

Springer Theses

Recognizing Outstanding Ph.D. Research

Antoine Simonneau

Gold-Catalyzed Cycloisomerization Reactions Through Activation of Alkynes

New Developments
and Mechanistic Studies



Springer

Springer Theses

Recognizing Outstanding Ph.D. Research

For further volumes:
<http://www.springer.com/series/8790>

Aims and Scope

The series “Springer Theses” brings together a selection of the very best Ph.D. theses from around the world and across the physical sciences. Nominated and endorsed by two recognized specialists, each published volume has been selected for its scientific excellence and the high impact of its contents for the pertinent field of research. For greater accessibility to non-specialists, the published versions include an extended introduction, as well as a foreword by the student’s supervisor explaining the special relevance of the work for the field. As a whole, the series will provide a valuable resource both for newcomers to the research fields described, and for other scientists seeking detailed background information on special questions. Finally, it provides an accredited documentation of the valuable contributions made by today’s younger generation of scientists.

Theses are accepted into the series by invited nomination only and must fulfill all of the following criteria

- They must be written in good English.
- The topic should fall within the confines of Chemistry, Physics, Earth Sciences, Engineering and related interdisciplinary fields such as Materials, Nanoscience, Chemical Engineering, Complex Systems and Biophysics.
- The work reported in the thesis must represent a significant scientific advance.
- If the thesis includes previously published material, permission to reproduce this must be gained from the respective copyright holder.
- They must have been examined and passed during the 12 months prior to nomination.
- Each thesis should include a foreword by the supervisor outlining the significance of its content.
- The theses should have a clearly defined structure including an introduction accessible to scientists not expert in that particular field.

Antoine Simonneau

Gold-Catalyzed Cycloisomerization Reactions Through Activation of Alkynes

New Developments and Mechanistic Studies

Doctoral Thesis accepted by
Université Pierre et Marie Curie, Paris, France

Author

Dr. Antoine Simonneau
Paris Institute of Molecular Chemistry
University Pierre and Marie Curie
Paris
France

Supervisor

Prof. Max Malacria
Institut de Chimie des Substances Naturelles
Gif-Sur-Yvette
France

ISSN 2190-5053

ISBN 978-3-319-06706-3

DOI 10.1007/978-3-319-06707-0

ISSN 2190-5061 (electronic)

ISBN 978-3-319-06707-0 (eBook)

Springer Cham Heidelberg New York Dordrecht London

Library of Congress Control Number: 2014939382

© Springer International Publishing Switzerland 2014

This work is subject to copyright. All rights are reserved by the Publisher, whether the whole or part of the material is concerned, specifically the rights of translation, reprinting, reuse of illustrations, recitation, broadcasting, reproduction on microfilms or in any other physical way, and transmission or information storage and retrieval, electronic adaptation, computer software, or by similar or dissimilar methodology now known or hereafter developed. Exempted from this legal reservation are brief excerpts in connection with reviews or scholarly analysis or material supplied specifically for the purpose of being entered and executed on a computer system, for exclusive use by the purchaser of the work. Duplication of this publication or parts thereof is permitted only under the provisions of the Copyright Law of the Publisher's location, in its current version, and permission for use must always be obtained from Springer. Permissions for use may be obtained through RightsLink at the Copyright Clearance Center. Violations are liable to prosecution under the respective Copyright Law. The use of general descriptive names, registered names, trademarks, service marks, etc. in this publication does not imply, even in the absence of a specific statement, that such names are exempt from the relevant protective laws and regulations and therefore free for general use.

While the advice and information in this book are believed to be true and accurate at the date of publication, neither the authors nor the editors nor the publisher can accept any legal responsibility for any errors or omissions that may be made. The publisher makes no warranty, express or implied, with respect to the material contained herein.

Printed on acid-free paper

Springer is part of Springer Science+Business Media (www.springer.com)

Part of this thesis have been published in the following journal articles:

1. Gold(I)-Catalysed Cycloisomerisation of 1,6-Enynes into Functionalised Allenes.
Harrak, Y.; Simonneau, A.; Malacria, M.; Gandon, V.; Fensterbank, L. *Chem. Commun.* **2010**, 46, 865–867.
2. Ring Expansions Within the Gold-Catalyzed Cycloisomerization of O-Tethered 1,6-Enynes. Application to the Synthesis of Natural-Product-like Macrocycles.
Simonneau, A.; Harrak, Y.; Jeanne-Julien, L.; Lemièrre, G.; Mouriès-Mansuy, V.; Goddard, J.-P.; Malacria, M.; Fensterbank, L. *Chem. Cat. Chem.* **2013**, 5, 1096.
3. Gold-Catalyzed 1,3-Acyloxy Migration/5-exo-dig Cyclization/1,5-Acyl Migration of Diynyl Esters.
Leboeuf, D.; Simonneau, A.; Aubert, C.; Malacria, M.; Gandon, V.; Fensterbank, L. *Angew. Chem. Int. Ed.* **2011**, 50, 6868.
4. Tracking Gold Acetylides in Gold(I)-Catalyzed Cycloisomerization Reactions of Enynes.
Simonneau, A.; Jaroschik, F.; Lesage, D.; Karanik, M.; Guillot, R.; Malacria, M.; Tabet, J.-C.; Goddard, J.-P.; Fensterbank, L.; Gandon, V.; Gimbert, Y. *Chem. Sci.* **2011**, 2, 2417.

Supervisor's Foreword

Antoine Simonneau's achievement during his Ph.D. work was really outstanding and I am convinced that everyone reading his thesis will appreciate his superb skills as a bright chemist.

His approach in solving scientific problems always involves great patience as well as enthusiasm and focused investment.

Antoine was extremely productive in a highly competitive field. So, in my group, he brought the topic of gold catalyzed cycloisomerization of polyunsaturated frameworks to the summit.

The reader will enjoy unprecedented migration processes, an original approach toward macrocycles, as well as the beauty of an exceptional cascade from a simple diyne involving a first -1,3-acyd shift, followed by gold catalyzed allenyne cycloisomerization, and then a previously unknown 1,5-acyl transfer delivering compounds of very high synthetic value in a one-pot operation.

Antoine is also very organized, extremely dedicated, and highly exigent researcher.

To conclude his work, he was the driver of a joint research program with theoreticians and mass spectrometry experts which allowed a better understanding of the intermediates involved in these catalytic processes.

Finally, I should say that he is an exceptionally brilliant researcher as well as a gentleman. His attitude within the group was consistently first class, his communication skills are excellent, and he has proved to have extraordinary leadership skills, which earned him the respect of all the members of my group.

Gif-Sur-Yvette, March 2014

Prof. Max Malacria

Abstract

The aim of this Ph.D. work was to develop new cycloisomerization reactions through activation of alkynes with gold complexes. We were first interested in 1,6-enynes and their direct conversion into allenes through 1,5-hydride or ester migration processes. By the use of appropriate propargylic functional groups, we could reach this goal. During the course of this study, it was observed that *O*-tethered 1,6-enynes carrying a strained cycloalkane at the propargylic position could undergo a cyclopropanation/ring expansion cascade reaction. This rearrangement was employed as the starting point in the design of a new macrocycle synthesis. We then turned our attention to the cycloisomerization of diynes involving as the first step of the process the rearrangement of one alkyne partner into an allene thanks to a gold-catalyzed 1,3-shift of a propargylic ester. A new cycloisomerization pattern featuring a 1,5-carbonyl transfer was thus disclosed, giving rise to unprecedented cross-conjugated diketones. To conclude, we investigated the gold-catalyzed cycloisomerization mechanism of 1,6-enynes and questioned the intermediacy of gold acetylides. By means of NMR and mass spectrometry analysis, theoretical treatment, and solution experiments, we were able to rule out the involvement of these species in the catalytic cycle.

Contents

1	Gold- and Platinum-Catalyzed Reactions of Enynes	1
1.1	Introduction	1
1.2	From Alder-Ene to Skeletal Reorganization in the Metal-Catalyzed 1,6-Enyne Cycloisomerization Reactions	2
1.3	Skeletal Rearrangements of Enynes with π -Acidic Metals	5
1.3.1	Early Works	5
1.3.2	Mechanistic Investigations with Platinum	8
1.3.3	Skeletal Rearrangement of 1,6-Enynes with Gold Catalysts	12
1.4	Gold- and Platinum-Catalyzed Cycloisomerizations of Enynes Without Skeletal Rearrangement	15
1.4.1	Alder-Ene Reaction	15
1.4.2	Reactions Involving Enols and Enol Ethers	16
1.4.3	Cyclopropanation Reactions: Endocyclic Au and Pt Carbene Intermediates	16
1.5	Trapping of Cationic Intermediates: Au- or Pt-Catalyzed Cyclization Reactions of Enynes in the Presence of Nucleophiles	22
1.5.1	Addition of Oxygen and Nitrogen Nucleophiles	23
1.5.2	Addition of Carbon Nucleophiles	24
1.6	Influence of Propargylic Free or Protected Hydroxy Substituents	26
1.6.1	Propargylic Esters	26
1.6.2	Propargylic Ethers and Alcohols	31
1.7	Allenynes: A Particular Case of Enynes	33
1.8	Conclusion	36
	References	36
2	New Advances in the Gold-Catalyzed Cycloisomerization Reactions of Enynes: 1,5-hydride Shifts and Access to Ketomacrolactones	43
2.1	Introduction	43
2.1.1	Bibliography	43
2.1.2	Presentation and Objectives of the Project	48

2.2	Validation of Our Hypothesis: Synthesis of Allenes Through a Gold-Catalyzed Cyclization and/or 1,5-migration Processes	48
2.2.1	Synthesis of Test Substrates and Reactivity	48
2.2.2	Oxygen-Protected Precursors	51
2.2.3	Vinyl and Benzyl Groups as Propargylic Substituents	54
2.3	Substrate Scope and Limitations	55
2.3.1	Carbon-Tethered Enynes	55
2.3.2	Heteroatom-Tethered 1,6-enynes	56
2.3.3	Rearrangement of Propargyl Ethers INTO Allenes	66
2.3.4	Conclusions and Perspectives	67
2.4	Synthetic Strategy Toward Macrolactones Based on a Gold-Catalyzed Enyne Cycloisomerization	68
2.4.1	Generality of the Endo Cyclization/Ring Expansion of Oxygen-Tethered 1,6-enynes	68
2.4.2	Access to Ketomacrolactones from Ring-Expansion Products	73
2.4.3	Perspective: Toward the Total Synthesis of Diplodialide D	79
2.5	Conclusion and Perspectives	81
	References	83
3	Synthesis of Polyconjugated Bis-Enones Through a Gold-Catalyzed 1,3-Acyloxy Migration-Cyclization-1,5-Acyl Shift Cascade Reaction	85
3.1	Introduction	85
3.1.1	Bibliography	85
3.1.2	Presentation and Objectives of the Project	95
3.2	First Results	96
3.2.1	Synthesis of the Precursors	96
3.2.2	Catalyst Optimization	99
3.2.3	Reaction Scope	99
3.3	Mechanistic Investigations	103
3.3.1	First Mechanistic Rationale	103
3.3.2	Toward an Intramolecular Acyl Transfer	104
3.3.3	DFT Calculations	104
3.4	Broadening the Scope of the Reaction	107
3.4.1	Non-terminal Alkynes	107
3.4.2	Acryloyl and Benzoyl Derivatives	108
3.4.3	Perspective: Alkynoyl and Allenoyl Derivatives	112
3.5	Conclusion	115
	References	116

4 Tracking Gold Acetylides in Gold(I)-Catalyzed Cycloisomerization Reactions of 1,6-Enynes	119
4.1 Introduction	119
4.1.1 Bibliography.	119
4.1.2 Presentation and Objectives of the Project	124
4.2 Preliminary Results with 1,6-Enynes	125
4.2.1 Catalysts Assessment.	125
4.2.2 Mass Spectrometry Analysis.	126
4.3 Solution and NMR Monitoring Experiments	130
4.3.1 Study with Free Enyne 25	130
4.3.2 Reactivity of Gold Acetylides.	133
4.4 Investigations on the Origin of the Diaurated Species	136
4.4.1 Mass Spectrometry Analysis.	136
4.4.2 Theoretical Investigations.	138
4.5 Preliminary Results with Allenynes	139
4.5.1 Reactivity of 1,6-Allenynes with Gold Catalyst 38	139
4.5.2 Reactivity of 1,n-Allenynes Gold Acetylides	141
4.5.3 Preliminary Results in Mass Spectrometry	143
4.6 Conclusion	145
References	145
General Conclusion	149
Experimental Section.	153

Abbreviations

Ac	Acetyl
AIBN	Azo-bis- <i>iso</i> -butyronitrile
Ar	Aryl
Bn	Benzyl
Bu	Butyl (n-normal-, t-tertio-)
cat.	Catalytic
Cbz	Benzyloxycarboxyl
Cy	Cyclohexyl
DCE	1,2-Dichloroethane
DCM	Dichloromethane
DFT	Density functional theory
DHP	Dihydropyran
DMAP	4-Dimethylaminopyridine
DMF	Dimethylformamide
DMSO	Dimethylsulfoxide
dr	Diastereomeric ratio
E	Electrophile
EDCI	1-Ethyl-3-(3-dimethylaminopropyl)carbodiimide
ee	Enantiomeric excess
equiv.	Equivalent
ESI	Electrospray ionization
Et	Ethyl
h	Hour
HMPT	Hexamethylphosphotriamide
HOMO	Highest occupied molecular orbital
HRMS	High resolution mass spectrometry
IMDA	Intramolecular Diels-Alder
IPr	<i>N,N'</i> -bis(2,6-Diisopropylphenyl) imidazol-2-ylidene
<i>i</i> -Pr	<i>iso</i> -Propyl
IR	Infra-red
L	Ligand
LA	Lewis acid
LDA	Lithium di- <i>iso</i> -propylamide
LUMO	Lowest unoccupied molecular orbital

M	Metal
<i>m</i>	Meta
<i>m</i> -CPBA	Metachloroperbenzoic acid
Me	Methyl
min	Minute
mp	Melting point
MS	Mass spectrometry
Ms	Mesyl
MW	Molecular weight
NBS	<i>N</i> -Bromosuccinimide
nd	Not determined
NHC	<i>N</i> -Heterocyclic carbene
NHS	Succinimide
NMR	Nuclear magnetic resonance
nOe	Nuclear Overhauser effect
Nu	Nucleophile
<i>o</i>	Ortho
<i>p</i>	Para
PCC	Pyridinium chlorochromate
PE	Petroleum ether
PG	Protecting group
Ph	Phenyl
PNB	<i>para</i> -Nitrobenzoate
PTSA	<i>para</i> -Toluenesulfonic acid
quant.	Quantitative
rt	Room temperature
T	Temperature
TBDMS	<i>tert</i> -Butyldimethylsilyl
TBDPS	<i>tert</i> -Butyldiphenylsilyl
Tf	Triflate
THF	Tetrahydrofuran
THP	Tetrahydropyran
TLC	Thin layer chromatography
TMS	Trimethylsilyl
Tol	Tolyl
TS	Transition state
Ts	Toluenesulfonyl
<i>vs</i>	Versus
$\Delta\epsilon$	Reflux

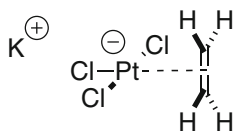
General Introduction: Gold, a Powerful Tool for the Activation of C–C Multiple Bonds

The end of the twentieth century has seen a growing number of reports on transition metal-based catalysis published in the scientific literature. These methodologies have been the object of intensive studies and still raise the interest of many research groups around the world as well as companies from the chemical industry, as they represent an expedient way to molecular complexity from simple building blocks. Examples include alkene metathesis and cross-coupling, two fields of organometallic catalysis that have emerged in the second half of the last century and were both awarded Nobel prizes. Most of the metal catalyzed processes discovered during this period rely on mid-to-late transition metal catalysts (eg. Ru, Rh, Ir, Pd). They often involve two different oxidation states of the considered metal in the catalytic cycle, the switch from one to the other being permitted by oxidative additions or reductive eliminations, which are two-electrons red-ox processes.

From the 1990s, significant results on homogeneous platinum and gold catalysis, dealing with the functionalization of carbon–carbon unsaturations were reported. They deeply contrast with the above-mentioned chemistry of cross-coupling, as these reactions are red-ox neutral. They can be seen, yet in an extremely simplified manner, as a Lewis acid/base interaction between the metallic center and the multiple bond, resulting in the consideration of monocoordinated metal-substrate adducts in the drawing of mechanistic rationales. This introduction will briefly present the possibilities offered by gold and platinum complexes in terms of catalysis, and underline the concepts at stake to understand the particular reactivity of these metals.

Implication of Relativistic Effects in the Coordination Chemistry of Gold and Platinum Salts to C–C Multiple Bonds

In homogeneous catalysis, gold is mainly used in complexes of +1 or +3 oxidation states. While gold(I), which features filled 5d orbitals, is mainly encountered as divalent complexes with linear geometry, gold(III) ($5d^8$) adopts a square planar



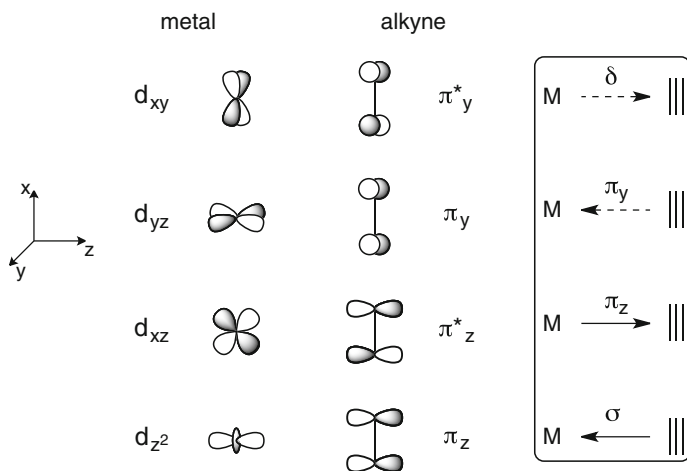
Scheme 1 Zeise's salt

configuration. The same geometry is observed for the isoelectronic platinum(II) complexes which are the most used as catalysts. Both gold(III) and platinum(II) complexes are preferentially obtained as tetracoordinated compounds. Platinum(IV) ($5d^6$) is octahedral. Historically, the first transition metal complex with an unsaturated hydrocarbon is Zeise's salt $K[PtCl_3(C_2H_4)]$ [1]. Its true nature was unraveled latterly, and it is with the advent of X-ray diffraction at the beginning of the 1950s that its structure was finally elucidated [2]. This will raise a series of interrogations about the nature of bonding between a metal center and the carbon–carbon multiple bond, and intense research from both the coordination and theoretical chemistry sides have bloomed from this period (Scheme 1).

In the 1950s, Dewar, Chatt and Duncanson devised a qualitative model accounting for the bonding situation of transition metal complexes with alkenes or alkynes based on the consideration of four couples of orbitals of different symmetry that overlap to form the complex [3, 4]. The four components that contribute to the bond between a metal and an alkyne are highlighted in Scheme 2.

In-plane interactions represent the major contributions of this bonding situation: a σ -symmetric bond emerge from overlapping of alkyne's p_z and metal's d_{z^2} . In this case, alkyne's electrons are delocalized toward the metallic center. A π -symmetric bond is formed by fusion of metal's d_{xz} and alkyne's p_z^* which can be seen as a back-donation from the metal onto the alkyne. With alkyne, a third component is at stake as the out-of-plane p_y orbital can participate to the alkyne-to-metal donation by forming another π -symmetric bond. Finally, the fourth component, of δ symmetry, represents a little contribution in bonding as metal's d_{xy} and alkyne's p_y^* orbitals weakly overlap. Rehybridization will ensue, as a consequence of the depletion of the bonding p orbitals in favor of the antibonding one, thanks to metal back-donation. This model thus predicts an elongation of the C–C bond, as well as a loss of linearity or planarity of the considered alkyne or alkene form. It is readily applicable to gold and platinum, but is nonetheless not enough to explain the particular reactivity displayed by these metals.

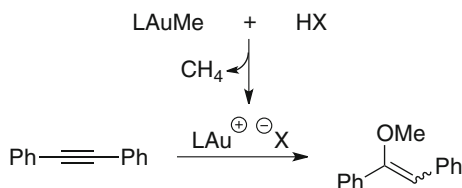
The outstanding reactivity of gold and platinum homogeneous catalysts finds another explanation by taking into account relativistic effects [5]. Due to the great velocity of electron orbiting around heavy nucleus, the theory of relativity predicts that their mass will considerably increase, and inversely, their radius will decrease. This results directly in a greater ionization energy and a contraction of s and p orbitals, and consequently by the expansion of d and f orbitals that are better shielded by the former. These effects reach a peak for platinum, gold, and mercury, and the stabilization of their valence orbitals gives these metals a high



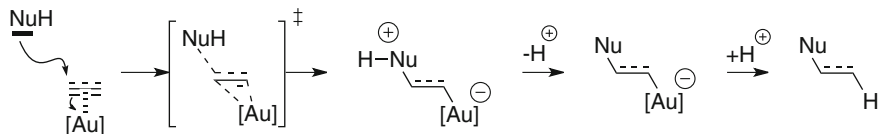
Scheme 2 The qualitative Dewar–Chatt–Duncanson (DCD) model for a metal–alkyne bond

electronegativity (gold, with an electronegativity of 2.4 according to Pauli's scale, is the most electronegative transition metal). Besides, the electrons of the diffuse 5d orbital are better held due to decreased electron repulsion, resulting in a low nucleophilicity of gold and platinum species and their propensity to avoid oxidative addition. This is well illustrated by the difference between organocopper(I) and organogold(I) complexes, the former being readily oxidized to a copper(III) species while the latter is relatively inert [6]. Likewise, reductive elimination from gold(III) is quite disfavored [7, 8]. These phenomena are consistent with the rare observation of red-ox cycles with these metals, and their relative tolerance to oxygen, particularly with gold(I). Again, keeping in mind the DCD model (Scheme 2), the amplified energy difference between the s and d orbitals results in a weak back-donation from the metal to the ligand, as pointed out by theoretical investigations on the $[\text{Au}(\text{C}_2\text{H}_2)]^+$ fragment. They revealed that the π interactions were the most prominent and contribute to almost two-thirds of the whole bonding.¹ Thus, the interaction of an alkyne or an alkene with platinum or gold approaches the purely donor–acceptor case described by the Lewis theory of acid/base behavior. This means that gold (and platinum) complexes can be seen as soft Lewis “p-acids”: their complexation to a C–C multiple bond will deprive the latter of a part of its electron density and engender a partial positive charge on it, as electron back-donation from the metal is poorly effective (but however must not be neglected). The unsaturated hydrocarbon ligand is thus made sensitive to any nucleophilic attack. Structural and spectroscopic data correlate well this fact, as X-ray diffraction studies of gold(I) or platinum(II) bound alkenes or alkynes

¹ This study also revealed that electrostatic interactions participate for half of the total bonding force: [9].



Scheme 3 Alkoxylation of alkynes with cationic gold(I)



Scheme 4 Generic mechanism for the nucleophilic addition of NuH onto a C–C multiple bond

revealed a very slight distortion of the unsaturated hydrocarbon's geometry and small changes in the stretching frequencies were observed by IR absorption. It accounts well for a limited population of the π antibonding orbital.²

The Concept of Alkynophilicity

In many cases of gold-catalyzed reactions, a competitive issue can arise, as both an alkyne and an alkene are present in the reaction mixture. The observation of a preferred alkyne over alkene activation is quite intriguing as gold was shown to build stronger bonds with alkenes than alkynes (See footnote 1). In fact, this phenomenon has a kinetic origin, as activated alkyne LUMOs are relatively low in energy compared to the alkene case [12]. This results in a favored attack on alkynes and accounts for this observed “alkynophilicity.”

Reactivity of C–C Multiple Bonds Upon Gold or Platinum Catalysis

In our view, the most significant and seminal example of the practical application of these catalysts is the addition of water or alcohols to alkynes. This reaction was previously known to work well upon mercury(II) catalysis, in place of simple Brønsted acids that usually require harsh conditions and present as a major

² For reviews on such coordination compounds see for Au: [10]. For Pt: [11].

drawback, numerous side reactions. Furthermore, mercury(II) salts are toxic, and their related reaction with olefins are plagued by the formation of stable alkylmercury bonds, which renders such reaction stoichiometric in mercury. The replacement of mercury by gold(I), carried out by the team of Teles from BASF, demonstrates well the power of this metal to activate alkynes. Taking into account that linear gold(I) complexes are reticent to coordinate a third ligand, they generated in situ cationic phosphine gold(I) species by protonolysis of a $C(sp^3)$ –Au bond and could perform very efficiently the nucleophilic addition (Scheme 3).

This paved the way for the use of cationic gold(I) salts as catalysts of choice for the activation not only of alkynes but also other C–C multiple bonds. Although platinum was also shown to display similar reactivity, gold overtook this field of catalysis thanks to its greater activity. A generic mechanistic pathway can be drawn for such reactions (Scheme 4).

First, complexation of the metal center causes a lowering of the electron density at the unsaturation and renders it electrophilic. The nucleophilic attack is then permitted by “slippage” of the metal fragment along the ligand’s axis.³ This η^2 to η^1 deformation considerably enhances the electrophilicity of the bound C–C multiple bond as it favors, by this slight change of orbitals’ geometry, the charge transfers from the nucleophile. It is now widely accepted that this occurs in an *anti* fashion. Concomitantly, with the formation of the C–Nu bond is formed a σ C-metal bond resulting in vinyl- or alkylgold species. The occurrence of such intermediates was recently demonstrated with their isolation in the gold series.⁴ The carbon-metal bond in these η^1 -complexes is quite labile and readily react with electrophiles, frequently a proton.⁵ This last step has for consequence the regeneration of the active catalytic species.

This kind of reaction was successfully performed on alkenes, alkynes, and allenes with various heteroatomic or carbon nucleophiles, and will not be detailed further in this introduction.⁶

References

1. Zeise WC (1827) Poggendorf’s. Ann Phys 9:632
2. Wunderlich JA, Mellor DP (1954) Acta Crystallogr 7:130
3. Dewar MJS (1951) Bull Soc Chim Fr 18:C71
4. Chatt J, Duncanson LA (1953) J Chem Soc 1953:2939
5. Gorin DJ, Toste FD (2007) Nature 446:395

³ For a seminal contribution in the study of this phenomenon see: [13]. For a solid state structure of a slipped gold-alkene complex see: [14].

⁴ Alkylgold complexes from alkenes: [15]. Vinylgold complexes from allenes: [16]. Vinylgold complexes from alkynes: [17, 18].

⁵ For studies on the reactivity of vinylgold complexes with electrophiles see: [19, 20].

⁶ Selected reviews: [21–27].

6. Nakanishi W, Yamanaka M, Nakamura E (2005) *J Am Chem Soc* 127:1446
7. Komiya S, Albright TA, Hoffmann R, Kochi JK (1976) *J Am Chem Soc* 98:7255
8. Komiya S, Kochi JK (1976) *J Am Chem Soc* 98:7599
9. Nechaev MS, Rayon VM, Frenking G (2004) *J Phys Chem A* 108:3134
10. Schmidbaur H, Schier A (2010) *Organometallics* 29:2
11. Belluco U, Bertani R, Michelin RA, Mozzon M (2000) *J Organomet Chem* 600:37
12. Garcia-Mota M, Cabello N, Maseras F, Echavarren AM, Perez-Ramirez J, López N (2008) *ChemPhysChem* 9:1624
13. Eisenstein O, Hoffmann R (1981) *J Am Chem Soc* 103:4308
14. Fürstner A, Alcarazo M, Goddard R, Lehmann CW (2008) *Angew Chem Int Ed* 47:3210
15. LaLonde RL, Brenzovich WE, Benitez D, Tkatchouk E, Kelley K, Goddard WA, Toste FD (2010) *Chem Sci* 1:226
16. Liu L.-P, Xu B, Mashuta MS, Hammond GB (2008) *J Am Chem Soc* 130:17642
17. Hashmi ASK, Schuster AM, Rominger F (2009) *Angew Chem Int Ed* 48:8247
18. Hashmi ASK, Ramamurthi TD, Rominger F (2009) *J Organomet Chem* 694:592
19. Hashmi ASK, Ramamurthi TD, Rominger F (2010) *Adv Synth Catal* 352:971
20. Hashmi ASK, Ramamurthi TD, Todd MH, Tsang ASK, Graf K (2010) *Aust J Chem* 63:1619
21. Hashmi ASK (2007) *Chem Rev* 107:3180
22. Hashmi ASK, Hutchings GJ (2006) *Angew Chem Int Ed* 45:7896
23. Li ZG, Brouwer C, He C (2008) *Chem Rev* 108:3239
24. Nevado C, Echavarren AM (2005) *Synthesis* 2:167
25. Reetz MT, Sommer K (2003) *Eur J Org Chem* 18:3485
26. Shen HC (2008) *Tetrahedron* 64:3885
27. Widenhoefer RA, Han XQ (2006) *Eur J Org Chem* 4555

Chapter 1

Gold- and Platinum-Catalyzed Reactions of Enynes

In this chapter we will introduce the reactivity of enynes toward gold catalysis. As many examples of gold-catalyzed enyne cycloisomerizations have been reported in the literature, we will only focus on examples we found relevant in view of the results that will be presented in the following chapters.

1.1 Introduction

Synthetic methodologies aimed at the synthesis of functionalized and/or functionalizable cyclic compounds have always been of particular interest for the synthetic chemist. In his continuing effort to try to be equal to, or even better than Nature for the synthesis of complex molecules, the organic chemist has known how to overcome many problems raised by the complexity of some molecular structures. Among them, the development of reliable and efficient synthesis of cyclic and polycyclic compounds remains maybe one of the most important challenges. Through the last 40 years, transition metal catalysis has emerged as a powerful tool for the formation, in a selective manner and with limited by-products, of carbon-carbon and carbon-heteroatom bonds that would be much more difficult, even impossible to achieve with conventional organic reagents alone or by thermal rearrangements. In this field, the metal-catalyzed cycloisomerization reactions of 1,n-enynes have emerged as a unique, conceptually and highly attractive tool for the synthesis of a broad range of cyclic compounds in a very easy one-pot process. Since the pioneering studies with palladium processed by the team of Trost in the mid-80s, several metals have been identified as excellent candidates for catalyzing these reactions, allowing the discovery of new reactions and contributing to answer to the constant demand of atom-economic reactions.

1.2 From Alder-Ene to Skeletal Reorganization in the Metal-Catalyzed 1,6-Enyne Cycloisomerization Reactions

From a historical point of view, the first metal-catalyzed cycloisomerization of enynes **1** was performed using palladium(II) catalysts and led to Alder-Ene products **2** [1], the latter being generally obtained by thermal isomerizations at high temperatures and on a limited range of substrates [2, 3]. The reaction was proposed to occur through a palladium(IV)-metallacycle **3** after coordination of both alkene and alkyne to the metal center, which formation is accompanied by a two electrons oxidation of the metal. A β -hydride elimination gives birth to vinylpalladium complex **4** which evolves through reductive elimination into Alder-Ene product **2**, concomitant with Pd(II)-catalyst regeneration (Scheme 1.1).

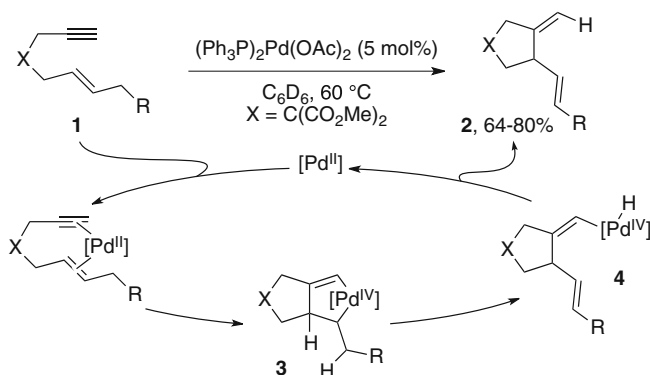
From this work will follow a series of investigations on related substrates, led by many research teams around the world, employing different metals and experimental conditions that allowed the discovery of new cyclization patterns and new mechanisms. As well, the decoration of the starting enyne with functional groups such as alcohols, aldehydes, ethers, alkenes or alkynes was often shown to have a dramatic influence on the reaction outcome and brought more complexity to the synthesized compound. Without going further into details, as some relevant reviews will fulfil this duty [4–6], three major mechanistic pathways rapidly emerged from the experimental observations made by different teams:

- (i) the metallacyclopentene pathway,
- (ii) the vinylmetal pathway,
- (iii) the π -allylmetal pathway,

each being depicted in Scheme 1.2. The first one has been explained above with the example of palladium-catalyzed Alder-ene reaction disclosed by the group of Trost. Scheme 1.2 adds the regioselectivity issue of the β -hydride elimination that can lead to two different products **5** and **6** and was shown to obey to stereoelectronic factors [7].

The chemistry of metallacycles is very rich and will not be further developed in this chapter, but one can cite insertion reaction occurring on these intermediates, such as the Pauson-Khand reaction with carbon monoxide, or electrophilic cleavage. Several metals were shown to display this reactivity apart from palladium.¹ The vinylmetal pathway, again discovered by the team of Trost [11] with in situ generated palladium(II) hydride catalysts has for main difference with the metallacyclopentene pathway to maintain the oxidation state of the metal. The first step is a metallation step occurring at the triple bond of the system to give vinylmetal intermediate **7**, then followed by a carbometallation step in which the carbon-carbon bond is formed. The resulting intermediate **8** then undergoes β -hydride

¹ Seminal report with Co: [8]. With Rh: [9, 10].



Scheme 1.1 Pd^{II}-catalyzed cycloisomerization of 1,6-enynes

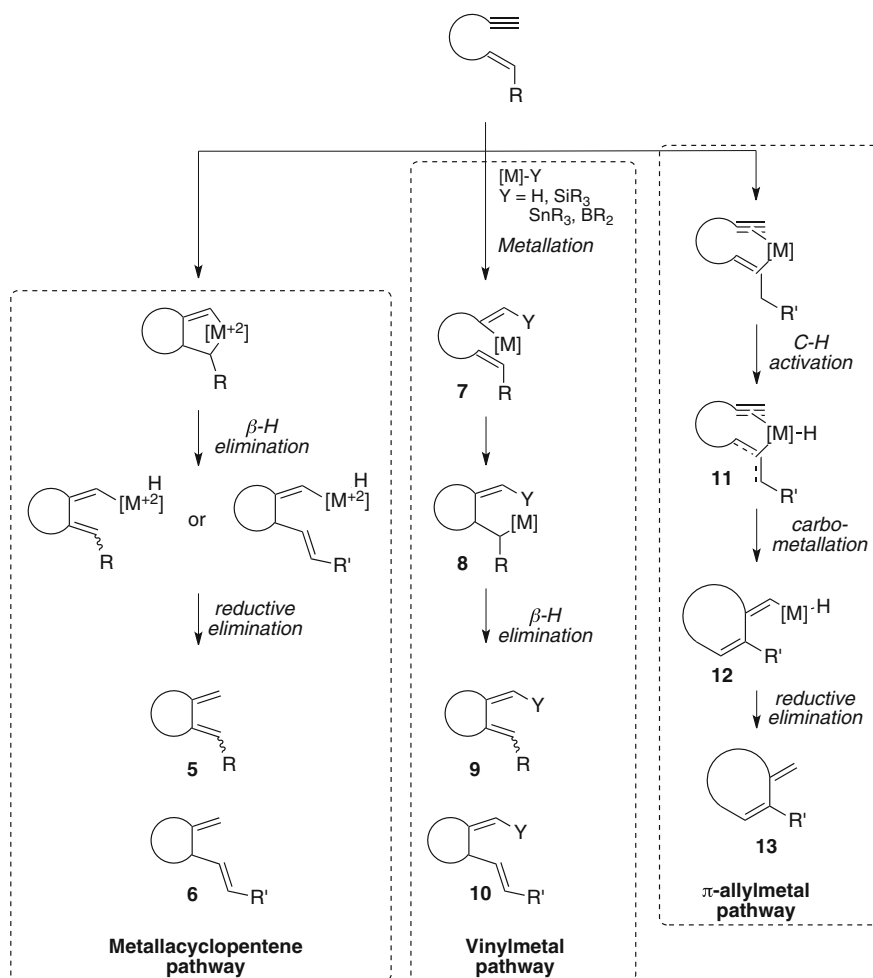
elimination to give cyclized products **9** and/or **10**. This pathway can be also encountered with nickel-chromium and ruthenium catalysts.² To finish, the last pathway features the occurrence of a π -allylmatal intermediate **11** generated through activation of an allylic C–H bond. A carbometallation step then occurs affording vinylmetal intermediate **12** which subsequently undergoes reductive elimination to yield cyclized product **13**. This cycloisomerization pathway, to the best of our knowledge, has only been observed in the enyne series with ruthenium catalysts. However, it was disclosed that rhodium catalysts were able to activate an allylic chlorine-carbon bond and then trigger an enyne cycloisomerization through a π -allylmatal pathway [14]. It is worth citing that recently a pathway involving a rhodium vinylidene was also evidenced, yet leading to other types of products [15].

While studying a novel electrophilic palladium catalyst for cycloisomerization of enynes, Trost and his team stumbled upon an intriguing cyclized compound **16** which skeletal reorganization could not be explained by classic metallacycle or vinylmetal pathways (Scheme 1.3) [16]. To account for the formation of diene **16**, named “metathesis product” as similar products were obtained by Katz and Sivavec upon catalysis with a Fischer-type tungsten carbene complex [17], it was initially postulated that it could arise from a reductive elimination on metallacycle **17** leading to cyclobutene **18** which subsequent thermal, conrotatory opening could deliver compound **16** (Scheme 1.3).³

However, ²H- and ¹³C-labelling studies have shown that two different kinds of rearranged dienes **20** and **21** are obtained, arising from either a *single cleavage* of the double bond or a *double cleavage* of both the double and the triple bond (Scheme 1.4) [20]. To explain this, another pathway was hypothesized, relying on the rearrangement of the palladacyclopentene **22** into cyclopropylcarbene **23**.

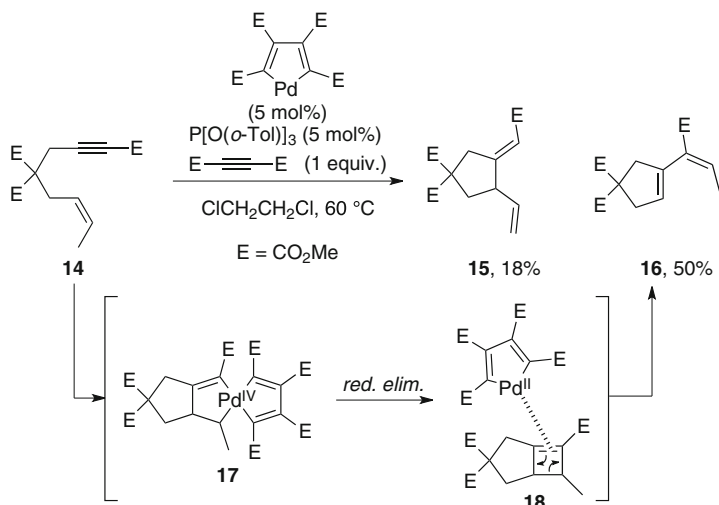
² Seminal report with Ni–Cr: [12]. With Ru: [13].

³ Cyclobutenes could have been isolated in some cases, see: [18, 19].

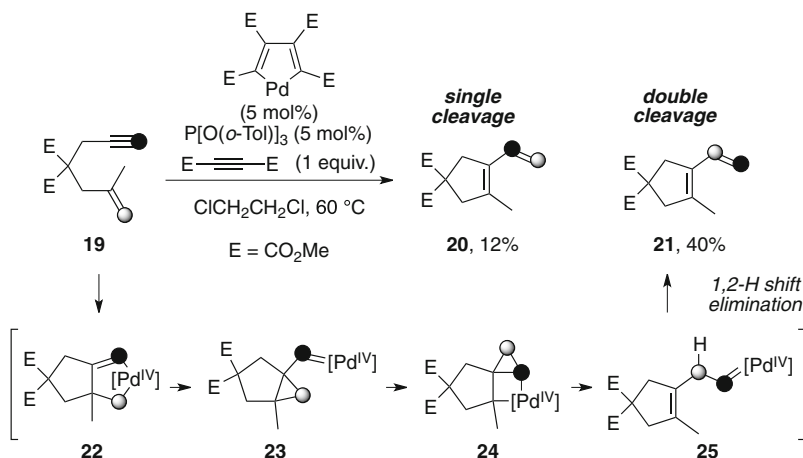


Scheme 1.2 The first three major pathways in metal-catalyzed enyne cycloisomerization reactions

The latter would undergo successive rearrangements through **23** and **24** to lead to carbene **25**. A 1,2-H shift/elimination sequence then allows regeneration of the catalyst and release of the formal metathesis product **21** [20]. This mechanism sets the basis to explain the skeletal rearrangement of enynes promoted by other electrophilic metal salts. The team of Trost and Hashmi latterly evidenced the implication of species **23** [21–23]. The use vinyl substituted enyne **26** in the presence of a 1,3-diene allowed them to obtain product **27** arising from a [4 + 2] cycloaddition of vinyl carbene **28** with the propargylic double bond of the diene (Scheme 1.5).



Scheme 1.3 Formation of an unexpected product

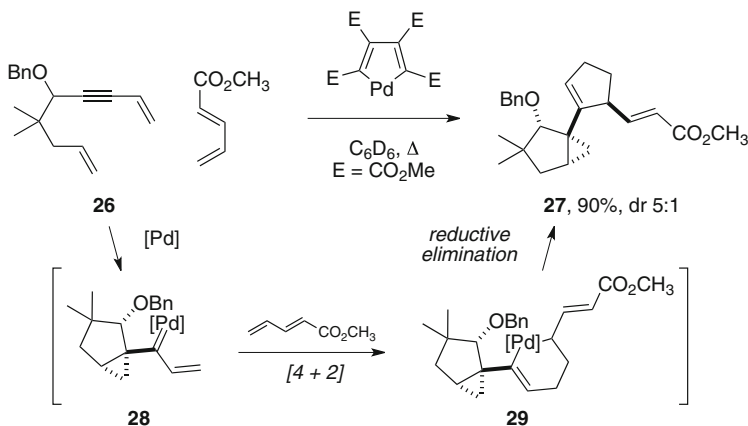


Scheme 1.4 Mechanism attesting to the formation of double cleavage metathesis products

1.3 Skeletal Rearrangements of Enynes with π -Acidic Metals

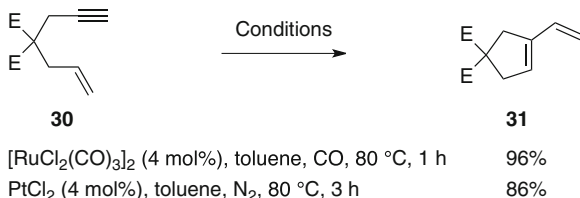
1.3.1 Early Works

Along the 90s decade, inspired by the pioneering studies of Trost, many research groups have shown that several non-alkylidene metal complexes are able to promote the formal metathesis of enynes. Again, intensive mechanistic studies clearly



Scheme 1.5 Evidence for a cyclopropylcarbene intermediate: a [4 + 2] cycloaddition trapping strategy

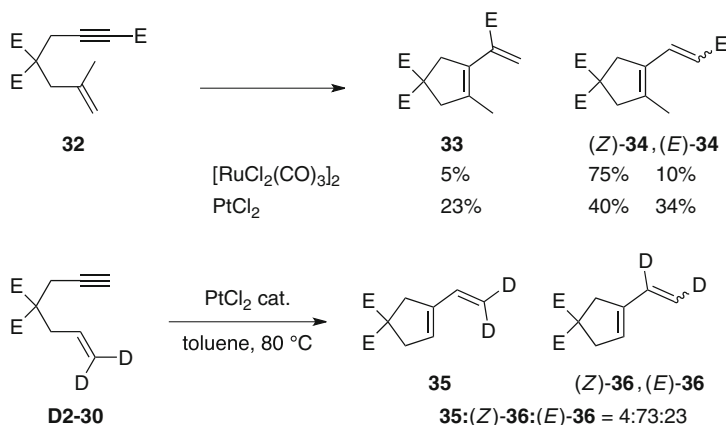
Scheme 1.6 Skeletal rearrangement of 1,6-enynes with Pt and Ru chloride salts



separate the metathesis process with carbene-based catalysts [17, 24–30] from the one with electrophilic complexes, which has thus been named “skeletal rearrangement” or “skeletal reorganization” instead of “metathesis”. The first team to report an efficient and selective skeletal reorganization of 1,6- and 1,7-enynes was the group of Chatani and Murai with the use of catalytic ruthenium dimer $[\text{RuCl}_2(\text{CO})_3]_2$ under an atmosphere of CO [31]. They noticed that the presence of both CO and a halide was crucial for the reaction to proceed. Interestingly, Murai and Chatani added at the end of their manuscript that rhodium, rhenium, iridium, platinum and gold chloride salts also caused similar skeletal reorganization. Shortly after, they published a complete study with platinum dichloride (Scheme 1.6) [32].

The reaction of ester-substituted enyne **32** showed that two mechanisms were at stake in the skeletal reorganization of enynes as a mixture of single and double cleavage products **33** and (*E*)-**34** (*Z*)-**34** was obtained. This result was confirmed with deuterium-labelled enyne **D2-30** upon platinum catalysis, this last experiment showing with product **36** that a 1,2-H shift was involved in its formation (Scheme 1.7).

Unlike the mechanism proposed by Trost with palladium(II) catalysts, the mechanism proposed by Murai for electrophilic metal complexes does not involve a metallacycle. He proposed, as the initial step, a single η -complexation of the



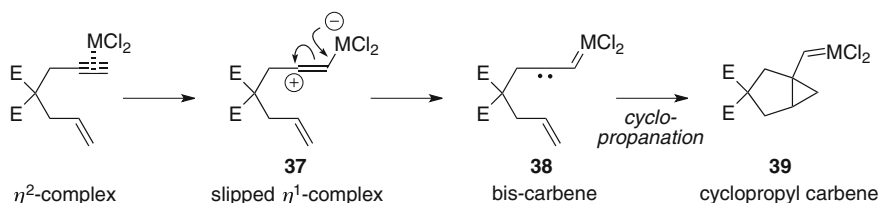
Scheme 1.7 Single and double cleavage products in the skeletal rearrangement of 1,6-enynes

metal to the alkyne, this complex would then evolve into a slipped η -alkyne complex **37** bearing a positive charge at the β position. The proposition of such carbocationic intermediate followed the observation by the group of Dixneuf of propargylic arenes 1,2-migrations triggered by ruthenium complexation onto an alkyne, and was rationalized by the occurrence of such slipped structures [33]. Slipped complex **37** would subsequently be transformed into the “bis-carbene” species **38** which undergoes cyclopropanation with the double bond to lead to cyclopropylcarbene intermediate **39** as proposed by Trost (Scheme 1.8).

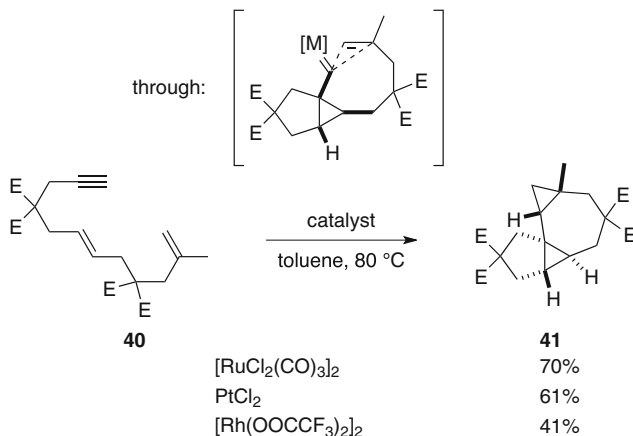
Intramolecular trapping by a pendant double bond, through submitting substrate **40** to electrophilic ruthenium, platinum and rhodium complexes, latterly evidenced the involvement of carbene **39** [34]. This experiment allowed Murai and Chatani to get complex fused tetracyclic compounds like **41** and settled the validity of the cyclopropylcarbene as intermediate in the skeletal reorganization of enynes (Scheme 1.9).

The team of Fensterbank, Malacria and Marco-Contelles latterly applied a similar strategy. They employed “branched” dienyynes like **42** and showed, upon platinum catalysis, that the putative cyclopropylplatinacarbene could be trapped in a comparable manner to Murai’s dienyne **40** to get polycyclic adducts **43** (Scheme 1.10) [35].

Some years after their study on platinum, Chatani and Murai reported two iridium(I) complexes, $[\text{IrCl}(\text{CO})_3]_n$ and $[\text{IrCl}(\text{cod})]_2$ to be efficient catalysts for the skeletal reorganization of 1,6- and 1,7-enynes [36]. Within this short period, other groups, notably Fürstner’s, Echavarren’s and Inoue’s ones, brought considerable insights to the understanding of skeletal rearrangement of enynes catalyzed by platinum then gold, finally found to be the ultimate catalyst for this reaction (and many others).



Scheme 1.8 Formation of cyclopropylcarbene through a slipped η -alkyne complex



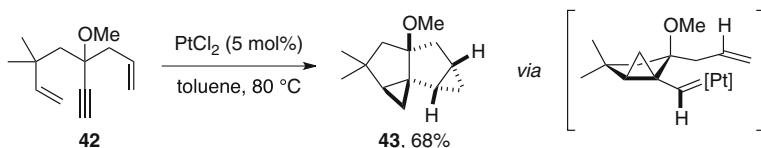
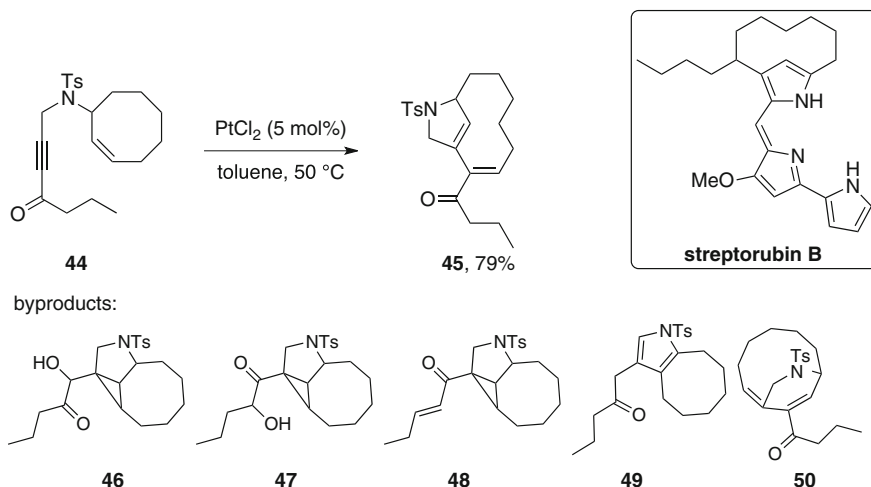
Scheme 1.9 Carbene trapping by cyclopropanation

1.3.2 Mechanistic Investigations with Platinum

Following Murai and Chatani's studies, the group of Fürstner employed the PtCl_2 -catalyzed skeletal rearrangement of 1,6-enynes as a key step in the total synthesis of streptorubin B and metacycloprodigosin alkaloids [37]. As they run the cycloisomerization reaction of precursor **44** on a large scale, they could isolate low amounts of minor byproducts **46–50** that shed light on the reaction mechanism (Scheme 1.11).

They thus proposed a “nonclassical” homoallyl-cyclopropylmethyl-cyclobutyl cation⁴ as reactive intermediate. Its formation is explained by the coordination of platinum onto the triple bond that triggers nucleophilic attack from the alkene partner, based on the idea that alkynes coordinated to platinum(II) had been shown

⁴ First description of nonclassical cation: [38]. Introduction of the term: [39, 40].

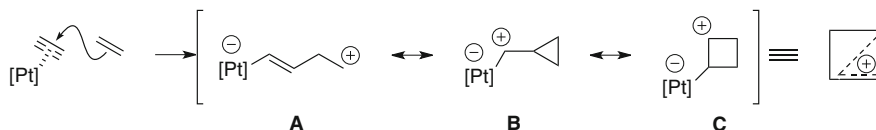
**Scheme 1.10** Trapping of carbene intermediates**Scheme 1.11** Skeletal rearrangement accompanied by minor by-products en route to streptorubin B

to display an electrophilic character,^{5,6} (Scheme 1.12). This mechanistic rationale allowed them to account for the formation of compounds **45–50**, the minor products arising from reaction with traces of water. In a later article, they showed that the skeletal rearrangement was also effective with terminal alkynes and carbon-tethered enynes [**42**, **43**].

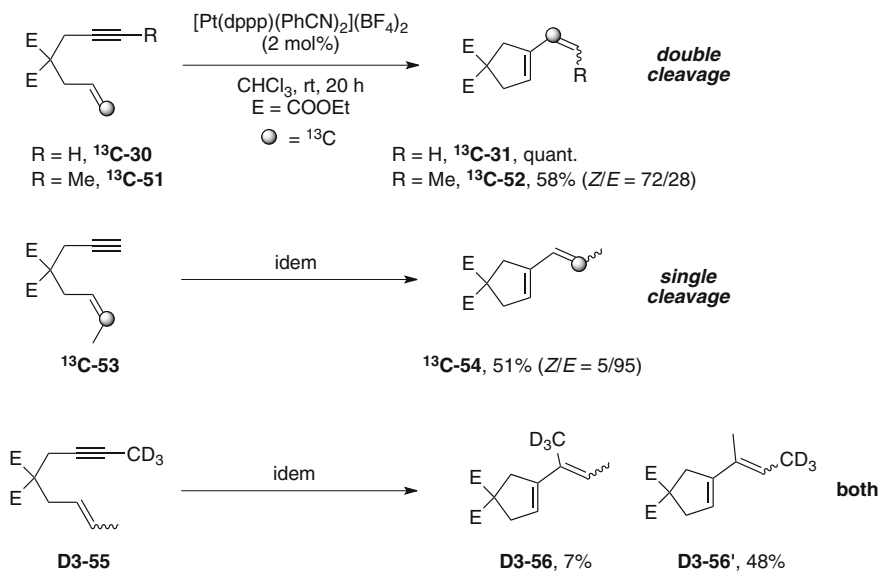
The groups of Echavarren and Inoue then made their own contribution to the understanding of the mechanism as they brought supplementary evidences to the cationic intermediate hypothesized by Fürstner. They both simultaneously proposed the occurrence of a cyclopropylcarbene intermediate. Whereas Echavarren came to this conclusion as he was working on PtCl_2 -catalyzed alkoxymercuration and Alder-Ene reactions of 1,6-enynes (vide infra) [**44**, **45**] with DFT calculations

⁵ This fact was also enforced by some effective skeletal reorganization promoted by either a Lewis or a Brønsted acid.

⁶ For a review see: [**41**].



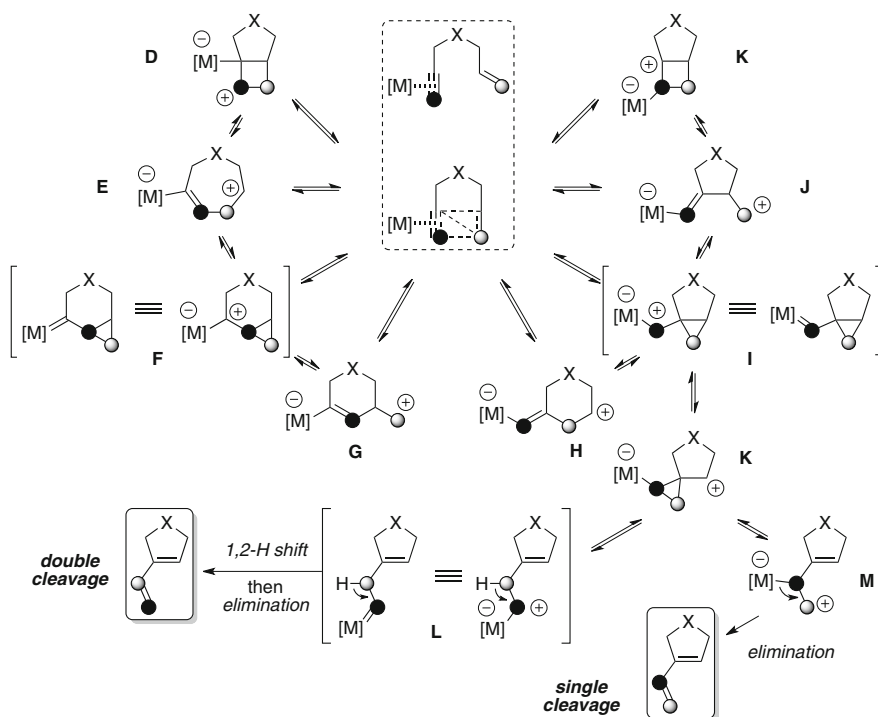
Scheme 1.12 A nonclassical carbocation intermediate in the Pt-catalyzed skeletal rearrangement



Scheme 1.13 Single and double cleavage skeletal reorganization of 1,6-enynes upon dicationic Pt(II) catalysis

giving support, Inoue showed on the basis of ^2H - and ^{13}C -labelling experiments that single and double cleavage skeletal rearrangement products of 1,6-enynes could be obtained upon catalysis with electrophilic, dicationic platinum complex $[\text{Pt}(\text{dppp})(\text{PhCN})_2](\text{BF}_4)_2$ (Scheme 1.13) [46].

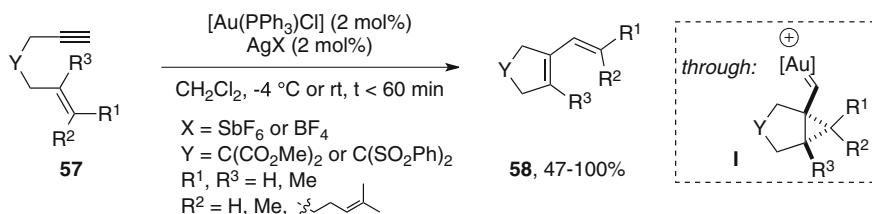
According to these results, he also invoked cationic intermediates to account for his observations. The mechanistic model proposed for the skeletal reorganization was thus magnified and has since been adopted and confirmed by numerous computational and experimental studies. It explains well a myriad of transformations relying on carbophilic activation of enynes by extension of the underlying principles, either with electrophilic salts of other transition metal such as gold (vide infra), gallium, [47] indium, [48] iridium, [36] ruthenium [31, 34] and rhodium [49, 50]. In view of the results collected by Fürstner and Inoue [37, 42, 46] and further studies by Echavarren, [44, 51] the carbene nature is a pertinent description of the



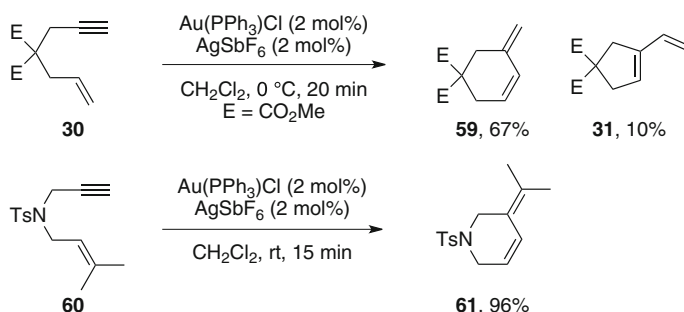
Scheme 1.14 Interpretation of metal-activated enynes in the sense of a nonclassical carbocation and mechanism of single and double cleavage postulated by Inoue

reactive intermediates in the platinum series. However, in the gold series, theoretical and experimental studies have shown its considerable cationic character, so that a debate will ensue on the genuine nature of the intermediates involved in the cycloisomerization of enynes with strongly electrophilic gold complexes. We will briefly present this controversy in Sect. 2.3.2, but we will keep the term “carbene” for intermediates **F**, **I**, **L** or **M** (Scheme 1.14).

From a practical point of view, the model depicted in Scheme 1.14 is in total adequacy with the results obtained by Inoue: single cleavage products are selectively obtained when stabilizing substituents are placed at the alkene terminus to give stability to cation **M**, whereas acetylenic substituents stabilizing cation **L** will favor double cleavage. In a general manner, the outcome of many reactions of enynes activated with carbophilic metals could be predicted by considering the most stable cationic resonance structure among all those depicted in Scheme 1.14.



Scheme 1.15 Exocyclic, single cleavage skeletal rearrangement of 1,6-enynes with cationic Au(I)



Scheme 1.16 Endocyclic skeletal rearrangement of 1,6-enynes with cationic Au(I)

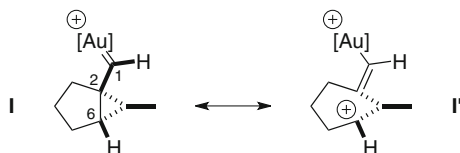
1.3.3 Skeletal Rearrangement of 1,6-Enynes with Gold Catalysts

1.3.3.1 Endo- and Exo-Skeletal Rearrangement

In 2004, Echavarren reported cationic gold(I) catalysts to be powerful complexes for the skeletal rearrangement of enynes **57** to give 1,3-dienes **58** (Scheme 1.15) [52].

These species were generated by chloride abstraction from a phosphinegold chloride complex by the use of silver salts [53], or by protonolysis of the related methyl complex [54–56]. They are isolobal to the H^+ ion [57, 58] so they cannot coordinate to both the alkene and the alkyne, ruling out competition of metallacyclic intermediates. DFT calculations with $[\text{Au}(\text{PH}_3)]^+$ showed that a highly polarized (η -alkyne) gold complex was formed displaying a substantial electron deficiency on the alkyne's internal carbon, which echoes back the propositions made by Murai and Fürstner with platinum (vide supra). The latter then evolves to cyclopropylcarbene **I** (Scheme 1.14) with lower activation energy than calculated with platinum for the same step, explaining room temperature procedures with cationic gold. Among all the 1,6-enynes Echavarren and his team have tested, enynes **30** and **60** gave unprecedented six-membered rings compounds **59** and **61** respectively, arising from a *6-endo-dig* skeletal rearrangement (Scheme 1.16).

Scheme 1.17 Cyclopropyl carbene with homoallylic cation-like structure

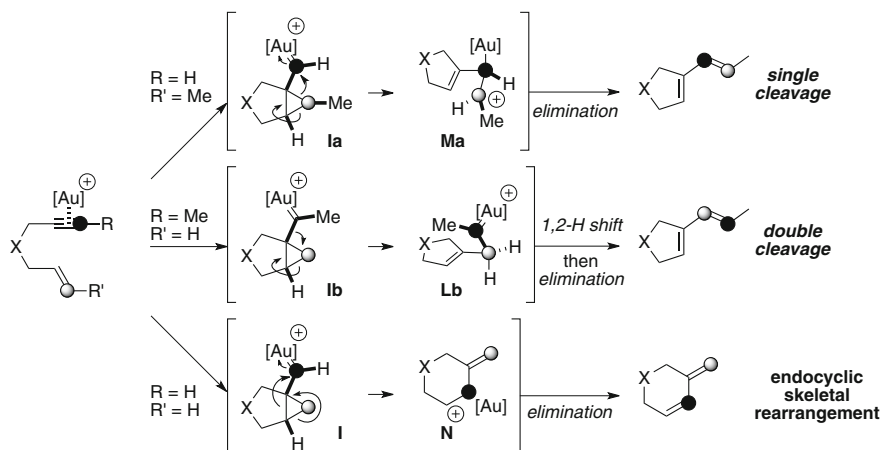


On the basis of DFT calculations and labelling experiments, Echavarren proposed the following mechanisms to account for the formation of *endo*- [59] and *exocyclic* [60] skeletal rearrangement. Complexation of gold(I) leads to cyclopropylcarbene **I** through a 5-*exo-dig* cyclization, by *anti* attack of the double bond, resulting in an *anti* geometry for **I**. The latter displays a very distorted structure in which the C2–C6 bond conjugated with the carbene is particularly long, while C1–C2 has more alkene character, so that **I** can also be seen as a gold(I)-stabilized homoallylic cation **I'** (Scheme 1.17).⁷

Unlike Inoue, who proposed a stepwise evolution from **I** to **M** or **L** through intermediate **K** (Scheme 1.14), DFT calculations showed that cyclopropylcarbene **Ia** evolves directly to intermediate **Ma**. Elimination of gold then furnishes the single cleavage product. For double cleavage products, carbene **Ib** suffers a concerted dyotropic rearrangement [62, 63] to give carbene **Lb**, the latter evolving to double cleavage product through a 1,2-H shift/elimination sequence. It is worth noting that in the gold series, this product is obtained with complete stereoselectivity, which is not the case with cationic platinum as the other isomer is obtained predominantly (Scheme 1.13). The studies on the endocyclic skeletal rearrangement led to the conclusions that it was occurring preferentially with unsubstituted enynes bearing weak electron-withdrawing substituents at the tether. Again, the favored pathway, according to DFT calculations, starts from cyclopropylcarbene **I** on which ring opening gives cation **N**. Gold elimination then furnishes the *endo* product (Scheme 1.18).

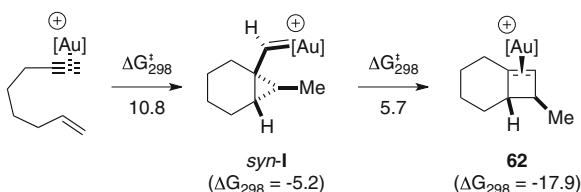
In addition, this DFT study has shown the feasibility of the skeletal rearrangement process without intermediacy of cyclobutenes as Trost initially proposed. Although some of them have been isolated as major products in 1,*n*-enyn cycloisomerizations (*n* = 6–8), [18, 19, 59, 64–68] they are thermally stable, which rule out their involvement in the mechanism leading to skeletal rearrangement products. Further DFT and experimental studies have revealed that in the case of 1,7-enynes, the formation of cyclobutene **62** was favorable and occurred through nucleophilic attack of the double bond in a *syn* fashion giving a cyclopropylcarbene **I** with a *syn* geometry (Scheme 1.19) [59].

⁷ For a study on the influence of alkene substituents on the structure of this intermediate see: [61].



Scheme 1.18 Reviewed mechanistic rationale for Au-catalyzed skeletal rearrangements

Scheme 1.19 Energy profile of the cyclobutene formation: occurrence of a *syn*-cyclopropylcarbene



1.3.3.2 Carbene or Cation?

The nature of intermediate **I** was a matter of debate to determine which representation, a gold carbene or a gold capped carbocation, was the closest to the real bonding situation [69, 70]. We have seen above that intermolecular trapping with a pendant double bond to form cyclopropanes brought evidences of carbene intermediates in the platinum series [34, 35, 71]. Similar experiments were carried out by the team of Echavarren with spectator alkenes in either intra- or intermolecular fashion [72–74]. Stereochemistry of the tetracyclic products obtained by intramolecular trapping confirmed the favored *anti* geometry adopted by carbene **I**. Interestingly, they were also able to trap intermolecularly carbene intermediates of type **L**, thus providing compelling evidence for the existence of such intermediates in the skeletal rearrangement of enynes. The high degree of stereospecificity of the cyclopropanation is in good agreement with carbene chemistry. Gold carbene were also encountered in solution by reaction of a cationic NHC gold(I) complex with ethyl diazoacetate, [75] or in the gas phase by decomposition in a mass spectrometer of a phosphonium ylide gold complex [76, 77]. In both cases, these entities were shown to display classic carbene reactivity, the most representative being cyclopropanation of olefins. However, structural data of

isolated Fischer-type gold carbenes shows particularly long C–Au bonds with very little double bond characters. This is more consistent with the metal-stabilized carbocation representation.⁸ The teams of Fürstner [82] and Toste [83] both studied model systems with gold to get insight in the nature of the proposed intermediates, not only in the enyne cycloisomerization reaction, but also in many other gold or platinum catalyzed reactions that will not be detailed here. Without detailing their results, the conclusions of these studies reject neither one nor the other representation. The carbene or cationic nature of the intermediates is dependent from the chemical environment of the “carbene” carbon, but also from the ligand carried by the metal center (Scheme 1.20). Thus, the carbene and cation representations are nothing but two extremes of the bonding situation.

1.4 Gold- and Platinum-Catalyzed Cycloisomerizations of Enynes Without Skeletal Rearrangement

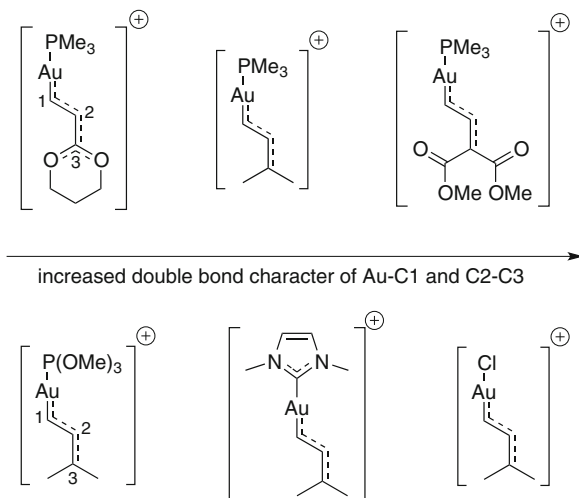
1.4.1 Alder-Ene Reaction

The Alder-Ene reaction of enynes with π -acidic transition metals is a rare event, as skeletal rearrangement is often the observed outcome. However, this pathway was encountered when cycloisomerization reactions were performed in polar solvents with enynes whose alkene moiety is carrying at least two substituents. Thus, it was possible to obtain Alder-Ene products **65** and **66** from enyne **63** with both platinum and gold catalysts (Scheme 1.21). However, deuterium-labelling experiments shown that a different mechanism was at stake for each metal [44, 45, 84]. While platinum-catalyzed Alder-Ene reaction occurs through a platinacycle, the gold-catalyzed process likely involves cationic intermediates.

Recently, the team of Chung has shown that the formal Alder-Ene reaction of 1,6-enynes with gold was a general process for heteroatom-tethered enynes bearing non-terminal alkynes and a prenyl double bond [85]. Attempts to render this reaction enantioselective with chiral gold catalysts resulted in low enantiomeric excesses. Formal Alder-Ene products were also obtained using 1,6-enynes bearing allylsilanes or—stannanes [86]: activation of the alkyne triggers nucleophilic attack of the electron rich olefin concomitant with departure of the Si or Sn atom. The resulting vinylmetal species is subsequently quenched by a proton source present in the reaction mixture. Although efficient, this reaction has for major shortcoming to be not atom-economical.

⁸ Selected examples: [78–81].

Scheme 1.20 Influence of chemical environment and ligands on the carbene character of gold-stabilized cations



1.4.2 Reactions Involving Enols and Enol Ethers

The addition of β -ketoesters to alkynes with cationic gold(I) has been disclosed by Toste and his team [87, 88], and represents the most efficient version of the Conia-Ene reaction.⁹ This transformation can be seen as intramolecular addition of the enol of the ketoester moiety with onto the activated alkyne in **67**, proceeding endo- or exocyclically to give rise to a vinylgold species. Protonolysis of the latter furnishes the five-membered ring derivatives **68** (*endo*) and **69** (*exo*) and regenerates the catalyst (Scheme 1.22).

An analogous reaction was achieved with compounds **69a,b** bearing iodoalkynes and silyl enol ethers in place of ketoesters.¹⁰ Cyclized compound **70a** was employed in the enantioselective synthesis of alkaloid (+)-licopadine [103], while **70b** is a key intermediate en route to (+)-fawcettimine (Scheme 1.23) [104].¹¹

1.4.3 Cyclopropanation Reactions: Endocyclic Au and Pt Carbene Intermediates

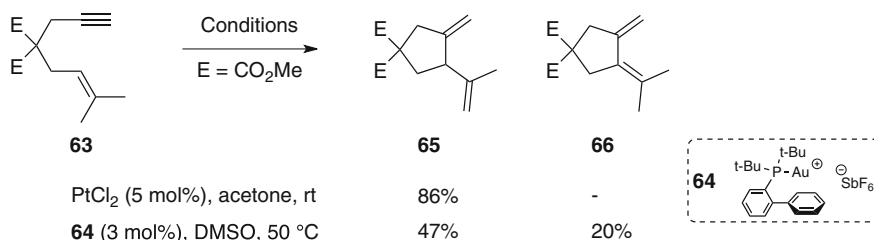
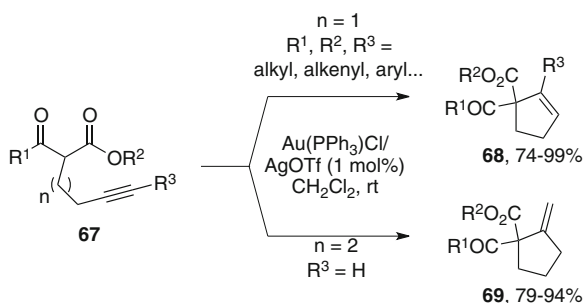
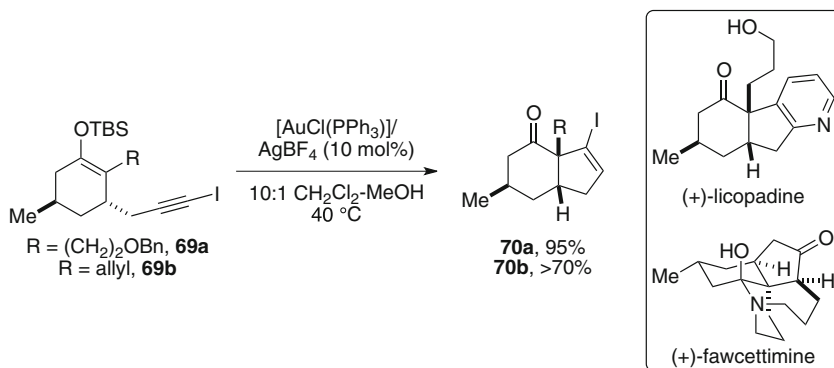
1.4.3.1 1,6-Enynes

In 1994, Blum and co-workers discovered a new and intriguing rearrangement of allyl propargyl ethers **72** into bicyclo[3.1.0]heptene derivatives **73**. The proposed

⁹ Leading references: [89–100].

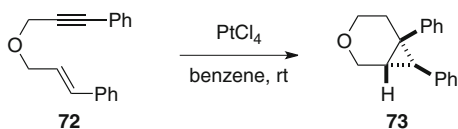
¹⁰ A similar reactivity with related substrates was observed with $W(CO)_5(thf)$, probably through the same type of intermediates: [101, 102].

¹¹ Similar products were obtained with silyl ketene amides and carbamates: [105].

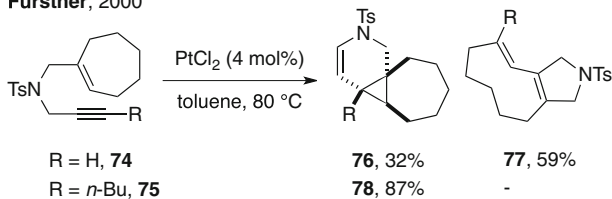
**Scheme 1.21** Alder-Ene reaction of enynes**Scheme 1.22** Au-catalyzed Conia-Ene reaction**Scheme 1.23** Au-catalyzed cyclization of alkynyl silyl enol ethers

mechanism to account for their observation was assumed (erroneously) to rely on a η -allenyl platinum complex formed after tautomerism of the triple bond [106]. Few years later, the group of Echavarren [44, 45] and Fürstner [43, 44] came upon a similar rearrangement with platinum chloride salts, mainly when heteroatoms were introduced as tether (Scheme 1.24). They therefore expanded its scope and drew a new mechanistic rationale in accordance with the deuterium labelling experiments. It was assumed that the key intermediate was the **F** resonance form of the

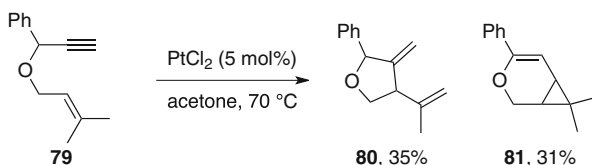
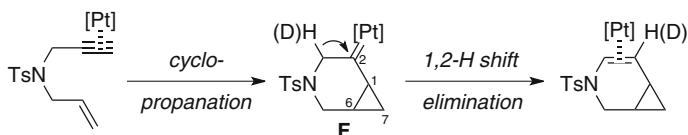
Blum, 1995



Fürstner, 2000



Echavarren, 2000

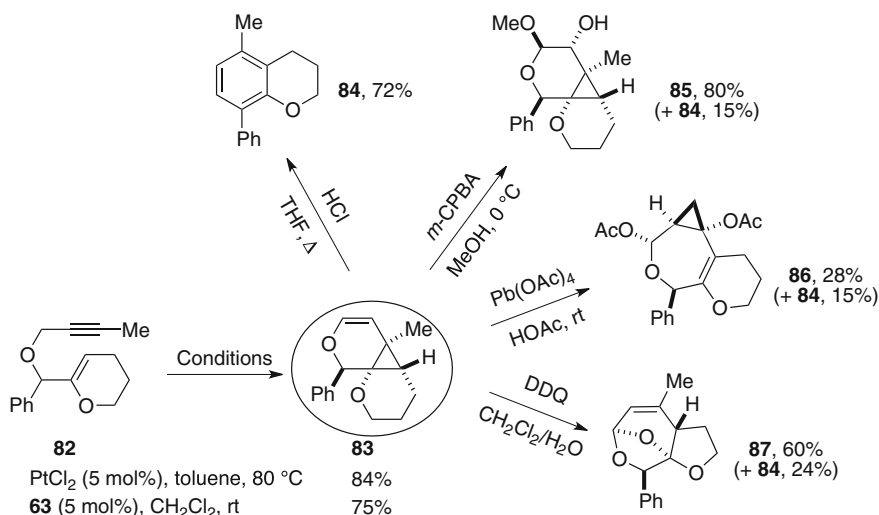
**Scheme 1.24** Formation of bicyclo[3.1.0]heptenes derivatives with Pt**Scheme 1.25** Cyclopropanation mechanism through *endo* platinum carbenes

nonclassical cation (Scheme 1.14), whose carbene character makes it able to undergo a rapid 1,2-H shift [107], presumably assisted by the presence of the heteroatom in the 3 position.

Deuterium labelling experiments or reaction in presence of D_2O [43] supported Fürstner's arguments, and DFT calculations led by Soriano and Marco-Contelles further confirmed this rationale [108]. Like cyclopropylcarbene of type **I**, the structure of carbenes **F** is very distorted, the C1–C2 bond displaying a strong double bond character whereas cyclopropane bonds are very elongated (Scheme 1.25). Aside from platinum,¹² many other metals were able to promote this rearrangement: gold, [52]¹³ rhodium, [49, 50, 115] gallium [116] and iridium [117–119].

¹² Asymmetric versions with Pt: [109–111].

¹³ Reference [112]. Asymmetric versions: [113, 114].



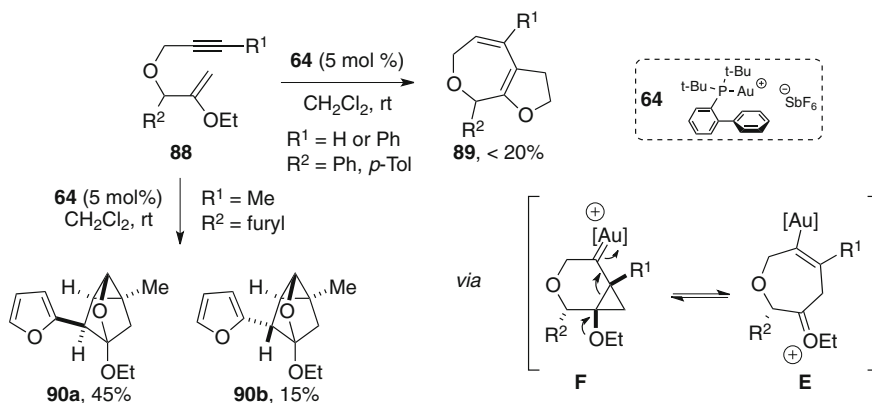
Scheme 1.26 Cyclopropanation of *O*-tethered alkynyl enol ethers

The team of Echavarren has shown that oxygen-tethered alkynyl enol ethers **82** were good candidates toward this kind of reaction [120]. Platinum and gold are both good catalysts for this rearrangement, allowing access to tricycles **83**. The synthetic potential of such structures is well illustrated by the several acidic and oxidative rearrangements these compounds could undergo to give polycyclic molecules **84–87** with relatively good yields, including the formation of seven-membered rings **86** through cyclopropane opening (Scheme 1.26).

In some cases, with gold catalyst **63** and substrates **88**, a different reaction outcome was observed that can only be explained by an endocyclic opening of the cyclopropane in **F** through a synergistic action of the enol ether oxygen and the cationic gold center. Products **89** and **90** were therefore the first examples where carbocation **E** (Scheme 1.14) is the best description of the reactive intermediate, its formation being allowed by the stabilizing effect of the heteroatom and the strong electrophilicity of cationic gold(I) catalyst **63** (Scheme 1.27) [121].

Recently, the team of Chung designed an elegant tandem reaction based on a platinum-catalyzed cyclopropanation of 1,6-enynes [122]. Substituting the external position of either the alkene or the alkyne (or both) allowed them to perform in a one-pot process a thermal Cope rearrangement of divinylcyclopropane moieties after a platinum-promoted cycloisomerization, to get bridged or fused bicyclic structures containing a seven-membered ring. Application of *endo* cyclopropanation was also successfully applied by GSK to the total synthesis of GSK1360707, an antidepressive drug candidate (Scheme 1.28) [123, 124].

This synthetic strategy using as a key step the cycloisomerization of enyne **91** into **92** greatly improved the overall yield of the synthesis compared to the patented precedents. Very recently, the team of Fürstner reported an optimized and



Scheme 1.27 Cyclizations of O-tethered alkynyl enol ethers where **E** is the reactive intermediate

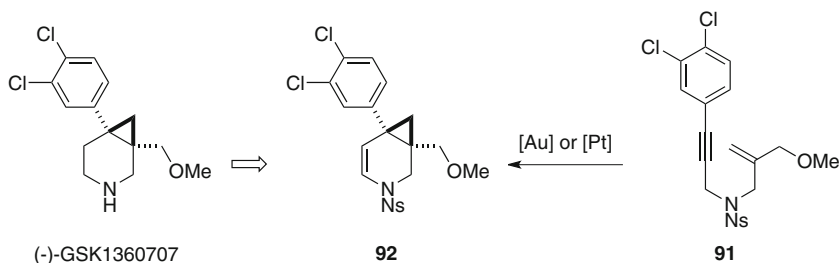
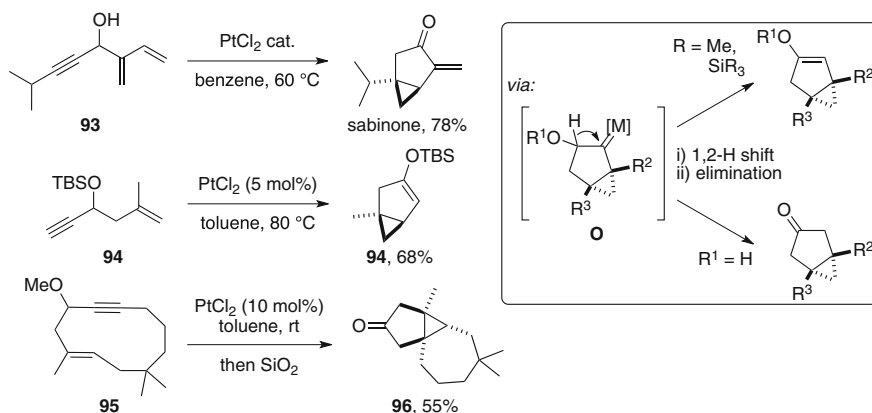
highly enantioselective synthesis of this drug, using chiral cationic gold(I) catalysts with phosphoramidite ligands [125].

1.4.3.2 1,5-Enynes

Unlike 1,6-enynes in which the intermediacy of two different carbenes **I** and **F** is possible in reactions catalyzed by gold or platinum, only *endo* cyclization is possible for 1,5-enynes. Indeed, an *exo* process would result in a highly strained bicyclo[2.1.0]pentanyl carbene intermediate, which is obviously not favorable. In 2004, the groups of Fürstner [126] and Malacria/Fensterbank [127] independently reported the gold and platinum cycloisomerization of 3-hydroxy-1,5-enynes **93** and **94** (Scheme 1.29).¹⁴ They could have obtained bicyclo[3.1.0] frameworks, a structural motif frequently encountered in natural terpenes such as sabinone. The latter team even designed an elegant transannular version with macrocyclic enynes such as **95**, giving easy access to the tricyclo[5.3.0.0.^{1,8}]undecane skeleton (**96**), which can be found in various natural products [129]. Either free alcohols or alkyl- or silyl-protected ones reacted in this fashion, and the reaction was found stereospecific, as (*Z*) and (*E*) isomers of styryl precursors gave distinct diastereoisomers [127].

The team of Toste showed the same year that the presence of a hydroxy group at the propargylic position was not crucial to achieve the same cycloisomerization with cationic gold(I) catalysts. Their study demonstrated that not only excellent chirality transfers were possible starting from enantioenriched enyne **98**, but also that it was possible to switch from 1,2-H shift to 1,2-alkyl shift at the end of the mechanism by introducing quaternary centers at the propargylic position. They

¹⁴ 3-hydroxy-1,5-allenynes reacted similarly with Pt: [128].

**Scheme 1.28** Au- or Pt-based synthetic route to GSK1360707**Scheme 1.29** Cycloisomerizations via *endocyclic* cyclopropylcarbene of 3-hydroxy-1,5-enynes

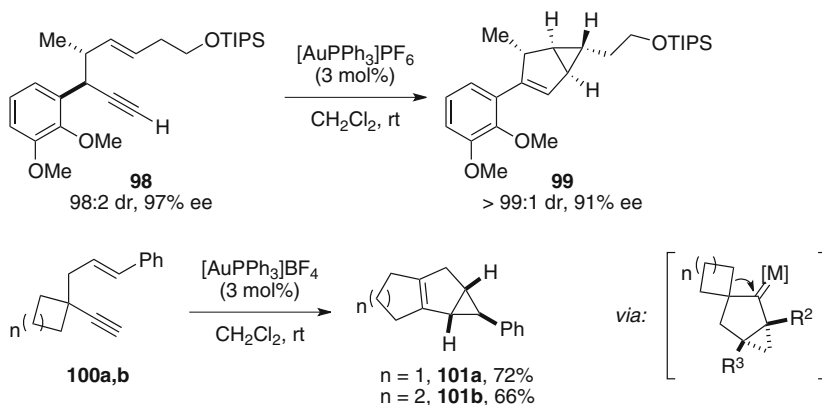
thus were able to isolate tricyclic products **101a,b** resulting from a tandem cycloisomerization-ring enlargement process [130] (Scheme 1.29).¹⁵ Interestingly, when seven-membered rings were placed at the propargylic position instead of four- or five-membered ones in **98** ($n = 4$), the ring enlargement process was not observed but an insertion of the gold carbene into a neighboring $Csp^3\text{-H}$ bond of the propargylic cycloalkane rather took place.¹⁶

A 1,2-alkyl shift was also proposed in the mechanism of the copper-catalyzed cycloisomerization of 1,5-enyne **102** bearing a tertiary alcohol at the propargylic position to account for the formation of bridged tetracyclic ketone **103** (Scheme 1.31) [136].

The reaction described above (Schemes 1.29, 1.30, 1.31) paved the way for a now rich chemistry of 1,5-enynes toward transition metal catalysis. In fact, before Fürstner' and Malacria/Fensterbank' studies, only scattered reports could be found

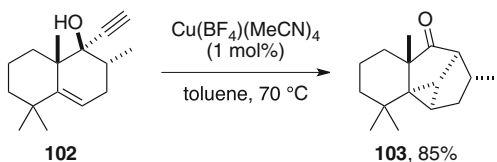
¹⁵ Other ring-enlargement triggered by complexation of gold onto an alkyne: [131–133].

¹⁶ Reference [134]. DFT calculations: [135].



Scheme 1.30 Au-catalyzed cycloisomerizations of non-hydroxylated 1,5-enynes

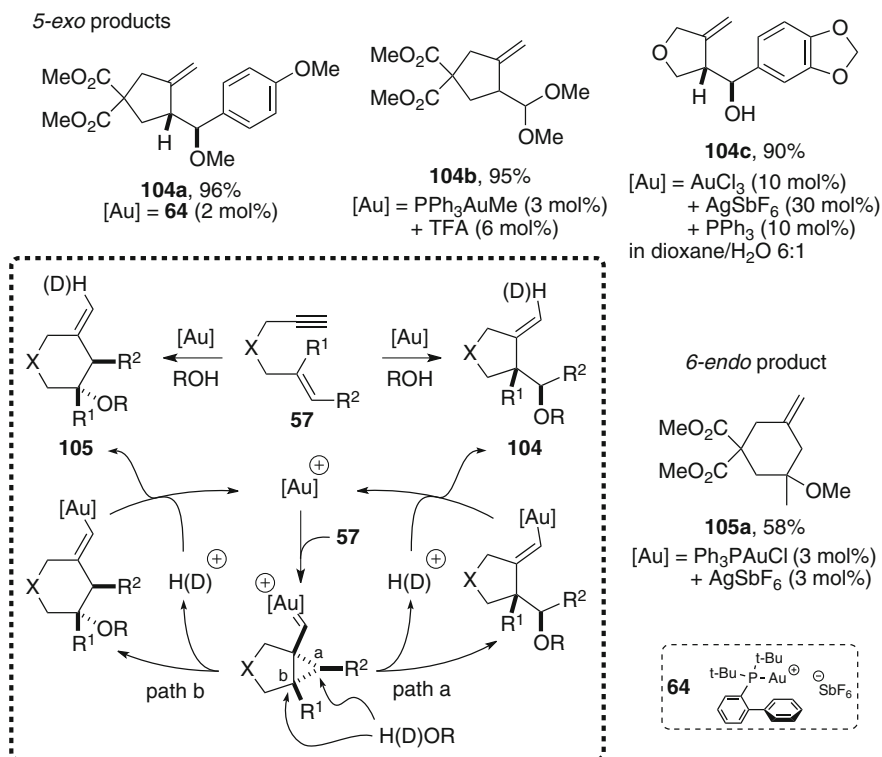
Scheme 1.31 Cycloisomerization of a 3-hydroxy-1,5-enyne ended by a 1,2-alkyl shift



in the literature, [101, 102, 137–139] unlike those related to 1,6-enynes. Since the early 2000s, the number of studies on these substrates has bloomed, mainly with electrophilic metal salts. Different reactivities were disclosed that will not be further detailed in this manuscript and because they are not essential for the understanding of the results presented in this manuscript. At least can be cited skeletal rearrangement [140–142], *endo* cyclizations [143, 144] and pinacol rearrangements [145, 146].

1.5 Trapping of Cationic Intermediates: Au- or Pt-Catalyzed Cyclization Reactions of Enynes in the Presence of Nucleophiles

The following section will briefly present some examples where the highly cationic nature of intermediates in the gold- and platinum-catalyzed cyclization reactions of enynes is well illustrated, through their reaction with various nucleophiles.



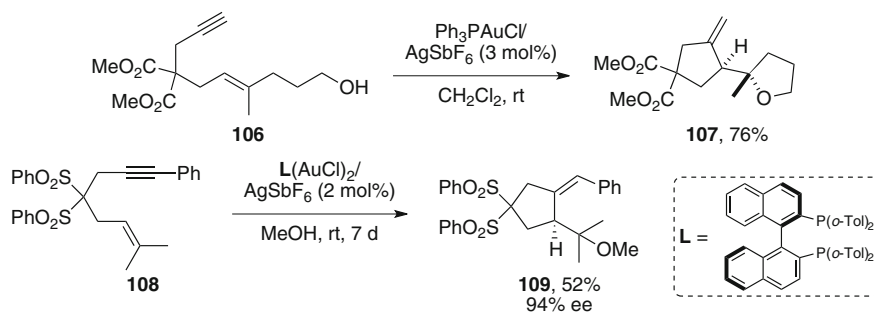
Scheme 1.32 Au-catalyzed alkoxy- and hydroxycyclization of 1,6 enynes

1.5.1 Addition of Oxygen and Nitrogen Nucleophiles

The hydroxycyclization of 1,6-enynes was first disclosed with palladium by the team of Genêt [147–149]. Some years later, Echavarren showed that platinum dichloride in refluxing methanol was a superior catalysts for both alkoxy- and hydroxycyclizations of 1,6-enynes [44, 45]. Although other catalysts were found efficient to achieve this reaction [150–152], the most competitive catalysts are cationic gold(I) complexes giving clean reactions at room temperature [52, 153]. Both products of *exo*- (**104a–c**) and *endo-trig* (**105a**) cyclization can be obtained, the outcome being directed by cation-stabilizing groups on the alkene that will direct the nucleophilic attack on cyclopropylcarbene **I** (path a or b, Scheme 1.32). Water can also act as nucleophile as illustrated by product **104b**. The reaction is stereospecific as (*E*) and (*Z*) isomers of internal double bonds will each give distinct diastereoisomers.

Intramolecular versions were developed [153], and a good enantiomeric excess was reached through the use of chiral bimetallic catalysts (Scheme 1.33).¹⁷ Inter-

¹⁷ References [154–156]. See also with Pt: [157].



Scheme 1.33 Intramolecular and asymmetric versions of alkoxycyclizations of 1,6-enynes

and intramolecular hydro- or alkoxycyclizations were also achieved in the 1,5-enyne series,¹⁸ through a mechanistically similar process. The addition of nitrogen nucleophiles has been less explored but some reports exist with both 1,5- [160] and 1,6-enynes [161], the aminocyclization reaction remaining closely related to the alkoxycyclization reaction. Intramolecular trapping of cationic intermediates was also achieved with carboxylic acids similarly to the gold-catalyzed reaction of **106** [162]. In this remarkable study, the analogy with acid-catalyzed polyene cyclization was drawn, which further revealed the highly cationic nature of reactive intermediates in gold-catalyzed enyne cycloisomerization reactions.

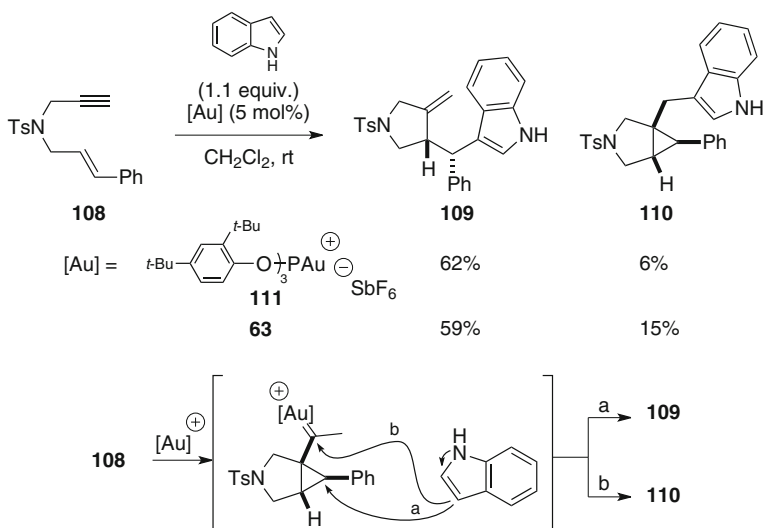
To finish with this section, it is worth saying that inter- and intramolecular addition of carbonyl compounds to enynes was also achieved through Prins-type reactions [163–166]. The mechanism is quite more complex and the outcome is substrate dependant. This methodology, which will not be further detailed in this manuscript, was successfully applied in its intramolecular version to the total synthesis of (+)-orientalol F [167] and (–)-englerin A [168].

1.5.2 Addition of Carbon Nucleophiles

1.5.2.1 Intermolecular Reactions

Nucleophilic attack at cyclopropylcarbene intermediate **I** was also achieved with carbon nucleophiles. The groups of Michelet and Echavarren were the first to report the successful addition of indoles to 1,6-enyne **110** to obtain products **111–112** [169–172]. Interestingly, addition onto carbene carbon was also observed, preferentially when bulky donor ligands were employed (path b, Scheme 1.34). The use of electrophilic catalyst **111** allowed them to promote this reaction with a high regioselectivity along path b (Scheme 1.34).

¹⁸ Intramolecular alkoxycyclizations: [157, 158]. Intermolecular alkoxycyclizations: [159].



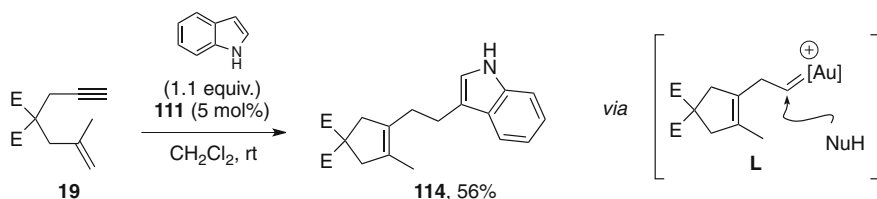
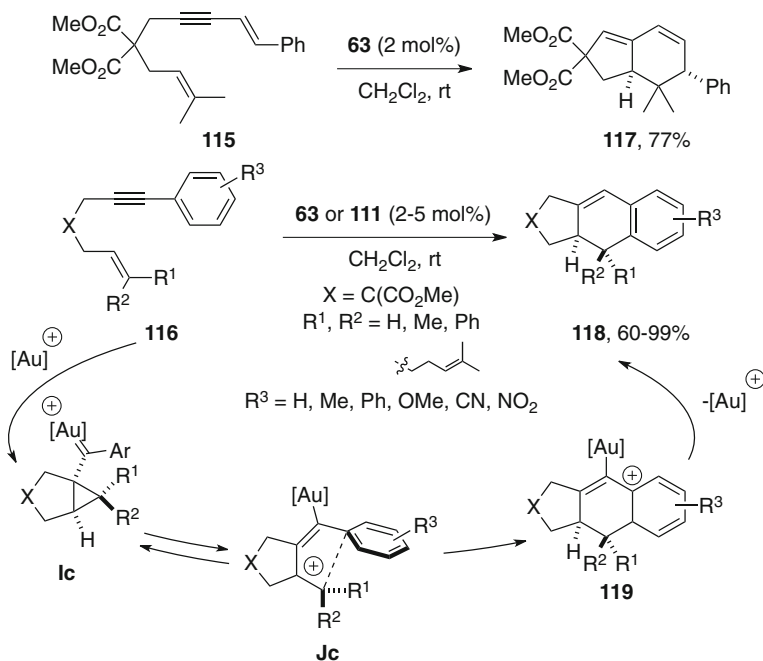
Scheme 1.34 Two different sites of nucleophilic attack in the arylation of 1,6-enynes

This reaction works well with other electron-rich arenes, but also with allyl-silanes and acetoketone derivatives [173]. Sporadically, other intermediates could have been trapped such as **G** or **H**, mainly with enynes bearing non-terminal alkynes (not depicted), and **L** (see Schemes 1.14, 1.19) in the case of enyne **19** (Scheme 1.35).

1.5.2.2 Intramolecular Reactions

Formal [4 + 2] adducts **117–118** were obtained when 1,6-enynes bearing aryl or alkenyl substituents **115–116** were submitted to catalytic amounts of cationic gold(I) salts [67] (Scheme 1.36).

The reaction is general and works well on a broad range of precursors. The mechanism was proposed on the basis of DFT calculations and cyclopropylcarbene **1c** was found to be the key intermediate in this cyclization reaction. Its opening leads to aryl-stabilized π -cation **1j** where the stereochemical information of the double bond is retained. A Friedel-Crafts type reaction then occurs stereospecifically, giving Wheland intermediate **119**. Proton loss followed by protodeauration finally yields the polycyclic compound **118** [174]. This concept was also further applied to a gold-catalyzed enantioselective polycyclisation reaction of polyene-ynes [175].

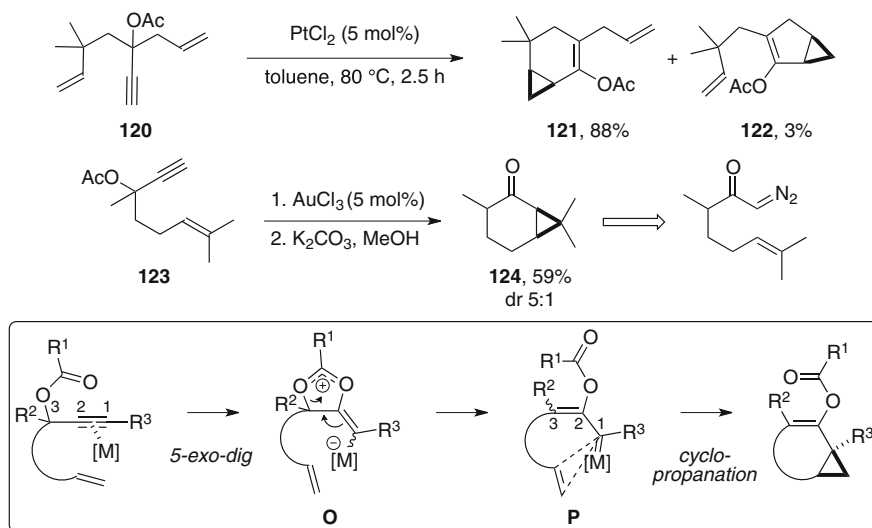
Scheme 1.35 Trapping of intermediate **L** with indoleScheme 1.36 Formal [4 + 2] cycloaddition by trapping of carbocation **Jc**

1.6 Influence of Propargylic Free or Protected Hydroxy Substituents

1.6.1 Propargylic Esters

1.6.1.1 Mechanistic Considerations

The chemistry of 1,*n*-enynes bearing an ester group in the 3 position is very rich and bloomed after the observation by our team [35] that replacing the methyl protecting group on precursor **42** by an acyl could lead to a divergent reaction outcome. We, and a couple of years later, Fürstner [126], initially postulated to



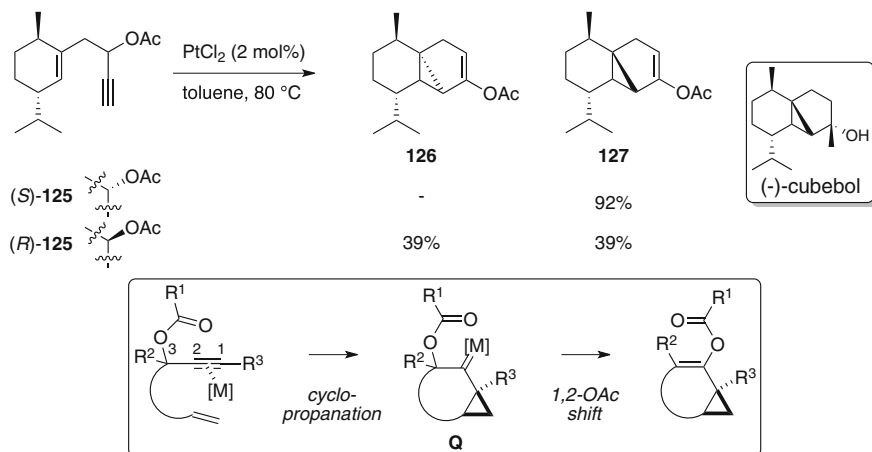
Scheme 1.37 1,2-OAc shift products obtained from enynes bearing propargylic acetates upon Pt catalysis

account for the formation of products **121**, **122** and **124**, that complexation of the alkyne triggers a 5-*exo-dig* cyclization of the ester's carbonyl oxygen to give dioxolium intermediate of type **O**, which subsequently rearranges into carbene **P**. Cyclopropanation of neighboring olefin thus lead to compounds **121**, **122** or **124**. (Scheme 1.37).

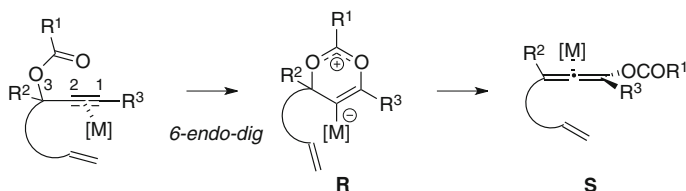
This rearrangement, in fact, knows precedents: Rautenstrauch, in the 80s, also proposed carbene **P** as a putative intermediate in the mechanism of formation of cyclopentenones from 1,4-enynyl acetates [176], and Ohloff, in the 70s, observed cycloprane compounds where the acetate has shifted when submitting 1,6-enynyl acetates to ZnCl_2 [177]. This rearrangement is thus coined as the “Ohloff-Rautenstrauch” rearrangement. One can notice that it represents an easier way to access compounds that are usually obtained by classical carbene methodologies starting from α -diazoketone substrates.

In the course of the total synthesis of (-)-cubebol and related terpenes, the teams of Fürstner [178] and Fehr [179, 180] observed with platinum catalysts that the configuration of the propargylic ester in compound **125** could influence the stereochemical outcome of the reaction. As the occurrence of planar carbene **P** was inconsistent with these results, they both proposed a mechanism where cyclization takes place prior to ester migration through cyclopropylcarbene **Q**, as illustrated in Scheme 1.38.

Calculations led by Soriano and Marco-Contelles came to further confirm this rationale, even if they did not exclude the fact that formation of carbene **P** could compete due to weak differences in the energy barriers [181, 182]. However, in the



Scheme 1.38 Divergent stereochemical outcomes depending on propargylic carbon configuration



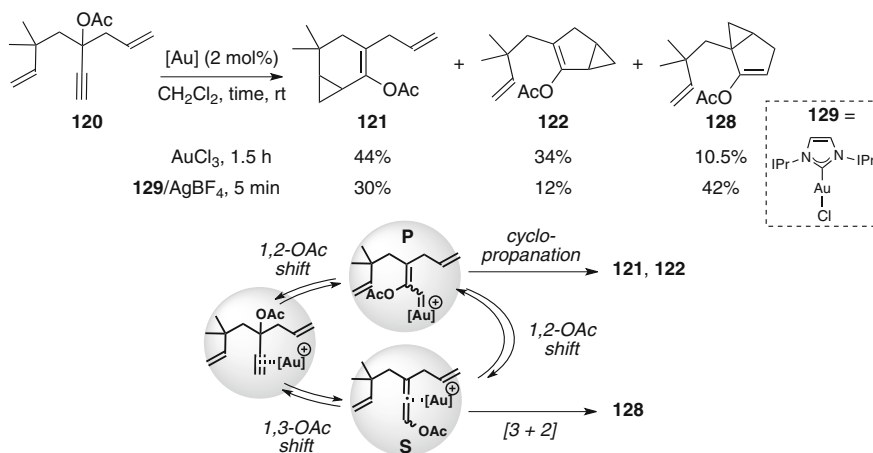
Scheme 1.39 Rearrangement of propargyl acetates into allenyl esters

intermolecular case¹⁹ where entropic factors govern, the rearrangement into free carbene **P** precedes the cyclopropanation step [188]. Other studies with platinum have shown that another pathway could compete leading to allenyl ester **S** [189] through dioxolium **R**. Such species display reactivities that will be detailed in Chap. 3. 6-*Endo-dig* cyclization of the carbonyl oxygen onto the activated alkyne leading to **R** mainly occurs when R^3 = alkyl or aryl substituents, which stabilize positive charges at C1, although other factors can be at stake [190]. On the opposite, esters [191] or halides [192] will strongly disfavor this pathway. It is worth noting that the formation of allenyl esters was already realized in the late 50s upon silver catalysis (Scheme 1.39).²⁰

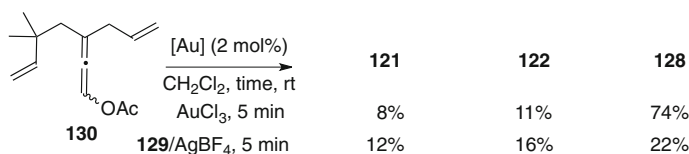
The numerous studies that have been published until nowadays about the use of propargylic esters in enyne systems upon π -acidic transition metal catalysis

¹⁹ With Ru: [183–186]. This study shows that the use of enantioenriched propargylic acetates results in racemic cyclopropane, but good ees were obtained using chiral gold catalysts. See also: [187].

²⁰ References [193–195]. See also: [196–198].



Scheme 1.40 Observation of a new cycloisomerization compound of **120** with gold



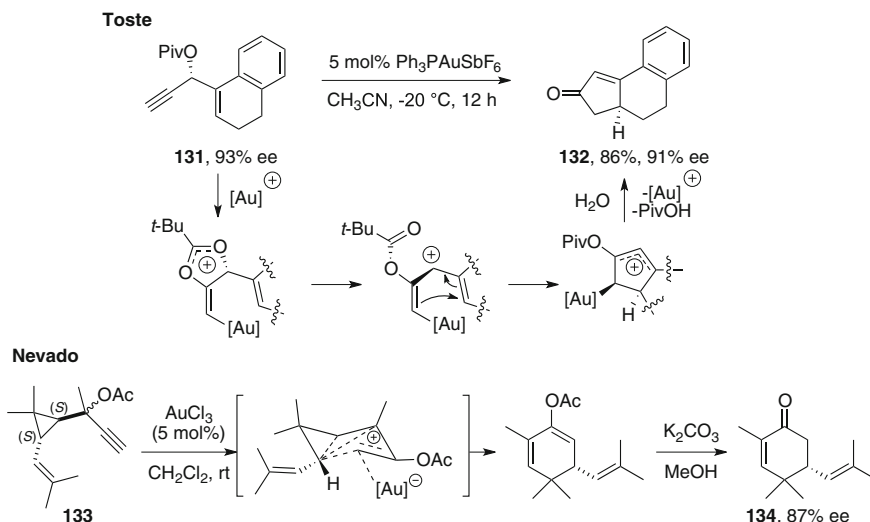
Scheme 1.41 Reaction of allenyl ester **130** with gold catalysts

revealed that several competing pathways can take place. It is reasonable to say that the overcoming of one over the others is highly dependent on the substrate, but catalysts and reaction conditions can play a role as well [199–201].

1.6.1.2 The Gold Catalysis Case

Early experiments by our team has shown that the situation in gold catalysis is more complex. Investigation of the behaviour of dienynne **120** with gold catalyst led to the observation of a third product **128**, which becomes major when cationic gold(I) catalyst **129** was used (Scheme 1.40, top) [202].

Theoretical studies show that a “golden carousel” interconnects the gold-complexed propargylic ester, carbene **P** and allenyl ester **S** through 1,2- or 1,3-OAc shifts in a rapid equilibrium (Scheme 1.40, bottom); [203, 204] it is thus unsurprising to observe compound **128**, which stems from a formal [3 + 2] cycloaddition of an allene-ene intermediate of type **S** [205]. Oxygen labelling



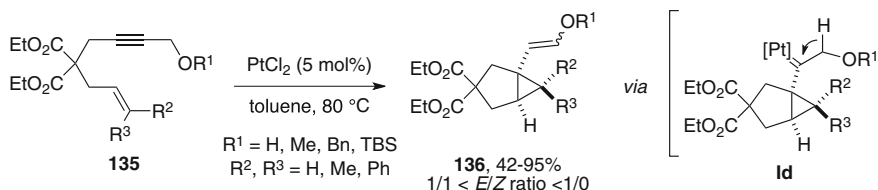
Scheme 1.42 Examples illustrating the cationic rendition of gold-activated propargylic esters

studies have shown a high degree of label scrambling in the resulting enol esters what is consistent with the calculated carousel [204]. The formation of **121** and **122** when the related allenyl ester of **120**, **130**, was submitted to gold catalysts is another proof of the reversibility of the OAc shifts (Scheme 1.41) [204].

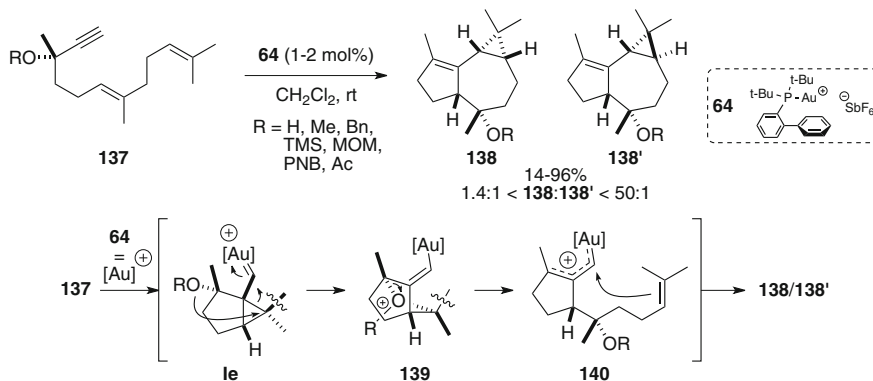
Unlike platinum catalysts, the rearrangement of propargylic acetates was shown to favorably occurs before cyclopropanation what correlates well with poor or no chirality transfers observed with enantioenriched **120**. It is worth adding that calculated structure of gold carbene **P** suggests that it is close to a gold-stabilized allyl cation [203]. This is consistent with the relative easiness of nucleophilic attack at the C1 position of carbene **P**.²¹ The cationic rendition is also well illustrated by studies led by Toste and Nevado where cation-stabilizing substituents were introduced at the propargylic position (Scheme 1.42). They thus were able to perform respectively the Rautenstrauch rearrangement of vinyl propargyl pivaloate **131** into **132**²² and homo-Rautenstrauch rearrangement of quaternary cyclopropyl propargyl acetate **133** into **134**, respectively [214]. Besides, these studies highlight the “nonclassical” character of cationic intermediates involved in these processes, as they kept memory of the chiral information of the starting material, allowing a high degree of chirality transfer.

²¹ Selected examples with Pt: Ref. [168] and also [206, 207]. With Au: [208–211].

²² Reference [212]. For a theoretical study see: [213].



Scheme 1.43 Cycloisomerization of 1,6-enynes bearing external propargylic alcohol or ethers



Scheme 1.44 1,5-migration of propargylic oxygenated groups

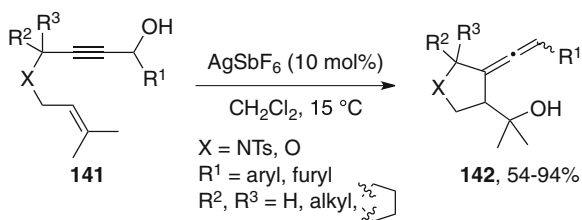
1.6.2 Propargylic Ethers and Alcohols

1.6.2.1 1,2-H Shift on Cyclopropylcarbene I

Keeping in mind that heteroatoms might facilitate a 1,2-H shift onto a neighbouring carbene (see Sect. 3.3), the team of Michelet, Chen and Zhang explored the reactivity of 1,6-enynes bearing an external propargylic alcohol or ether assuming that such substrate should undergo a rapid 1,2-H shift onto carbene **I** to give bicyclo[3.1.0]hexane derivatives [215]. They successfully implemented their concept and obtained bicyclic molecules **136** displaying a cyclopropylenol ether (or a β -cyclopropylaldehyde in the case of free alcohols). For this purpose, they submitted malonate-tethered 1,6-enynes **136** to catalytic amounts of platinum dichloride (Scheme 1.43). However, heteroatom-tethered enynes did not react along this new cycloisomerization pattern, and classic bicyclo[4.1.0]heptene skeletons arising from a favored endocyclic carbene of type **F** were obtained (not depicted).

It is worth adding that similar substrates where R^1 is an acetyl substituent were also explored toward cationic gold(I) catalysis, leading to comparable products.

Scheme 1.45 Allene synthesis through Ag-catalyzed enyne cyclization reactions



Cyclopropylcarbene **Id** was also invoked in the catalytic cycle, but in this case a 1,2-OAc shift onto the carbene is preferred over a 1,2-H shift [216].

1.6.2.2 1,5-Migration of Ethers and Hydroxy Group

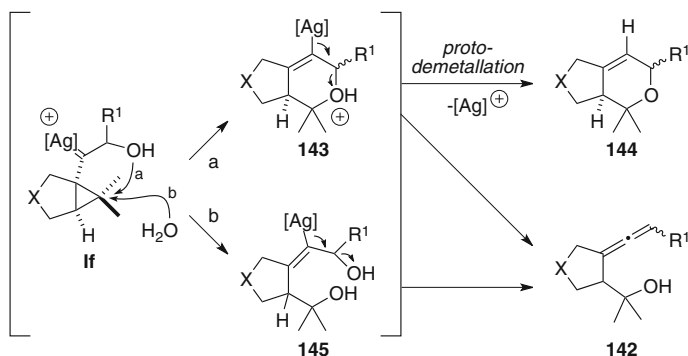
Coordination of gold on a triple bond was also shown to promote the migration of adjacent hydroxy and ether groups. Hydroxy-, silyloxy- or alkoxyated enynes **137** with a (*E*) double bond geometry submitted to catalytic amounts of **64** were rearranged stereoselectively and stereospecifically into tricyclic scaffolds **138** where a 1,5-migration of the oxygenated group has operated [217]. (*Z*) precursors gave products with inverted configuration at the carbon carrying the oxygen. In both cases, minor products **138'** arising from *endo* cyclopropanation were also obtained. The mechanism is supposed to occur through cyclopropyl gold carbene **Ie**. Thanks to its cationic nature, the OR group could then migrate at the cyclopropyl head carbon to give oxonium intermediate **139**, which subsequently opens to give allylgold cation **140** (Scheme 1.44). Deuterium labelling experiments have shown that this process was intramolecular. A final cyclopropanation allows the formation of the bicyclo[5.1.0]octane skeleton.

Another 1,5-migration was also observed by Liang and co-workers in the cycloisomerization of 1,6-enynes **141** bearing a hydroxy group at the external propargylic position [218]. The reaction was carried out in the presence of silver(I) salts which are not commonly used in metal catalyzed cycloisomerization reaction of enynes.²³ As the reaction products can roughly be seen as 1,5-migration products, we chose to present this reaction in this section. It is besides important for the experimental results described below. Reaction products are exocyclic allenes **142**, a rarely encountered cyclization pattern of 1,6-enynes (Scheme 1.45).²⁴

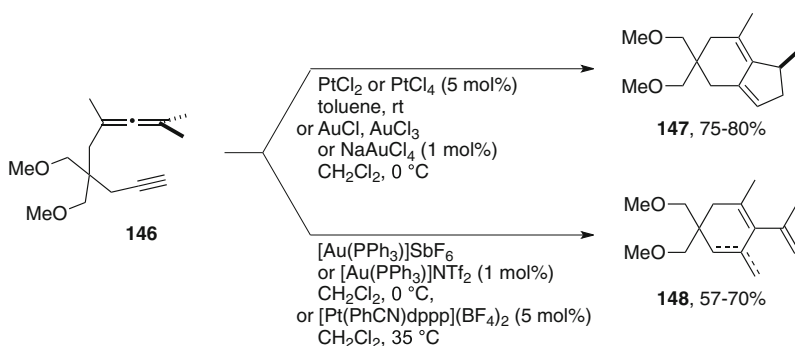
Regarding to the mechanism, no literature report invokes cyclopropylcarbenes as reactive intermediates in silver catalyzed processes. However, the reaction outcome can be explained by the involvement of such species. From **If**, intramolecular cyclopropane opening could lead to **143**, which can then undergo either demetallation/fragmentation giving **142**, or a simple protodemetallation to give

²³ Some examples are described in the following review: [219].

²⁴ Comparable products were also obtained from the cyclization of 1,6-enynes with stoichiometric amounts of TiCl₄: [220].



Scheme 1.46 Mechanistic hypothesis accounting for the formation of 138



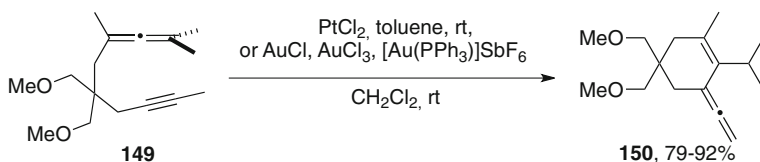
Scheme 1.47 Different reaction outcomes depending on the catalysts in the cycloisomerization of 1,6-allenynes **146**

144. The non-observation of the latter decribilizes such mechanism. Otherwise, intermolecular trapping of **If** by a water molecule could lead to **145**, and subsequent demetallation/dehydration furnish *exocyclic allene* **142** (Scheme 1.46).

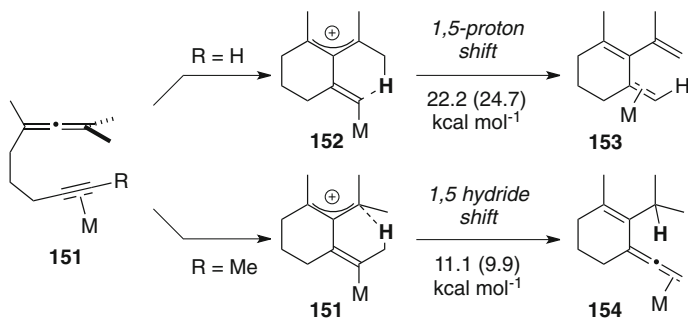
As the reaction needs traces of water to be performed, the authors rather inclined toward the last hypothesis than for an intramolecular shift of the hydroxy group. Nonetheless, no labelling experiments were carried out to confirm this assumption.

1.7 Allenynes: A Particular Case of Enynes

Following the seminal works of Trost on enynes, allenynes rapidly emerged as powerful substrates for the discovery of new cycloisomerization reactions [221]. The exploration of such substrates toward π -acidic transition metals began in our



Scheme 1.48 Formation of vinyl allenes in the case of acetylenic methyl precursors

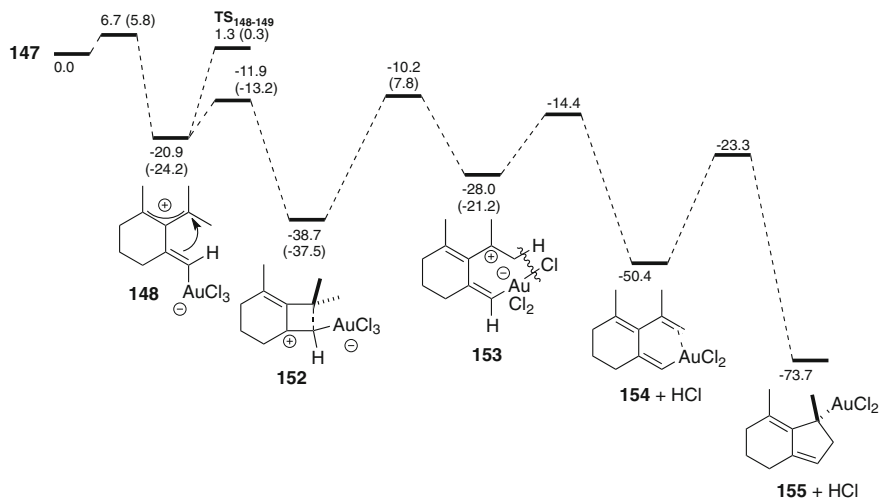


Scheme 1.49 Mechanistic proposal for the formation of Alder-ene and vinylallene products: ΔG_{298}° were calculated for $M = \text{AuCl}_3$ (and AuPH_3^+)

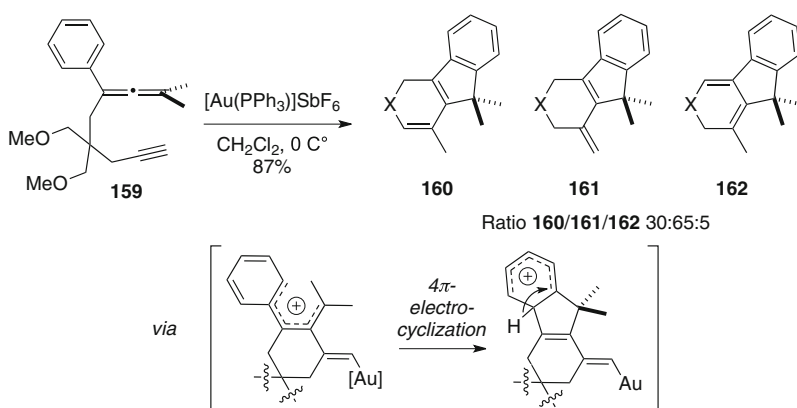
laboratory, first with platinum catalysis [222] and then with gold [223]. Will follow a plethora of reports in this field, which reflect, like enynes, a high substrate and catalyst dependancy [221]. An exhaustive description of these works is out of the scope of this chapter. However, a focus on our work seems pertinent to briefly illustrate the power of such substrates and point out the common points and differences with enynes in the mechanistic rationales. It is moreover valuable in view of the results presented in Chaps. 3 and 4. The reactivity of 1,6-allenyne substrate **146** has been investigated with various platinum and gold catalysts, and the results are summarized in Scheme 1.47. In our first study, we hypothesized the occurrence of platinacyclopentene in the mechanistic pathway, which was further supported by DFT calculations [224]. However, such mechanistic rational is inconsistent in the case of gold(I), gold(III) and platinum(IV), these catalysts being particularly reticent to give rise to metalacyclic intermediates.

While studying gold catalyst, our team noticed that the presence of chloride ligand on the platinum and gold complexes had a dramatic impact on the reactivity: chloride-containing catalysts allowed the formation of hydrindiene product **147**, while cationic, phosphine-ligated catalysts resulted in the selective formation of an isomeric mixture of formal Alder-ene regioisomers **148**.²⁵ Switching to methyl-substituted alkyne substrate **149** allowed the discovery of a third cycloisomerization pathway affording vinylallene **150** which is effective either with gold or platinum chloride salts or cationic halide-free complexes (Scheme 1.48).

²⁵ Ligand effects in gold catalysis have been recently reviewed, see: [225].



Scheme 1.50 Energy profile [kcal mol⁻¹] for the transformation of **147** into hydriindene **155** calculated for M = AuCl₃ (and AuPH₃⁺)



Scheme 1.51 Tandem cyclization/Friedel-Crafts reaction of phenyl-substituted 1,6-allenynes

The proposed mechanisms, supported by a computational study, starts for each product by a 6-*exo*-dig cyclization triggered by gold complexation onto the alkyne,²⁶ giving birth to a stabilized allylic carbocationic intermediate **151/153**, respectively. Then, depending on the substrate and the catalyst, diverging

²⁶ Gold's "alkynophilicity" results in a preferred reaction of activated alkynes rather than activated allenes. However, some reports dealing with allenynes are consistent with initial activation of the allene, see: [226–228]. See also ref. [128].

pathways were unveiled with DFT calculations. The Alder-Ene products were computationally reachable if $R = H$ and their formation would proceed through a direct 1,5-proton shift. Vinylallene **154** is also obtained in a single step by a 1,5-hydride shift (Scheme 1.49).

As only chloride-containing catalysts could promote the formation of hydrindiene products, a mechanistic rationale was proposed involving isomerization of the vinyl metal species **148** followed by elimination of HCl (Scheme 1.48). The next step is a 5-*endo* carboauration which after protolysis with HCl delivers the final product and restores the catalytic species (Scheme 1.50).

This cationic manifold echoes back the mechanisms of cycloisomerization of enynes with gold and particularly in this case a direct parallel can be drawn with the gold-catalyzed Alder-ene of enynes (compare products **65**, Scheme 1.20 and **148**, Scheme 1.47) [84, 85]. Although no intermediates similar to cyclopropylcarbenes were invoked in this case, intermediates similar to **D**, **E**, **F**, **G** resulting from *endo* cyclization (Schemes 1.14, 1.25) were proposed in the cycloisomerization of heteroatom tethered 1,6-allenynes upon platinum catalysis [229].

Trapping of cationic intermediates was achieved with deuterated methanol and evidenced by intramolecular Friedel-Crafts reaction (Scheme 1.51), in a closely similar manner than Echavarren did in the 1,6-enynes series (see Sect. 4.2.2, Refs. [67, 174]).

1.8 Conclusion

Activation of enynes by electrophilic metal salts has raised considerable interest from the community of synthetic chemists. The high reactivity of such compounds coupled to the easiness of their “decoration” with a variety of functional groups has allowed the discovery of a lot of cyclization reactions leading to complex cyclic and polycyclic frameworks, which have sometimes been applied in the total synthesis of natural products [37, 103, 104, 167, 168, 178–180, 230]. All these compounds often arise from common intermediates, which can be seen as a cyclopropylcarbenes **I** or **F**, originating from a 5-*exo*-dig or a 6-*endo*-dig cyclization of the activated enyne, respectively. Both nonetheless display a highly cationic character, and this duality is well illustrated by the reactions presented above.

References

1. Trost BM, Lautens M (1985) J Am Chem Soc 107:1781
2. Hoffmann HM (1969) Angew Chem Int Ed 8:556
3. Oppolzer W, Snieckus V (1978) Angew Chem Int Ed 17:476
4. Trost BM (1990) Acc Chem Res 23:34
5. Aubert C, Buisine O, Malacria M (2002) Chem Rev 102:813
6. Michelet V, Toullec PY, Genet JP (2008) Angew Chem Int Ed 47:4268

7. Trost BM, Lautens M, Chan C, Jebaratnam DJ, Mueller T (1991) *J Am Chem Soc* 113:636
8. Llerena D, Aubert C, Malacria M (1996) *Tetrahedron Lett* 37:7353
9. Cao P, Wang B, Zhang XJ (2000) *J Am Chem Soc* 122:6490
10. Sturla SJ, Kablaoui NM, Buchwald SP (1999) *J Am Chem Soc* 121:1976
11. Trost BM, Romero DL, Rise F (1994) *J Am Chem Soc* 116:4268
12. Trost BM, Tour JM (1987) *J Am Chem Soc* 109:5268
13. Nishida M, Adachi N, Onozuka K, Matsumura H, Mori M (1998) *J Org Chem* 63:9158
14. Tong XF, Li D, Zhang ZG, Zhang XM (2004) *J Am Chem Soc* 126:7601
15. Kim H, Lee CB (2005) *J Am Chem Soc* 127:10180
16. Trost BM, Tanoury GJ (1987) *J Am Chem Soc* 109:4753
17. Katz TJ, Sivavec TM (1985) *J Am Chem Soc* 107:737
18. Trost BM, Trost MK (1991) *Tetrahedron Lett* 32:3647
19. Trost BM, Yanai M, Hoogsteen K (1993) *J Am Chem Soc* 115:5294
20. Trost BM, Tanoury GJ (1988) *J Am Chem Soc* 110:1636
21. Trost BM, Hashmi ASK (1993) *Angew Chem Int Ed* 32:1085
22. Trost BM, Hashmi ASK (1994) *J Am Chem Soc* 116:2183
23. Trost BM, Hashmi ASK, Ball RG (2001) *Adv Synth Catal* 343:490
24. Mori M, Watanuki S (1992) *Chem Commun* 1082
25. Kinoshita A, Mori M (1994) *Synlett* 1020
26. Kim SH, Bowden N, Grubbs RH (1994) *J Am Chem Soc* 116:10801
27. Watanuki S, Mori M (1995a) *Organometallics* 14:5054
28. Watanuki S, Ochifuji N, Mori M (1995b) *Organometallics* 14:5062
29. Mori M, Kitamura T, Sato Y (2001) *Synthesis* 654
30. Kitamura T, Sato Y, Mori M (2002) *Adv Synth Catal* 344:678
31. Chatani N, Morimoto T, Muto T, Murai S (1994) *J Am Chem Soc* 116:6049
32. Chatani N, Furukawa N, Sakurai H, Murai S (1996) *Organometallics* 15:901
33. Pilette D, Moreau S, Lebozec H, Dixneuf PH, Corrigan JF, Carty AJ (1994) *Chem Commun* 409
34. Chatani N, Kataoka K, Murai S, Furukawa N, Seki Y (1998) *J Am Chem Soc* 120:9104
35. Mainetti E, Mouries V, Fensterbank L, Malacria M, Marco-Contelles J (2002) *Angew Chem Int Ed* 41:2132
36. Chatani N, Inoue H, Morimoto T, Muto T, Murai S (2001) *J Org Chem* 66:4433
37. Fürstner A, Szillat H, Gabor B, Mynott R (1998) *J Am Chem Soc* 120:8305
38. Winstein S, Trifan DS (1949) *J Am Chem Soc* 71:2953
39. Roberts JD, Mazur RH (1951) *J Am Chem Soc* 73:3542
40. Roberts JD, Lee CC (1951) *J Am Chem Soc* 73:5009
41. Chisholm MH, Clark HC (1973) *Acc Chem Res* 6:202
42. Fürstner A, Szillat H, Stelzer F (2000) *J Am Chem Soc* 122:6785
43. Fürstner A, Stelzer F, Szillat H (2001) *J Am Chem Soc* 123:11863
44. Mendez M, Muñoz MP, Echavarren AM (2000) *J Am Chem Soc* 122:11549
45. Mendez M, Muñoz MP, Nevado C, Cárdenas DJ, Echavarren AM (2001) *J Am Chem Soc* 123:10511
46. Oi S, Tsukamoto I, Miyano S, Inoue Y (2001) *Organometallics* 20:3704
47. Chatani N, Inoue H, Kotsuna T, Murai S (2002) *J Am Chem Soc* 124:10294
48. Miyano Y, Chatani N (2006) *Org Lett* 8:2155
49. Ota K, Chatani N (2008) *Chem Commun* 2906
50. Ota K, Lee SI, Tang JM, Takachi M, Nakai H, Morimoto T, Sakurai H, Kataoka K, Chatani N (2009) *J Am Chem Soc* 131:15203
51. Martin-Matute B, Nevado C, Cárdenas DJ, Echavarren AM (2003) *J Am Chem Soc* 125:5757
52. Nieto-Oberhuber C, Muñoz MP, Buñuel E, Nevado C, Cárdenas DJ, Echavarren AM (2004) *Angew Chem Int Ed* 43:2402
53. Preisenberger M, Schier A, Schmidbaur H (1999) *Dalton Trans* 1645
54. Teles JH, Brode S, Chabanas M (1998) *Angew Chem Int Ed* 37:1415

55. Mizushima E, Sato K, Hayashi T, Tanaka M (2002) *Angew Chem Int Ed* 41:4563
56. Mizushima E, Hayashi T, Tanaka M (2003) *Org Lett* 5:3349
57. Hoffmann R (1982) *Angew Chem Int Ed* 21:711
58. Hall KP, Mingos DMP (1984) *Prog Inorg Chem* 32:237
59. Nieto-Oberhuber C, López S, Muñoz MP, Cárdenas DJ, Buñuel E, Nevado C, Echavarren AM (2005) *Angew Chem Int Ed* 44:6146
60. Cabello N, Jiménez-Núñez E, Buñuel E, Cárdenas DJ, Echavarren AM (2007) *Eur J Org Chem* 4217
61. Jiménez-Núñez E, Claverie CK, Bour C, Cárdenas DJ, Echavarren AM (2008) *Angew Chem Int Ed* 47:7892
62. Reetz MT (1972a) *Angew Chem Int Ed* 11:130
63. Reetz MT (1972b) *Angew Chem Int Ed* 11:129
64. Marion F, Coulomb J, Courillon C, Fensterbank L, Malacria M (2004) *Org Lett* 6:1509
65. Furstner A, Davies PW, Gress T (2005) *J Am Chem Soc* 127:8244
66. Odabachian Y, Gagosz F (2009) *Adv Synth Catal* 351:379
67. Nieto-Oberhuber C, López S, Echavarren AM (2005) *J Am Chem Soc* 127:6178
68. Lee YT, Kang YK, Chung YK (2009) *J Org Chem* 74:7922
69. Hashmi ASK (2008) *Angew Chem Int Ed* 47:6754
70. Echavarren AM (2009) *Nat Chem* 1:431
71. Bruneau C (2005) *Angew Chem Int Ed* 44:2328
72. López S, Herrero-Gómez E, Perez-Galan P, Nieto-Oberhuber C, Echavarren AM (2006) *Angew Chem Int Ed* 45:6029
73. Nieto-Oberhuber C, López S, Muñoz MP, Jiménez-Núñez E, Buñuel E, Cárdenas DJ, Echavarren AM (2006) *Chem Eur J* 12:1694
74. Kim SM, Park JH, Choi SY, Chung YK (2007) *Angew Chem Int Ed* 46:6172
75. Fructos MR, Belderrain TR, de Frémont P, Scott NM, Nolan SP, Diaz-Requejo MM, Pérez PJ (2005) *Angew Chem Int Ed* 44:5284
76. Fedorov A, Moret M-E, Chen P (2008) *J Am Chem Soc* 130:8880
77. Fedorov A, Chen P (2009) *Organometallics* 28:1278
78. Aumann R, Fischer EO (1981) *Chem Ber* 114:1853
79. Fischer EO, Bäck M, Aumann R (1983) *Chem Ber* 116:3618
80. Fischer EO, Bäck M (1985) *J Organomet Chem* 287:279
81. Raubenheimer HG, Esterhuysen MW, Timoshkin A, Chen Y, Frenking G (2002) *Organometallics* 21:3173
82. Seidel G, Mynott R, Fürstner A (2009) *Angew Chem Int Ed* 48:2510
83. Benitez D, Shapiro ND, Tkatchouk E, Wang Y, Goddard WA, Toste FD (2009) *Nat Chem* 1:482
84. Nieto-Oberhuber C, Muñoz MP, López S, Jiménez-Núñez E, Nevado C, Herrero-Gómez E, Raducan M, Echavarren AM (2006) *Chem Eur J* 12:1677
85. Lee SI, Kim SM, Kim SY, Chung YK (2006) *Synlett* 2256
86. Fernandez-Rivas C, Mendez M, Echavarren AM (2000) *J Am Chem Soc* 122:1221
87. Kennedy-Smith JJ, Staben ST, Toste FD (2004) *J Am Chem Soc* 126:4526
88. Staben ST, Kennedy-Smith JJ, Toste FD (2004) *Angew Chem Int Ed* 43:5350
89. Conia JM, Leperchec P (1975) *Synthesis* 1
90. Boaventura MA, Drouin J, Conia JM (1983) *Synthesis* 801
91. Balme G, Bouyssi D, Faure R, Gore J, Vanhemelryck B (1992) *Tetrahedron* 48:3891
92. Stammmler R, Malacria M (1994) *Synlett* 92
93. Cruciani P, Aubert C, Malacria M (1994) *Tetrahedron Lett* 35:6677
94. Cruciani P, Stammmler R, Aubert C, Malacria M (1996) *J Org Chem* 61:2699
95. McDonald FE, Olson TC (1997) *Tetrahedron Lett* 38:7691
96. Renaud J-L, Petit M, Aubert C, Malacria M (1997) *Synlett* 931
97. Kitagawa O, Suzuki T, Inoue T, Watanabe Y, Taguchi T (1998) *J Org Chem* 63:9470
98. Bouyssi D, Monteiro N, Balme G (1999) *Tetrahedron Lett* 40:1297
99. Renaud JL, Aubert C, Malacria M (1999) *Tetrahedron* 55:5113

100. Kuminobu Y, Kawata A, Takai K (2005) *Org Lett* 7:4823
101. Maeyama K, Iwasawa N (1998) *J Am Chem Soc* 120:1928
102. Iwasawa N, Miura T, Kiyota K, Kusama H, Lee K, Lee PH (2002) *Org Lett* 4:4463
103. Staben ST, Kennedy-Smith JJ, Huang D, Corkey BK, LaLonde RL, Toste FD (2006) *Angew Chem Int Ed* 45:5991
104. Linghu X, Kennedy-Smith JJ, Toste FD (2007) *Angew Chem Int Ed* 46:7671
105. Minnihan EC, Colletti SL, Toste FD, Shen HC (2007) *J Org Chem* 72:6287
106. Blum J, Beerkraft H, Badrieh Y (1995) *J Org Chem* 60:5567
107. Kirmse W (1971) *Carbene Chemistry*, 2nd edn. Academic Press, New York
108. Soriano E, Ballesteros P, Marco-Contelles J (2004) *J Org Chem* 69:8018
109. Brissy D, Skander M, Jullien H, Retailleau P, Marinetti A (2009a) *Org Lett* 11:2137
110. Brissy D, Skander M, Retailleau P, Frison G, Marinetti A (2009b) *Organometallics* 28:140
111. Jullien H, Brissy D, Sylvain R, Retailleau P, Naubron JV, Gladiali S, Marinetti A (2011) *Adv Synth Catal* 353:1109
112. Lee SI, Kim SM, Choi MR, Kim SY, Chung YK, Han WS, Kang SO (2006) *J Org Chem* 71:9366
113. Chao CM, Beltrami D, Toullec PY, Michelet V (2009) *Chem Commun* 6988
114. Pradal A, Chao CM, Toullec PY, Michelet VB (2011) *J Org Chem* 7:1021
115. Kim SY, Chung YK (2010) *J Org Chem* 75:1281
116. Kim SM, Lee SI, Chung YK (2006) *Org Lett* 8:5425
117. Shibata T, Kobayashi Y, Maekawa S, Toshida N, Takagi K (2005) *Tetrahedron* 61:9018
118. Benedetti E, Simonneau A, Hours A, Amouri H, Penoni A, Palmisano G, Malacria M, Goddard JP, Fensterbank L (2011) *Adv Synth Catal* 353:1908
119. Barbazanges M, Augé M, Moussa J, Hamouri H, Desmarests C, Fensterbank L, Gandon V, Malacria M, Ollivier C (2011) *Chem Eur J* 17:13789
120. Nevado C, Ferrer C, Echavarren AM (2004) *Org Lett* 6:3191
121. Ferrer C, Raducan M, Nevado C, Claverie CK, Echavarren AM (2007) *Tetrahedron* 63:6306
122. Kim SY, Park Y, Chung YK (2010) *Angew Chem Int Ed* 49:415
123. Deschamps NM, Elitzin VI, Liu B, Mitchell MB, Sharp MJ, Tabet EA (2011) *J Org Chem* 76:712
124. Elitzin VI, Liu B, Sharp MJ, Tabet EA (2011) *Tetrahedron Lett* 52:3518
125. Teller H, Fürstner A (2011) *Chem Eur J* 17:7764
126. Mamane V, Gress T, Krause H, Fürstner A (2004) *J Am Chem Soc* 126:8654
127. Harrak Y, Blaszykowski C, Bernard M, Cariou K, Mainetti E, Mouries V, Dhimane AL, Fensterbank L, Malacria M (2004) *J Am Chem Soc* 126:8656
128. Zriba R, Gandon V, Aubert C, Fensterbank L, Malacria M (2008) *Chem Eur J* 14:1482
129. Blaszykowski C, Harrak Y, Goncalves MH, Cloarec JM, Dhimane AL, Fensterbank L, Malacria M (2004) *Org Lett* 6:3771
130. Markham JP, Staben ST, Toste FD (2005) *J Am Chem Soc* 127:9708
131. Sethofer SG, Staben ST, Hung OY, Toste FD (2008) *Org Lett* 10:4315
132. Kleinbeck F, Toste FD (2009) *J Am Chem Soc* 131:9178
133. Luzung MR, Markham JP, Toste FD (2004) *J Am Chem Soc* 126:10858
134. Horino Y, Yamamoto T, Ueda K, Kuroda S, Toste FD (2009) *J Am Chem Soc* 131:2809
135. Liu YX, Zhang DJ, Zhou JH, Liu CB (2010) *J Phys Chem A* 114:6164
136. Fehr C, Farris I, Sommer H (2006) *Org Lett* 8:1839
137. Imamura K, Yoshikawa E, Gevorgyan V, Yamamoto Y (1998) *J Am Chem Soc* 120:5339
138. Imamura K, Yoshikawa E, Gevorgyan V, Yamamoto Y (1999) *Tetrahedron Lett* 40:4081
139. Ajamian A, Gleason JL (2003) *Org Lett* 5:2409
140. Zhang LM, Kozmin SA (2004) *J Am Chem Soc* 126:11806
141. Gagosz F (2005) *Org Lett* 7:4129
142. Sun JW, Conley MP, Zhang LM, Kozmin SA (2006) *J Am Chem Soc* 128:9705
143. Grise CM, Rodrigue EM, Barriault L (2008) *Tetrahedron* 64:797
144. Li GJ, Liu YH (2010) *J Org Chem* 75:2903

145. Kirsch SF, Binder JT, Crone B, Duschek A, Haug TT, Liebert C, Menz H (2007) *Angew Chem Int Ed* 46:2310
146. Menz H, Binder JT, Crone B, Duschek A, Haug TT, Kirsch SF, Klahn P, Liebert C (2009) *Tetrahedron* 65:1880
147. Galland JC, Savignac M, Genêt JP (1997) *Tetrahedron Lett* 38:8695
148. Galland JC, Dias S, Savignac M, Genêt JP (2001) *Tetrahedron* 57:5137
149. Charruault L, Michelet V, Genêt JP (2002) *Tetrahedron Lett* 43:4757
150. Nevado C, Charruault L, Michelet V, Nieto-Oberhuber C, Muñoz MP, Mendez M, Rager MN, Genêt JP, Echavarren AM (2003a) *Eur J Org Chem* 706
151. Nevado C, Cárdenas DJ, Echavarren AM (2003b) *Chem Eur J* 9:2627
152. Michelet V, Charruault L, Gladiali S, Genêt JP (2006) *Pure Appl Chem* 78:397
153. Nieto-Oberhuber C, Muñoz MP, López S, Jiménez-Núñez E, Nevado C, Herrero-Gómez E, Raducan M, Echavarren AM (2006) *Chem Eur J* 12:1677
154. Muñoz MP, Adrio J, Carretero JC, Echavarren AM (2005) *Organometallics* 24:1293
155. Chao CM, Genin E, Toullec PY, Genet JP, Michelet V (2009) *J Organomet Chem* 694:538
156. Pradal A, Chao CM, Vitale MR, Toullec PY, Michelet V (2011) *Tetrahedron* 67:4371
157. Charruault L, Michelet V, Taras R, Gladiali S, Genêt J-P (2004) *Chem Commun* 850
158. Toullec PY, Blarre T, Michelet V (2009) *Org Lett* 11:2888
159. Buzas AK, Istrate FM, Gagosz F (2007) *Angew Chem Int Ed* 46:1141
160. Zhang LM, Kozmin SA (2005) *J Am Chem Soc* 127:6962
161. Leseurre L, Toullec PY, Genet JP, Michelet V (2007) *Org Lett* 9:4049
162. Furstner A, Morency L (2008) *Angew Chem Int Ed* 47:5030
163. Jiménez-Núñez E, Claverie CK, Nieto-Oberhuber C, Echavarren AM (2006) *Angew Chem Int Ed* 45:5452
164. Schelwies M, Dempwolff AL, Rominger F, Helmchen G (2007) *Angew Chem Int Ed* 46:5598
165. Schelwies M, Moser R, Dempwolff AL, Rominger F, Helmchen G (2009) *Chem Eur J* 15:10888
166. Escribano-Cuesta A, López-Carrillo V, Janssen D, Echavarren AM (2009) *Chem Eur J* 15:5646
167. Jiménez-Núñez E, Molawi K, Echavarren AM (2009) *Chem Commun* 7327
168. Molawi K, Delpont N, Echavarren AM (2010) *Angew Chem Int Ed* 49:3517
169. Toullec PY, Genin E, Leseurre L, Genet JP, Michelet V (2006) *Angew Chem Int Ed* 45:7427
170. Amijs CHM, Ferrer C, Echavarren AM (2007) *Chem Commun* 698
171. Leseurre L, Chao CM, Seki T, Genin E, Toullec PY, Genet JP, Michelet V (2009) *Tetrahedron* 65:1911
172. Chao CM, Vitale MR, Toullec PY, Genet JP, Michelet V (2009) *Chem Eur J* 15:1319
173. Amijs CHM, López-Carrillo V, Raducan M, Perez-Galan P, Ferrer C, Echavarren AM (2008) *J Org Chem* 73:7721
174. Nieto-Oberhuber C, Perez-Galan P, Herrero-Gómez E, Lauterbach T, Rodriguez C, López S, Bour C, Rosellon A, Cárdenas DJ, Echavarren AM (2008) *J Am Chem Soc* 130:269
175. Sethofer SG, Mayer T, Toste FD (2010) *J Am Chem Soc* 132:8276
176. Rautenstrauch V (1984) *J Org Chem* 49:950
177. Strickler H, Davis JB, Ohloff G (1976) *Helv Chim Acta* 59:1328
178. Fürstner A, Hannen P (2006) *Chem Eur J* 12:3006
179. Fehr C, Galindo J (2006) *Angew Chem Int Ed* 45:2901
180. Fehr C, Winter B, Magpantay I (2009) *Chem Eur J* 15:9773
181. Soriano E, Marco-Contelles J (2005a) *J Org Chem* 70:9345
182. Soriano E, Ballesteros P, Marco-Contelles J (2005b) *Organometallics* 24:3182
183. Miki K, Ohe K, Uemura S (2003a) *Tetrahedron Lett* 44:2019
184. Miki K, Ohe K, Uemura S (2003b) *J Org Chem* 68:8505
185. Miki K, Fujita M, Uemura S, Ohe K (2006) *Org Lett* 8:1741
186. Johansson MJ, Gorin DJ, Staben ST, Toste FD (2005) *J Am Chem Soc* 127:18002

187. Garayalde D, Krüger K, Nevado C (2011) *Angew Chem Int Ed* 123:941
188. Soriano E, Marco-Contelles J (2008) *Chem Eur J* 14:6771
189. Cariou K, Mainetti E, Fensterbank L, Malacria M (2004) *Tetrahedron* 60:9745
190. Hardin AR, Sarpong R (2007) *Org Lett* 9:4547
191. Prasad BAB, Yoshimoto FK, Sarpong R (2005) *J Am Chem Soc* 127:12468
192. Wang Y, Biao L, Zhang L (2010) *Chem Commun* 46:9179
193. Saucy G, Marbet R, Lindlar H, Isler O (1959) *Helv Chim Acta* XLII:1945
194. Schlossarczyk H, Sieber W, Hesse M, Hansen H-J, Schmid H (1973) *Helv Chim Acta* 56:875
195. Oelberg DG, Schiavelli MD (1977) *J Org Chem* 42:1804
196. Cookson RC, Cramp MC, Parsons PJ (1980) *Chem Commun* 197
197. Bowden B, Cookson RC, Davis HA (1973) *J Chem Soc, Perkin Trans. 1*:2634
198. Sromek AW, Kel'in AV, Gevorgyan V (2004) *Angew Chem Int Ed* 43:2280
199. Moreau X, Goddard JP, Bernard M, Lemièrre G, López-Romero JM, Mainetti E, Marion N, Mouries V, Thorimbert S, Fensterbank L, Malacria M (2008) *Adv Synth Catal* 350:43
200. Moreau X, Hours A, Fensterbank L, Goddard JP, Malacria M, Thorimbert S (2009) *J Organomet Chem* 694:561
201. Harrak Y, Makhlof M, Azzaro S, Mainetti E, Romero JML, Cariou K, Gandon V, Goddard JP, Malacria M, Fensterbank L (2011) *J Organomet Chem* 696:388
202. Marion N, de Frémont P, Lemièrre G, Stevens ED, Fensterbank L, Malacria M, Nolan SP (2006) *Chem Commun* 2048
203. Correa A, Marion N, Fensterbank L, Malacria M, Nolan SP, Cavallo L (2008) *Angew Chem Int Ed* 47:718
204. Marion N, Lemièrre G, Correa A, Costabile C, Ramón RS, Moreau X, de Frémont P, Dahmane R, Hours A, Lesage D, Tabet JC, Goddard J-P, Gandon V, Cavallo L, Fensterbank L, Malacria M, Nolan SP (2009) *Chem Eur J* 15:3243
205. Buzas A, Gagosz F (2006) *J Am Chem Soc* 128:12614
206. Pujanauskis BG, Prasad AB, Sarpong R (2006) *J Am Chem Soc* 128:6786
207. Motamed M, Bunnelle EM, Singaram SW, Sarpong R (2007) *Org Lett* 9:2167
208. Witham CA, Mauleon P, Shapiro ND, Sherry BD, Toste FD (2007) *J Am Chem Soc* 129:5838
209. Shapiro ND, Toste FD (2008) *J Am Chem Soc* 130:9244
210. Davies PW, Albrecht SJ-C (2008) *Chem Commun* 238
211. Shapiro ND, Shi Y, Toste FD (2009) *J Am Chem Soc* 131:11654
212. Shi X, Gorin DJ, Toste FD (2005) *J Am Chem Soc* 127:5802
213. Nieto Faza O, Silva López C, Alvarez R, de Lera AZJ (2006) *Am Chem Soc* 128:2434
214. Zou Y, Garayalde D, Wang Q, Nevado C, Goeke A (2008) *Angew Chem Int Ed* 47:10110
215. Ye L, Chen Q, Zhang JC, Michelet V (2009) *J Org Chem* 74:9550
216. Gung BW, Bailey LN, Craft DT, Barnes CL, Kirschbaum K (2010) *Organometallics* 29:3450
217. Jiménez-Núñez E, Raducan M, Lauterbach T, Molawi K, Solorio CR, Echavarren AM (2009) *Ang Chem Int Ed* 48:6152
218. Ji KG, Shu XZ, Zhao SC, Zhu HT, Niu YN, Liu XY, Liang YM (2009) *Org Lett* 11:3206
219. Belmont P, Parker E (2009) *Eur J Org Chem* 6075
220. Zhang Z, Shi M (2011) *Eur J Org Chem* 2610
221. Aubert C, Fensterbank L, Garcia P, Malacria M, Simonneau A (2011) *Chem Rev* 111:1954
222. Cadran N, Cariou K, Hervé G, Aubert C, Fensterbank L, Malacria M, Marco-Contelles J (2004) *J Am Chem Soc* 126:3408
223. Lemièrre G, Gandon V, Agenet N, Goddard JP, de Kozak A, Aubert C, Fensterbank L, Malacria M (2006) *Angew Chem Int Ed* 45:7596
224. Soriano E, Marco-Contelles J (2005) *Chem Eur J* 11:521
225. Gorin DJ, Sherry BD, Toste FD (2008) *Chem Rev* 108:3351

- 226. Yang C-Y, Lin G-Y, Liao H-Y, Datta S, Liu R-S (2008) *J Org Chem* 73:4907
- 227. Wei H, Zhai H, Xu P-F (2009) *J Org Chem* 74:2224
- 228. Gonzalez-Gómez A, Dominguez G, Pérez-Castells J (2009) *Eur J Org Chem* 5057
- 229. Matsuda T, Kadowaki S, Goya T, Murakami M (2006) *Synlett* 4:575
- 230. Sethofer SG, Staben ST, Hung OY, Toste FD (2008) *Org Lett* 10:4315

Chapter 2

New Advances in the Gold-Catalyzed Cycloisomerization Reactions of Enynes: 1,5-hydride Shifts and Access to Ketomacrolactones

In this chapter will be presented some new results obtained in the field of gold catalyzed cycloisomerizations of 1,6-enynes. A new reaction based on a 1,5-hydride shift process has been disclosed, allowing the formation of functionalized allenes. The end of this chapter gathers some results we got toward the synthesis of macrocycles using a gold catalyzed cycloisomerization reaction of oxygen-tethered 1,6-enynes. Before the results being described and discussed, we will briefly introduce other gold catalyzed reactions that feature 1,5-hydride shifts.

2.1 Introduction

2.1.1 Bibliography

2.1.1.1 C(sp³)-H Functionalization Through 1,5-hydride Shifts

Methodologies allowing the direct functionalization of relatively unreactive C–H bonds have raised a growing interest from the organic chemists community, as it facilitates the formation of C–C and C-heteroatom bonds without requiring a prefunctionalized C–X bond (X = halogens, triflates...).¹ The majority of these methodologies deals with C(sp²)-H bonds, even if recently some promising catalytic systems have emerged toward the activation of the strong C(sp³)-H bond. In general, they rely on the direct insertion of a metal into the desired C–H bond. However, a turn in this chemistry appeared in 2005 with the work of Sames and co-workers [6–8]. They proposed an alternative approach based on an initial activation of an unsaturation by an electrophilic metal catalyst that triggers the cleavage of a C–H bond in 1,5-relationship to the activated π -system.²

¹ For a selection of recent reviews on C–H bond functionalization, see: [1–4]. See also [5].

² For a review gathering some examples of this type of reaction see: [9].

The resulting ate-complex **1** then reacts intramolecularly on the electrophilic position generated by the departure of the H atom to form a C–C bond (Scheme 2.1).

Although the reaction is limited due to its intramolecular character and requires the presence of a stabilizing group (mainly heteroatoms such as O or N), this strategy allows the activation of sterically hindered C(sp³)–H bonds, a strong limitation in the direct metal insertion based processes. Some examples are presented in Scheme 2.2, and it is worth adding that aryl can also play the role of the stabilizing group, rather than nitrogen or oxygen.

2.1.1.2 Related Reactions Catalyzed by Gold and Platinum

Given the fact that gold and platinum are excellent and selective activators of C–C unsaturations, the transposition of the Sames' strategy into the realm of gold and platinum catalyzed reactions came naturally. Indeed, these metals efficiently promoted the 1,5-migration of an hydride onto an activated triple bond when starting from precursors **6** and **8**,³ resulting in products **7**, **9**, **10** of formal alkyne hydroalkylation (Scheme 2.3).

The gold version of this rearrangement can be plagued by side reactions,⁴ and a selectivity issue between 5-*exo* (such as **9**) or 6-*endo* products (such as **10**) is also met, mainly due to steric interactions. The proposed mechanism starts complexation by the electrophilic metal center onto the alkyne that triggers the 1,5-hydride shift.⁵ The C–C bond formation occurs at the resulting vinylmetal species **11** in a 5-*exo* manner, to give carbene **12**. Then, depending on steric factors that allow the requisite conformation of carbene **12**, a 1,2-H or a 1,2-alkyl shift takes place, leading to products **7/9** or **10**, respectively (Scheme 2.4).

The team of Gagosz further extended this rearrangement to propargyl ethers **13** and thus disclosed a practical method for the synthesis of substituted allenes **14** [12]. In this case the vinylgold species **15** rather undergoes a gold elimination concomitant with the adjacent C–O bond cleavage, leading to the obtention of substituted allene **14** and benzaldehyde as products (Scheme 2.5).

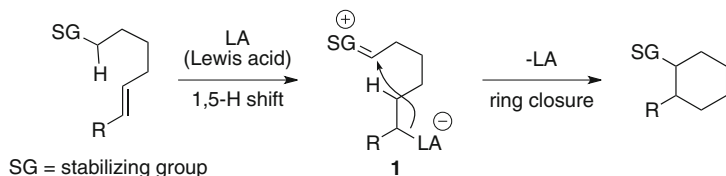
It is worth noting that substrates similar to **13** with R¹ = ester gave *endo* hydroalkylation products upon the conditions reported in Scheme 2.3. This mechanistic divergence still lacks rationalization. The team of Gagosz also developed the allenic version of the hydroalkylation reaction depicted in Scheme 2.3 [13]. This study also features a comparison with strong Brønsted acids. The latter were shown to give a different outcome than gold, though able to perform the 1,5-migration process (Scheme 2.6).

The postulated mechanism starts with activation of the allene inducing the migration of the hydride α to the oxygen atom. From intermediate **19** two different pathways are then likely to occur: with gold, carbometalation of the oxonium

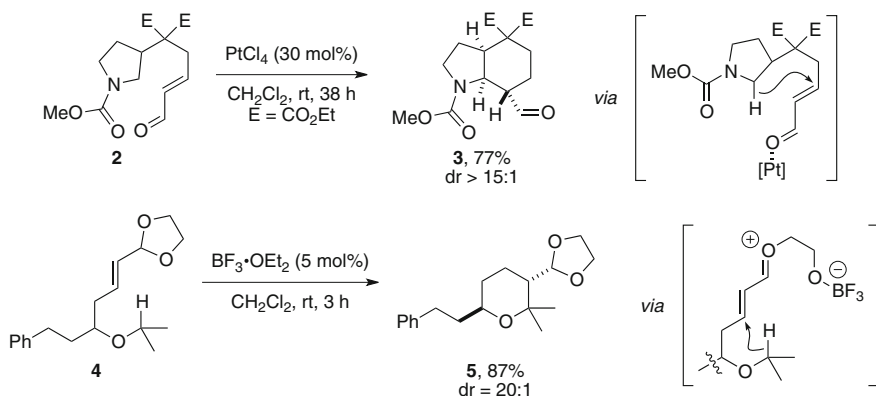
³ With Pt(IV): [10].

⁴ With cationic Au(I): [11].

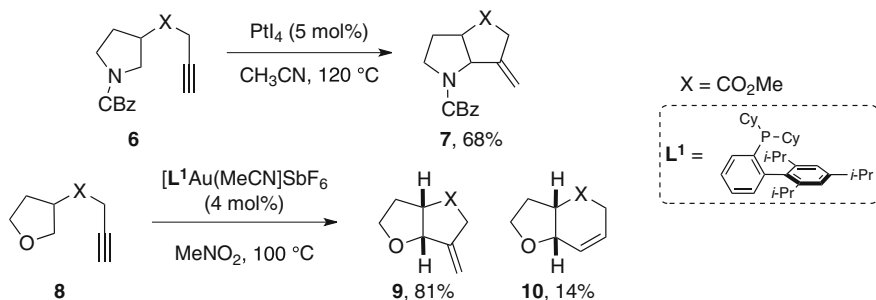
⁵ Sames also invoked the possibility of a platinum vinylidene, see Ref. [10].



Scheme 2.1 Sames' strategy for the activation of C(sp³)-H bonds

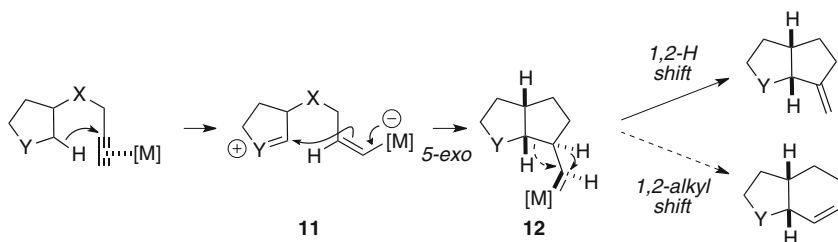


Scheme 2.2 Examples of the indirect C(sp³)-H functionalization strategy developed by Sames

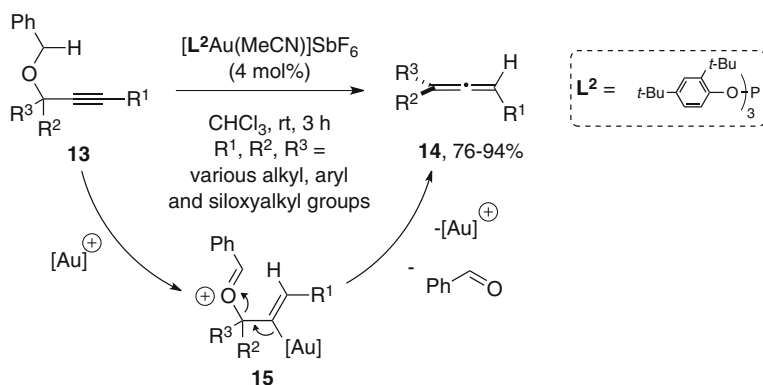


Scheme 2.3 1,5-hydride shifts onto a Pt- or Au-activated C-C triple bond

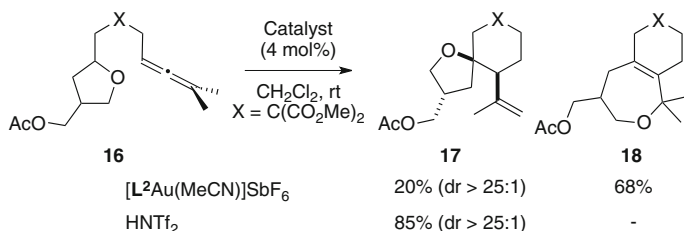
moiety can take place giving complex **20**, on which a gold-triggered furan opening allows rearrangement into **18** through allylic carbocation **21**. On the other hand, the pathway leading to product **17** involves the nucleophilic attack of the double bond in **19** onto the oxonium to produce carbocation **22** (which may evolve to **20** through gold elimination). The latter, depending on the catalyst, furnishes the spiro compound **17** in a one or two steps sequence. Neither **17** nor **18** rearranged into the other upon gold or acid catalysis, which is consistent with such mechanistic divergence (Scheme 2.7).



Scheme 2.4 Mechanism of the Pt- or Au-catalyzed hydroalkylation



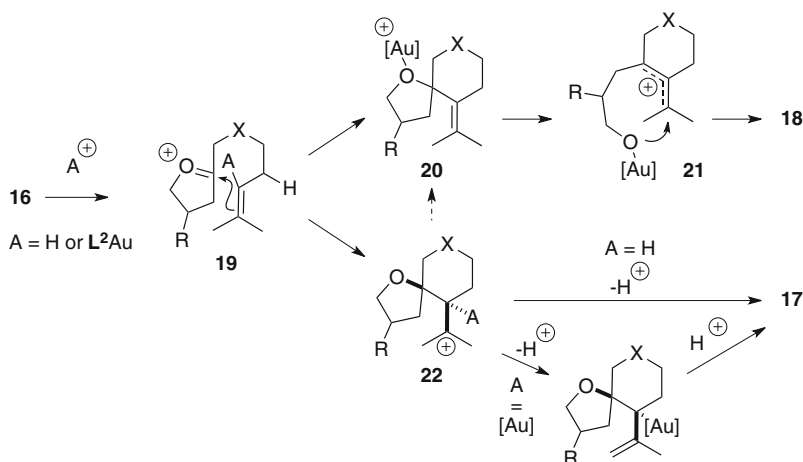
Scheme 2.5 Synthesis of allenes through 1,5-hydride shift/aldehyde elimination sequence



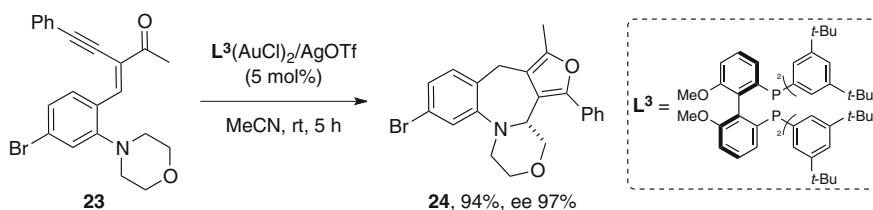
Scheme 2.6 Gold and acid catalyzed hydroalkylation of allenes

Cationic intermediates generated in gold catalysis can also react with a hydride through 1,5-intramolecular migration providing the design of the substrate allows it. This concept was successfully realized in an enantioselective version by the team of Zhang, starting from compound **23** (Scheme 2.8) [14, 15].

The mechanism of this reaction begins with the activation of the triple bond by cationic gold that induces a 5-*endo* nucleophilic attack of the neighboring carbonyl



Scheme 2.7 Mechanism for the Au- or acid-catalyzed hydroalkylation of allenes

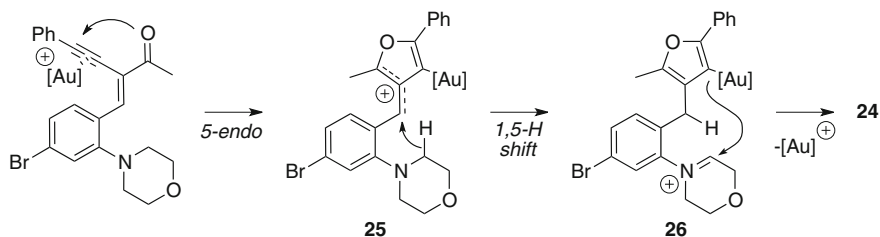


Scheme 2.8 Zhang's enantioselective Au-catalyzed functionalization of C(sp³)-H bonds

oxygen. The resulting stabilized carbocation **25** and the hydride α to nitrogen are in 1,5 relationship, therefore a migration process is likely to occur, leading to iminium **26**. The latter then reacts with the nucleophilic C-Au bond to form the seven-membered ring in an enantioselective manner and regenerates the catalyst (Scheme 2.9).

It is worth mentioning that a 1,6-hydride shift was proposed to occur in a particular case of enynes cycloisomerization upon platinum catalysis [16]. 1,5-sigmatropic shifts were also catalyzed by this metal [17]. 1,3-Hydride shifts onto platinum or gold carbenes have been more frequent [18, 19], and a sporadic example of a 1,5-hydride shift onto a platinum carbene has been reported to this date by the team of Oh [20].⁶

⁶ See also Ref. [21].



Scheme 2.9 Mechanism of Zhang's Au-catalyzed functionalization of C(sp³)-H bonds

2.1.2 Presentation and Objectives of the Project

As we were interested in the formation of allenes through gold-catalyzed processes for the development of tandem reactions, the direct transformation of enynes into allenes appeared to us as a promising tool. In view of our own results in the 1,6-allenynes series [22, 23], those of Liang and co-workers [24] and those presented above, we sought it was possible to obtain allenes upon gold catalysis, based on a 1,5-shift of an external propargylic substituent that could occur on an intermediate cyclopropylcarbene.

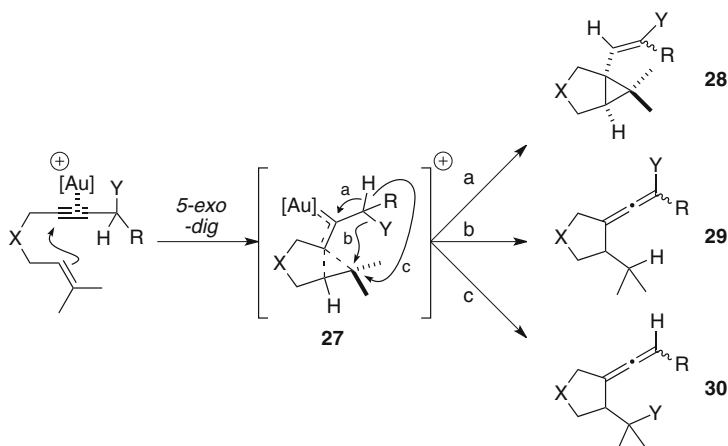
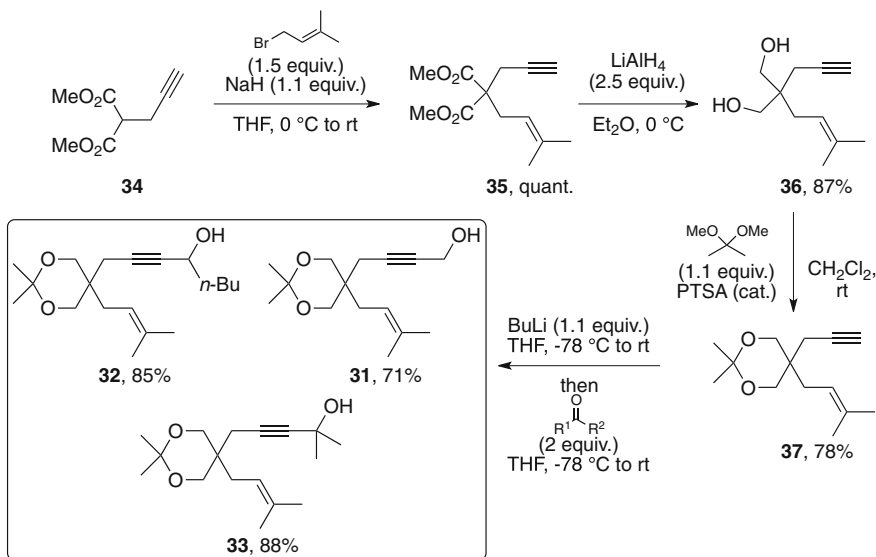
Considering cyclopropylcarbene **27**, several competitive processes could be at stake: a donor Y substituent could promote either a 1,2-H shift (path a, Scheme 2.10) to give a bicyclo[3.1.0]hexane derivative **28** [26] or a 1,5-H shift onto the cyclopropane head carbon to lead to exocyclic allene **29** (path b). If Y is also a good leaving group, its own migration could also be envisioned (path c). To enhance the carbocationic character of the cyclopropane head carbon and thus, to increase the chance to perform selectively the 1,5-migration process, geminal substitution at the external olefinic carbon should be decisive.

Below are presented the results we obtained in the development of such reaction.

2.2 Validation of Our Hypothesis: Synthesis of Allenes Through a Gold-Catalyzed Cyclization and/or 1,5-migration Processes

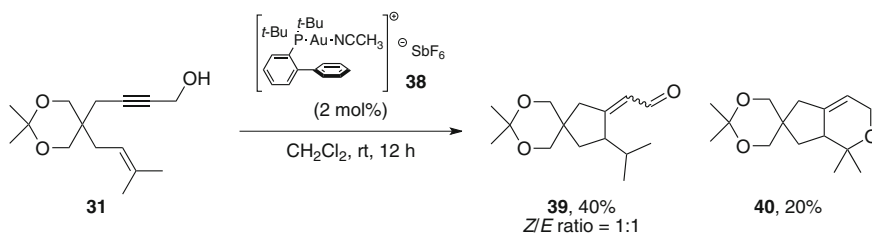
2.2.1 Synthesis of Test Substrates and Reactivity

We first assessed 1,6-enynes substituted at the external propargylic position by a primary, a secondary or a tertiary alcohol **31–33**, and displaying a prenyl group to give better chances to perform the migration process. The synthesis of such precursors was straightforward starting from commercially available dimethylpropargyl malonate **34** (Scheme 2.11). Deprotonation of the latter using sodium hydride in the presence of dimethylallyl bromide furnishes 1,6-enyne **35**. Reduction

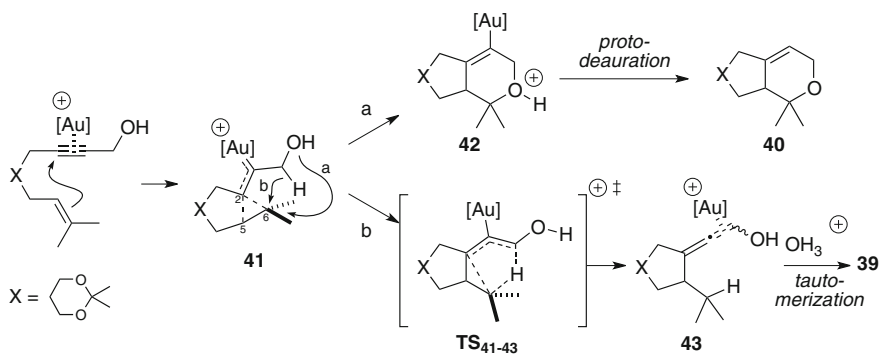
**Scheme 2.10** Anticipated mechanistic scenarii**Scheme 2.11** Synthesis of test substrates **31–33**

of the *gem*-diester moiety with lithium aluminium hydride followed by transacetalization with 2,2-dimethoxypropane led to dioxane tethered enyne **37**. Then, formation of the lithium acetylide by treatment with *n*-butyllithium followed by addition onto either formaldehyde, valeraldehyde or acetone gives 1,6-enyne precursors **31**, **32** or **33**, respectively.

With these substrates in hand, we could assess their reactivity toward gold catalysis. We chose cationic gold(I) catalyst **38** [25] to carry out the experiment,



Scheme 2.12 Au-catalyzed cycloisomerization of 1,6-enyne **31**

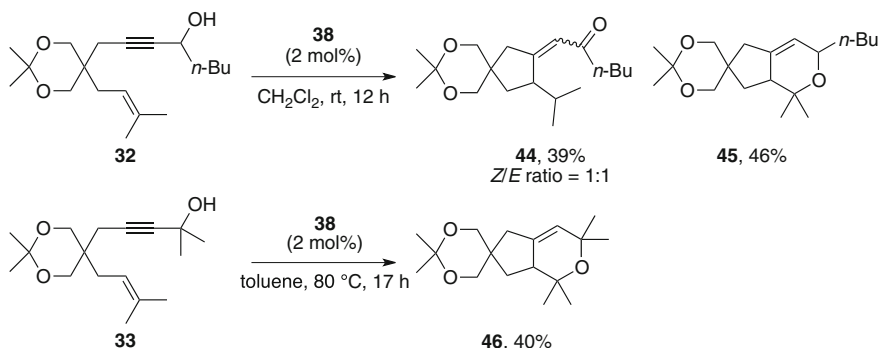
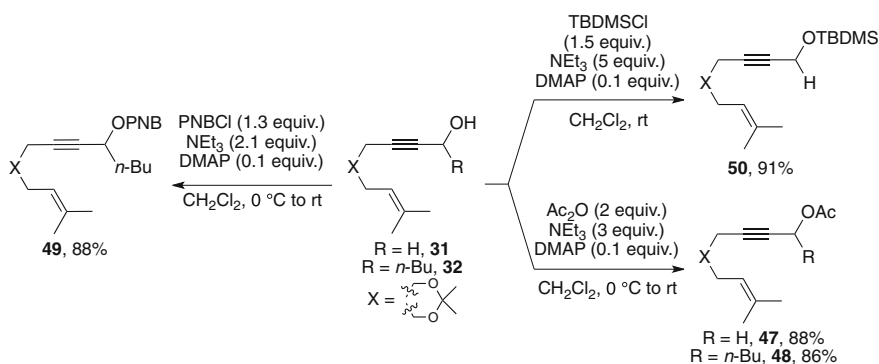


Scheme 2.13 Mechanistic rationale accounting for the formation of **39** and **40**

on one hand for practical reason because it is air-stable and easy to handle and on the other hand, it has been shown to be very efficient in promoting various enyne rearrangement. Its cationic nature also avoids recourse to silver salts which have been shown to promote cyclization reactions on related substrates [24]. Submission of **31** to catalytic amounts of **38** gave after 12 h at room temperature a mixture of products **39** and **40** (Scheme 2.12).

The mechanism accounting for the formation of **39** and **40** is depicted below. Complexation of gold onto the triple bond triggers the formation of cyclopropylgold carbene **41**. The latter can then evolve along two different pathways: nucleophilic attack of the free hydroxy group onto C6 delivers vinylgold oxonium **42** which after protodeauration gives dihydropyranyl derivative **40** (path a, Scheme 2.13).

The mechanism leading to **39** is somewhat original. Formation of this product can only be explained by a 1,5-hydride shift from the propargylic position to C6. This process was most probably made possible by assistance of the hydroxy group whose non bonding electron pairs can delocalize into the σ -antibonding orbital of the adjacent C–H bond. Gold-complexed allenol **43** is thus formed which upon decooordination/ tautomerization delivers aldehyde **39** (path b). The discovery of this new rearrangement of enynes prompted us to explore the scope and optimize this process.

Scheme 2.14 Reaction of substrates **32** and **33** with catalyst **38**

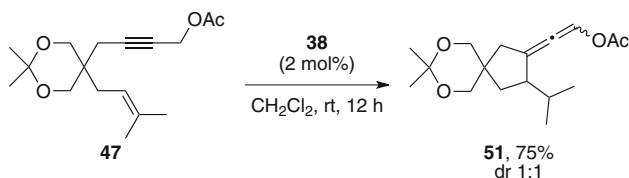
Scheme 2.15 Synthesis of esters and silylether derivatives

Precursor **32** gave a comparable yield of 1,5-hydride shift product upon catalysis with **38**, nonetheless the amount of dihydropyranyl derivative **45** was more than doubled. Unsurprisingly, substrate **33** that does not have any hydrogen at the external propargylic position reacted only along path a, nonetheless with harsher conditions than for **31** and **32** (Scheme 2.14).

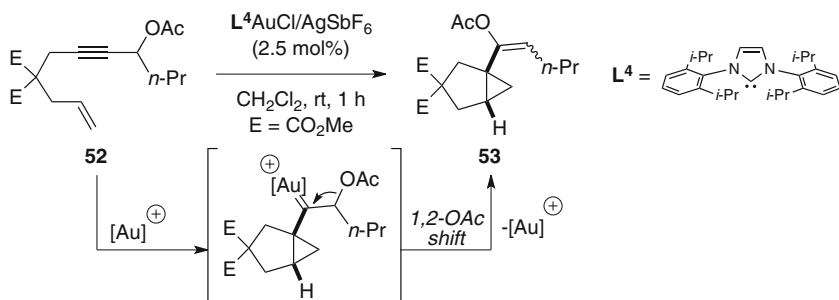
To prevent nucleophilic attack from the oxygen, we then synthesized a series of O-protected substrates, assuming they would exclusively react along path b.

2.2.2 Oxygen-Protected Precursors

Starting from alcohols **31** and **32**, we synthesized a range of ester and silyl protected precursors. Acylation or benzylation were realized with the acetic anhydride or *p*-nitrobenzoyl chloride (PNBCl) in the presence of triethylamine and 4-dimethylaminopyridine, and allowed us to obtain precursors **47–49**. Silylation of



Scheme 2.16 Efficient and selective 1,5-hydride shift



Scheme 2.17 Gung's study on a related system: importance of the prenyl substituent

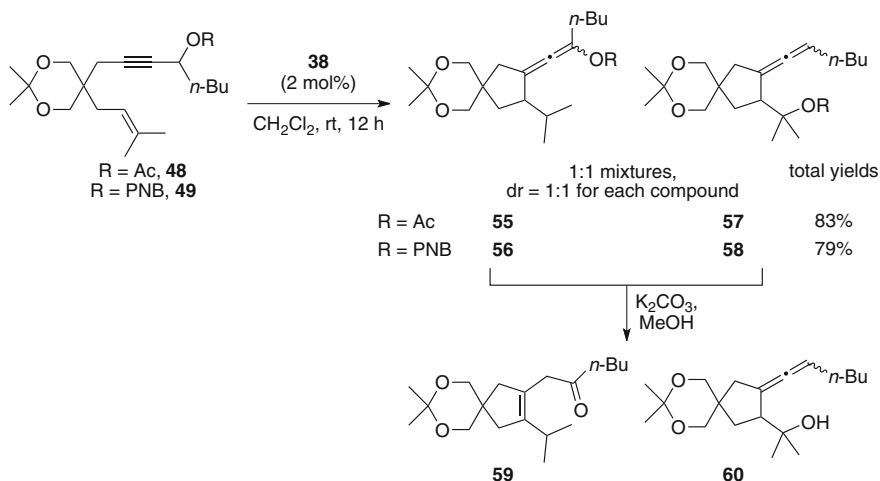
31 under classical conditions led to compound **50**. Alkylethers were not explored, as we assumed the risk to see them react similarly to benzylether derivatives upon platinum catalysis [26].

We then submitted precursors **47–50** to our reaction conditions. We were pleased to find that substrate **47** gave selectively the product of 1,5-hydride shift **51** in a satisfying 75 % yield and in a 1:1 diastereomeric ratio (Scheme 2.16).

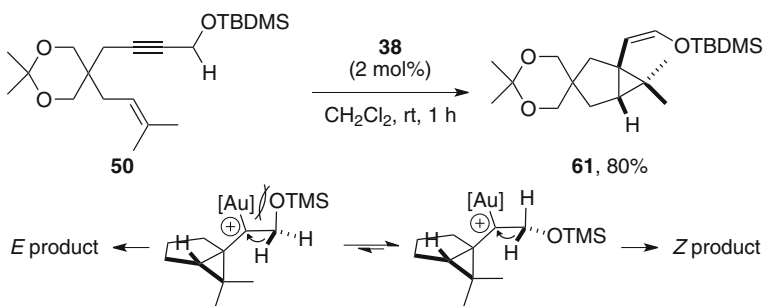
The preferred nucleophilic attack of the double bond over acetate migration is quite surprising, but consistent with the observation made by Gung on similar substrate **52** [27]. In his case, the olefin is monosubstituted and formation of cyclopropylcarbene prevails over any acyloxy migration process.⁷ A 1,2-OAc shift ends the catalytic cycle, thus delivering bicyclo[3.1.0]hexane compound **53** (Scheme 2.17). Therefore, the importance of using prenyl substituents is decisive to render the 1,5-hydride shift favourable rather than 1,2-OAc shift.

Secondary esters **48** and **49** both led to unseparable 1:1 mixtures of compounds resulting of either a 1,5-hydride shift (**55** and **56**) or a 1,5-carbonyloxy shift (**57** and **58**). As it was anticipated in Scheme 2.10, when the propargylic substituent is a good leaving group, competition between hydride or the latter migration could take place. Each product of the mixture was separated after methanolysis of the ester groups, leading to the corresponding ketone **59** or alcohol **60** (Scheme 2.18). Finally, no products that could arise from an initial rearrangement of the

⁷ However, as discussed in Chap. 1, Sect. 1.5.1, formation of **53** can also arise from a 1,2-OAc shift/cyclopropanation sequence, but it was not evoked by the authors.



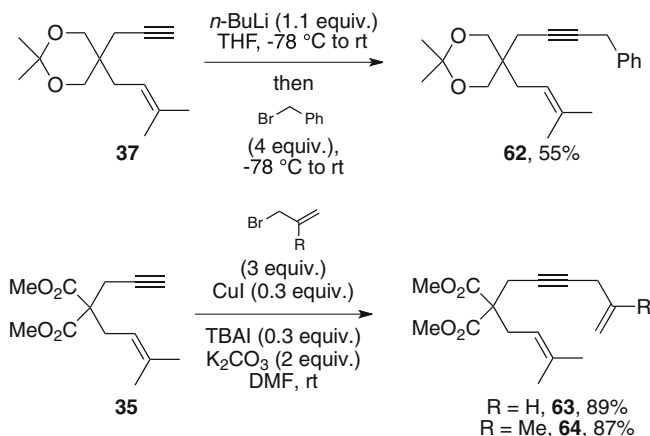
Scheme 2.18 Competition between 1,5-hydride or 1,5-carbonyloxy shift



Scheme 2.19 Bicyclo[3.1.0]hexane compound formation from silyl-protected precursor **164**

propargylic ester (refer to [Chap. 1](#), Sect. 1.5.1) were observed in the reactions of compounds **47** and **49**.

Silyl-protected substrate **50** did not undergo any 1,5-migration process, but selectively rearranged into bicyclo[3.1.0]hexane derivative **61** bearing a double bond of (*Z*) configuration (Scheme 2.19). This time, the 1,2-hydride shift/gold elimination process seems kinetically more favourable than any other process. This result could have been foreseen in view of Michelet's study with closely similar precursor, nonetheless with platinum(II) catalysis [26]. The selectivity toward the (*Z*) isomer is also consistent with her study, although she did not give any explanation for this phenomenon. It can reasonably be assumed that it resides in steric factors according to the model depicted in Scheme 2.19. In view of the above described results, a fine tuning between the leaving ability and the electron



Scheme 2.20 Synthesis of 1,6-enynes bearing allyl and benzyl acetylenic substituents

withdrawing character of the protected hydroxy group at the external propargylic position seems to be the key to selectively perform a 1,5-hydride shift.

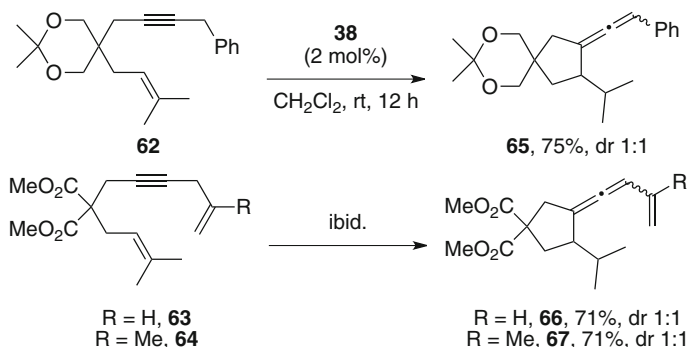
We then thought about benzyl and allyl as acetylenic substituents. They are clearly not leaving groups, and delocalization of their π -electrons into the σ -antibonding orbital of the vinylic or benzylic C-H bond could maybe help to the realization of a 1,5-hydride migration process.

2.2.3 Vinyl and Benzyl Groups as Propargylic Substituents

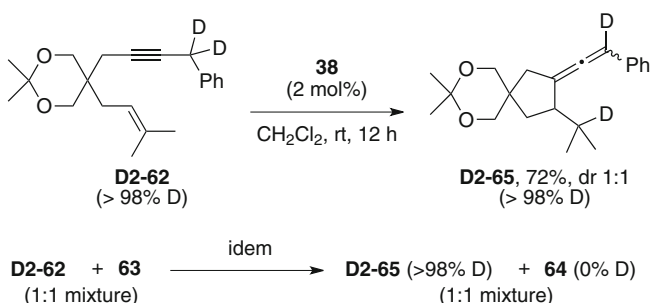
Benzyl derivative **62** was synthesized by treatment of 1,6-enyne **37** with n -butyllithium followed by addition of benzyl bromide. We also synthesized allyl and methallyl precursors **63** and **64** starting from malonate-tethered enyne **63** through palladium-free Sonogashira conditions (Scheme 2.20) [28].

We were pleased to find that submission of substrates **62–64** to catalytic amounts of **38** resulted in a clean conversion to the corresponding aryl- and vinylallenes **65–67** arising from a gold-catalyzed cyclization/1,5-hydride shift process (Scheme 2.21). Again, no diastereoselectivity was attained. Intriguingly, whereas vinylallenes of type **67** have been shown in the literature to undergo a Nazarov-type reaction upon gold or platinum catalysis, leading to cyclopentene derivatives [18, 29, 30], a prolonged reaction time of **67** resulted only in a complex mixture of unidentified products.

To further validate our proposed mechanism, we synthesized the deuterated analogue of **62**, **D2-62**, by reaction of 1,1-dideuteroallyl bromide with the corresponding lithium acetylide of **62** (60 % yield). When this substrate was reacted with 2 mol% of **38**, fully deuterated products **D2-65** was obtained. We also performed a deuterium scrambling experiment to confirm the intramolecular nature:



Scheme 2.21 Synthesis of aryl- and vinyl-allenes by a Au-catalyzed cyclization/1,5-H shift tandem reaction



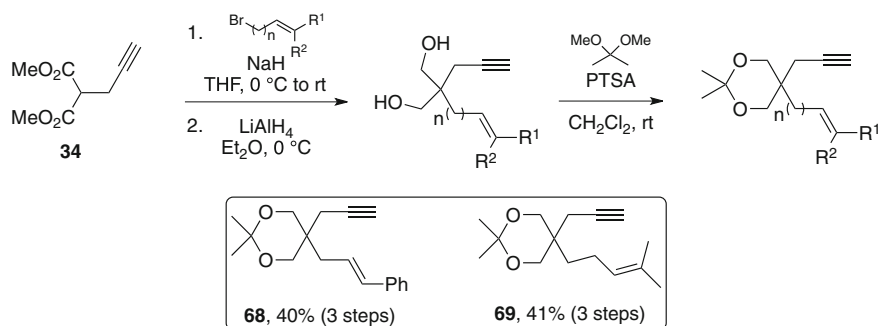
Scheme 2.22 Deuterium-labelling experiments

equimolar amounts of substrates **D2-62** and **63** were mixed together in a dichloromethane solution and submitted to the gold catalyst. A 1:1 mixture of product **D2-65** and **66** was obtained, the latter exhibiting no deuterium incorporation while it was superior than 98 % for **D2-65**, thus proving the intramolecular character of the migration process (Scheme 2.22).

2.3 Substrate Scope and Limitations

2.3.1 Carbon-Tethered Enynes

Encouraged by our preliminary results with carbon-tethered enynes, we next attempted to extend the scope of this new rearrangement to styryl precursors and 1,7-enynes. For this purpose we synthesized enynes **68** and **69** from propargyl-malonate **34** through a similar sequence of organic reactions than for the synthesis of **37** (Scheme 2.23).



Scheme 2.23 Synthesis of substrates **68** and **69**

Enynes **68** and **69** were alkylated under classical conditions using *n*-butyllithium followed by addition of valeraldehyde. Subsequent acetylation furnished acetate precursors **70** and **71** (Table 2.1).

A benzyl derivative was also synthesized by alkylation with benzyl bromide, delivering 1,7-enyne precursor **72** (Scheme 2.24).

When submitted to cationic gold(I) catalyst **38** in dichloromethane at rt, styryl precursor **70** was totally recovered after 12 h. The use of harsher conditions resulted in full conversion of the starting material within 5 h, but unfortunately a complex mixture of unseparable products was obtained (Scheme 2.25).


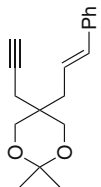
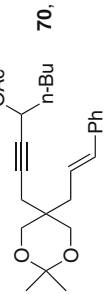
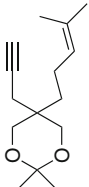
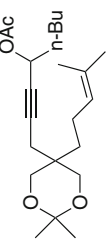
1,7-enynes precursors **71** and **72** both gave disappointing results. When submitted to catalyst **38**, substrate **71** led to a complex, unseparable mixture of unidentified compounds. Lowering the temperature to 0 °C slowed down conversion, but a mixture was still obtained. Precursor **72** was unreactive under the normal conditions. Harsher ones (dichloroethane, 60 °C) allowed full conversion of the starting material within 4 h, however NMR of the crude mixture revealed a complete decomposition of the starting material (Scheme 2.26).

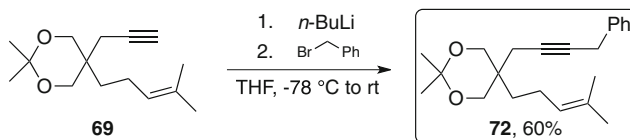
Clearly, the 1,5-migration process is strongly limited by the length of the tether and the nature of the double bond. The 1,5-relationship of the hydride toward its acceptor seems to be determinant, as suggest our results on 1,7-enynes **71** and **72**. The disappointing reactivity of styryl precursor could find explanations in steric repulsions avoiding the hydride and the benzylic cation to have the requisite geometry for the 1,5-migration process. Carbon-tethered enynes were abandoned, and we next focused our study on heteroatom-tethered enynes.

2.3.2 Heteroatom-Tethered 1,6-enynes

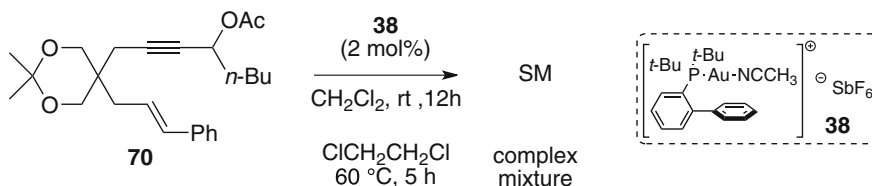
As a starting point to the synthesis of heteroatom-tethered enynes, we synthesized various propargyl alcohols or amines. The precursor of N-tethered enynes we used

Table 2.1 Synthesis of 1,6-enynes **70** and **71**

		1. $n\text{-BuLi}$ then  THF, -78 °C to rt 2. Ac_2O , NEt_3 , cat. DMAP CH_2Cl_2 , 0 °C to rt	
Entry	Enyne	Product (yield, 2 steps)	
1		 70 , 84%	
2		 71 , 81%	

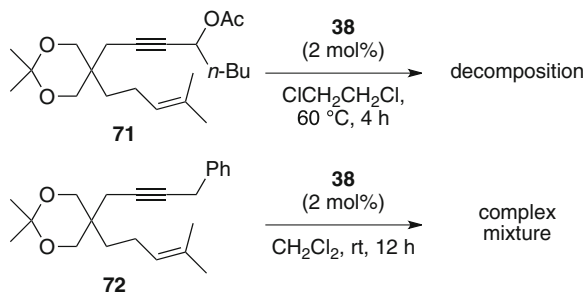


Scheme 2.24 Synthesis of benzyl-substituted 1,7-enyne precursor **72**

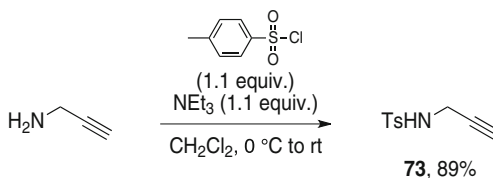


Scheme 2.25 Failure to promote the cycloisomerization of styryl precursor **70** through 1,5-migration

Scheme 2.26 Failed attempts to promote 1,5-migration on 1,7-enynes



Scheme 2.27 Synthesis of *N*-tosyl propargyl amine **73**



was *N*-tosyl propargyl amine **73** obtained in one step in 89 % yield by tosylation of commercially available propargyl amine (Scheme 2.27).

Propargyl alcohols **74–76** were prepared in excellent yields by addition of lithium acetylides onto aldehydes or ketones. Propargyl alcohol **76** was subsequently desilylated under classical methanolysis conditions to give precursor **77** (Table 2.2).

Propargyl amine and alcohols **73–75** and **77** were next alkylated by treatment with sodium hydride and an allyl bromide in 73–83 % yield. 1,6-Enynes **78–80** bearing a terminal alkyne can be further functionalized at the acetylenic position. Precursor **81** displays an alkyl-substituted triple bond, so that we can check the

possibility of a 1,5-hydride shift without the assistance of an adjacent π -donor group. Enyne **82**, bearing a mono-substituted olefin, will allow us to test the limit of the 1,5-migration process as well (Table 2.3).

Terminal alkynes in enynes **78–80** were alkylated with valeraldehyde upon treatment with *n*-butyllithium, and subsequent acetylation furnished cyclization precursors **83–85**, the latter bearing a quaternary propargylic center (Table 2.4).

Benzyl derivatives **86** and **87** were also synthesized starting from enynes **79** and **80**, respectively (Table 2.5).

Finally, substrate **88** with a methylene cyclohexane moiety was synthesized. Wittig-Horner olefination of cyclohexanone followed by reduction using LAH furnished allylic alcohol **89**. Alkylation of the latter with propargyl bromide and subsequent alkylation of the acetylenic position gave enyne precursor **88** (Scheme 2.28).

We then assessed the reactivity of substrates **81–88** when submitted to catalytic amounts of catalyst **38**. *n*-Butyl precursors **81** and **82** both rearranged into bicyclo[4.10]heptene skeletons **90** and **91**, the latter with ring expansion of the cyclopentane framework (Scheme 2.29).

The cycloisomerization of **81** into **89** clearly demonstrates that the presence of an adjacent π -donor group is critical to perform the 1,5-hydride shift. Thus, it is not surprising that enyne **82**, bearing a mono-substituted olefin, reacts in a similar manner. The mechanism of this transformation is detailed in the box of Scheme 2.29 and involves an *endo* cyclopropylcarbene **92** (refer to Sect. 1.3.3 of Chap. 1). The latter would then undergo a 1,2-alkyl shift/ring expansion followed by gold elimination consistent with precedents in the 1,6- and 1,5-enynes series (*ibid.*).

O-acyl precursors **83–85** gave contrasting results. *N*-tethered substrate **83** was unreactive under the classical gold catalysis conditions. When switching to harsher ones (refluxing dichloroethane), a complex mixture of unseparable products was obtained (Scheme 2.30).

O-tethered substrate **84** led selectively upon cationic gold(I) catalysis to allene **93** arising from a 1,5-acetate shift process. This is in sharp contrast with carbon-tethered substrate **47** also bearing a primary acetate at the external propargylic position that gave selectively a 1,5-hydride shift product (Scheme 2.16). This example is a nice illustration of a mechanistic divergence directed by the tether (Scheme 2.31).

Enyne **85** bearing a quaternary propargylic center exhibited a particular reactivity when submitted to catalyst **38**, as diene **94** was obtained in quantitative yield with a (*E*)/(*Z*) ratio of 1:0.4 (Scheme 2.32).

As we detected a downfield signal in the ^1H NMR of the crude mixture, we assumed that this product could arise from a gold-triggered elimination of 3,3-dimethylacrolein. This process would be possible if a 1,5-hydride shift occurs from the allylic position onto the external carbon of the triple bond, leading to vinylgold oxonium **95**. Gold elimination would then take place concomitant with elimination of 3,3-dimethylacrolein, to lead to allene **96**. A 3,3-sigmatropic shift, probably gold-catalyzed, would finally deliver the mixture of dienes **92** through dioxonium intermediate **97** (Scheme 2.33).

Table 2.4 Synthesis of 1,6-enynes **83**–**85**

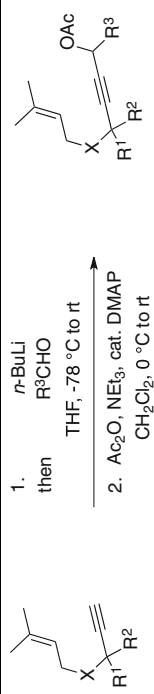
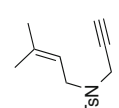
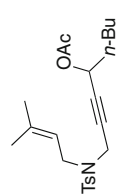
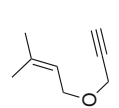
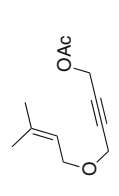
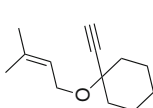
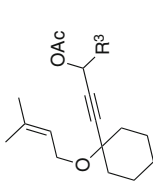
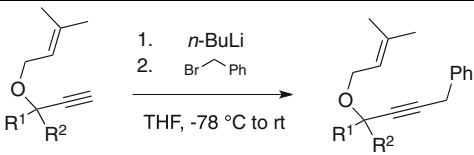
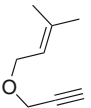
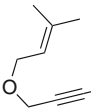
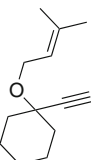
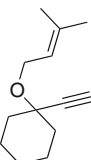
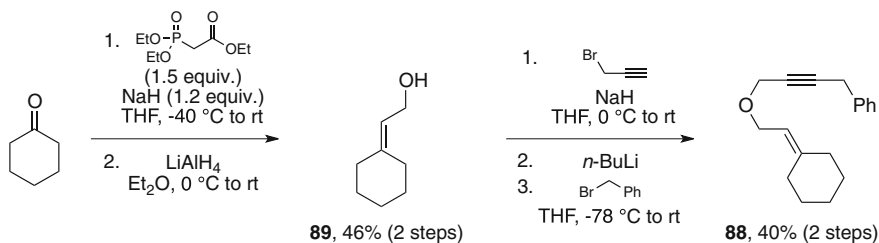
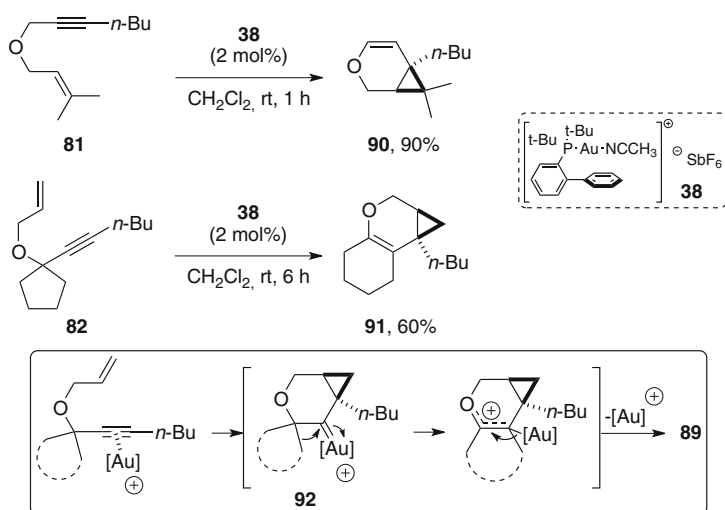
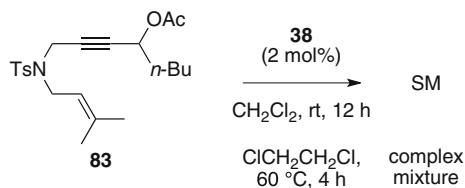
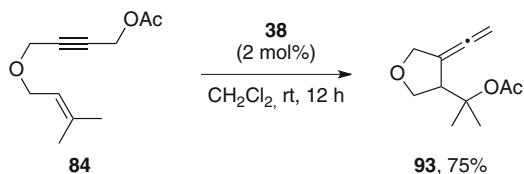
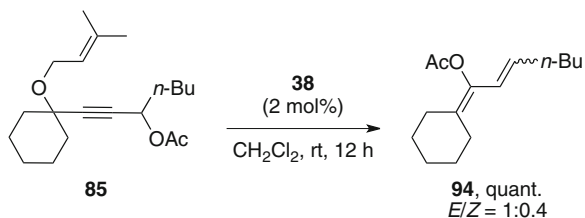
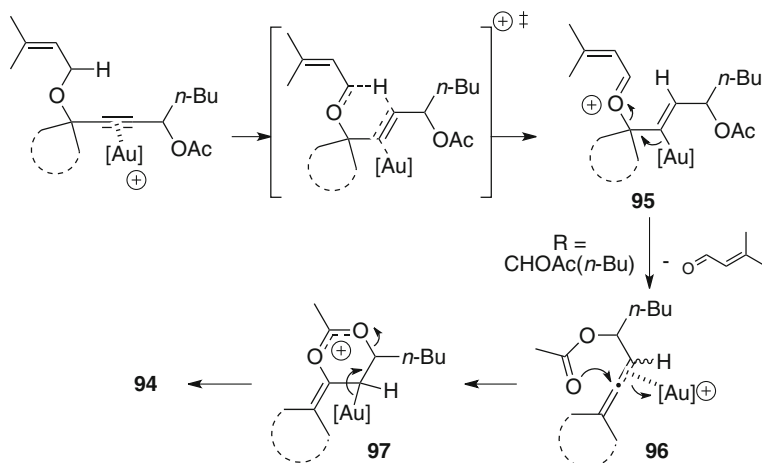
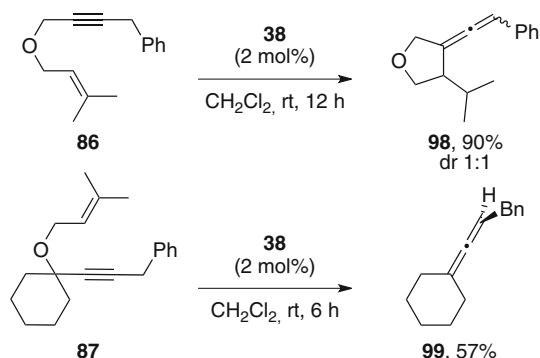
<div>  </div>		Entry	Enyne	R ³	Product (yield, 2 steps)
		1		<i>n</i> -Bu	 83 (77%)
		2		H	 84 (82%)
		3		<i>n</i> -Bu	 85 (56%)

Table 2.5 Benzylation of the acetylenic position of enynes **79–80**

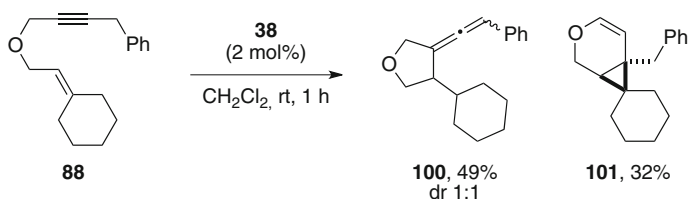
		
Entry	Enyne	Product (yield)
1	 79	 86 (56%)
2	 80	 87 (56%)

**Scheme 2.28** Synthesis of substrate **88** bearing a methylene cyclohexane**Scheme 2.29** Cycloisomerization of enynes **81** and **82** into fused polycyclic compound **90** and **91**

**Scheme 2.30** Failed attempts to cyclize *N*-tethered precursor **83****Scheme 2.31** Cyclization of *O*-tethered enyne **84** through a 1,5-OAc shift process**Scheme 2.32** Particular reactivity of substrate **85** bearing a quaternary propargylic center**Scheme 2.33** Mechanistic hypothesis accounting for the formation of product **92**



Scheme 2.34 Reactivity of benzyl derivatives **86** and **87**



Scheme 2.35 Competition between *endo* cyclization and 1,5-hydride shift in the cycloisomerization of **88**

Gratifyingly, benzyl derivative **86** was cleanly converted to cyclized compound **98** through a 1,5-hydride shift upon gold catalysis, in 90 % yield. However, enyne **87** bearing a quaternary propargylic center selectively rearranged into allene **99**. This product presumably arise from a mechanistic sequence similar to the one leading to allene **96** in the rearrangement of enyne **85** into diene **94** (Scheme 2.34).

These examples show that two 1,5-hydride shift processes can compete when using *O*-tethered enynes, one leading to compounds **94** or **99**, the other leading to **98**. The nature of the internal propargylic center has a dramatic influence in the overcoming of one pathway over the other.

When reacted with a catalytic amount of **38**, substrate **88** led, within a short reaction time, to a 3:2 mixture exocyclic allene **100** and *endo* cyclization product **101**, the allene derivative being, once more, obtained as a 1:1 mixture of diastereoisomers (Scheme 2.35).

This last example suggests that using trisubstituted, sterically hindered double bond may rise issues of selectivity, *endo* cyclization becoming competitive with 1,5-hydride migration.

Table 2.6 Synthesis of propargyl ethers **102** and **103**

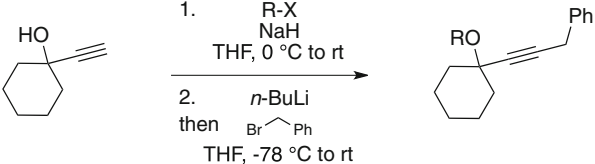
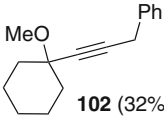
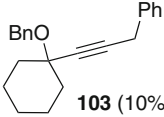
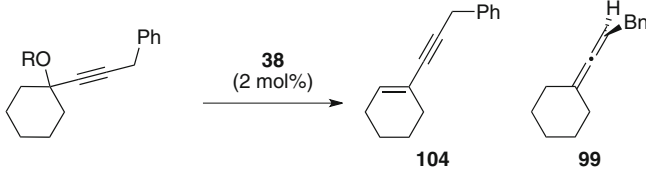
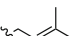
		
Entry	R-X	Product (yield, 2 steps)
1	Mel	 102 (32%)
2	Br-CH ₂ -Ph	 103 (10%)

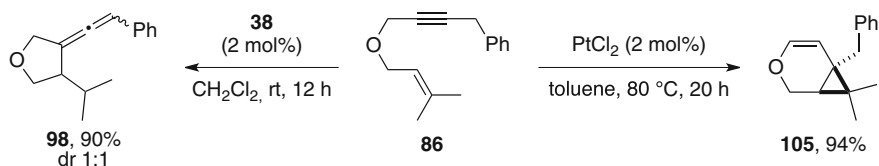
Table 2.7 Reactivity of propargyl ethers **87**, **102** and **103** toward gold catalysis

			
Propargyl ether	Conditions	Yield	
102 , R = Me	ClCH ₂ CH ₂ Cl, 80 °C, 5 h	70%	-
103 , R = Bn	CH ₂ Cl ₂ , rt, 12 h	-	47% (90% brsm)
87 , R = 	CH ₂ Cl ₂ , rt, 6 h		57%

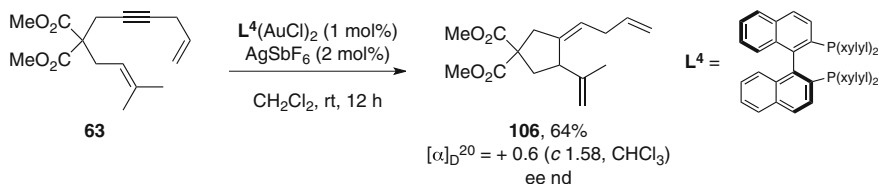
2.3.3 Rearrangement of Propargyl Ethers into Allenes

Another 1,5-hydride migration process was disclosed, leading to diene **94** or allene **99** (vide supra). A study of its scope was started with propargyl ethers **102** and **103** bearing a quaternary propargylic center. They were synthesized from propargyl alcohol **77** through a Williamson reaction/alkylation sequence (Table 2.6).

The reactivity of propargyl ethers **102** and **103** and **87** when submitted to catalyst **38** are summarized in Table 2.7. Precursor **102** was unreactive under room-temperature conditions. Running the reaction in refluxing dichloroethane led to **104** resulting from methanol elimination as the single product (70 % yield). Benzyl ether **103** cleanly afforded allene **99** in 47 % yield, however conversion



Scheme 2.36 Distinct mechanistic pathways between **38** and PtCl_2



Scheme 2.37 Alder-ene product reaction upon catalysis with a chiral bimetallic gold complex

was incomplete. As a matter of comparison, dimethallyl precursor **87** reacted faster under room-temperature conditions.

During the course of this study, another team reported the direct formation of allenes from benzyl propargyl ethers with cationic gold(I) catalysts through the same process as described above (Scheme 2.5) [12]. Therefore, we did not go further into the exemplification of this reactivity.

2.3.4 Conclusions and Perspectives

This overall study has shown that the gold catalyst could promote different, substrate-dependant rearrangements on the enyne precursors that have been tested. These rearrangements can enter in competition as illustrated by the example depicted in Scheme 2.35. The tether, the external propargylic substituent and the nature of the double bond have an influence on the reactivity preference of a considered substrate. One study still have to be done, dealing with the catalyst's influence. For example, we noticed that enyne **86** behaved differently in the presence of a platinum catalyst (Scheme 2.36).

In an attempt to render the 1,5-hydride shift process enantioselective with a chiral bimetallic gold complex [31], a formal Alder-ene product was selectively obtained (Scheme 2.37). This clearly shows that the nature of the catalyst is also at stake in these processes.

2.4 Synthetic Strategy Toward Macrolactones Based on a Gold-Catalyzed Enyne Cycloisomerization

2.4.1 Generality of the *Endo* Cyclization/Ring Expansion of Oxygen-Tethered 1,6-enynes

2.4.1.1 Catalyst Optimization

We briefly looked at the scope of the reactivity displayed by enynes **81** and **82** upon gold catalysis. First, we optimized the reaction of **82** with cationic gold(I) catalyst **38**, running it on a larger scale within a shorter time. We also screened other catalysts, and intriguingly, platinum chloride salts showed no activity toward this cycloisomerization process (Table 2.8, entries 1–3), as well as neutral gold(I) and gold(III) salts, giving sometimes elimination product **121** (entries 4–5).

Pentamethylcyclopentadienyl iridium chloride dimer, which was recently shown by our group to perform *endo* cycloisomerization of nitrogen- and oxygen-tethered enynes, [32] was also inactive (entry 11). However, other cationic gold(I) complexes were able to promote *endo* cyclization. Among them, catalyst **38** and L^5Au^+ with a bulky donor ligand, the latter being generated by chloride abstraction in presence of silver hexafluoroantimonate, were found to be the most efficient. It is worth noting that bulkiness of the ligand seems to play a role, as tri-*tert*-butylphosphine allows the reaction to proceed with efficiency. According to these results, we kept either **38** or L^5Au^+ as catalysts of choice to perform this rearrangement.

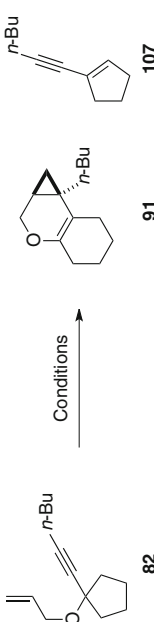
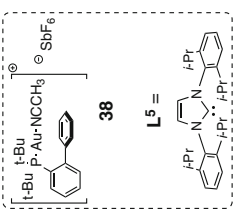
2.4.1.2 Reaction Scope

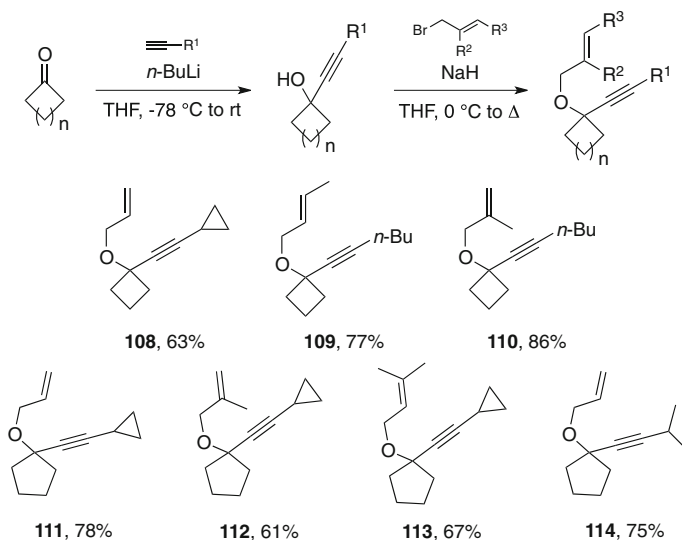
We then synthesized a series of oxygen-tethered 1,6-enynes starting from different commercial cycloalkanones. A two-step sequence consisting of addition of a lithium acetylide onto the carbonyl moiety of the cycloalkanone followed by alkylation with an alkyl bromide in refluxing THF furnish the targeted enyne. According to this procedure, 1,6-enynes **108–114** were synthesized from either cyclobutanone (Scheme 2.38, **108–110**) or cyclopentanone (**111–114**) in yields ranging from 63 to 86 %. We first focus on precursors bearing non terminal alkyne, substituted by various alkyl groups, such as *n*-butyl (**109** and **110**), cyclopropyl (**108**, **111–113**) and isopropyl (**114**).

Four membered-ring precursors **108–110** reacted well when submitted to catalyst **38**, and cleanly afforded compounds **115–117** in good yields (Table 2.9).

Enyne **108** and **110** cleanly afforded in good isolated yields fused tricyclic compounds **115** and **117**, respectively (entries 1 and 3). Cycloisomerization product of **109**, **116** was isolated in a lower yields (entry 2). Apolar by-products, which were not isolated, formed during the reaction. The poor diastereoselectivity


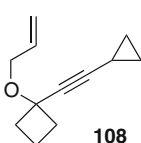
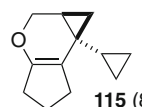
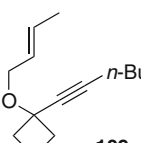
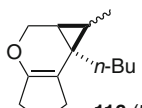
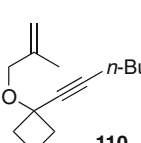
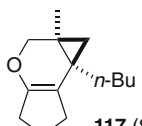
Table 2.8 Catalyst optimization

			
Entry	Conditions	Product(s)	
1	PtCl ₂ (5 mol%), toluene, 80 °C, 5 h	SM	
2	PtCl ₂ (5 mol%), toluene, Δ, 15 h	SM	
3	PtCl ₄ (5 mol%), toluene, 80 °C, 5 h	SM	
4	AuCl (2 mol%), CH ₂ Cl ₂ , rt, 27 h	SM	
5	AuCl ₃ (2 mol%), CH ₂ Cl ₂ , rt, 27 h	SM + 107 , 33%	
6	Ph ₃ PAuCl/AgSbF ₆ (2 mol%), CH ₂ Cl ₂ , rt, 30 min	82 , 50%	
7	(t-Bu) ₃ PAuCl/AgSbF ₆ (2 mol%), CH ₂ Cl ₂ , rt, 1 h 30	82 , 75%	
8	[Ph ₃ PAu]NTf ₂ (2 mol%), CH ₂ Cl ₂ , rt, 30 min	82 , 49%	
9	38 (2 mol%), CH ₂ Cl ₂ , rt, 1 h 30	82 , 84%	
10	L ⁵ AuCl/AgSbF ₆ (2 mol%), CH ₂ Cl ₂ , rt, 1 h 30	82 , 85%	
11	[IrCp*Cl] ₂ (5 mol%), ClCH ₂ CH ₂ Cl, Δ, 12 h	SM	



Scheme 2.38 Synthesis of enynes precursors with a quaternary propargylic center

Table 2.9 Cycloisomerization/ring expansion of enynes **108**–**110** catalyzed by cationic gold(I)

			
Entry	Enyne	Time	Product (yield)
1	 108	4 h	 115 (81%)
2	 109	6 h	 116 (51%, dr 3:2)
3	 110	6 h	 117 (85%)

in this last example suggests that a planar carbocation corresponding to an opened form of the intermediate *endo* cyclopropylcarbene might be involved (see [Chap. 1](#), Sect. 1.3.3).

On the opposite, five-membered ring derivatives **111–114** gave contrasting results. For these enyne precursors, catalyst L^5Au^+ with a NHC ligand gave better results than catalyst **38** (Table 2.10). While enyne **114** reacted well in the presence of catalyst L^5Au^+ (77 % yield, entry 4), substrates with acetylenic cyclopropyl substituents were more capricious. For example product **119** issued from the cycloisomerization of **112** was formed with unidentified polar by-products and was isolated in a poor 37 % yield (entry 2).

In only 2 h, **111** led to a mixture of products from which a major one was isolated and assigned to structure **137** after full-NMR analysis. A mechanistic proposal accounting for the formation of **118** would involve a vinyl cyclopropane rearrangement [33–37]⁸ on cycloisomerization compound **123** leading to the strained tricyclic intermediate **124**. An elimination step would finally lead to compound **118** (Scheme 2.39).

Why this divergence in the reaction outcome is observed remains unanswered. Probably the poor yield of **119** could result from this side reaction, however the related alcohol was not isolated. Regarding to precursor **113**, a considerable amount of allene **121** was detected in the crude reaction mixture after 2 h at room temperature with catalyst L^5Au^+ , starting material being totally consumed. It is likely that this by-product arise from the 1,5-hydride shift/aldehyde elimination reaction that was discussed above (Sect. 1.2.2). This process might be favored in the presence of a prenyl double bond. Only 12 % of the desired cycloisomerized product **120** was isolated (Table 2.10, entry 3). Formation of allenes could possibly be responsible for the moderate yield obtained in the cycloisomerization of enyne **109** (Table 2.9, entry 2).

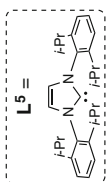
We next turned our attention to precursors remaining unsubstituted at the acetylenic position. We synthesized enynes **125–127** starting from commercially available cycloalkanones (Table 2.11). Alkynylation using *n*-butyllithium in the presence of trimethylsilyl acetylene followed by desilylation under classical methanolysis afforded propargyl alcohols **128–130**. This two steps sequence worked quite well except the addition onto indanone (entry 2) which proved to be difficult (41 % yield), probably because dehydration of alcohol **129** might occur. Final alkylation in DMF delivered the *O*-tethered 1,6-enynes **125–127**. In the case of substrates **125** and **126**, an impurity remained after column chromatography that could be eliminated by Kugelrohr distillation, but seriously decreasing the overall yield (entries 1 and 2).

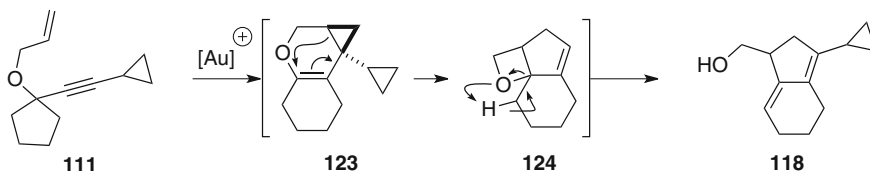
The results of the gold-catalyzed rearrangements of enynes **125–127** are summarized in Table 2.12. Gold-catalyzed reaction of **125** led to a mixture of

⁸ See also: [37].

Table 2.10 Cycloisomerization/ring expansion of enynes **111**–**114** catalyzed by cationic gold(I)

Entry	Enyne	Time	Product (yield)	
1		2 h	 118 (50%)	
2		18 h	 119 (37%)	
3		2 h	 120 (12%)	 121 (48%)
4		5 h	 122 (77%)	





Scheme 2.39 Mechanistic rationale for the cycloisomerization of **111**

cyclopropanation/ring expansion product **130** and skeletal rearrangement product **131** (entry 1). Enyne **126** produced an unseparable mixture of several compounds when submitted to catalyst **38**, in which the ring expansion product **132** was the major component. Purification by flash column chromatography did not allowed the isolation of pure **132**, but the yield could be assessed by ^1H NMR of the fraction containing the cyclized compound (entry 2). The crude reaction mixture resulting from submission of enyne **127**, bearing a prenyl double bond, to catalyst **38**, did not reveal any ring expansion product at all. In place, skeletal rearrangement compounds **133** and **134** were isolated in 11 and 58 % yield, respectively (entry 3).

These results clearly indicate that skeletal rearrangement enters in competition with *endo* cyclopropanation for 1,6-enynes bearing no acetylenic substituents (entries 1 and 3). They are sometimes exclusive as demonstrated with the cycloisomerization of **127**, bearing a prenyl double bond (entry 3).⁹

2.4.2 Access to Ketomacrolactones from Ring-Expansion Products

The platinum- and gold-catalyzed cycloisomerization of 1,6-enynes into bicyclo[3.1.0]heptene derivatives, through an endocyclic cyclopropylcarbene, was rarely applied to natural and/or biologically active compounds [39–41]. By our side, we envisioned the possible access to ketomacrolactones from of cycloisomerization/ring expansion products by realizing first the oxidative cleavage of the enol ether, followed by cyclopropane opening (Scheme 2.40).

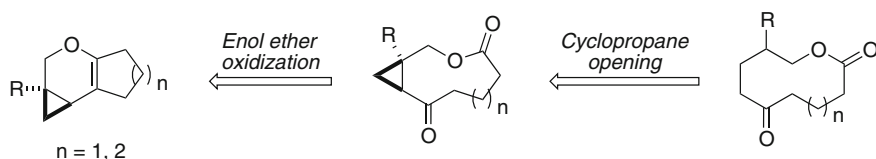
It is worth noting that the 5-ketodecalactone skeleton we could obtain by this synthetic sequence is found in some natural products of biological interest, such as diplodialide D, sporostatin and xestodecalactone A (Scheme 2.41).

In order to validate our approach, we chose **91** as a model substrate. The oxidative cleavage of its enol ether moiety was successfully realized using either pyridinium chlorochromate [42] or a combination of ruthenium dioxide and sodium periodate, [43] and 10-membered ring lactone **136** was isolated in similar yields (Table 2.13).

⁹ For a study where prenyl double bonds showed distinct behaviors, see Ref. [38].

Table 2.11 Synthesis of 1,6-enynes **125–127**

Entry	Ketone	Propargyl alcohol	Bromide	Product (yield, 3 steps)
1				
2			idem	
3				



Scheme 2.40 Envisioned approach to the 5-ketodecalactone and 6-ketoundecalactone skeletons

Table 2.13 Oxidative cleavage of enol ether **91**

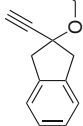
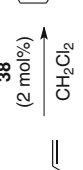
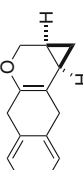

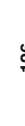






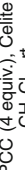

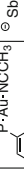

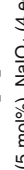





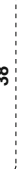




















































































<p>91</p>	<p>Conditions</p> <p>→</p>	<p>136</p>
	<p>PCC (4 equiv.), Celite CH₂Cl₂, rt</p>	<p>58%</p>
	<p>RuO₂ (5 mol%), NaIO₄ (4 equiv.) CCl₄/H₂O 1:1</p>	<p>59%</p>

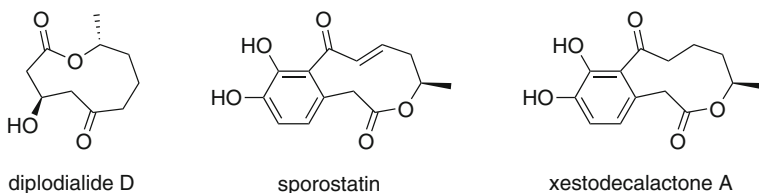
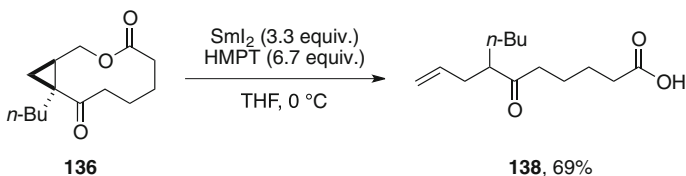
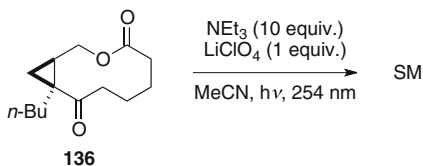
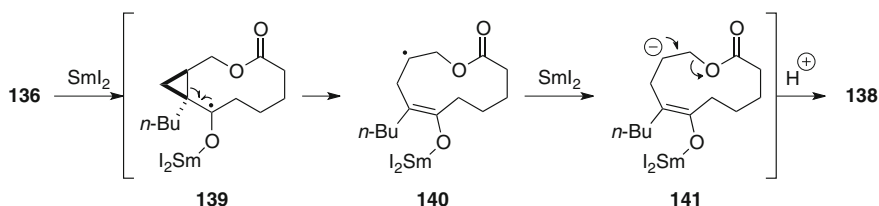
Encouraged by these results, we applied these oxidation conditions to the mixture from which we were not able to isolate **133**, the cycloisomerization product of **126**. We expected that the polar ketolactone thus obtained could be easily separated from the other unidentified components of the mixture. However, a totally different outcome was reached with enol ether **133**, and aromatized naphthyl derivative **136** was obtained, in excellent yield with ruthenium dioxide. When ozone was used as the oxidant, only a mixture of products from which **137** could be isolated in poor yield. To the best of our knowledge, such reaction had never been reported. It seems that aromaticity of the final compound may act as a driving force that discriminates oxidative cleavage of the double bond in favor of aromatization (Table 2.14).

We then tried several methods to open the cyclopropane in compound **136**. We assumed that the presence of a carbonyl group in α position might facilitate its opening through radical-based methodologies. We first tried a photochemical procedure consisting in irradiation in the presence of NEt₃ and LiClO₄, reported by Cossy et al. [44]. Unfortunately, in these conditions, the starting material was totally recovered (Scheme 2.42).

Several reports describe samarium diiodide as a good reductor of cyclopropyl ketones. We tried the conditions reported by the team of Motherwell (SmI₂, HMPT in THF) [45] and this time the starting material was fully consumed, but led to the linear carboxylic acid derivative **138** (Scheme 2.43).

Table 2.14 Oxidation of cyclized compound **133**

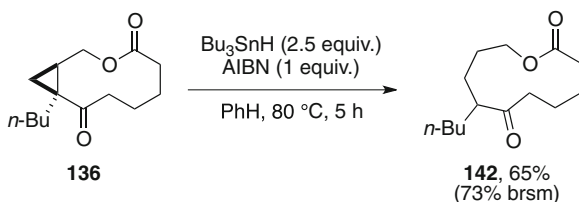
 <p>126</p>	 <p>38</p>	 <p>133</p>	 <p>137</p>
 <p>126</p>	 <p>38</p>	 <p>133</p>	 <p>137</p>
 <p>126</p>	 <p>38</p>	 <p>133</p>	 <p>137</p>
 <p>126</p>	 <p>38</p>	 <p>133</p>	 <p>137</p>
 <p>126</p>	 <p>38</p>	 <p>133</p>	 <p>137</p>
 <p>126</p>	 <p>38</p>	 <p>133</p>	 <p>137</p>
 <p>126</p>	 <p>38</p>	 <p>133</p>	 <p>137</p>
 <p>126</p>	 <p>38</p>	 <p>133</p>	 <p>137</p>
 <p>126</p>	 <p>38</p>	 <p>133</p>	 <p>137</p>
 <p>126</p>	 <p>38</p>	 <p>133</p>	 <p>137</p>
 <p>126</p>	 <p>38</p>	 <p>133</p>	 <p>137</p>
 <p>126</p>	 <p>38</p>	 <p>133</p>	 <p>137</p>
 <p>126</p>	 <p>38</p>	 <p>133</p>	 <p>137</p>
 <p>126</p>	 <p>38</p>	 <p>133</p>	 <p>137</p>
 <p>126</p>	 <p>38</p>	 <p>133</p>	 <p>137</p>
 <p>126</p>	 <p>38</p>	 <p>133</p>	 <p>137</p>
 <p>126</p>	 <p>38</p>	 <p>133</p>	 <p>137</p>
 <p>126</p>	 <p>38</p>	 <p>133</p>	 <p>137</p>
 <p>126</p>	 <p>38</p>	 <p>133</p>	 <p>137</p>
 <p>126</p>	 <p>38</p>	 <p>133</p>	 <p>137</p>
 <p>126</p>	 <p>38</p>	 <p>133</p>	 <p>137</p>
 <p>126</p>	 <p>38</p>	 <p>133</p>	 <p>137</p>
 <p>126</p>	 <p>38</p>	 <p>133</p>	 <p>137</p>
 <p>126</p>	 <p>38</p>	 <p>133</p>	 <p>137</p>
 <p>126</p>	 <p>38</p>	 <p>133</p>	 <p>137</p>
 <p>126</p>	 <p>38</p>	 <p>133</p>	 <p>137</p>
 <p>126</p>	 <p>38</p>		

**Scheme 2.41** Natural products exhibiting the 5-ketodecalactone skeleton**Scheme 2.42** Failed attempt to open cyclopropane in **136** photochemically**Scheme 2.43** Reaction of cyclopropylketolactone **136** with SmI_2 **Scheme 2.44** Mechanism accounting for the formation of **138**

Although the cyclopropane was indeed opened, product **138** was certainly not the one expected. The following mechanism can account for the formation of this product: first, reaction of samarium diiodide with the keto group generates ketyl radical **139**, and cyclopropane opening led to the corresponding enolate **158**. A fast reduction of the secondary radical then occurs, accompanied by departure of the carboxylate group to lead, after protonation, to acid derivative **156** (Scheme 2.44).

Clearly the fast reduction of radical **158** must be avoided to get selectively the product of cyclopropane opening. This could be achieved if a good hydrogen donor is present in the reaction mixture. For this purpose the use of the combination of tributyltin hydride and azo-isobutyronitrile (AIBN) appeared as a

Scheme 2.45 Successful opening of cyclopropane **136** to the 5-ketodecalactone skeleton



satisfying option [46]. Application of these reaction conditions to **136** gratifyingly led to the desired 11-membered ring lactone **142**. Let us underline that full conversion was not reached, but the reaction conditions have not been optimized to date (Scheme 2.45). Thus, our approach was validated starting from model substrate **91**.

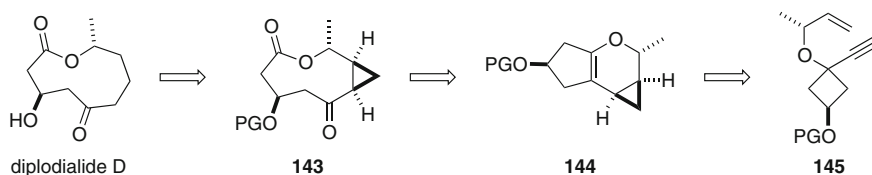
2.4.3 Perspective: Toward the Total Synthesis of *Diplodialide D*

We envisioned a possible total synthesis of diplodialide D through the below depicted retrosynthetic analysis: the aimed 5-ketodecalactone could be built from cyclopropyl ketone **143** by a sequence of deprotection and cyclopropane opening steps. **143** would result from the oxidative cleavage of enol ether **144**, the latter coming from the gold-catalyzed cyclosomerization of enyne **145** (Scheme 2.46).

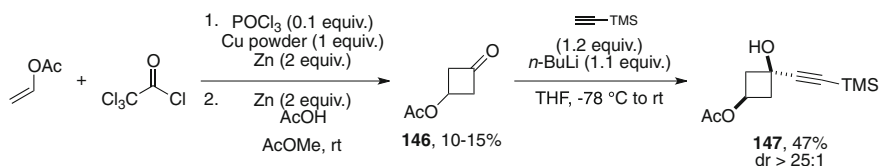
Therefore, we started the synthesis of enyne **163**. Cyclobutanone **164** was first synthesized through a one-pot procedure by reaction of trichloroacetyl chloride and vinyl acetate in the presence of copper and zinc [47]. Addition of trimethylsilyl lithium acetylide furnished alcohol **165** in an acceptable yield, which relative *syn* configuration was addressed according to literature precedents (Scheme 2.47) [48–50].

The functionalization of alcohol **147–145** proved to be difficult. Classical conditions involving deprotonation of the alcohol and alkylation with an alkyl bromide were dispelled as competitive $\text{S}_{\text{N}}2'$ could lead to a mixture of products. Several methodologies based on Lewis acid-assisted propargylic substitution were reported in the literature, but either sodium tetrachloroaurate, [51] copper bromide [52] or bismuth chloride [53] resulted in recovery of the starting material, even at higher temperature than used in the original reports. Another procedure was reported by the team of Toste that did not rely on a Lewis acid activation but is supposed to proceed through an allenic intermediate resulting from the 3,3-sigmatropic shift of an oxopropargyloxyrhenium species [54]. Unfortunately, these new conditions failed to give the desired product (Scheme 2.48).

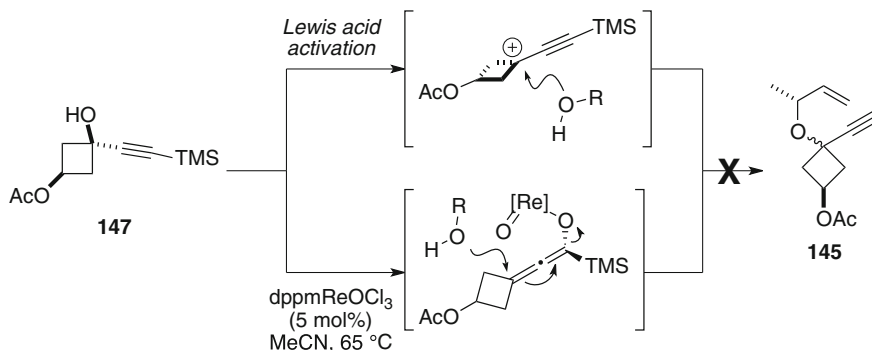
Other possibilities could be envisioned for the synthesis of **145**: other Lewis, and even Brønsted acid could be assessed, and the Nicholas reaction could also be a solution. Otherwise, direct allylation via a π -allyl transition metal complex can



Scheme 2.46 Retrosynthetic analysis of dipodialide D



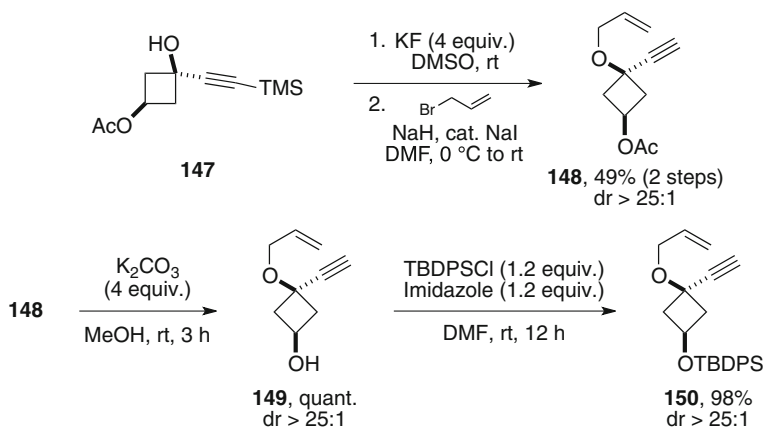
Scheme 2.47 Toward the synthesis of enyne **147**



Scheme 2.48 Failed attempts to realize the last step in the synthesis of **145**

also be envisioned. For time reason, all these methods have not been tried. However, to get an idea of the behaviour of enynes of type **145** bearing a substituted cyclobutane ring, we synthesized enynes **148–150**. Propargyl alcohol was first desilylated using potassium fluoride, and classic alkylation in the presence of sodium hydride furnished enyne **148**. Further steps allowed variation of the hydroxy protecting group (Scheme 2.49).

The submission of these precursors to gold catalysts gave unfortunately disappointing results (Table 2.15). Hydroxy-protected enynes **148** and **150** reacted slowly, and gave skeletal reorganization products **151** and **152** in moderate yields (entries 1 and 3). Catalyst **38** was inactive toward enyne **150**, but cationic gold(I) catalyst $[\text{Ph}_3\text{PAu}]\text{NTf}_2$ led to complete conversion overnight. Only traces of cyclopropanic products could be observed in the crude reaction mixtures of **148** and **150** that we did not manage to isolate. Regarding enyne **149**, its reaction with



Scheme 2.49 Synthesis of 1,6-enynes **148**–**150**

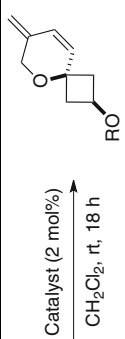
cationic phosphinegold(I) catalyst **38** led to an unseparable, complex mixture of unidentified compounds (Table 2.15).

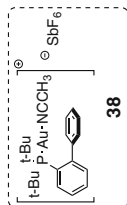
These results predict a consequent work of optimization for the gold-catalyzed key-step en route to diplodialide D. A fine tuning between the catalyst, the hydroxy-protecting group and the reaction conditions should be found to promote the desired, selective cycloisomerization of these cyclobutane-based enynes.

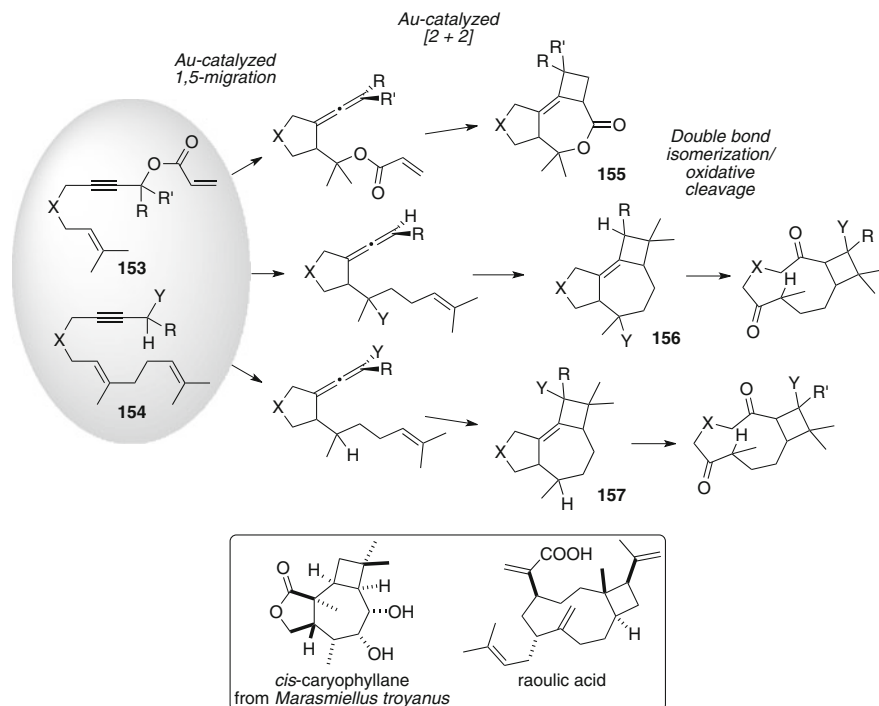
2.5 Conclusion and Perspectives

This work on 1,6-enynes enlightens and illustrates well the “substrate dependency” frequently met in the cycloisomerizations of enynes upon carbophilic activation. It is further amplified if working with substrates decorated with various functional groups inserted at key position in the enyne backbone. To our part, we disclosed that donor groups at the external propargylic position could promote a 1,5-migration process triggered by the 5-*exo* cyclization of a prenyl double bond onto the gold-activated alkyne. Interesting findings were also done with oxygen-tethered enynes: with prenyl double bonds, a 1,5-hydride shift followed by dimethylacrolein elimination can give rise to allene, while inserting a strained cycloalkane at the internal propargylic position can lead to products of *endo* cyclization with expansion of the strained ring. Synthetic value was brought to these products, as they were efficiently transformed into ketomacrolactones. A total synthesis of natural product diplodialide D was begun. To put an end to this chapter, we would like to give a prospect for the 1,5-migration process. Considering acrylate derivative **153** or geraniol-based enyne **154**, a gold-catalyzed 1,5-migration should give rise to the corresponding 1,7-allenene compounds (Scheme 2.50). Gold is also known to promote the [2 + 2] cycloaddition of

Table 2.15 Cycloisomerization reactions of enynes **148–150**

Entry	Enyne			Product (yield)
		Catalyst		
1		38	151 (53%) dr > 25:1	
2		idem	complex mixture	
3		$[\text{Ph}_3\text{PAu}]\text{NTf}_2$	152 (40%) dr > 25:1	





Scheme 2.50 Perspective: a tandem, gold-catalyzed 1,5-migration/[2 + 2] cycloaddition reaction

allenes. It would be therefore possible that, at this stage, these allenes underwent a [2 + 2] cycloaddition, thus leading to tricyclic compounds **155–157**, which skeletons resemble to those of some members of the caryophyllane family (Scheme 2.50, box). To go further, it would be also possible after isomerization and oxidative cleavage of the double bond to access the bicyclo[8.2.0]dodecane skeleton of raoulic acid (Scheme 2.50, box).

References

1. Alberico D, Scott ME, Lautens M (2007) *Chem Rev* 107:174
2. Bergman RG (2007) *Nature* 446:391
3. Godula K, Sames D (2006) *Science* 312:67
4. Davies HML (2006) *Angew Chem Int Ed* 45:6422
5. C-H Activation in *Topics in Current Chemistry*; Yu, J.-Q.; Shi, M. Ed; 2010, Vol 292
6. Pastine SJ, McQuaid KM, Sames D (2005) *J Am Chem Soc* 127:12180
7. McQuaid KM, Long JZ, Sames D (2009) *Org Lett* 11:2972
8. McQuaid KM, Sames D (2009) *J Am Chem Soc* 131:402
9. Zhang SY, Zhang FM, Tu YQ (1937) *Chem Soc Rev* 2011:40
10. Vadola PA, Sames D (2009) *J Am Chem Soc* 131:16525

11. Jurberg ID, Odabachian Y, Gagosz F (2010) *J Am Chem Soc* 132:3543
12. Bolte B, Odabachian Y, Gagosz F (2010) *J Am Chem Soc* 132:7294
13. Bolte B, Gagosz F (2011) *J Am Chem Soc* 133:7696
14. Zhou G, Zhang J (2010) *Chem Commun* 46:6593
15. Zhou G, Liu F, Zhang J (2011) *Chem Eur J* 17:3101
16. Vasu D, Das A, Liu RS (2010) *Chem Commun* 46:4115
17. Shu XZ, Ji KG, Zhao SC, Zheng ZJ, Chen J, Lu L, Liu XY, Liang YM (2008) *Chem Eur J* 14:10556
18. Horino Y, Yamamoto T, Ueda K, Kuroda S, Toste FD (2009) *J Am Chem Soc* 131:2809
19. Funami H, Kusama H, Iwasawa N (2007) *Angew Chem Int Ed* 46:909
20. Oh CH, Lee JH, Lee SM, Yi HJ, Hong CS (2009) *Chem Eur J* 15:71
21. Cadran N, Cariou K, Hervé G, Aubert C, Fensterbank L, Malacria M, Marco-Contelles J (2004) *J Am Chem Soc* 126:3408
22. Lemiere G, Gandon V, Ageton N, Goddard JP, de Kozak A, Aubert C, Fensterbank L, Malacria M (2006) *Angew Chem Int Ed* 45:7596
23. Ji KG, Shu XZ, Zhao SC, Zhu HT, Niu YN, Liu XY, Liang YM (2009) *Org Lett* 11:3206
24. Herrero-Gomez E, Nieto-Oberhuber C, Lopez S, Benet-Buchholz J, Echavarren AM (2006) *Angew Chem Int Ed* 45:5455
25. Ye L, Chen Q, Zhang JC, Michelet V (2009) *J Org Chem* 74:9550
26. Gung BW, Bailey LN, Craft DT, Barnes CL, Kirschbaum K (2010) *Organometallics* 29:3450
27. Bieber LW, da Silva MF (2007) *Tetrahedron Lett* 48:7088
28. Lee JH, Toste FD (2007) *Angew Chem Int Ed* 46:912
29. Lemiere G, Gandon V, Cariou K, Fukuyama T, Dhiman AL, Fensterbank L, Malacria M (2007) *Org Lett* 9:2207
30. Muñoz MP, Adrio J, Carretero JC, Echavarren AM (2005) *Organometallics* 24:1293
31. Benedetti E, Simonneau A, Hours A, Amouri H, Penoni A, Palmisano G, Malacria M, Goddard JP, Fensterbank L (1908) *Adv Synth Catal* 2011:353
32. Neureiter N (1959) *J Org Chem* 24:2044
33. Overberger CG, Borchert AE (1960) *J Am Chem Soc* 82:1007
34. Overberger CG, Borchert AE (1960) *J Am Chem Soc* 82:4896
35. Vogel E (1960) *Angew Chem* 72:4
36. Tomas HT, Reed JW (1991) Rearrangements of Vinylcyclopropanes and related systems. In: Trost BM, Fleming I (eds) *Comprehensive organic synthesis*, vol 5. Pergamon, Oxford, pp 899–970
37. Harrak Y, Makhoul M, Azzaro S, Mainetti E, Romero JML, Cariou K, Gandon V, Goddard JP, Malacria M, Fensterbank L (2011) *J Organomet Chem* 696:388
38. Deschamps NM, Elitzin VI, Liu B, Mitchell MB, Sharp MJ, Tabet EA (2011) *J Org Chem* 76:712
39. Elitzin VI, Liu B, Sharp MJ, Tabet EA (2011) *Tetrahedron Lett* 52:3518
40. Teller H, Fürstner A (2011) *Chem Eur J* 17:7764
41. Baskaran S, Islam I, Raghavan M, Chandrasekaran S (1987) *Chem Lett* 1175
42. Lu H, Yuan X, Zhu S, Sun C, Li C (2008) *J Org Chem* 73:8665
43. Cossy J, Furet N (1993) *Tetrahedron Lett* 34:8107
44. Batey RA, Motherwell WB (1991) *Tetrahedron Lett* 32:6211
45. Enholm EJ, Zhaozhong JJ (1997) *J Org Chem* 62:174
46. Zajac MA (2008) *Tetrahedron Lett* 49:4763
47. Jain R, Sponsler MB, Combs FD, Dougherty DA (1988) *J Am Chem Soc* 110:1356
48. Seiser T, Cramer N (2008) *Angew Chem Int Ed* 47:9294
49. Creary X, Kochly ED (2009) *J Org Chem* 74:9044
50. Georgy M, Boucard V, Campagne J-M (2005) *J Am Chem Soc* 127:14180
51. Hui H-H, Zhao Q, Yang M-Y, She D-B, Chen M, Huang G-S (2007) *Synthesis* 191
52. Zhan Z-P, Yang W-Z, Yang R-F, Yu J-L, Li J-P, Liu H-J (2006) *Chem Commun* 3352
53. Sherry BD, Radosevich AT, Toste FD (2003) *J Am Chem Soc* 125:6076
54. Luzung MR, Mauleon P, Toste FD (2007) *J Am Chem Soc* 129:12402

Chapter 3

Synthesis of Polyconjugated Bis-Enones Through a Gold-Catalyzed 1,3-Acyloxy Migration-Cyclization-1,5-Acyl Shift Cascade Reaction

The following part will deal with a new reaction we designed in our laboratory. Initial gold catalyzed rearrangement into an allenyl ester triggers a series of elementary steps to fully rearrange the starting material. Before the results being presented and discussed, we will shortly introduce the reactivities accessible from allenyl esters upon gold catalysis and focus on their use in allenyne-type cycloisomerizations.

3.1 Introduction

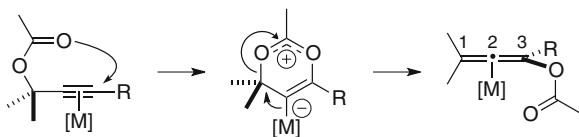
3.1.1 Bibliography

3.1.1.1 Allenyl Esters and Gold Catalysis: Generation and Reactivity

We have seen in [Chap. 1](#) that propargylic esters could rearrange upon gold or platinum catalysis in two manners affording a metal carbene, mainly in the case of terminal alkynes, or an allenyl ester (Scheme 3.1). The rearrangement of propargylic acetates into allenyl esters offers a myriad of possible further reactivity, as allene species are known to be activated by π -acidic transition metal such as gold [1].

The bonding mode of gold to allenyl esters has been the subject of a computational and experimental study in our group [2], which disclosed the η^1 , C2-coordination mode to be the most favored. These gold complexes exhibit a more or less distorted allylic cation structure, depending on the allenyl ester substitution pattern (for practical reason we decided to represent it as depicted in Scheme 3.1). The delocalized cation character of these complexes makes them prompt to undergo a variety of rearrangements/reactions. For example, Zhang has shown it was possible to access Knoevenagel products through a 1,3-acyl shift upon cationic gold(I) catalysis (Scheme 3.2) [3]. Propargylic acetate **1** is first rearranged into allenyl ester **4** which upon gold coordination can evolve to the

Scheme 3.1 Rearrangement of propargylic esters into allenyl esters



reactive oxonium **5**. Reaction between the σ Au–C bond with the neighboring carbonyl results in strained oxetanium **6** which opening delivers Knoevenagel compound **3**. In hydrated conditions, intermediate **5** can also be hydrolyzed by a molecule of water to furnish α,β -unsaturated ketones and acetic acid [4, 5].

The cationic character of the gold complexed allenyl ester is also illustrated by the opening of small strained rings linked to the propargylic position, as studied by Gevorgyan [6] and Nevado [7–9] (Scheme 3.3).

Starting from the gold-complexed allenyl ester, the appearance of a formal positive charge at C1 in Gevorgyan's case triggers a Wagner–Meerwein rearrangement giving diene **8** after proton elimination/deauration. In Nevado's case, the formal positive charge at C3 is responsible for the opening of the cyclopropane ring in **TS**₁₃₋₁₀ that leads to cyclopentene derivative **10** (Scheme 3.4). It is worth noting that in Nevado's study, chirality transfers from the cyclopropane configuration to the final product have been observed, thanks to the “nonclassical” character of the gold stabilized cation **TS**₁₃₋₁₀ that retains the chiral information. However, competition with the cyclopropane opening leading to a “classic” carbocation prevented the transfer to be complete.

Activation of one double bond of the allenyl ester make it sensitive to nucleophilic attack at one of the two external carbons,¹ giving rise to hydroalkoxylation, hydroamination and hydroarylation products (Scheme 3.5).²

With π -systems as nucleophiles (alkenes, dienes, alkynes, allenes, ketones...), the formation of a bond at the external allene carbon may be followed, in a stepwise or asynchronous concerted fashion, by the creation of a second C–C bond at the other end (Scheme 3.6). Thus, allenyl esters can also be activated as formal 3-carbon dipoles of type **14** in $[3C + n]$ cycloaddition reactions.³ The isolated product will then depend on the evolution or trapping of the resulting cyclic carbene **16**.⁴ On the other hand, the cationic intermediate **15** can be trapped by nucleophiles such as alcohols, amines or arenes.

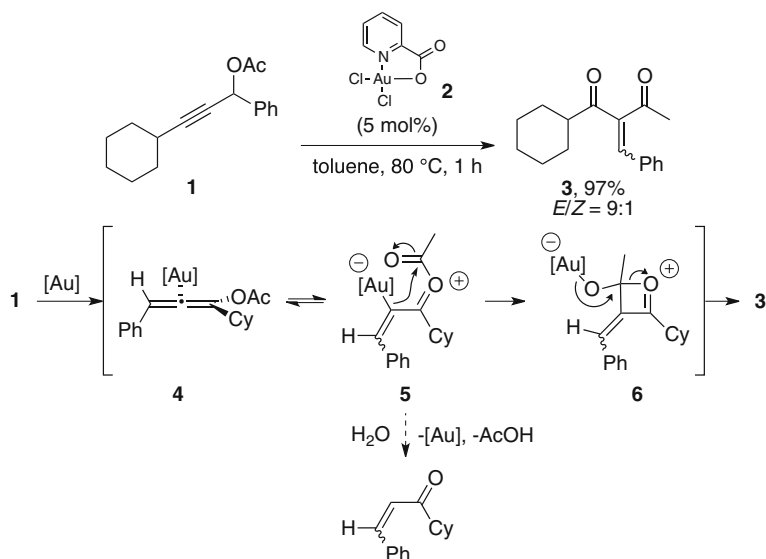
Allenyl esters, as electron rich allenes, can also act as nucleophiles in gold-catalyzed reactions, when a neighbouring gold-activated triple bond is present on the molecule, resulting in an allenyne-type reactivity (see Chap. 1, Sect. 1.6).

¹ To the best of our knowledge, the only example of nucleophilic attack at the central carbon atom of the allenyl ester was reported in the hydration of α -acyloxy- α -alkynyl silanes, thanks to the β -silicon effect, see: [10].

² Selected examples, *O*-nucleophiles [11, 12], *N*-nucleophiles [13], *C*-nucleophiles [14, 15].

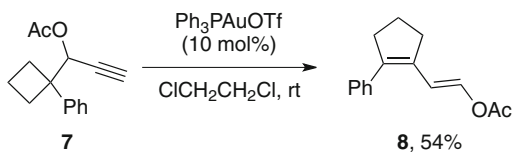
³ Selected examples, $[2 + 2]$ [16], $[3 + 2]$ [17], $[4 + 3]$ [18, 19], Nazarov [20].

⁴ For intramolecular trapping of this carbene with double bonds in the metal-Nazarov reaction of vinyl allenyl esters, see: [21, 22].

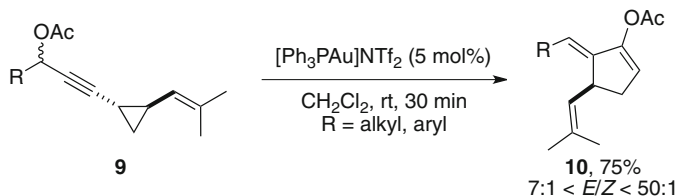


Scheme 3.2 Au-catalyzed rearrangement of propargylic acetates through a 1,3-acyl shift

Gevorgyan



Nevado

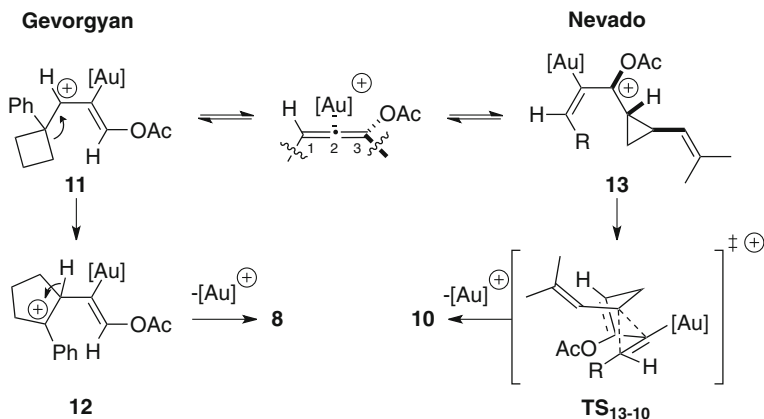


Scheme 3.3 Opening of small ring through rearrangement of propargylic acetates

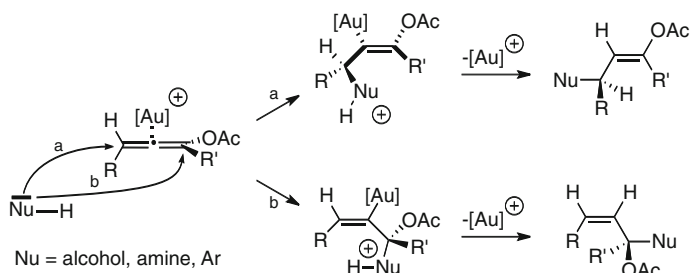
3.1.1.2 Allenyl Esters as Nucleophiles in Allenynes Systems

The first example where allenyl esters displayed this reactivity was performed by our team with platinum (Scheme 3.7) [23].

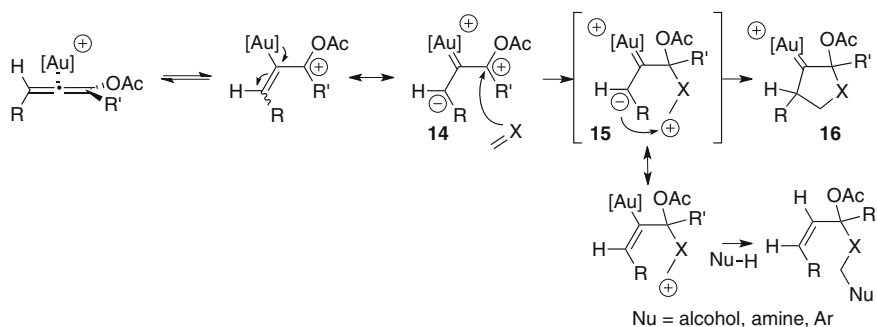
Starting from diynyl ester **17**, a platinum-catalyzed 1,3-OAc shift generates allenynyl ester **19** which undergoes cycloisomerization to furnish bicyclic derivative **20**. Subsequent methanolysis furnish ketone **18**.



Scheme 3.4 A cationic interpretation for the mechanisms leading to **8** and **10**

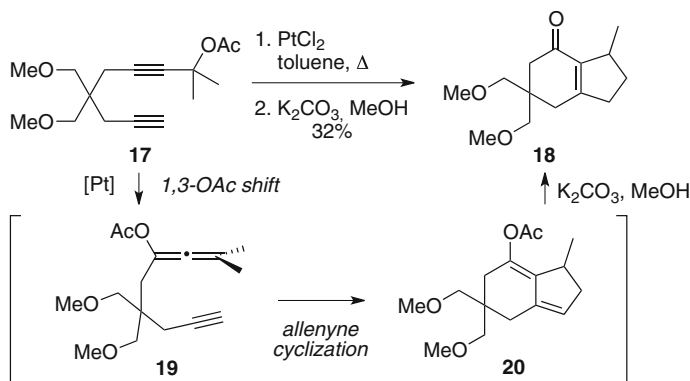


Scheme 3.5 Nucleophilic attack onto a gold activated allenyl ester

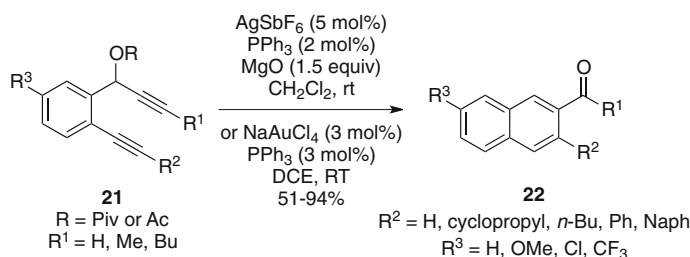


Scheme 3.6 Reaction of a gold activated allenyl ester with π -systems

A couple of years later, Toste and co-workers developed a tandem process based on the same strategy, starting from ene-diynes **21** and leading to aromatic ketones **22** (Scheme 3.8) [24]. Better yields were obtained by the use of silver salts



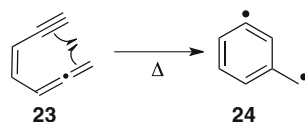
Scheme 3.7 Diynyl esters for in situ generation of allenynyl esters followed by allenyne-type cyclization



Scheme 3.8 Synthesis of aromatic ketones with silver or gold catalysts

Scheme 3.9 Myers-Saito rearrangement

Myers-Saito cyclization of yne-ene-allene:



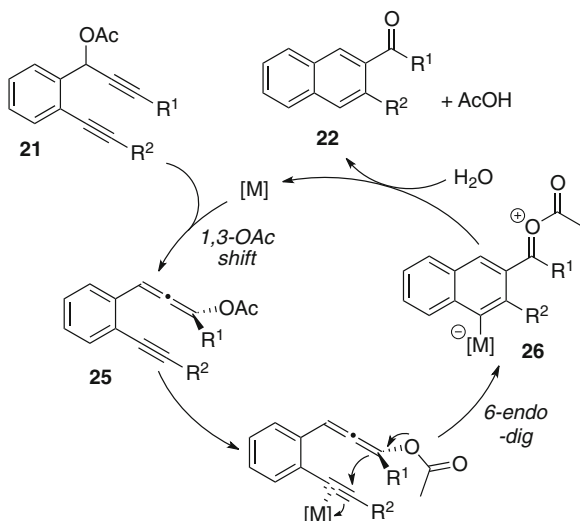
but the team of Oh have shown that gold(III) salts in combination with triphenylphosphine was also a efficient catalytic system for this reaction [25].

This transformation is the first efficient transition metal-catalyzed equivalent of the Myers-Saito cyclization that consists in the thermal cyclization of (*Z*)-allene-ene-yne systems **23** through 1,4-biradical intermediates **24** (Scheme 3.9).^{5,6}

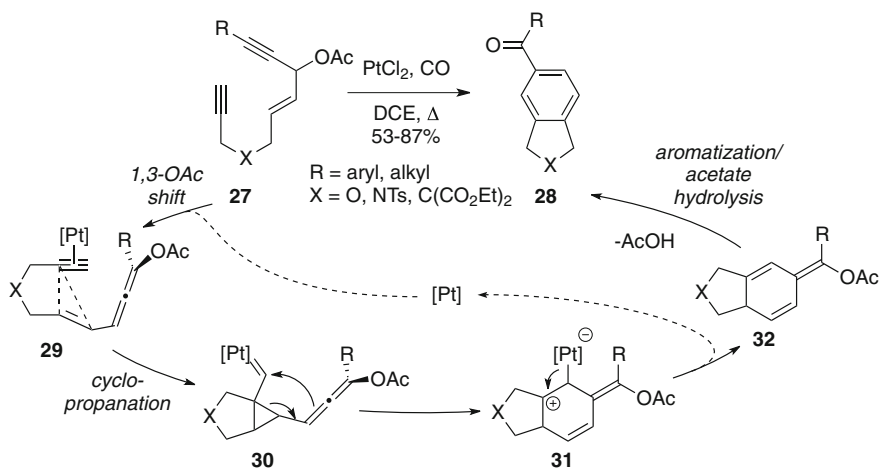
The mechanism begins with allenyl-ester **25** generation upon π -Lewis acid catalysis (Scheme 3.10). Then, upon activation of the triple bond, a 6-*endo* cyclization takes place affording naphthyl metal oxonium **26** which is further hydrolyzed to give aromatic ketone **22** and acetic acid. The use of MgO in Toste's

⁵ Mo-mediated carbonylation of allenyl arene-yne gave by-products derived from the Myers-Saito rearrangement, see [26].

⁶ For seminal works on the Myers-Saito rearrangement, see [27, 28].



Scheme 3.10 Mechanistic rationale accounting for the formation of aromatic ketones

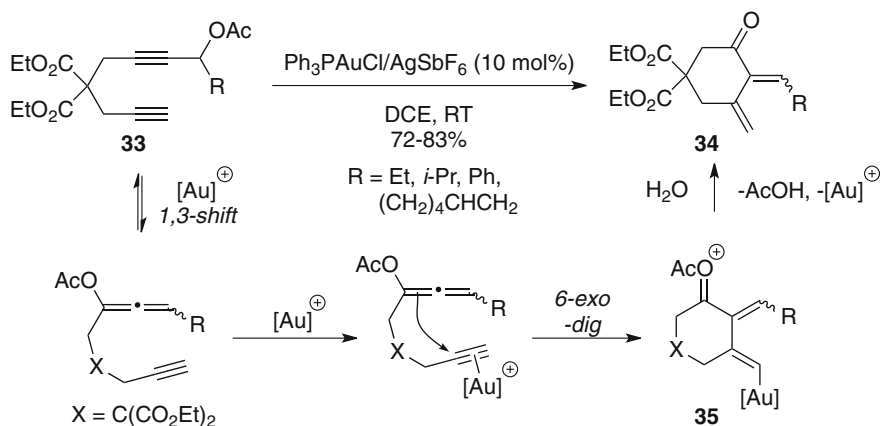


Scheme 3.11 Liang's synthesis of aromatic ketones

conditions is aimed at scavenging this equivalent of released acid at the end of the catalytic cycle. The reaction is not limited to phenyl-tethered substrates, which can be replaced by either pyrroles [24] or simple double bonds [29].

A similar approach for the construction of aromatic rings was lately designed by Liang, which relies on the coupling of a 1,6-enyne cycloisomerization and a [3, 3] sigmatropic rearrangement of a propargylic ester (Scheme 3.11).

It is worthy to note that this is a rare case of platinum superiority over gold in a cycloisomerization reaction involving a 3,3-sigmatropic shift of a propargylic



Scheme 3.12 Ketone synthesis through a tandem 1,3-OAc shift/allenyne cyclization pathway

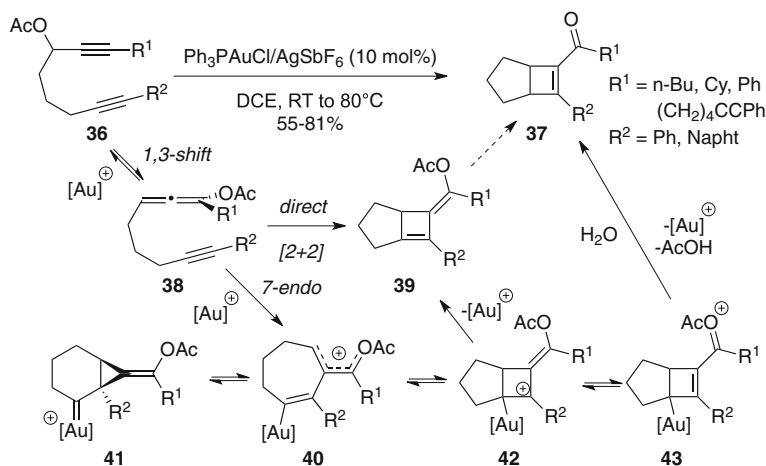
acetate, the latter (cationic and neutral gold(I), gold(III)) only leading to traces of desired product and/or decomposition [30]. This allowed them to obtain bicyclic compounds **28** through a two-sequences mechanism. After generation of allenyl ester **29**, the cyclization of the 1,6-enyne moiety occurs, giving rise to a cyclopropyl platinum carbene **30** that further rearranges⁷ to give carbocation **31**. Finally, elimination of platinum gives the formal Diels-Alder adduct **32**, which is converted into aromatic ketone **28** through an isomerization/aromatization sequence accompanied by a loss of acetic acid.

The group of Oh also explored the reactivity of diynyl esters toward gold catalysis. Thus, they were able to cyclize 1,6-diynyl acetates **33** into 2,3-bis(alkylidene)cycloalkanones **34** in the presence of phosphinegold(I) salts (Scheme 3.12). Again, a tandem 1,3-OAc shift/allenyne cyclization pathway is responsible for the formation of the cyclic ketone. Upon activation of the triple bond by gold, nucleophilic attack from the electron-rich allene occurs in a 6-*exo-dig* manner to give delocalized acylium **35**. Then, hydrolysis and protodeauration afford the desired diene **34**. Interestingly, when a third carbon-carbon non-terminal triple bond was added to the cyclization precursor the authors obtained fused tricyclic compounds arising from a further intramolecular [4 + 2] cycloaddition/oxidation sequence.

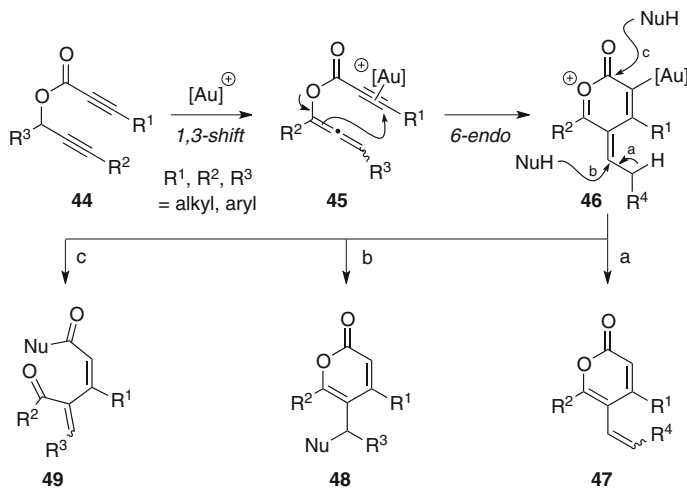
In the continuity of this work, Oh's group studied 1,7-diynyl esters **36** bearing this time the migrating acetate in internal position [32]. The outcome of the reaction, using the same catalytic system, was directed towards formal [2 + 2] cycloaddition products **37** (Scheme 3.13).

The reaction mechanism is not clear and the authors were not able to state for the most probable pathway. They yet proposed a direct [2 + 2] cycloaddition

⁷ Comparable intermediates were invoked in the intramolecular Diels-Alder reaction of dienyynes, see [31].

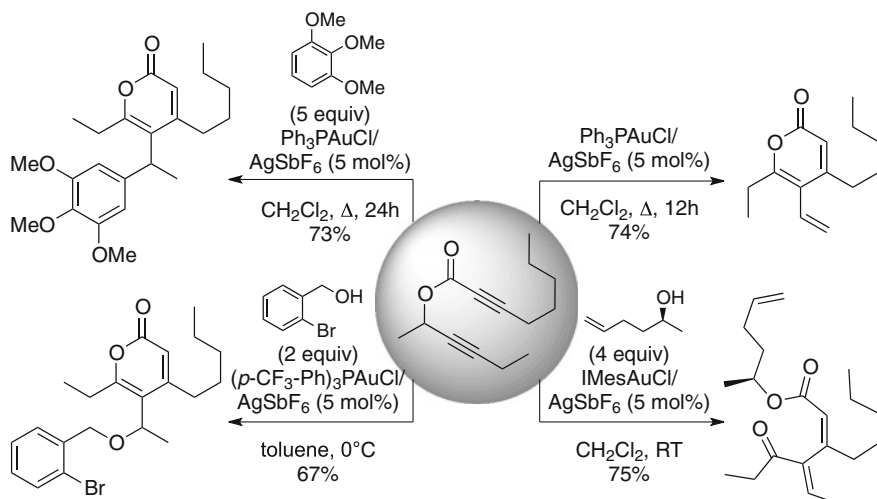


Scheme 3.13 Formal [2 + 2] cycloaddition of 1,7-diynyl esters



Scheme 3.14 Schreiber's strategy for the synthesis of variously substituted α -pyrones

pathway from the allenynyl-ester **38** to cyclobutenylidene **39**, followed by hydrolysis, but no experimental evidence of this intermediate was collected. Thoughtfully, one can imagine that a gold-promoted 7-endo-dig cyclization could take place affording delocalized carbocation **40**. The latter is probably in equilibrium with cyclopropylcarbene **41** and with the two bicyclic intermediates **42** and **43**. Carbocation **42**, relatively stable due to its possible delocalization to aromatic R^2 group, could evolve, through gold elimination, to product **39**. Otherwise, acylium **43** could undergo hydrolysis and subsequent protodeauration would give the bicyclo[3.2.0]ketone **37** (Scheme 3.13).

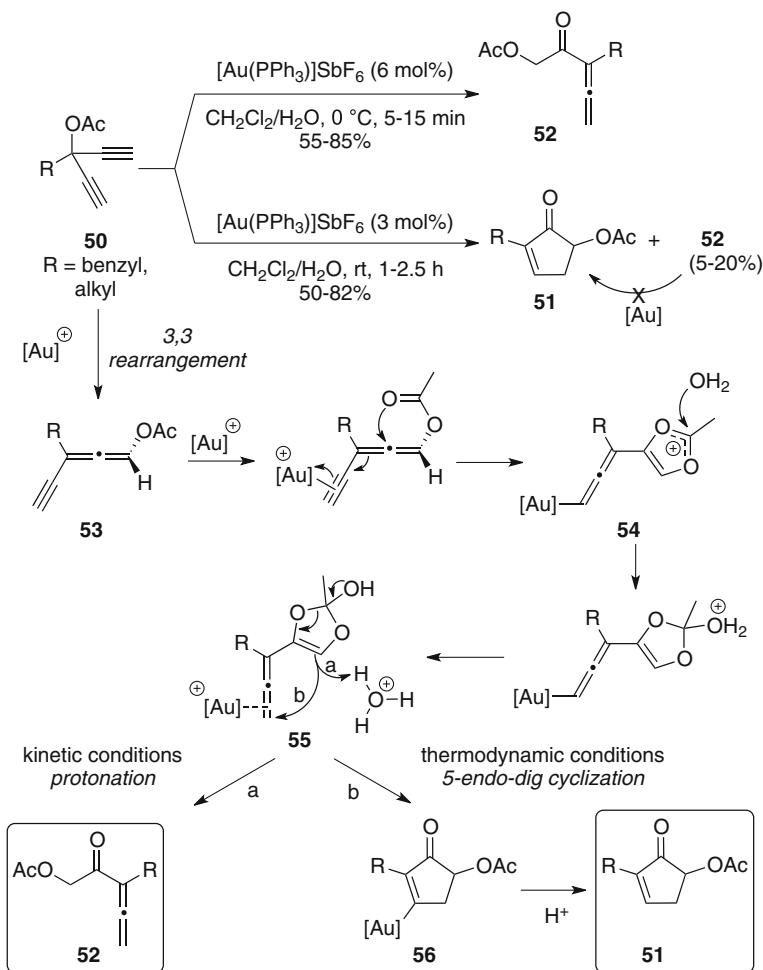


Scheme 3.15 The conditions tuning drives the reaction outcome in Schreiber's work

The team of Schreiber reported an elegant application of tandem 1,3-OAc shift/cyclization to build a large library of small molecules. Starting from propargyl propiolates **44**, they elaborated 3 different strategies to get diversely functionalized α -pyrones and/or polyconjugated dienones, from the same intermediate **46** arising from 6-*endo* cyclization of the in situ generated allenyne **45** (Scheme 3.14) [33, 34].

The first strategy (path a) is a simple cycloisomerization leading to triene **47** after a proton elimination/protodeauration sequence. The second and third strategies consist in performing a nucleophilic addition either on the exocyclic double bond (path b) to give a substituted α -pyrone **48**, or on the carbonyl moiety which results in cycle opening and affords bis-enone **49** (Scheme 3.14). For this purpose, nucleophiles such as alcohols and electron-rich aromatics were introduced in the reaction mixture, allowing the synthesis of compounds **48** and **49** in a one-pot process. Favoring either path a or path b was achieved by fine tuning of the reaction conditions (Scheme 3.15).

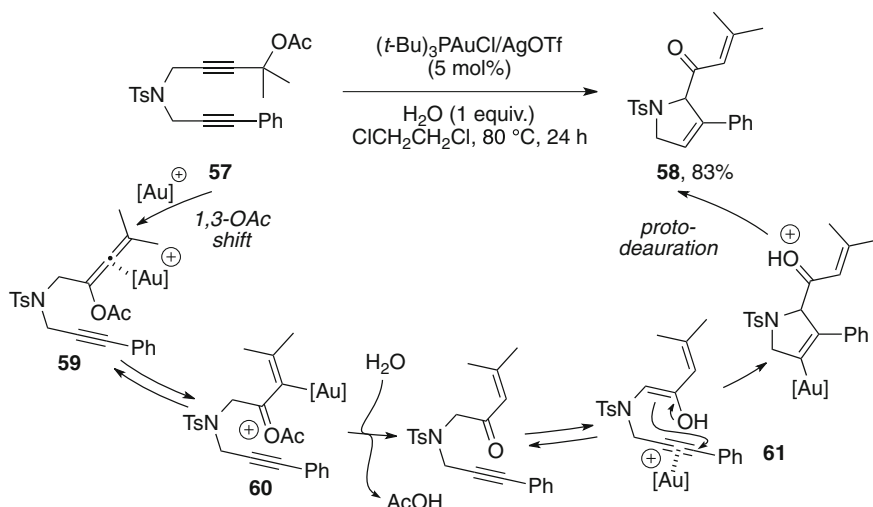
In 2009, Oh reported the gold-catalyzed hydrative rearrangement of 1,1-dieithynylcarbinol acetates **50** into cyclopentenones **51** [35] or allenone **52**, depending on the temperature, the catalyst loading and the reaction time (Scheme 3.16). Allenone **52** did not furnish cyclopentenone **51** when submitted to the gold catalyst. Nonetheless both products **51** and **52** share the first steps of the rearrangement mechanism. First, a 1,3-OAc shift of the propargyl acetate gives rise to a 1,3-allenynes system **53**. Activation of the triple bond by gold then induces oxacyclization that generates the cationic 1,3-dioxolium intermediate **54**. Subsequent nucleophilic attack by a molecule of water and protodemetalation lead to intermediate **55**. Then, depending on conditions, the latter can evolve into two different manners: kinetic conditions furnish allenone **52** after opening of the dioxole ring (path a), while thermodynamic conditions afforded cyclopentenone **51** (path b).



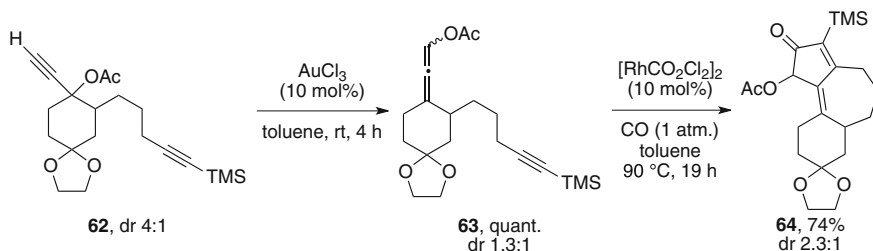
Scheme 3.16 Kinetic versus thermodynamic conditions in the rearrangement of diethynylcarbinol acetates

This thermodynamic product probably originates from a *5-endo-dig* cyclization upon activation of the allene by gold giving intermediate **56**, which undergoes protodemetalation to deliver cyclopentenone **51** (Scheme 3.16).

The group of Shi recently disclosed an interesting hydrative rearrangement of 3-acyloxy-1,6-diyne **57** leading to substituted pyrrolidine derivatives **58** (Scheme 3.17) [36]. Nonetheless, in view of deuterium labelling experiments, it seems that the propargyl acetate acts as an α,β -unsaturated ketone precursor through hydrolysis of acyloxonium intermediate **60**. The cyclization would then occur by nucleophilic attack of enol onto the remaining triple bond activated by gold in **61**. This represents a new way to perform tandem reactions by the mean of propargylic acetates but strictly speaking is not an allenyne cycloisomerization-type reaction.



Scheme 3.17 Synthesis of pyrrolidines from 3-acyloxy-1,6-diynes in hydrative conditions



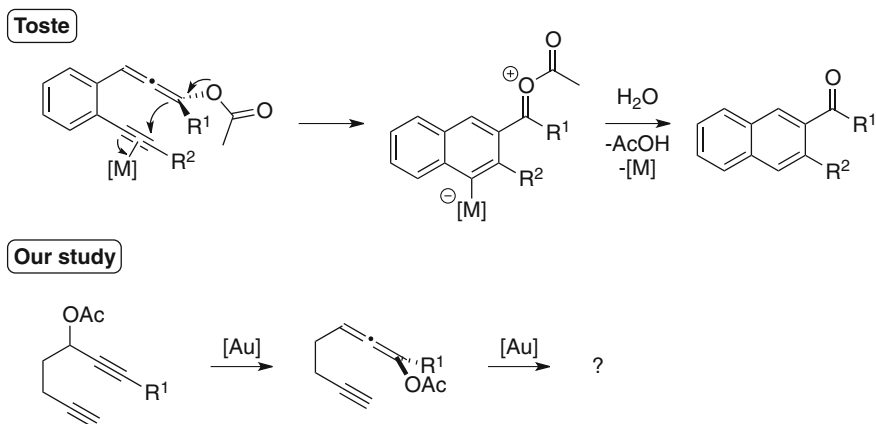
Scheme 3.18 Use of allenynyl esters in Pauson-Khand reactions

To end with this bibliographical section, it is worth adding that allenynyl esters generated from diynyl esters with AuCl₃ were employed in rhodium catalyzed Pauson-Khand reaction and lead to fused tricyclic compound **64**.⁸ Nonetheless they were isolated prior to submission to the rhodium catalysts (Scheme 3.18) [42].

3.1.2 Presentation and Objectives of the Project

We have seen above the potential of propargylic esters to generate allenes in situ by the means of gold catalysis, which can then be involved in a further metal-catalyzed process. More precisely, they are practical tools to generate in situ

⁸ Selected reviews: [37–41].



Scheme 3.19 Objectives of the project

allenynes systems. In view of the reports of Toste on ene-diyne precursors, we assumed that the double bond tethering the two alkyne partners would bias the reaction toward the formation of aromatic ketones (Scheme 3.8). We began our study with related substrates where no unsaturation was introduced in the tether. Below are presented our results in the study of such system (Scheme 3.19).

3.2 First Results

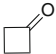
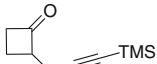
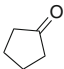
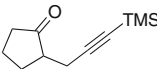
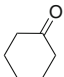
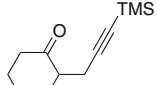
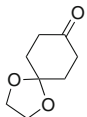
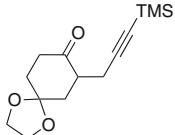
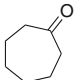
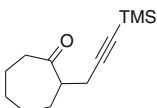
3.2.1 Synthesis of the Precursors

The synthesis of diyne precursors was started with the preparation of α -alkylated ketones **65–69**, starting from commercially available cycloalkanones. Protection of the carbonyl moiety was realized with *N,N*-dimethylhydrazine, and alkylation of the resulting hydrazone was preformed by treatment with *n*-butyllithium followed by addition of silylated propargyl bromide. Final hydrolysis of the hydrazone with aqueous HCl afforded the desired ketones in excellent overall yields (Table 3.1).

Ketones **65–69** were next converted into propargyl alcohols by addition of various lithium acetylides. Acetylation under classical conditions followed by desilylation using potassium fluoride furnished the desired 3-acyloxy-1,6-diyne precursors **70–84**, of various ring sizes and acetylenic substituents, as mixtures of diastereomers (Scheme 3.20).

The synthesis of acyclic precursors was realized from pent-4-yn-1-ol, which was monosilylated at the acetylenic position by double deprotonation with *n*-butyllithium, addition of two equivalent of trimethylsilyl chloride and subsequent treatment with aqueous HCl. Oxidation of the resulting alcohol, operated with pyridinium chlorochromate, furnished aldehyde **85**. Various lithium

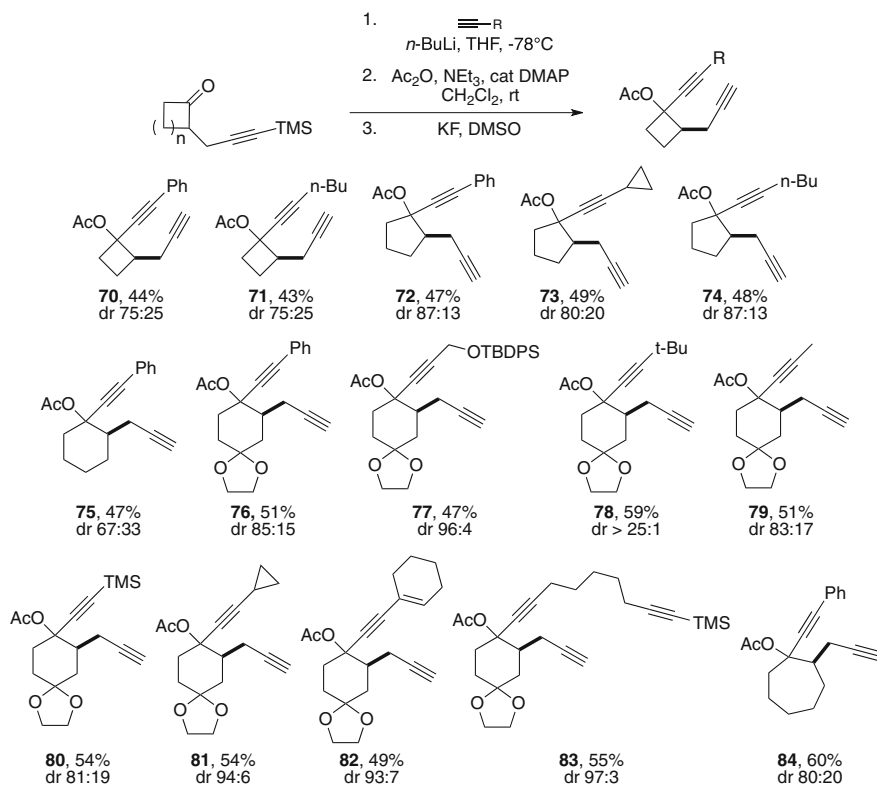
Table 3.1 Synthesis of α -propargylated ketones **65–69**

1. H_2NNMe_2 2. $n\text{-BuLi}$ (1.1 equiv), THF, -78°C then $\text{Br}-\text{C}\equiv\text{C}-\text{TMS}$ (1.2 equiv.) 3. HCl aq.		
Entry	Ketone	Product (yield, 3 steps)
1		 65 (85%)
2		 66 (88%)
3		 67 (88%)
4		 68 (91%)
5		 69 (95%)

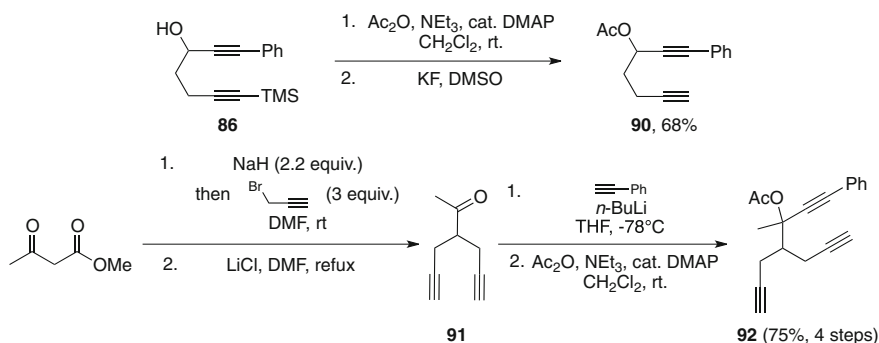
acetylides were added on **85** with good yields and alcohols **86–89** were obtained in 80–88 % (Table 3.2).

From alcohol **86**, we synthesized precursor **90** through a two-step acetylation/desilylation sequence 52 % yield over two steps (Scheme 3.21). Another acyclic precursor, bearing a quaternary acetate was synthesized according the following procedure: 3-oxo butyric acid methyl ester was treated with two equivalent of sodium hydride and two equivalent of propargyl bromide. The crude dialkylated compound was then submitted to Krapcho's decarboxylation conditions to give diyne **91**. Addition of phenylacetylene lithium acetylide was performed on the crude product, and the resulting alcohol was converted into acetate **95** following the same conditions described above, in 75 % yield for these 4 steps (Scheme 3.21).

We thus were able to synthesize a broad range of substrates for our study, according to simple and well-working procedures. Exploration of the potential of these substrates toward cycloisomerization reactions using gold catalysts was first run with compound **76**.

**Scheme 3.20** Cyclic precursors to be tested**Table 3.2** Synthesis of acyclic precursors **86–89**

	1. $n\text{-BuLi}$ (2.1 equiv.) TMSCl (2.2 equiv.) THF , -78°C to rt		
	2. HCl aq. 3. PCC , CH_2Cl_2 , rt		
		85 , 68% (2 steps)	
		R	Product (yield)
		Ph	86 (88%)
		$n\text{-Bu}$	87 (85%)
		$-\frac{1}{2}-\triangle$	88 (87%)
		$t\text{-Bu}$	89 (80%)



Scheme 3.21 Synthesis of acyclic precursors **90** and **92**

3.2.2 Catalyst Optimization

We were pleased to find that precursor **76** underwent a rapid and clean conversion into cross-conjugated dicarbonyl compound **93** at our first attempts with cationic gold(I) catalysts (Table 3.3).

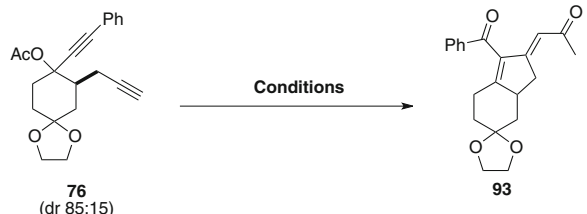
While the presence of two carbonyl functionalities could be evidenced by ^{13}C NMR, the rest of the structure was assigned on the basis of 2D spectroscopic studies and nOe experiments (vide infra). Cationic gold(I), generated in situ by reaction of a silver(I) salt with a triphenylphosphinegold(I) chloride complex quantitatively converted the substrate into diketone **93** (Table 3.3, entry 1), which was isolated spectroscopically pure by simple filtration of the reaction mixture on a small plug of silica gel. Silver alone was not efficient and slowly decomposes the starting material (entry 2), thus proving its exclusive chloride abstraction role. Triphenylphosphinegold(I) chloride was inactive in the absence of silver salts (entry 3). On the opposite, commercial cationic gold(I) salts such as Echavarren's catalyst [43] (entry 4) and Gagosz' catalysts [44, 45] [Ph_3PAu] NTf_2 (entry 4) proved to be highly efficient for this transformation as full conversion was reached in 40 min at room temperature, and products were isolated in almost quantitative yields. Neutral gold(I), gold(III), platinum(II) and platinum(IV) chloride salts were also assessed for this rearrangement and although the reaction occurred, they yet provided inferior results (Table 3.4).

With decided to keep either triphenylphosphinegold chloride in combination with silver hexafluoroantimonate and catalyst **94** as catalytic systems to extend the scope of the reaction.

3.2.3 Reaction Scope

Substrate with alkyl or phenyl acetylenic substituents promptly rearranged in our optimized conditions within less than 1 h (Table 3.5). Thus, five-membered ring precursors **72–74** were converted into cross conjugated products **95–97** in good to

Table 3.3 Catalyst screening: gold(I) and silver(I)

					
Conditions					
Entry	Catalyst	Solvent	T (°C)	Time	Isolated yield (%)
1	Ph ₃ PAuCl/AgSbF ₆ (2 mol%/2 mol%)	CH ₂ Cl ₂	0	20 min	99
2	AgSbF ₆ (2mol%)	CH ₂ Cl ₂	rt	24 h	decomposition
3	Ph ₃ PAuCl	CH ₂ Cl ₂	rt	24 h	no reaction
4	94 (2 mol%)	CH ₂ Cl ₂	rt	40 min	98
5	[Ph ₃ PAu]NTf ₂ (2 mol%)	CH ₂ Cl ₂	rt	40 min	95

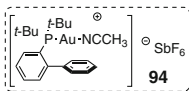
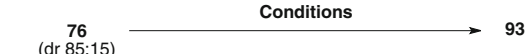


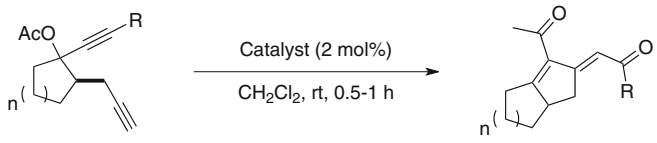
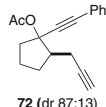
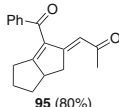
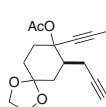
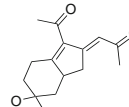
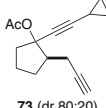
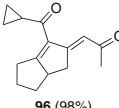
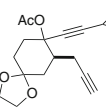
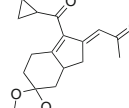
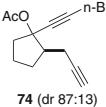
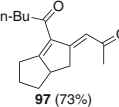
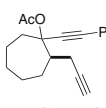
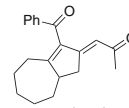
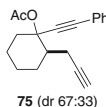
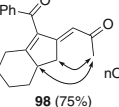
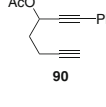
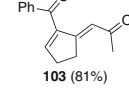
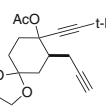
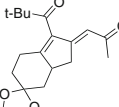
Table 3.4 Catalyst screening: halide salts of gold and platinum

					
Conditions					
Entry	Catalyst	Solvent	T (°C)	Time	Isolated yield (%)
1	AuCl (2 mol%)	CH ₂ Cl ₂	rt	1 h	80
2	AuCl ₃ (2mol%)	CH ₂ Cl ₂	rt	1 h	90
3	PtCl ₂ (5 mol%)	toluene	reflux	1 h	92
4	PtCl ₄ (5 mol%)	toluene	reflux	1 h	91

excellent yields (entries 1–3). Similarly, six-membered ring substrates behaved well and afforded the expected products (entries 4–7). The presence of a methylene acetal on the ring did not influence the reaction outcome (entries 5–7). Seven-membered ring precursor **84** delivered dicarbonyl compound **102** in an excellent 94 % yield (entry 8). As well, acyclic tertiary acetate **90** was cyclized into **103** in good yield under our reaction conditions (entry 9). nOeSY experiments on compound **98** (entry 4) allowed us to see through-space interaction between the protons of the acyl group and the protons of the two sp³-carbons of the five membered-ring backbone, thus validating the exocyclic double bond of (*E*)-geometry.

Four-membered ring derivatives **70–71** led to disappointing results, and exposure to gold catalysts for 20 h resulted in their slow decomposition (Scheme 3.21). The ring strain inherent to cyclobutane derivatives probably prevents the cyclizing partners (a triple bond and an allenyl ester, vide infra) to get close enough to each other and the cyclization to occur (Scheme 3.22).

Table 3.5 Catalytic rearrangement of substrates **72–75**, **78**, **79**, **81**, **84** and **90**

							
Entry	Substrate	Catalyst	Product (yield)	Entry	Substrate	Catalyst	Product (yield)
1	 72 (dr 87:13)	94	 95 (80%)	6	 79 (dr 83:17)	Ph_3PAuCl AgSbF_6	 100 (98%)
2	 73 (dr 80:20)	94	 96 (98%)	7	 81 (dr 94:6)	Ph_3PAuCl AgSbF_6	 101 (90%)
3	 74 (dr 87:13)	94	 97 (73%)	8	 84 (dr 80:20)	94	 102 (94%)
4	 75 (dr 67:33)	94	 98 (75%)	9	 90	Ph_3PAuCl AgSbF_6	 103 (81%)
5	 78 (dr 85:15)	Ph_3PAuCl AgSbF_6	 99 (97%)				

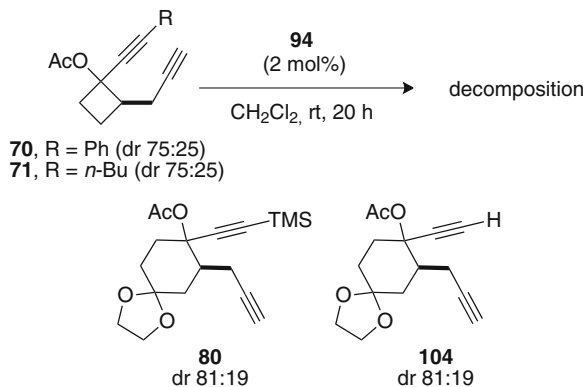
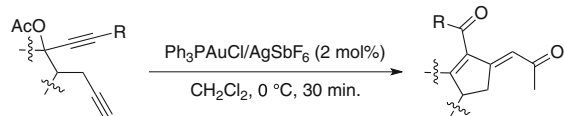
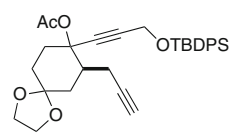
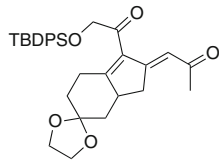
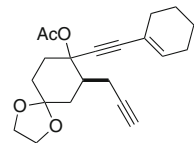
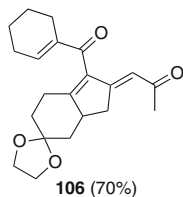
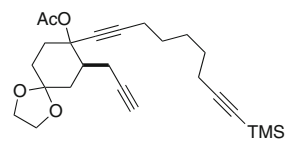
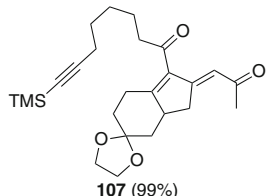
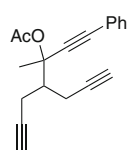
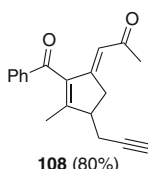
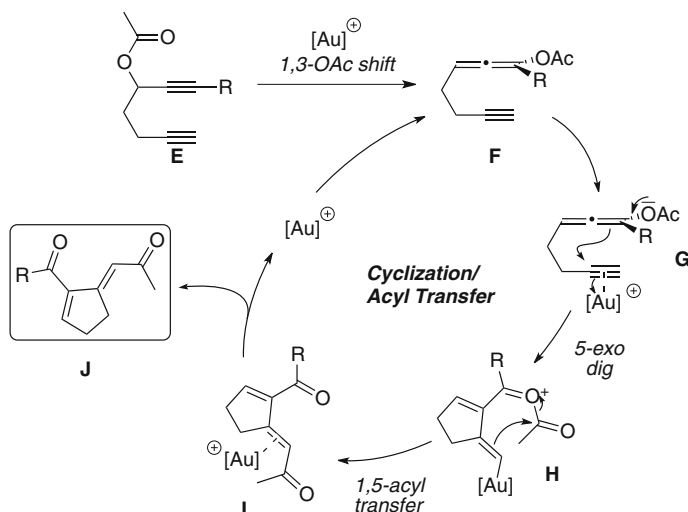
Scheme 3.22 Substrates that failed to react

Table 3.6 Functional group tolerance of the new reaction

		
Entry	Substrate	Product (yield)
1	 77 (dr 96:4)	 105 (95%)
2	 83 (dr 93:7)	 106 (70%)
3	 83 (dr 97:3)	 107 (99%)
4	 92	 108 (80%)

Trimethylsilyl- or hydrogen-substituted propargylic acetates **80** and **104** resulted in no reaction. For the former, formation of an allenyl ester is not favorable as it would involve the appearance, through gold coordination, of a formal positive charge α to the silicon atom. The latter, synthesized by desilylation of **79** under classical conditions (78 % yield) is probably rearranged into a gold carbene through a 1,2-acyloxy shift rather than into an allenyl ester which formation is necessary for the cycloisomerization process to take place (vide infra).

We were pleased to find that this new cycloisomerization reaction was tolerant of functional groups (Table 3.6). Silylether precursor **77** delivered the cyclized compound **105** in an almost quantitative yield (entry 1). The reaction also tolerates



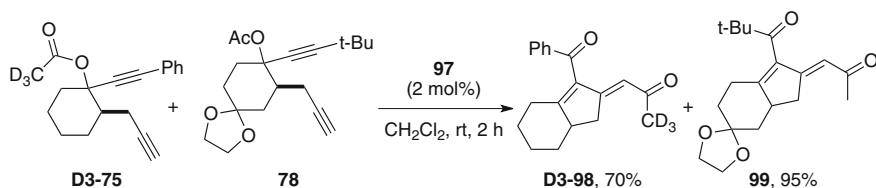
Scheme 3.23 Our first mechanistic proposal

well the presence of other carbon-carbon multiple bonds (entries 2–4). Substrate **83** bearing an alkene moiety was converted into the cross conjugated product **106** in 70 % yield. Likewise, precursor **83** carrying a silyl-protected alkyne reacted well (entry 3), and so did substrate **92** bearing a spectator terminal alkyne (entry 4). The results described above show that the reaction is very general and can lead to a broad range of cross-conjugated dicarbonyl compounds. Moreover, the process is fast and often high-yielding. With all these results in hand, we then came to the investigation of the mechanism.

3.3 Mechanistic Investigations

3.3.1 First Mechanistic Rationale

The first mechanism we proposed to account for the formation of cross-conjugated diketones is depicted in Scheme 3.23. We believed that rearrangement of the propargylic acetate **E** into allenylester **F** occurred prior to cyclization. Then, coordination of gold to the pendant triple bond on **F** could then trigger cyclization from the electron-rich allene onto the activated alkyne in a 5-exo-dig manner to afford vinylgold species **H**. Subsequently, the π -systems of the vinylgold and the acyl substituent could react together to result in the $1,5\text{-acyl transfer}$. Release of diketone **J** would follow gold decooordination in **I**.



Scheme 3.24 Deuterium labelling experiment

However, two questions raised from this proposal:

- is the acyl transfer intra- or intermolecular? Indeed, because of the (*E*)-stereochemistry of the exocyclic double bond, an intramolecular shift may seem difficult;
- is the acyl transfer stepwise or concerted?

Moreover, this mechanism hardly accounts for the complete stereoselectivity of this process. To find answers to these questions, we set up a series of experiments.

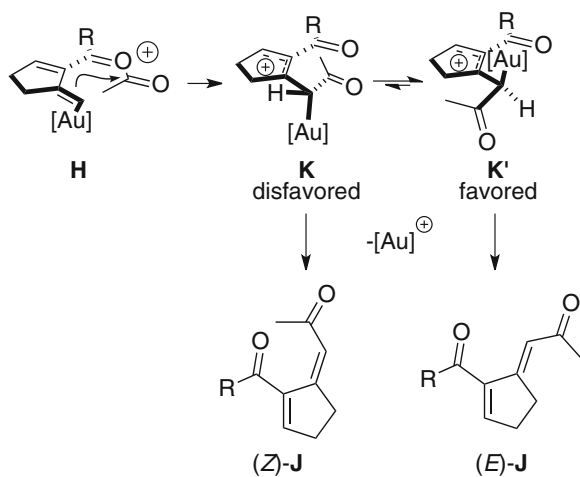
3.3.2 Toward an Intramolecular Acyl Transfer

To shed light on the inter- or intramolecular character of the acyl transfer, we ran the following experiment: cationic gold(I) catalyst **94** was added to a dichloromethane solution of labelled compound **D3-75** and precursor **77**. After 2 h both compound were totally consumed and cyclized products were isolated. No deuterium scrambling was observed, what accounted for an intramolecular mechanism (Scheme 3.24).

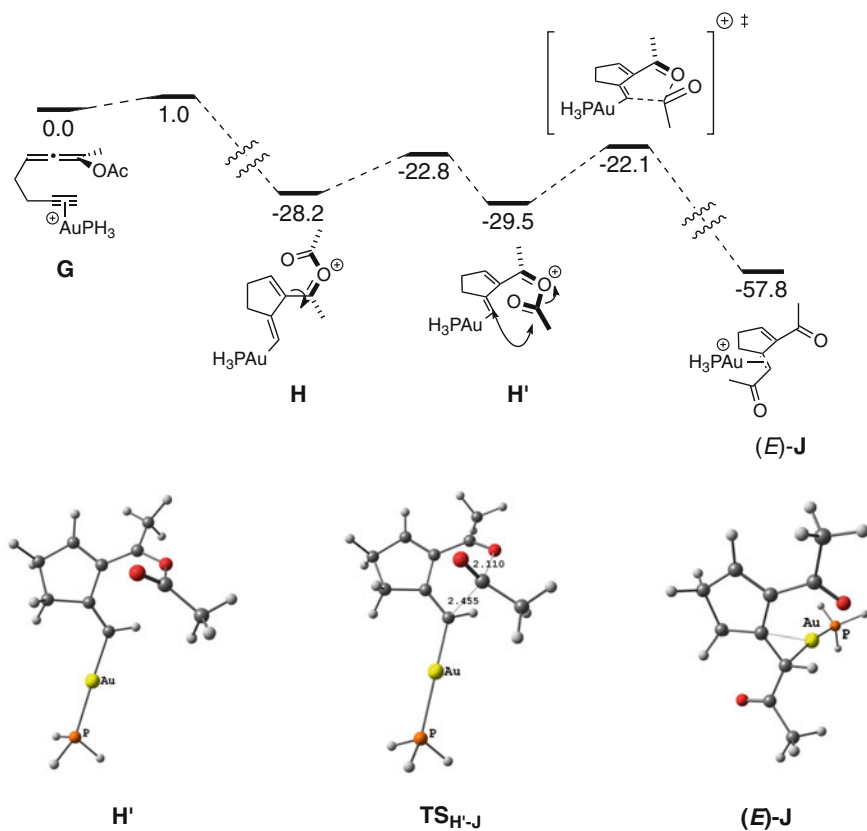
We then drew a stereoselectivity model, supposing a stepwise acyl transfer on **H** giving rise to cations **K/K'** (Scheme 3.25). **K** and **K'** are both in a favorable conformation for gold elimination to give compound **J**, as the C-Au σ bond is coplanar with the vacant π orbital. However, conformation **K** that leads to (*Z*)-**J** suffers from more steric repulsions than **K'** on which gold elimination will drive to (*E*)-**J**. Equilibration between conformations **K** and **K'** should thus be displaced in favor of **K'**, and could explain the observed stereoselectivity. As no trace of compounds (*Z*)-**J** was observed among all the cyclization reactions we performed, we decided to investigate this mechanism by the means of quantum mechanics computations to shed light on this stereoselectivity issue.

3.3.3 DFT Calculations

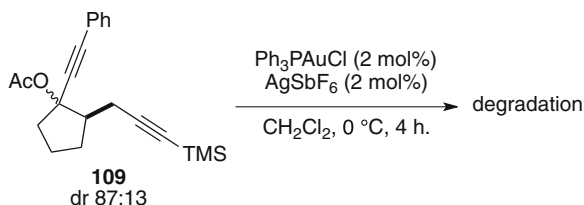
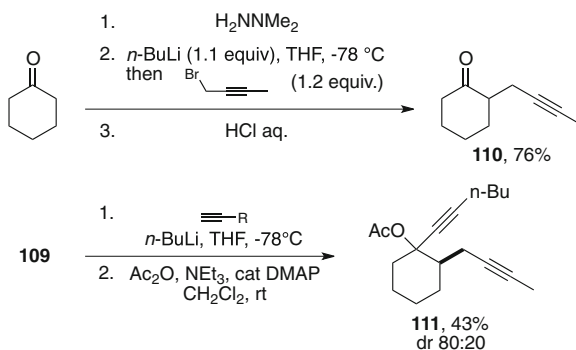
Prof. V. Gandon ran DFT computations, carried out using the B3LYP functional. The free enthalpy profile of the reaction is depicted in Scheme 3.26, and energies are given in $\text{kcal}\cdot\text{mol}^{-1}$. According to calculation, the first step, starting from allenynyl



Scheme 3.25 Stereoselectivity model for the acyl transfer

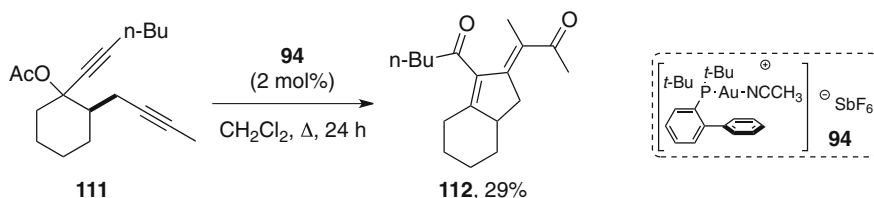


Scheme 3.26 Computed enthalpy profile of the process

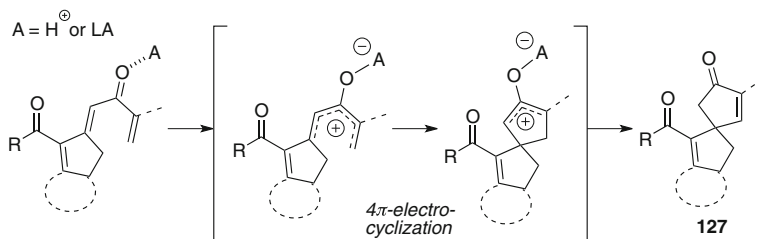
**Scheme 3.27** Decomposition of a silyl-substituted substrate**Scheme 3.28** Synthesis of a methyl-substituted substrate

ester **G**, is a low energy demanding, outer-sphere 5-*exo*-dig cyclization that gives vinylgold species **H** in an exothermic manner. A C–C bond rotation on **H** leads to reactive conformation **H'**, an almost thermoneutral process. In **H'**, the p orbitals at the terminal carbons of the π system are well oriented for an efficient overlap. 1,5-acyl migration to give the final product (*E*)-**J** can take place in a concerted, asynchronous fashion through a transition state lying 7.8 kcal·mol^{−1} above **H'**. This process is accompanied by the liberation of 28.3 kcal·mol^{−1} (Scheme 3.26).

Thus, these calculations show the feasibility of an intramolecular 1,5-acyl shift giving rise to a (*E*)-exocyclic double bond, the weak energy barriers accounting well for a process occurring at room temperature. The Au–C bond is cleaved by the acylium in a stereoselective fashion, the electrophile being delivered intramolecularly. The formation of the (*Z*) stereoisomer would require either an unfavorable inner sphere 5-*exo*-dig cyclization or the isomerization of the vinyl-gold moiety in **H**, which is kinetically very difficult to achieve [46]. The stereochemical outcome is therefore dictated by the cyclization step. Cationic intermediates **K**, **K'** we proposed in our initial model (Scheme 3.28) could not be modelled as such structure converged to a coordinated double bond as in **J** displaying a pronounced “slipped” gold fragment but nonetheless ruling out any possibility of bond rotation.



Scheme 3.29 Cycloisomerization of the methyl-substituted precursor **114**



Scheme 3.30 Possible Nazarov pathway for products **122–126**

3.4 Broadening the Scope of the Reaction

3.4.1 Non-terminal Alkynes

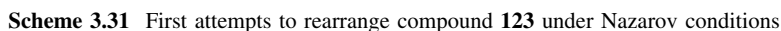
In view of the mechanism we proposed, it would be predictable that substituting the free alkyne will result in difficulties at the acyl transfer step. Our experimental results confirmed this fact. When submitted to cationic gold(I) catalysis, silyl alkyne compound **109** slowly decomposed (Scheme 3.27).

We switched to methyl-substituted triple bonds, and performed the synthesis of substrate **111** (Scheme 3.28). Commercially available cyclohexanone was quantitatively converted into the corresponding hydrazone by addition of *N,N*-dimethylhydrazine. α -Alkylated ketone **110** was obtained upon treatment of the hydrazone with *n*-butyllithium followed by addition of 1-bromobut-2-yne (76 % yield, 3 steps). Recovery of the carbonyl function was performed by acidic hydrolysis using aqueous HCl. Addition of *n*-hexyne lithium acetylide on ketone **110** and subsequent acetylation under classical conditions furnished the desired precursor **111** bearing a methyl-substituted alkyne in 43 % yield over the last two steps and 80:20 diastereomeric ratio.

Submission of substrate **111** to our optimized conditions resulted in low conversion, but full conversion was reached in 24 h in refluxing dichloromethane.¹ ¹H NMR of the crude material revealed a complex mixture from which 29 % of cyclized product **112** were isolated (Scheme 3.29).

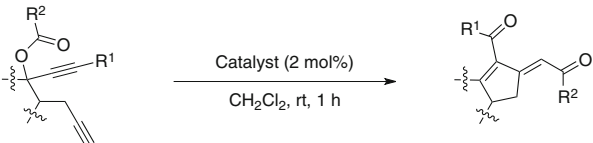
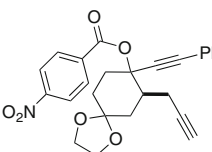
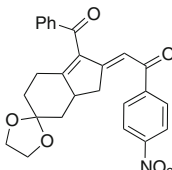
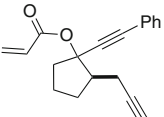
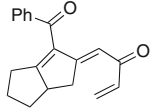
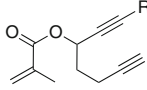
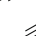
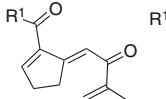
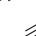
As we have supposed, this reaction, although possible, is rendered difficult by using disubstituted alkynes.

Entry	Alcohol	Acyl chloride	Product (yield, 2 steps)
		1. R ² COCl, NEt ₃ , cat. DMAP CH ₂ Cl ₂ , rt. 2. KF, DMSO	
1	 113 (dr 85:15)		 115 (57%) dr 85:15
2	 114 (dr 90:10)		 116 (72%) dr 90:10
3	 R ¹ = Ph 86 <i>n</i> -Bu 87 -CH ₂ - 88 <i>t</i> -Bu 89		 R ¹ = Ph 117 (46%)
4			 R ¹ = <i>n</i> -Bu 118 (53%)
5			 R ¹ = -CH ₂ - 119 (54%)
6			 R ¹ = <i>t</i> -Bu 120 (47%)



To our delight, these benzoyl and acryloyl derivatives **115–120** were cleanly converted within 1 h into the desired cyclized products **121–126** in good to

Table 3.8 Rearrangement of substrates **115–120** in the presence of cationic gold(I) catalysts

			
Entry	Substrate	Catalyst	Product (yield)
1	 115 dr 85:15	Ph ₃ PAuCl AgSbF ₆	 121 (99%)
2	 116 dr 90:10	94	 122 (66%)
3	 R ¹ = Ph 117 R ¹ = <i>n</i> -Bu 118 R ¹ =  119 R ¹ = <i>t</i> -Bu 120	94	 R ¹ = Ph 123 (98%)
4			R ¹ = <i>n</i> -Bu 124 (64%)
5			R ¹ =  125 (99%)
6			R ¹ = <i>t</i> -Bu 126 (99%)

excellent yields (Table 3.8). These compounds feature a highly cross-conjugated skeleton that is rarely encountered in the literature.

The conjugated skeleton displayed by compounds **121–126** makes them interesting candidates to be tested toward nucleophilic attack, thanks to their extended Michaël acceptor structure. As well, the cross-conjugation of two carbonyl groups and three carbon-carbon double bonds could raise interrogations about the potential of such compounds to undergo cationic rearrangements promoted either by a Brønsted or a Lewis acid (LA). For example, one can imagine that the divinylketone moiety of diketones **122–126** could undergo a conrotatory 4π-Nazarov electrocyclization,⁹ thus allowing access to spiroketones such as **127** (Scheme 3.30). We decided to focus our attention toward the latter rearrangement, using compound **123** as test substrate.

Unfortunately, Brønsted (PTSA) or Lewis (BF₃•OEt₂) acid conditions failed to give satisfying results and led to complex mixtures of unidentified products (Scheme 3.31).

Nonetheless, flash chromatography of both crude mixtures allowed isolation of what was supposed to be a cycloisomerization product of **123**, still bearing two carbonyl groups,¹⁰ in 15–20 % yield. During purification of these mixtures, we

⁹ For recent reviews on Nazarov cyclization, see [47–50].

¹⁰ According to ¹H, ¹³C NMR and mass spectrometry.

Scheme 3.32 X-ray diffraction study of product **128**. Anisotropic displacement parameters are drawn at the 50 % probability level and hydrogen atoms are omitted for clarity

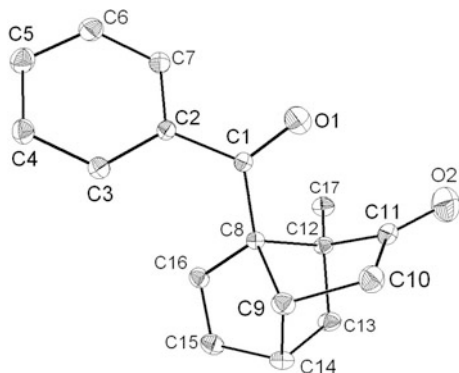


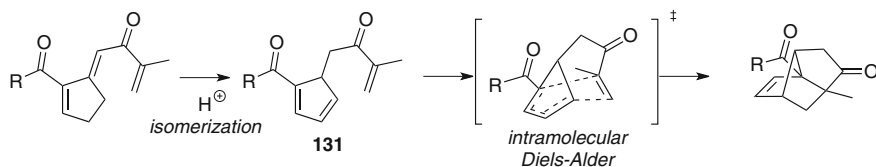
Table 3.9

Substrate			Product (yield)	
R =	Ph	123	128 (75%)	
		125	129 (quant.)	
	<i>t</i> -Bu	126	130 (55%)	

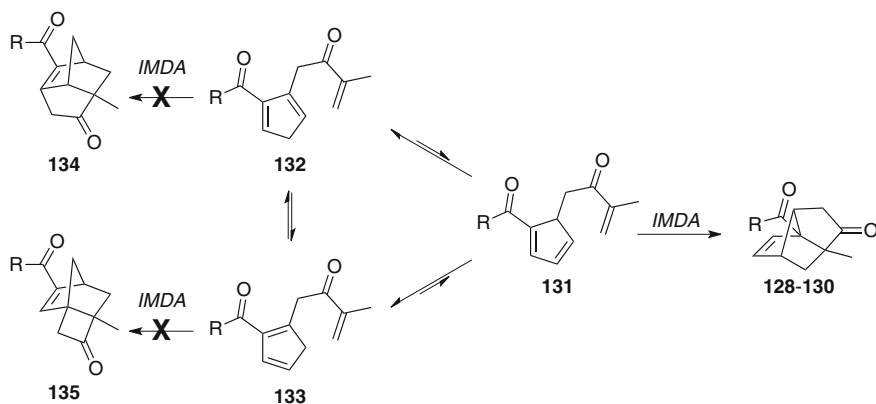
realized that eluting a TLC spot of a solution of **123** with dichloromethane led to the appearance of a spot having the same R_f than the unknown product. We thus came to the conclusion that the smooth acidic mixture of silica and dichloromethane could perform selectively the rearrangement of **123**. To our great pleasure, heating a dichloromethane solution of **123** with 100 equivalents of silica in a sealed tube à 70 °C for 3 days allowed the exclusive formation of this unknown compound. Structure elucidation of the latter was achieved by X-ray diffraction analysis of monocrystals obtained by slow evaporation of a 8/1.5/0.5 hexane/diethyl ether/dichloromethane solution and revealed that this product was norbornene derivative **128** (Scheme 3.32 and Table 3.9). The relative tricyclo[4.3.0.0^{3,7}]nonane skeleton has been trivially named “brexane” due to its *bridge* involving an *exo*-norbornyl bond [51]. Interestingly, the 4-brexene skeleton displayed by compound **128** is encountered in key intermediates toward the total synthesis of natural compounds (±)-sativene and (±)-sativendiol [52–55].

Similarly, cross-conjugated dicarbonyl compounds **125** and **126** could have been rearranged under the optimized acidic conditions into 4-brexene derivatives **129** and **130** in 100 and 55 % yield, respectively (Table 3.9).

Tricyclic skeletons of compounds **139–141** presumably arise from an intramolecular Diels-Alder (IMDA) reaction involving a 5-substituted cyclopentadiene intermediate **131**, generated by an acid-promoted double bond isomerization of the



Scheme 3.33 Hypothesized pathway to explain formation of products **128–130**



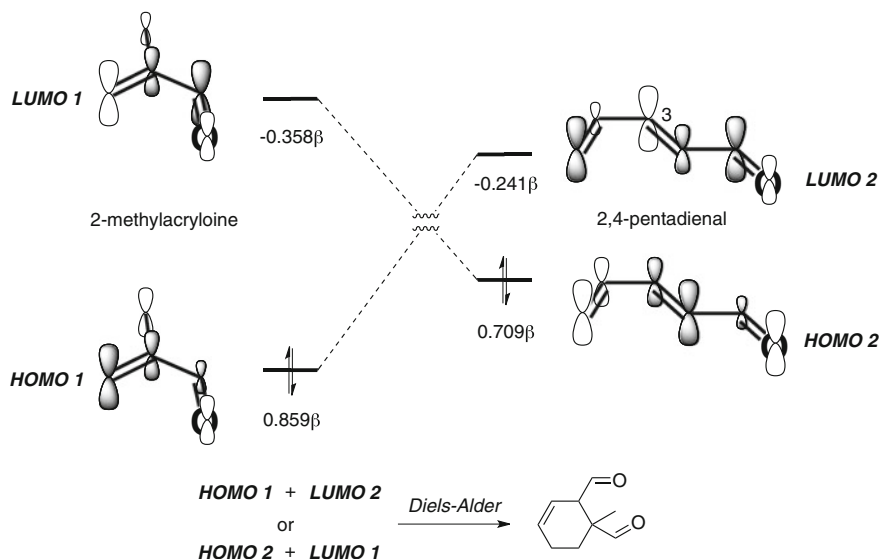
Scheme 3.34 Only one possible IMDA pathway

cyclopentenylidene moiety (Scheme 3.33). As 5-, 1- and 2-alkyl substituted cyclopentadienes all readily interconvert by 1,3-hydrogen shift (for example, the equilibrium concentrations of 5-, 1- and 2-methylcyclopentadiene at 20 °C are 1, 44 and 55 % respectively [56]), the exclusive observation of products **128–130** resulting from the IMDA of 5-substituted cyclopentadiene **131** raises questions.

Previous works conducted on the IMDA of homoallyl-substituted cyclopentadienes to obtain 4-brexene¹¹ derivatives explained this selectivity by the highly strained character of the alternative cycloaddition transition states. Thus, it is impossible for 2- or 1-substituted cyclopentadienes **143** and **144** to undergo IMDA. As a result, and according to the Curtin-Hammett principle [61], tricyclic adducts **145** and **146** were never observed upon heating of homoallyl-substituted cyclopentadienes. Displacement of the tautomeric equilibrium by continuous conversion of **142** led to the formation of a single brexene-type product (Scheme 3.34).

To finish, the regioselectivity of the reaction is well explained by the theory of frontier orbitals [62, 63]. Regarding the intramolecular Diels-Alder of 2,4-pentadienal and 2-methylacrolein as a model [64], the HOMO and LUMO's Hückel

¹¹ See Ref. [57] and also [58–60].



Scheme 3.35 Prediction of regioselectivity with the frontier orbital theory

atomic coefficients reveal that HOMO/LUMO's great lobes interactions will favor the observed cycloaddition regioselectivity in both cases (Scheme 3.35). If the interaction of HOMO 1 and LUMO 2 is considered, the desired regioselectivity is ensured by orbital control, through overlap of the methyl lobe on methylacroleine with the one at C3 in pentadienal's LUMO. In the other case, only one overlapping situation is possible, also leading to the right regioselectivity.

3.4.3 Perspective: Alkynoyl and Allenoyl Derivatives

Encouraged by the good results obtained with acryloyl precursors, we decided to explore the potential of alkynoyl and allenoyl derivatives toward this reaction. We thus synthesized the alkynoyl derivatives **136** and **137** according to the following procedures (Table 3.10). 3-Hydroxy-1,6-diynes **86** and **88** were first desilylated under methanolysis conditions. For the esterification step the Steglich conditions were chosen, as the use of chloride was plagued by 1,4-addition of chloride onto the alkynyl ester, resulting in inseparable mixtures. However these conditions did not prove to be efficient. The reaction was not total with pentynoic acid and ester **136** was isolated in 53 % yield over two steps (76 % brsm, entry 2). When the reaction was ran with alcohol **88** and 3-trimethylsilylpropynoic acid, a mixture of starting material **88**, ester **137** and unknown by-products was obtained from which the desired ester was isolated in only 18 % yield (entry 1).

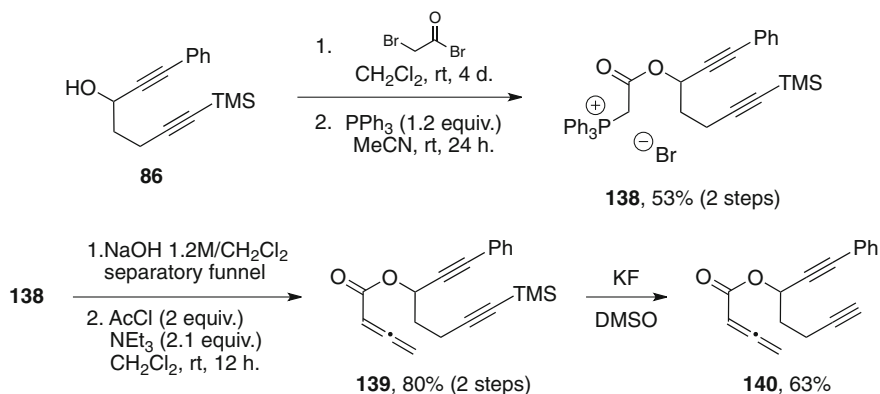
Table 3.10 Synthesis of substrates **136** and **137**

Entry	Alcohol	Acid	Product (yield, 2 steps)
1	 88		 136 (18%)
2	 86		 137 (53%)

To synthesize an allenoyl derivative, the use of a Wittig reaction between a phosphorus ylide and a ketene was envisioned [65–70]. Alcohol **88** was first esterified with bromoacetyl bromide and subsequently converted into phosphonium salt **138** by reaction with triphenylphosphine in acetonitrile (53 %, 2 steps). Deprotonation with sodium hydroxide to generate the phosphorus ylide was followed without purification by a Wittig reaction with ketene generated in situ from acyl chloride and triethylamine. Allenoyl derivative **139** was thus obtained in 80 % yield over the last two steps. Subsequent desilylation using potassium fluoride afforded the desired precursor **140** in 63 % yield (Scheme 3.36).

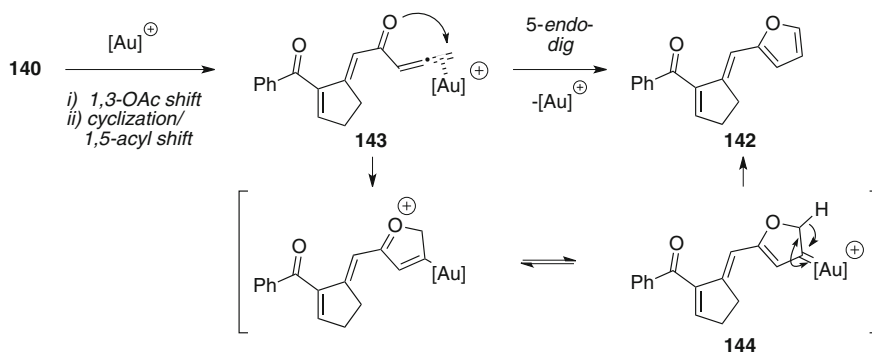
With this triad of substrates in hand, we then looked at their behavior toward gold(I) catalysis to check if they could undergo the cyclization/acyl transfer cascade reaction (Table 3.11). Silicon-protected precursor **147**, unfortunately, led to a complex mixture of products (entry 1). On the opposite, we were pleased to find that 2-pentynoate derivative **148** reacted the desired way with 4 mol% of catalyst **97**.¹² Intriguingly, this compound led to a mixture of (*E*)/(*Z*) exocyclic double bonds. Isomers (*E*)-**141** and (*Z*)-**141** were separated by flash chromatography and the double bond geometry was ascertained by nOeSY experiments, which showed a strong through-space interaction between the aromatic core and the ethyl on (*Z*)-**255**. This last result is not consistent with our previous findings and their rationalization. Indeed, 1,5-acyl transfer is stereospecific and only (*E*) product should have been obtained. Here, the major product is the (*Z*) product, which is

¹² In previous tests with 2 mol% of the catalyst, the conversion was blocked at about 50 %.

Scheme 3.36 Synthesis of allenyl derivative **140**Table 3.11 Rearrangement of substrates **136**, **137** and **140** with catalyst **94**

Entry	Substrate	Product (yield)
1	 136	 141 (98%, <i>E/Z</i> 2:3)
2	 137	 142 (74%)
3 ^a	 140	 143 (74%)

^a 2 mol% of catalyst were used



Scheme 3.37 Proposed mechanism attesting for furan formation

also the most sterically hindered. The parameters controlling this reaction outcome are not clear and deserve investigations, but it can be assumed that the activated alkyne could probably play a role. At what stage, however, the two different isomers are formed remains uncertain: during the 1,5-shift or once the cyclization is over, by simple double bond isomerisation? To finish, allenyl derivative **151** displayed a remarkable reactivity as it led to the unexpected compound **157** in the presence of 2 mol% of catalyst **97** in 3 h (74 %, entry 3).

The proposed mechanism of this reaction starts with the rearrangement of the precursor through the cyclization/1,5-acyl shift cascade we disclosed to afford intermediate **143** (Scheme 3.37). The allenyl ketone moiety is subsequently activated by gold and cyclised into a furan through carbene intermediate **144** [71, 72].

3.5 Conclusion

The potential of propargylic acetates to discover new tandem reactions with gold, platinum, copper and recently, rhodium [73–76], is no more debatable, as many publications report the use of this functional group to generate reactive carbenes or allenyl esters. Our group, in the early 2000, re-discovered the Ohloff-Rautenstrauch rearrangement with platinum and exploited it for the discovery of new reactions. We kept our interest toward this synthetic tool while we switched to gold catalysis, and interesting reactivities and cascade processes were discovered. Among them, the tandem cyclization/1,5-acyl transfer reaction of allenynyl ester, generated in situ by 1,3-acyloxy shift of a propargylic acetate moiety, adds to the now important number of transition-metal catalyzed processes involving such moieties. The special feature of this reaction is a rarely encountered acyl shift from an acyloxonium onto a nucleophilic vinylgold, whose modalities were investigated by the means of DFT computations. It allowed us, with the discovery of a stereospecific and concerted acyl shift, to explain the total stereoselectivity of the

process. This reaction was successfully extended to acryloyl, alkynoyl and allenoyl derivatives. We have shown that cyclised acryloyl precursors could be rearranged into complex 4-brexene skeletons through a 1,3-H shift/intramolecular Diels-Alder sequence. Finally, allenoyl derivatives led one-pot to furan-containing conjugated molecules, thanks to a further, gold-catalyzed cycloisomerization of the in situ generated allenyl ketone, thus showing the possibility to involve one of the carbonyl group in another gold-catalyzed process.

References

1. Krause N, Winter C (2011) *Chem Rev* 111:1994
2. Gandon V, Lemièrre G, Hours A, Fensterbank L, Malacria M (2008) *Angew Chem Int Ed* 47:7534
3. Wang S, Zhang L (2006) *J Am Chem Soc* 128:8414
4. Yu M, Li G, Wang S, Zhang L (2007) *Adv Synth Catal* 349:871
5. Marion N, Carlqvist P, Gealaeas R, de Fremont P, Maseras F, Nolan SP (2007) *Chem Eur J* 13:6437
6. Dudnik AS, Schwiert T, Gevorgyan V (2009) *J Organomet Chem* 694:482
7. Garayalde D, Gómez-Bengoa E, Huang XG, Goeke A, Nevado C (2010) *J Am Chem Soc* 132:4720
8. Mauleon P, Krinsky JL, Toste FD (2009) *J Am Chem Soc* 131:4513
9. Garayalde D, Krüger K, Nevado C (2011) *Angew Chem* 123:941
10. Sakaguchi K, Okada T, Shinada T, Ohfuné Y (2008) *Tetrahedron Lett* 49:25
11. Buzas A, Istrate F, Gagosz F (2006) *Org Lett* 8:1957
12. De Brabander JK, Liu B, Qian M (2008) *Org Lett* 10:2533
13. Huang J, Huang X, Liu B (2010) *Org Biomol Chem* 8:2697
14. Marion N, Díez-González S, de Frémont P, Noble AR, Nolan SP (2006) *Angew Chem Int Ed* 45:3647
15. Dudnik AS, Schwiert T, Gevorgyan V (2008) *Org Lett* 10:1465–1468
16. Zhang L (2005) *J Am Chem Soc* 127:16804
17. Buzas A, Gagosz F (2006) *J Am Chem Soc* 128:12614
18. Alonso I, Trillo B, López F, Montserrat S, Ujaque G, Castedo L, Lledos A, Mascareñas JL (2009) *J Am Chem Soc* 131:13020
19. Gung BW, Craft DT, Bailey LN, Kirschbaum K (2010) *Chem Eur J* 16:639
20. Zhang LM, Wang SZ (2006) *J Am Chem Soc* 128:1442
21. Lemièrre G, Gandon V, Cariou K, Fukuyama T, Dhimané AL, Fensterbank L, Malacria M (2007) *Org Lett* 9:2207
22. Lemièrre G, Gandon V, Cariou K, Hours A, Fukuyama T, Dhimané AL, Fensterbank L, Malacria M (2009) *J Am Chem Soc* 131:2993
23. Cadran N, Cariou K, Hervé G, Aubert C, Fensterbank L, Malacria M, Marco-Conteilles J (2004) *J Am Chem Soc* 126:3408
24. Zhao J, Hughes CO, Toste FD (2006) *J Am Chem Soc* 128:7436
25. Oh CH, Kim A, Park W, Park DI, Kim N (2006) *Synlett* 2781
26. Datta S, Liu R-S (2005) *Tetrahedron Lett* 46:7985
27. Myers AG, Dragovich PS, Kuo EY (1992) *J Am Chem Soc* 114:9369
28. Sugiyama H, Fujiwara T, Kawabata H, Yoda N, Hirayama N, Saito I (1992) *J Am Chem Soc* 114:5573
29. Oh CH, Kim A (2007) *New J Chem* 31:1719
30. Lu L, Liu X-Y, Shu X-Z, Yang K, Ji K-G, Liang Y-M (2009) *J Org Chem* 74:474

31. Fürstner A, Stimson CC (2007) *Angew Chem Int Ed* 46:8845
32. Oh CH, Kim A (2008) *Synlett* 777
33. Luo T, Schreiber SL (2007) *Angew Chem Int Ed* 46:8250
34. Luo T, Schreiber SL (2009) *J Am Chem Soc* 131:5667
35. Karmakar S, Oh CH (2009) *J Org Chem* 74:370
36. Zhang D-H, Yao L-F, Wei Y, Shi M (2011) *Angew Chem Int Ed* 50:2583
37. Brummond KM, Kent JL (2000) *Tetrahedron* 56:3263
38. Gibson SE, Stevenazzi A (2003) *Angew Chem Int Ed* 42:1800
39. Blanco-Urgoiti J, Anorbe L, Perez-Serrano L, Dominguez G, Perez-Castells J (2004) *Chem Soc Rev* 33:32
40. Shibata T (2006) *Adv Synth Catal* 348:2328
41. Lee HW, Kwong FY (2010) *Eur J Org Chem* 789
42. Brummond KM, Davis MM, Huang C (2009) *J Org Chem* 74:8314
43. Herrero-Gomez E, Nieto-Oberhuber C, Lopez S, Benet-Buchholz J, Echavarren AM (2006) *Angew Chem Int Ed* 45:5455
44. Mezaillies N, Ricard L, Gagosz F (2005) *Org Lett* 7:4133
45. Ricard L, Gagosz F (2007) *Organometallics* 26:4704
46. Lemiere G, Gandon V, Agenet N, Goddard JP, de Kozak A, Aubert C, Fensterbank L, Malacria M (2006) *Angew Chem Int Ed* 45:7596
47. Frontier AJ, Collison C (2005) *Tetrahedron* 61:7577
48. Pellissier H (2005) *Tetrahedron* 61:6479
49. Tius MA (2005) *Eur J Org Chem* 2193
50. Habermas KL, Denmark SE, Jones TK (1994) *Org React* 45:1–158
51. Nickon A, Kwasnik H, Swartz T, Williams RO, DiGiorgio JB (1965) *J Am Chem Soc* 87:1613
52. Snowden RL (1981) *Tetrahedron Lett* 22:101
53. Snowden RL (1986) *Tetrahedron* 42:3277
54. Antonsson T, Malmberg C, Moberg C (1988) *Tetrahedron Lett* 29:5973
55. Sigrist R, Rey M, Dreiding AS (1988) *Helv Chim Acta* 71:788
56. McLean S, Haynes P (1965) *Tetrahedron* 21:2329
57. Ferrer C, Raducan M, Nevado C, Claverie CK, Echavarren AM (2007) *Tetrahedron* 63:6306
58. Snowden RL (1981) *Tetrahedron Lett* 22:101
59. Wallquist O, Rey M, Dreiding AS (1983) *Helv Chim Acta* 66:1891
60. Nickon A, Stern AG (1985) *Tetrahedron Lett* 26:5915
61. Curtin DY (1954) *Rec Chem Prog* 15:111
62. Fukui K, Yonezawa T, Shingu H (1952) *J Chem Phys* 20:722
63. Fukui K, Yonezawa T, Nagata C, Shingu H (1954) *J Chem Phys* 22:1433
64. Nguyễn TA (2007) *Orbitales Frontières*. CNRS Éditions, Paris
65. Tömösközi I, Bestmann HJ (1964) *Tetrahedron Lett* 1293
66. Bestmann HJ, Hartung H (1966) *Chem Ber* 99:1198
67. Bestmann HJ, Tömösközi I (1968) *Tetrahedron* 24:3299
68. Bestmann HJ, Graf G, Hartung H, Kolewa S, Vilsmaier E (1970) *Chem Ber* 103:2794
69. Lang RW, Hansen HJ (1980) *Helv Chim Acta* 63:438
70. Oppolzer W, Chapuis C, Dupuis D, Guo M (1985) *Helv Chim Acta* 68:2100
71. Hashmi ASK, Schwarz L, Choi J-H, Frost TM (2000) *Angew Chem Int Ed* 39:2285
72. Sromek AW, Rubina M, Gevorgyan V (2005) *J Am Chem Soc* 127:10500
73. Shibata Y, Noguchi K, Tanaka K (2010) *J Am Chem Soc* 132:7896
74. Brancour C, Fukuyama T, Ohta Y, Ryu I, Dhimane A-L, Fensterbank L, Malacria M (2010) *Chem Commun* 46:5470
75. Shu D, Li X, Zhang M, Robichaux PJ, Tang W (2011) *Angew Chem Int Ed* 50:1346
76. Shu X, Huang S, Shu D, Guzei IA, Tang W (2011) *Angew Chem Int Ed* 50:8153

Chapter 4

Tracking Gold Acetylides in Gold(I) -Catalyzed Cycloisomerization Reactions of 1,6-Enynes

In this last chapter, we will question the intermediacy of gold acetylides in the gold(I)-catalyzed cycloisomerization of 1,6-enynes, as such intermediates have been postulated to intervene in some gold-catalyzed processes involving free alkynes. This study has been conducted as a joint project with mass spectrometry specialists and theoretical chemists.

4.1 Introduction

4.1.1 Bibliography

We have seen in the introduction of this manuscript how relativistic effects are at the origin of the fantastic ability of gold to activate π systems and stabilize cationic intermediates, properties that are relevant in the field of organic chemistry. However, another consequence of these effects has not been evoked, as it is mainly an observation that emerged from the field of coordination chemistry: “aurophilicity”, or the tendency for Au-Au interactions to be stabilizing on the order of hydrogen bonds, as illustrated in the chemistry of polyaurated coordination compounds [1].¹ Until recently, this phenomenon has not been taken into account since gold-catalyzed reactions are run with monometallic complexes in rather dilute media.

4.1.1.1 Gem-Diaurated Intermediates in Gold-Catalyzed Reactions

In, the majority of gold catalyzed reactions, the proposed mechanisms involve the nucleophilic attack at a metal activated C–C unsaturations. This results either in an alkyl- or a vinylgold complex. The isolation of such organogold species resulting

¹ For a review, see: [2].

from these processes confirmed this proposal.² The catalyst is then regenerated by protonolysis of the C-Au bond. However, some recent reports have laid the doubt on these now commonly accepted intermediates, as theoretical and experimental evidences of the occurrence of *gem*-diaurated species in some gold catalyzed organic reactions were reported.

The propensity of vinylgold resulting from the nucleophilic addition to allenes and alkynes to bind another cationic gold(I) fragment resulting in a *gem*-diaurated species has been recently provided by the teams of Gagné [7, 8] and Fürstner [9] (Scheme 4.1). The former observed the formation of diaurated species **3** while monitoring by ³¹P NMR the intramolecular hydroarylation of allenes, [10] and selectively synthesized this complex by reacting vinylgold **2** with 1 equivalent of cationic gold. The team of Fürstner studied the *gem*-diauration of vinylgold **4** that one can see as the result of nucleophilic attack of ethanol onto a gold activated alkyne. Likewise, they noticed that **4** readily binds another gold fragment to lead to diaurated species **5**. However, the relative stability of these species, notably toward protolytic cleavage, makes them unlikely intermediates in gold-catalyzed reactions that exhibit quite high turnovers. Therefore, **3** and **5** are rather considered as catalyst resting states. It is worth adding that similar three-centers two-electrons digold complex were already characterized, yet without any connection to the gold catalysis field [11, 12].³

4.1.1.2 Dual Activation of a Gold Acetylide in Cycloisomerization Reactions

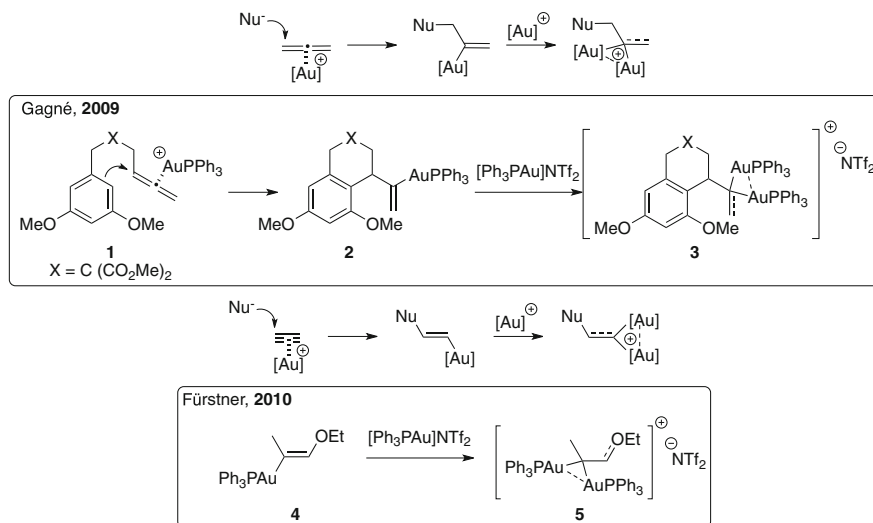
The experimental and theoretical studies on the gold-catalyzed cycloisomerization reaction of 1,5-allenynes into formal Alder-ene products (Scheme 4.2) conducted by Houk and Toste was the first report proposing the intervention of diaurated species along the catalytic cycle [14].

As they noticed the inertness of non-terminal alkynes, as well as exchange of acetylenic deuterium, the authors suggested the occurrence of gold acetylides in the catalytic cycle. According to DFT calculations, its formation is thermodynamically favorable, and moreover this species can easily binds another gold fragment to lead to diaurated compound **8** (Scheme 4.3).

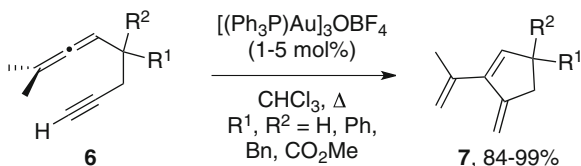
The cyclization starting from digold complex **8** was shown more favorable than starting from a mono-activated allenynes. The nucleophilic attack of the external allenic double bonds on the dually activated alkyne lead to the *gem*-diaurated intermediate **9**, which upon proton transfer produces a three-centers two-electrons digold complex **10** similar to those characterized by Gagné and Fürstner. The viability of an intermediate gold acetylide was confirmed by reacting a previously

² Alkylgold complexes from alkenes: [3] Vinylgold complexes from allenes: [4] Vinylgold complexes from alkynes: [5, 6].

³ For a review, see: [13].



Scheme 4.1 Characterized *gem*-diaurated species of significance in Au-catalyzed processes

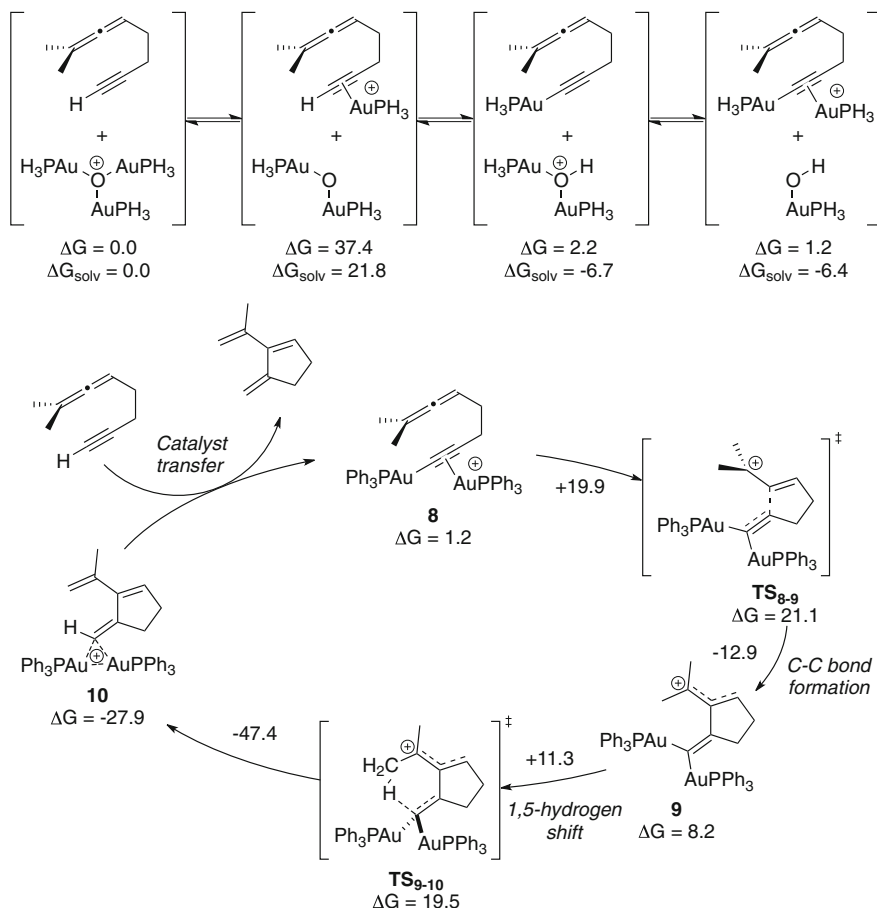


Scheme 4.2 Au-catalyzed cycloisomerization of 1,5-allenynes

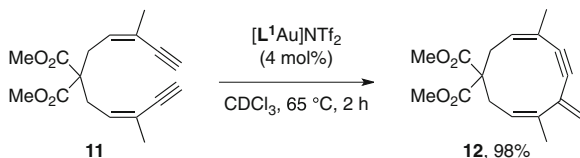
synthesized one with catalytic amounts of gold(I), which produced the Alder-ene product. Although no experimental evidences were collected on such diaurated species, some recent reports have however shown the ability of gold acetylides to evolve into polynuclear species upon coordination of another $[Ph_3PAu]^+$ or $[(Ph_3P)_2Au]^+$ fragment [15, 16].

On the same basis than Toste and Houk, the intermediacy of gold acetylides has also been proposed in the cycloisomerization of diynes: non-terminal alkyne were unreactive and partial deuterium exchange at the acetylenic position was observed on either the starting material and the cyclized compound (Scheme 4.4) [17].

Two mechanisms were proposed to account for the formation of ten-membered ring cycloalkyne **12** from diyne **11**. Both start with the evolution of a gold complexed alkyne into gold acetylide **13**. At this point, the coordination of a second gold center on either the free alkyne or the gold acetylide would give birth to two distinct mechanistic pathways. In path a, a nucleophilic attack from the gold acetylide onto the gold activated free alkyne in **14** would furnish diaurated

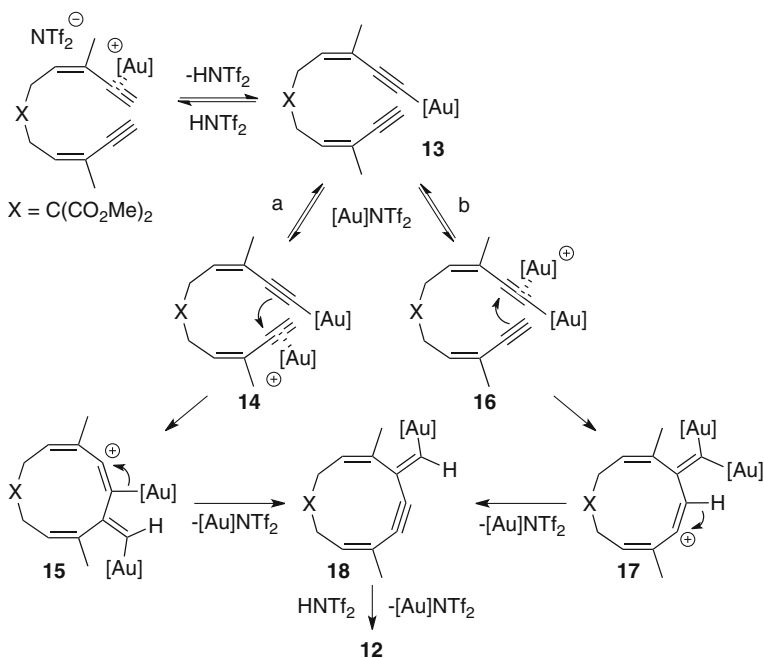


Scheme 4.3 Formation of a reactive digold complex in the catalytic cycle of the Alder-ene reaction of 1,5-allenyne. Energies are given in kcal.mol^{-1}



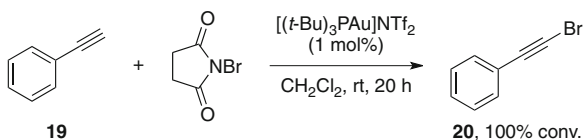
Scheme 4.4 Cycloisomerization reaction of diyne

intermediate **15**, which upon gold elimination evolves into vinylgold **18**. In path b, the second gold fragment would activate the gold acetylide moiety and trigger a nucleophilic attack onto the latter to produce *gem*-diaurated species **17**, which



Scheme 4.5 Two possible mechanisms in the cyclization of diynes

Scheme 4.6 Au-catalyzed bromination of terminal alkynes



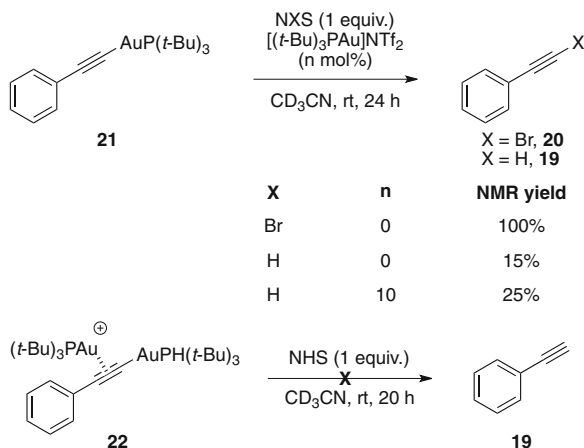
echoes back the proposal of Toste and Houk. A stereospecific protodeauration leads to **18**, which links paths a and b together. A final protodeauration delivers the cyclized compound **12** (Scheme 4.5).

4.1.1.3 Gold Acetylides in Acetylenic Functionalization Reactions

The team of Corma also proposed the intermediacy of gold acetylides in the gold catalyzed bromination of terminal alkynes in the presence of NBS, and brought compelling evidences to support this hypothesis (Scheme 4.6) [18].

The gold acetylide **21** was shown to react either with NBS or NHS to give respectively **20** or **19**. Interestingly, the protonolysis reaction slightly accelerated in the presence of catalytic amounts of the cationic gold(I) catalyst, a fact that would be consistent with a “dual activation” mechanism as proposed by Toste and

Scheme 4.7 Reactivity of Au acetylide **21** and diAu complex **22** toward bromo- and protolysis

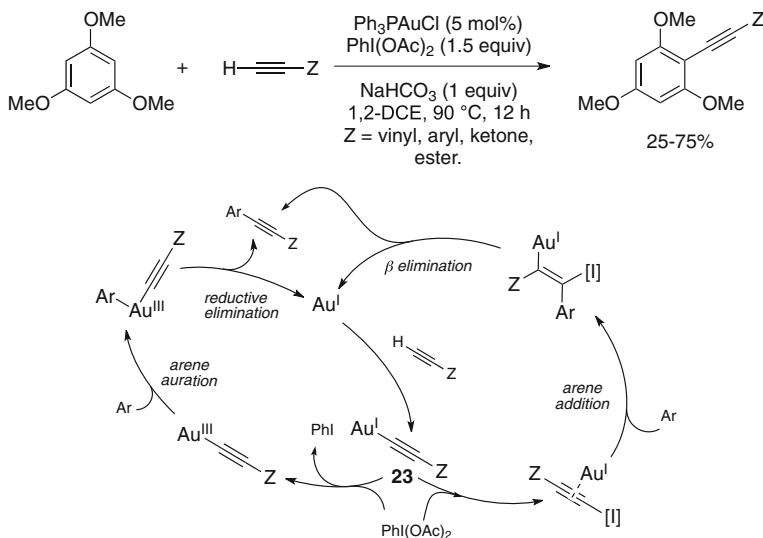


Houk. However, the isolated complex **22** showed no reactivity toward NHS, which dispelled this hypothesis (Scheme 4.7).

To finish, it is worth adding that some reports exist on gold catalyzed Sonogashira-type cross-coupling [19–21]. If there is still a debate on the role of palladium impurities [22] and gold nanoparticles [23] in such processes, the occurrence of gold acetylides along the catalytic cycle was of course proposed. Some comparable methodologies were developed where the gold(I)/gold(III) redox cycle was forced thanks to the use of stoichiometric oxidants [24–27]. Spectroscopic evidences on the occurrence of gold acetylide **23** during the gold catalyzed ethynylation of arenes were collected by the group of Nevado [26]. They could detect ^{31}P and ^1H NMR signals matching those of the independently synthesized acetylide **23**. They thus proposed two mechanisms for this coupling process, involving the above mentioned gold acetylide (Scheme 4.8) and differing on the role of the hypervalent iodine reagent.

4.1.2 Presentation and Objectives of the Project

The ability of gold(I) to easily insert into acetylenic C–H bonds raises some questions about the occurrence of gold acetylides in every gold catalyzed process involving a free alkyne. The study of Toste and Houk on the gold catalyzed cycloisomerization of 1,5-allenynes shows that their formation is thermodynamically favored, and they readily bind another gold fragment to give birth to a reactive species that evolves into *gem*-diaurated species along the catalytic cycle. Belonging to the vast area of 1,*n*-enynes cyclization reactions, this study thus lays some doubt on the now commonly accepted mechanisms that generally involve coordination of gold on the free alkyne followed by nucleophilic attack of the neighboring double bond. Our study simply questions the validity of such species



Scheme 4.8 Nevado's ethynylation of electron-rich arenes

in the cycloisomerization of 1,6-enynes. For this purpose we have called upon theoretical treatment through DFT computations, NMR spectroscopy and mass spectrometry, and solution experiments.

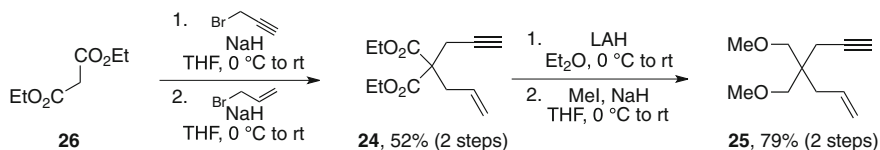
4.2 Preliminary Results with 1,6-Enynes

4.2.1 Catalysts Assessment

We decided to focus on 1,6-enynes **24** and **25** as they are readily accessible and serve as generic substrates in many experimental and theoretical studies on such substrates. As a background study, their reactivity toward three gold catalysts was assessed in deuterated chloroform. Enynes **24–25** were synthesized according to reported procedures depicted in Scheme 4.9, starting from diethylmalonate **26**. Subsequent alkylations of the latter furnished enyne **24** with a *gem*-diester group as tether. Dimethoxy enyne **25** was prepared from **24** by reduction of the ester groups followed by protection of the alcohol functions.

With these substrates in hand, we submitted them to cationic gold(I) catalysts **27**, [28, 29] **28**⁴ and **29** [30] (Table 4.1). As it is commonly observed with these substrates, *endo* products **30/31** are the major ones, accompanied by varying amounts of formal metathesis products **32/33**. Echavarren's catalyst **29** has shown

⁴ First synthesis: [32]. Use in catalysis: [33]. See also ref. [14].



Scheme 4.9 Synthesis of the “test” 1,6-enynes **24** and **25**

the better activity and produced high yields of cyclized compounds within 1 h at rt, starting from either **24** or **25**. Gagosz’ catalyst **27** was highly active and selective for malonate tethered enyne **24**, but, for unknown reasons, gave inferior results with dimethoxy precursor **25**. Finally, oxonium complex **28** is a poorly active catalyst for the cycloisomerization of 1,6-enynes, as heating is needed to perform the reaction, which is incomplete after several hours.

4.2.2 Mass Spectrometry Analysis

In many cases in organometallic catalysis, a comprehensive study of the considered process is supported by spectroscopic analysis, labelling studies and/or theoretical treatment. Less developed is the mass spectrometry (MS) approach. Since the development of the electrospray (ESI) technique that allows the intact transfer of molecular ions from a dilute solution directly to the gas phase through a gentle ionization,⁵ a growing number of studies have relied on this technique, coupled to a mass spectrometer, to get insight in mechanistic intermediates [31]. This technique is ideal when the species of interest is already present in ionic form in solution, which is frequently the case in gold(I) catalysis, and the soft ionization process allows to keep the catalyst’s coordination sphere intact. Thanks to mass spectrometry techniques, it is also possible to isolate the ion to be studied, and operate collisions with other molecules. Collision induced dissociation (CID) is employed to get thermochemical parameters by collision with an argon atom of known energy, and collision activated reaction (CAR) allows reactivity studies in the gas phase of the isolated ion, by collision with neutral molecules. In our laboratory, this approach, combined with DFT calculations, helped to confirm the crucial role of water traces in the cationic Pt(II)-catalyzed cycloisomerization reaction of enynes [36]. We therefore decided to take advantage of the ESI-MS technique to get in-depth understanding of the intermediates involved in the gold(I) catalyzed skeletal rearrangement of enynes. For this purpose, we used a modified triple-quadrupole mass spectrometer (Scheme 4.10) [37, 38].

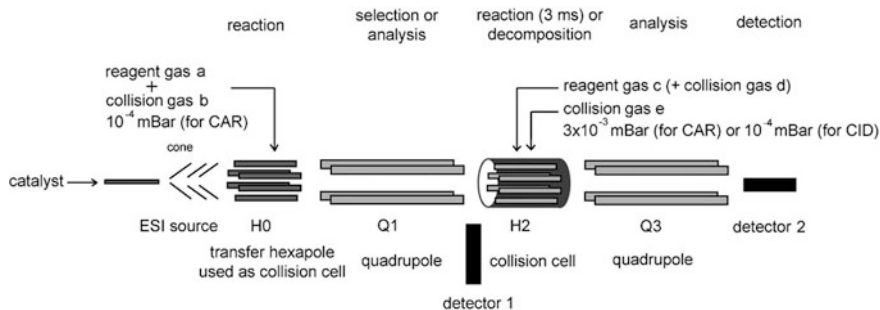
⁵ According to a complicated process involving charged droplet formation, fission, and field desorption, see: [34, 35].

Table 4.1 Reactivity of 1,6-enynes **24–25** with various gold catalysts

Entry	24	30	31
	catalyst (2 mol%) CDCl ₃ (0.025M)		
1	27	rt, 1 h	87% (20:1)
2	28	reflux, 7 h	35% (1:0) ^a
3	29	rt, 1 h	quant. (5:1)
4	27	rt, 3 d	38% (6:1) ^b
5	28	reflux, 15 h	47% (4:1) ^c
6	29	rt, 1 h	95% (1:6:1)

^a a 60% of the starting material was recovered. ^b idem, 55%. ^c idem, 38%

^a a 60% of the starting material was recovered. ^b idem, 55%. ^c idem, 38%



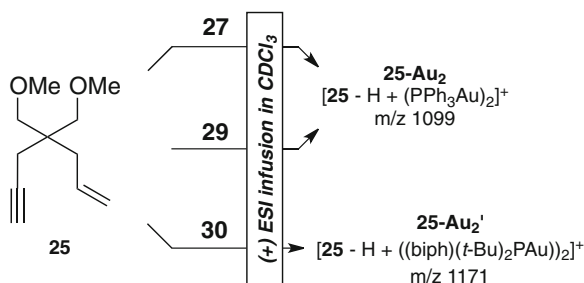
Scheme 4.10 The modified triple quadrupole mass spectrometer

The analyte is injected into the instrument via a syringe pump and pumped through a narrow, stainless steel capillary. A high voltage of 3 or 4 kV is applied to the tip of the capillary, which is situated within the ionisation source of the mass spectrometer. As a consequence of this strong electric field, the sample emerging from the tip is dispersed into an aerosol of highly charged droplets, a process that is aided by a co-axially introduced nebulizing gas flowing around the outside of the capillary. This gas, usually nitrogen, helps to direct the spray emerging from the capillary tip towards the mass spectrometer. The charged droplets diminish in size by solvent evaporation, assisted by a warm flow of nitrogen known as the drying gas, which passes across the front of the ionisation source. The ions produced in the electrospray source are transmitted into an intermediate vacuum region through a heated capillary where desolvation is completed, and from there through a small aperture into the analyser of the mass spectrometer, which is held under high vacuum. They first cross hexapole H0 which is connected to a gas inlet to perform collision with neutral gaseous reagents. Ions pass then into the first quadrupole analyzer Q1 in which the ions or reaction products can be selected and separated for a subsequent reaction. The mass-selected ions are then passed into a collision cell H2 where they can react again with neutral reagent gases, and then mass-analyzed in the second quadrupole Q3. High-resolution measurements at Q3 exit were acquired with a recent ultra-high resolution mass spectrometer, the hybrid linear ion trap LTQ-Orbitrap.

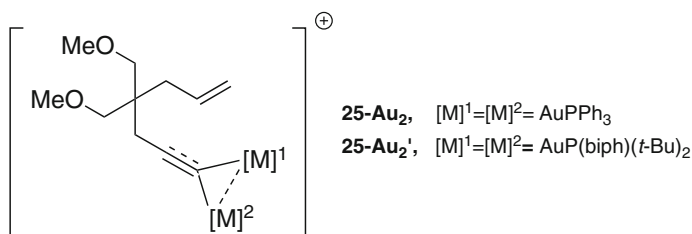
We engaged enyne **25** with catalysts **27–29**, in solution in CDCl_3 , into this mass spectrometer. With catalyst **27** and **28**, we observed the rapid and abundant formation of a peak at $m/z = 1,099$, corresponding to the formula $[\mathbf{25-H} + (\text{Ph}_3\text{PAu})_2] + (\mathbf{25-Au}_2)$. With catalyst **29**, the same type of adduct was also observed with a relatively high abundance, at $m/z = 1,171$ ($\mathbf{25-Au}_2'$) (Scheme 4.11).

The observation of these ions could suggest the formation of diaurated complexes similar to those proposed by Toste and Houk, by coordination of a cationic gold fragment to a gold acetylide (Scheme 4.12).

We thus synthesized gold acetylides **24-Au** and **25-Au** in order to submit them to the same mass spectrometry conditions and compare the experiments spectra. They were synthesized by treating Ph_3PAuCl with three equivalent of the lithium



Scheme 4.11 Observation of diaurated adducts in mass spectrometry conditions



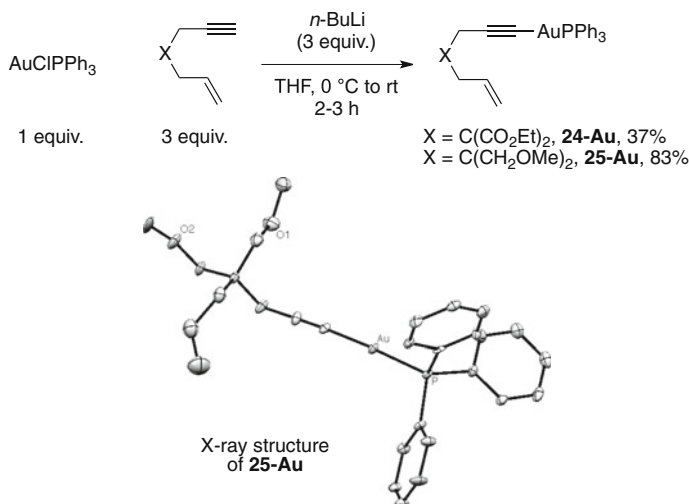
Scheme 4.12 Proposed structure for **25-Au₂** and **25-Au₂'**

acetylide of **24** or **25** (Scheme 4.13). The structure of **25-Au** was ascertained by the means of X-ray diffraction.

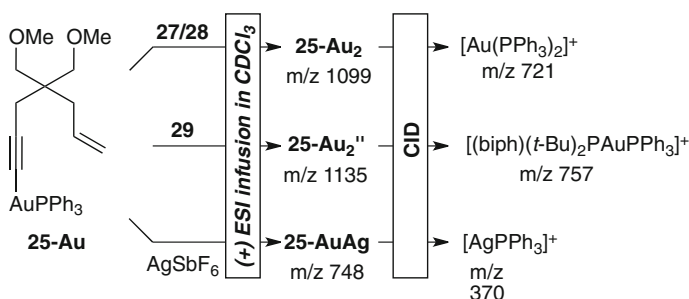
We engaged **25-Au** in the ESI source in a CDCl_3 mixture with either catalysts **27–29** or AgSbF_6 . We also noticed the formation of ions **25-Au₂** and **25-Au₂'**, while with AgSbF_6 a dinuclear silver-gold **25-AuAg** complex was observed. The isolated ions were submitted to CID experiments, which resulted in all cases in the detection of metallic ions ligated by the two phosphines (Scheme 4.14).

The neutral counterpart lost in each case correspond to the formula $[\text{25-H} + \text{Au}]$, but its structure remained unknown. DFT computations at the B3LYP/LANL2DZ(Au)/6-31G(d,p) level of theory were carried out by Prof. V. Gandon to learn more about the nature of this counterpart. Thermodynamic results using hept-1-en-6-yne **34** and PH_3 as model have shown that either the naked gold acetylide **35** or its related chelate **36** require prohibitive energies to be formed upon dissociation in the CID conditions. However, the formation of the cyclized form of the enyne bound to one gold atom **37** is endergonic by only $6.0 \text{ kcal.mol}^{-1}$, which suggests that the neutral counterpart could be **37** (Scheme 4.15).

All these data tended to suggest the formation of gold acetylides and their corresponding diaurated species in the reaction mixture. However, nothing indicates that they are really implicated in the catalytic cycle of the cycloisomerization of 1,6-enynes, and moreover, the observation of such species could simply arise from the instrument used for such measurements, which makes hazardous the transposition of these results to a solution phase catalytic event. It therefore appeared obvious that more accurate data could be gleaned from NMR monitoring.



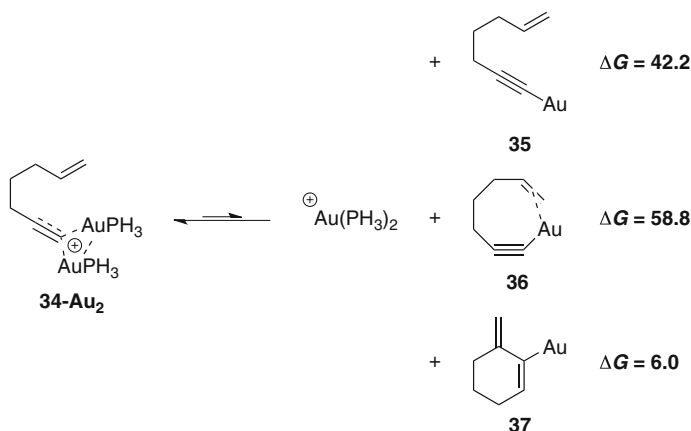
Scheme 4.13 Synthesis of gold acetylides

Scheme 4.14 Observation of diaurated adducts from **25-Au** and CID experiments

4.3 Solution and NMR Monitoring Experiments

4.3.1 Study with Free Enyne **25**

The NMR monitoring of the reaction of **24/25** with 1 equivalent of catalyst **27** or **29** could not be achieved, even at low temperature (−60 °C) because cycloisomerization took place at once. Catalyst **28** appeared as a good candidate as it requires heat to perform the cycloisomerization of 1,6-enynes. Thus, we followed the evolution of a solution of **25** with 0.33 equivalent of **28** in CDCl₃ by the means of ¹H and ³¹P NMR. After 5 min the signal of the free enyne were still clearly visible in ¹H NMR, but a new compound **38** exhibiting downfield shifted

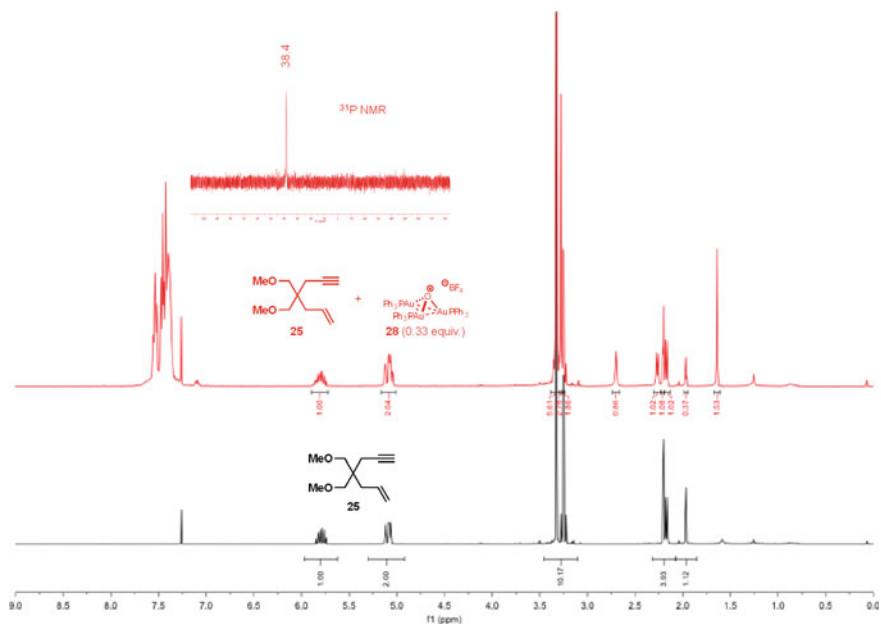


Scheme 4.15 Calculated free energies of dissociation ($\text{kcal}\cdot\text{mol}^{-1}$)

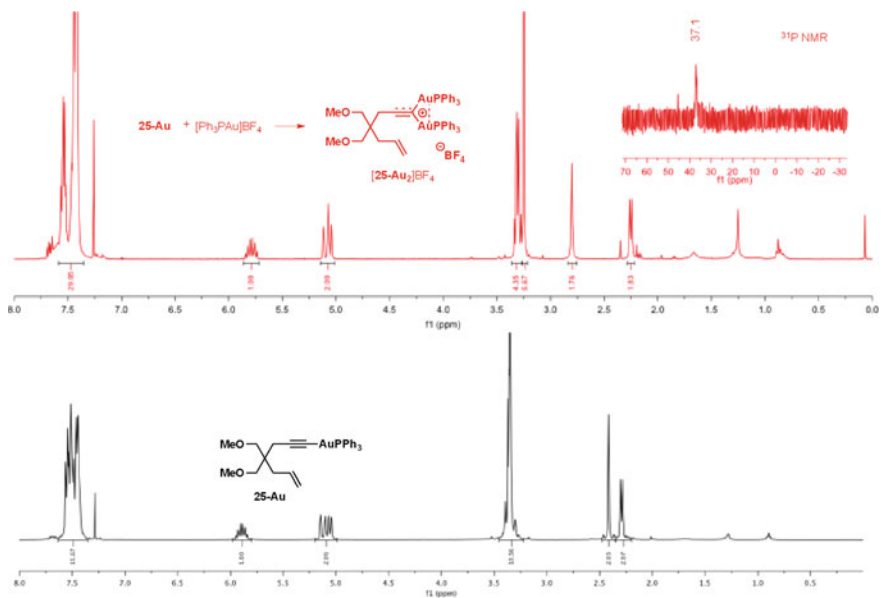
propargylic protons (2.16–2.69 ppm) and a priori no acetylenic proton was also present. A broad peak at 1.64 ppm was also observed, which strongly diminished in intensity upon addition of D_2O to the mixture, suggesting complexed water. ^{31}P NMR showed a single peak at 38.4 ppm, the signal of catalyst **28** at 23.9 ppm being no longer visible (Scheme 4.16).

We assumed from these data that this unknown compound **38** could be the $[\mathbf{25}\text{-Au}_2]\text{BF}_4$ species we observed by mass spectrometry. To validate this hypothesis, we reacted gold acetylide **25-Au** with one equivalent of the pre-generated cationic gold(I) salt $[\text{Ph}_3\text{PAu}]\text{BF}_4$ in CDCl_3 and monitored this reaction by NMR. We noticed after 5 min the formation of a new complex, while **25-Au** signals completely disappeared. Again, a strong downfield shifting of the propargylic signals (2.39–2.80 ppm) was recorded in ^1H NMR, and a single peak at 37.1 was visible in ^{31}P NMR. Clearly digold complex $[\mathbf{25}\text{-Au}_2]\text{BF}_4$ was formed in the NMR tube, but its spectroscopic profile did not match the one of **38** (Scheme 4.17).

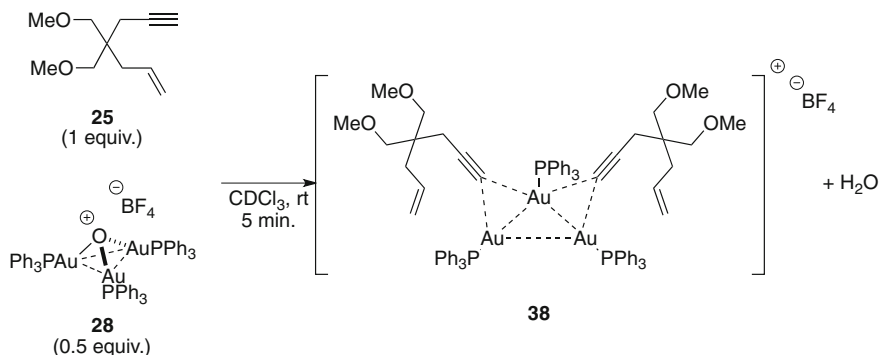
A close look on the **25**:**38** ratio by varying the amount of catalyst **28** mixed with enyne **25** in the NMR tube brought more suggestive data on the actual structure of **37**. When reacting enyne **25** with 0.33 equivalent of **28**, the **25**:**38** ratio was about 1:1 based on the integration of the propargylic protons and remained unchanged after 1 h. Increasing the amount of catalyst **28** to 0.5 equivalent lead to complete consumption of the free enyne **25** after 1 h, and only **38** is observed in both ^1H and ^{31}P NMR. When 0.66 or 1 equivalent is added, only **38** is visible in ^1H NMR but ^{31}P NMR revealed that a proportion of **28** was unreacted. Thus, at least 0.5 equivalent of catalyst is necessary to reach full consumption of enyne **25** and its clean conversion into **38** with no **28** remaining. This corresponds to a enyne:gold ratio of 2:3, which made us assume that **38** could possibly be the trinuclear dimer depicted in Scheme 4.18. This assumption is also consistent with the 1:1 ratio deducted from the integration of the propargylic protons in the experience **25** + 0.33 equiv. of **28** described above.



Scheme 4.16 NMR monitoring of **25** + 0.33 equiv. of **28** in CDCl_3



Scheme 4.17 Formation of a diaurated complex upon coordination of a cationic gold(I) center onto a gold acetylide



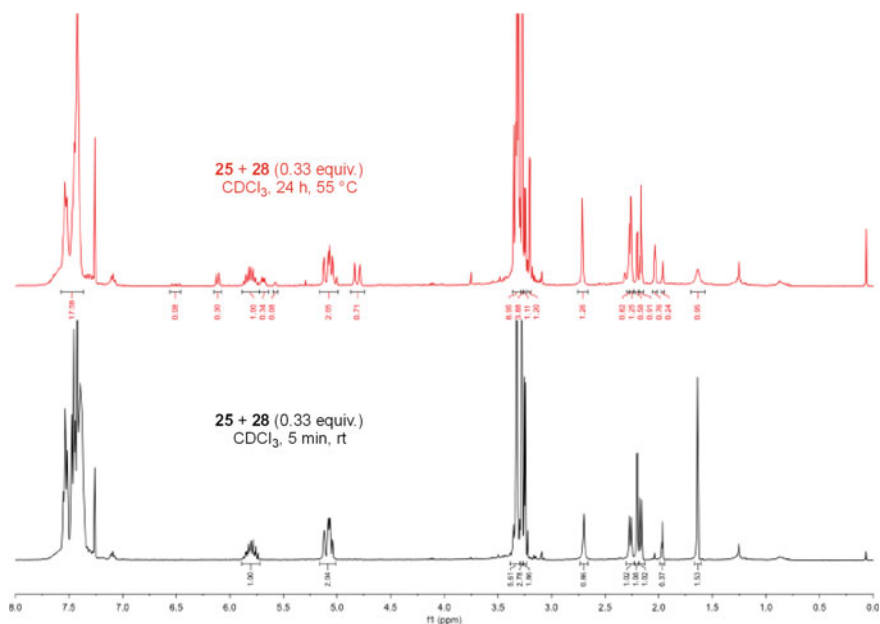
Scheme 4.18 Proposed structure of complex **38**

This structure can be seen as two gold acetylides sharing the same $[\text{Ph}_3\text{PAu}]^+$ fragment. This complex could have been isolated as a white, air-stable solid by evaporation of the CDCl_3 solution and precipitation in Et_2O . However, all attempts to grow crystals to confirm this structure by an X-ray diffraction study have failed. The non-observation of **38** by mass spectrometry (only **25-Au2** was observed) presumably arises from its fragility in the previously used ESI conditions. This was confirmed by using a low “cone voltage” (diminishing the voltage in the ESI chamber to get smoother ionization conditions). A peak at $m/z = 1,739$ corresponding to the formula $[\text{225-2H} + 3\text{AuPPh}_3]^+$ was now observed. Using deuterated **25**, the formation of **38** appeared slower (**25:38** ratio of 95:5 after 5 min, compared to 34:66 without deuterium), the kinetic isotope effect being consistent with a deprotonation of the acetylenic position.

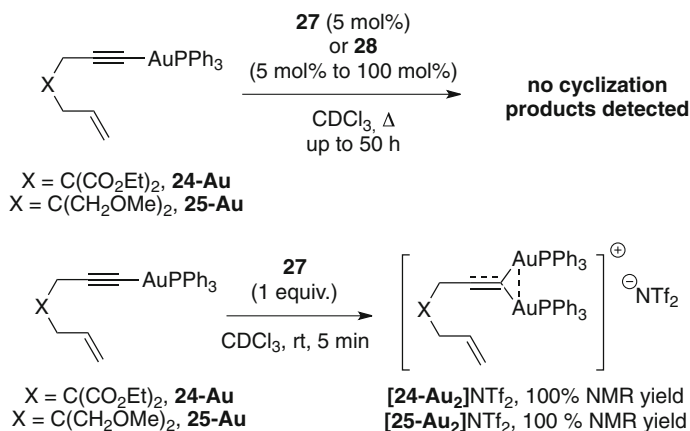
The solution obtained by reacting **25** and 0.33 equivalent of **28** furnished, upon heating at 50°C during 24 h, a mixture of free enyne **25**, **38** and cyclization compounds **32**, **33** in a **25:38:32:33** ratio of 27:32:32:9 (Scheme 4.19). Compared to the **25:38** ratio of 34:66 before heating, one can notice that the amount of dimer **38** is almost constant, which strongly support the fact that **38** is not an intermediate in the cycloisomerization of enynes, and discredit the intermediacy of gold acetylides in this process. To further confirm this hypothesis, we decided to study the reactivity of gold acetylides **24-Au** and **25-Au**.

4.3.2 Reactivity of Gold Acetylides

Gold acetylides **24-Au** and **25-Au** were submitted to 5–100 mol% of catalyst **27** or **28**. No cycloisomerization products were detected even after several hours in refluxing CDCl_3 . We noticed however the fast formation of digold complexes $[\text{24-Au}_2]\text{NTf}_2$ and $[\text{25-Au}_2]\text{NTf}_2$ while monitoring the reactions of **24-Au** and **25-Au** with stoichiometric amounts of catalyst **27** at rt in CDCl_3 (Scheme 4.20), but the



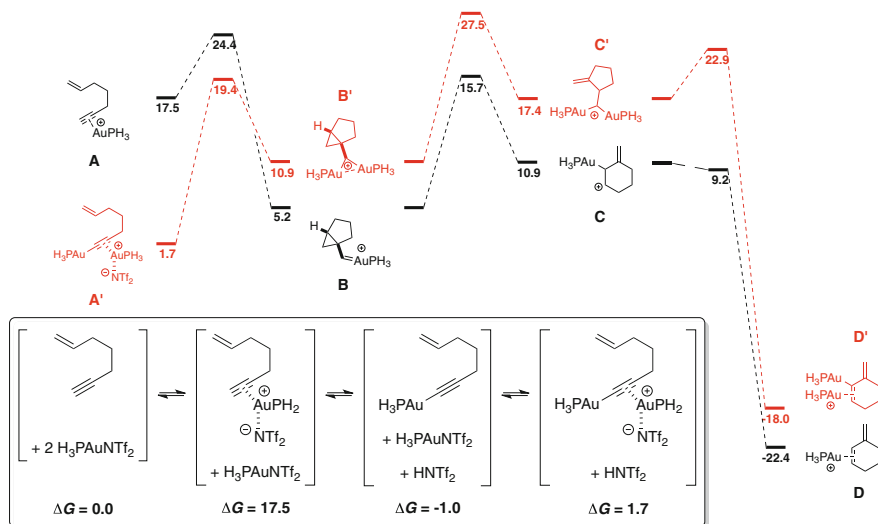
Scheme 4.19 Formation of cyclized compounds from a 34:66 mixture of **37** and **25** upon heating



Scheme 4.20 Reactivity of the gold acetylides

absence of cyclized compounds in the reaction mixture further discredited the intermediacy of gold acetylides in the catalytic cycle.

Based on the computations led by Tost and Houk, Prof. V. Gandon was able to model the formation of gold acetylide and digold complex with catalyst **27**



Scheme 4.21 Mono versus dual activation: DFT computations (energies given in kcal.mol⁻¹)

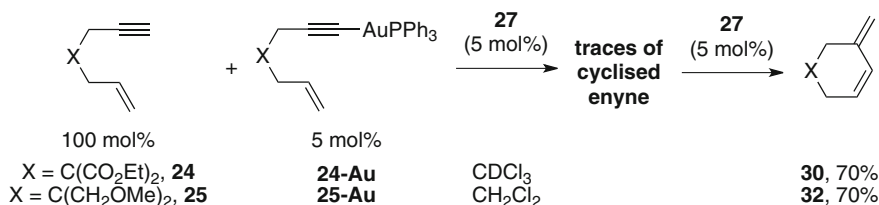
(Scheme 4.21, box) and the energy profile of the cyclization starting either from the monocoordinated enyne or from the diaurated complex (Scheme 4.21).

As noticed by Toste and Houk, the formation of a gold acetylide is favorable, as well as the coordination of a second gold fragment onto the latter. However, the energy profiles reveal that higher energy barriers have to be crossed in “digold” path. The theory thus predicts a favored “monogold” cyclization pathway. Intriguingly, in the latter case, the rearrangement of the nonclassical cation from **B'** to **D'** occurred through a five-membered ring intermediate **C'** rather than a six-membered one, as modeled in the single activation pathway.

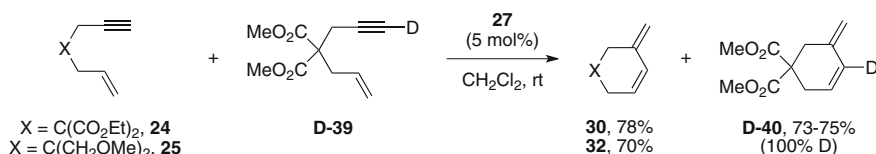
The great affinity of cationic gold(I) for a gold acetylide was also well illustrated experimentally: free enyne **24** or **25** was mixed with 5 mol% of its corresponding acetylide in either dichloromethane or deuterated chloroform. Then, 5 mol% of catalyst **27** were added to the solution. After 1 h, no cycloisomerization could be detected in the reaction mixture, but adding extra 5 mol% of **27** resulted in clean conversion of the free enyne (Scheme 4.22). Thus, complexation of a cationic gold fragment results in a catalytically unactive species, at least at rt.

Considering the work of Toste and Houk, it can be argued that a proton source is needed to complete the catalytic cycle. In their article, this role is held by the acetylenic proton of a free allenyne. Thus, in the 1,6-enyne series, the cycloisomerization reaction of a mixture of enynes **24** or **25** with **D-39** should result in a certain level of deuterium scrambling if a mechanism involving gold acetylides is operative. However, no deuterium exchange was observed using catalyst **30** (Scheme 4.23).

Clearly in this process the enyne cannot act as a proton donor. The unreactivity of gold acetylides and their related diaurated complexes is quite intriguing, as



Scheme 4.22 Greater affinity of Au(I)⁺ for Au acetylides inhibits the cycloisomerization reaction of enynes



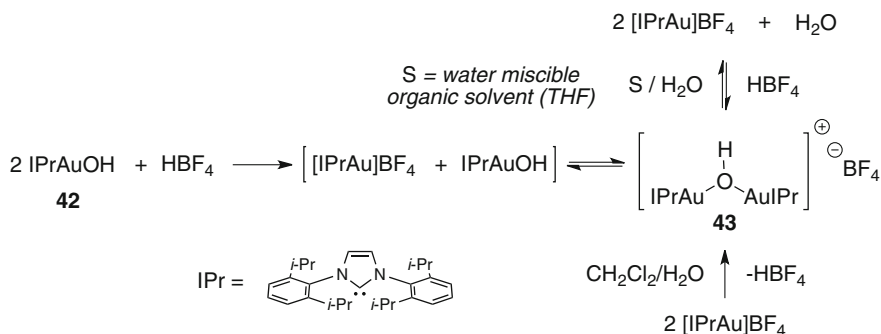
Scheme 4.23 Deuterium scrambling experiment

complex **38**, which resembles the structure of diaurated complexes [24-Au₂]NTf₂ and [25-Au₂]NTf₂, do furnish cyclized compounds upon heating. The major difference between the trinuclear complex **38** and his parent diaurated ones is that its formation is accompanied by the appearance in ¹H NMR of a broad peak at 1.64 ppm that suggests complexed water. This could finally act as the proton source in the cycloisomerization promoted by catalyst **28**.

4.4 Investigations on the Origin of the Diaurated Species

4.4.1 Mass Spectrometry Analysis

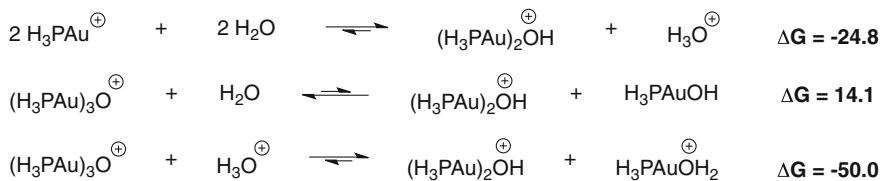
Recent literature reports by Nolan and co-workers have shown that gold(I) hydroxide species **42** [39] could readily insert into an acetylenic C–H bond to produce gold acetylides [40]. This species was shown by DFT to possibly form from cationic NHC gold(I) and water and to be key intermediates in the gold-catalyzed hydrative synthesis of enones and enals from propargylic acetates [41] or propargylic alcohols [42]. An in-depth study of the solution behaviour of such species revealed that protonolysis of a gold hydroxy species can lead to a [(IPrAu)₂(μ-OH)]⁺ complex **43** [43]. The latter can be seen as a reservoir of what is supposed to be the catalytically active species in gold catalyzed processes, say, [IPrAu]⁺. Upon acidic treatment, it can easily release [IPrAu]⁺, while the reaction of [IPrAu]⁺ with water inversely furnish **43** [44] (Scheme 4.24).



Scheme 4.24 Solution behaviour of gold(I) hydroxide and related species investigated by Nolan and coll.

This study suggests that in the presence of water, cationic gold(I) complexes can readily bind H₂O to form complex such as **43**. In an environment containing traces of water and acid, one can reasonably envision equilibrium between species **42–43**. That is why we wondered if one of these could not be responsible for the occurrence of diaurated complexes **24-Au₂** and **25-Au₂** we observed in MS conditions. Preliminary confirmation came after a closer look at the recorded MS spectra of **25** + **27/28/29** solutions. With catalyst **27** or **28**, the protonated gold hydroxide [Ph₃PAuOH]H⁺ (*m/z* = 477) was weakly observed, as well as [(biphenyl)(*t*-Bu)₂PAuOH]H⁺ (*m/z* = 513) with catalyst **29**. With the first two catalysts, we also noticed a peak at *m/z* = 935 corresponding to complex [(Ph₃PAu)₂OH]⁺, the phosphine equivalent of **43**. The parent complex [{(biphenyl)(*t*-Bu)₂PAu}₂OH]⁺ (*m/z* = 1,007) was found more abundant in the analysis of the solution of **25** + **29**, and he was accompanied by an ion at *m/z* = 1,189 that corresponds to the [**25** + [(biphenyl)(*t*-Bu)₂PAu]₂OH]⁺ adduct. This ion was shifted to *m/z* = 1,190 using deuterated **25**, whereas the *m/z* = 1,171 ion corresponding to **25-Au₂'** was unchanged. Although not categorical, these data support the structure we proposed for the diaurated complexes and suggest the involvement of gold hydroxy species in their formation.

By using CH₃CN, a coordinating solvent, to infuse a solution of **25** + **28** in the ESI source, we noticed this time the peak of **25-Au₂** displayed relatively low intensity. Adding 5 % of water to the solution dramatically increased its intensity, while a peak at *m/z* = 1,117, potentially corresponding to [**25** + (Ph₃PAu)₂OH]⁺ was now weakly observed, which further support the role of water in the observation of diaurated species.



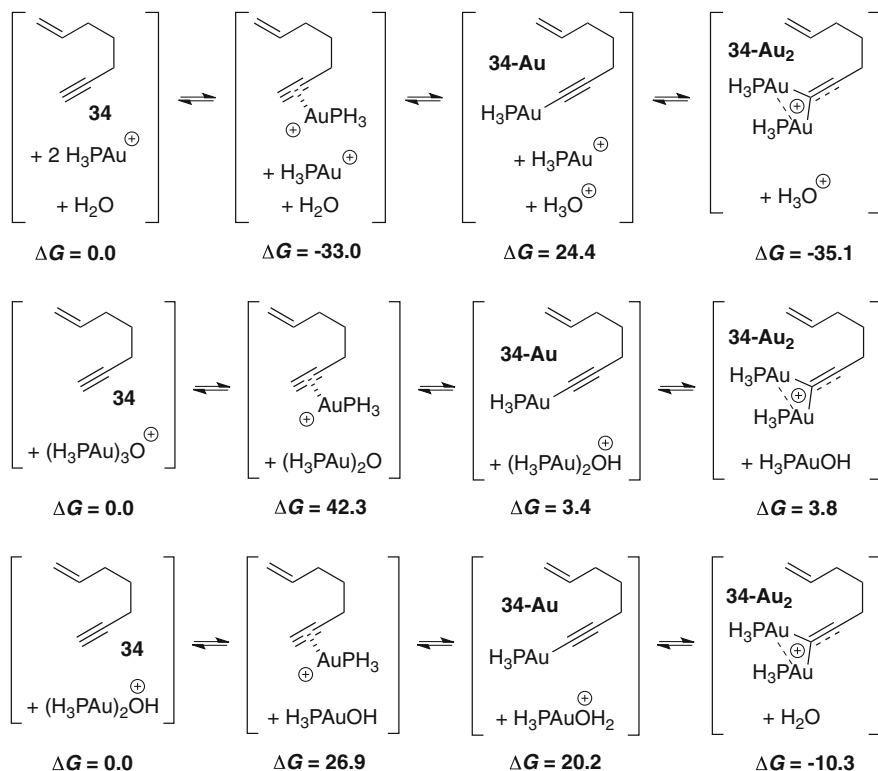
Scheme 4.25 Thermodynamic data on the formation of $[(\text{H}_3\text{PAu})_2\text{OH}]^+$

4.4.2 Theoretical Investigations

Prof. V. Gandon compared by the means of DFT various routes to $[(\text{H}_3\text{PAu})_2(\mu\text{-OH})]^+$ complex to see if in the phosphine series the formation of such species was possible. Its formation is thermodynamically favored by reaction of two $[\text{H}_3\text{PAu}]^+$ fragments with two molecules of water, as well by acidic hydrolysis of catalyst **28**. In the latter case, this process is strongly exothermic (Scheme 4.25).

We next had a look at the formation of diaurated species **33-Au₂** from a thermochemical point of view, with hept-1-en-6-yne **34** and PH_3 as model, starting either from $[\text{H}_3\text{PAu}]^+$, $[(\text{H}_3\text{PAu})_3\text{O}]^+$ or $[(\text{H}_3\text{PAu})_2\text{OH}]^+$, with water as proton acceptor in the former case (Scheme 4.26).

With $[\text{H}_3\text{PAu}]^+$, the formation of complexed alkyne is strongly exothermic, but the subsequent formation of gold acetylide **34-Au** is made difficult by a substantial endothermicity. However, the observed affinity of LAu^+ fragments for gold acetylides was well reproduced computationally, as illustrated by the exothermicity of the last step leading to **34-Au₂**. Starting from $[(\text{H}_3\text{PAu})_3\text{O}]^+$ (a simplified **28**), the first complexation could be achieved if $42.3 \text{ kcal.mol}^{-1}$ are furnished to the system, which is in sharp contrast compared to the first row of Scheme 4.26 and probably arises from the need to break a Au-O bond. From there, the formation of **34-Au** is exothermic, and we noticed in this case that the diaurated species **34-Au₂** is found less stable than the corresponding acetylide. The overall process, unlike with $[\text{H}_3\text{PAu}]^+$, is slightly endothermic and correlates well the results obtained by modelling by Toste and Houk with 1,5-allenynes. Finally, with $[(\text{H}_3\text{PAu})_2\text{OH}]^+$ as the gold source, the dissociation/alkyne complexation as well as gold acetylide formation are both quite endothermic processes, but the overall process leading to **34-Au₂** is exothermic by $10.3 \text{ kcal.mol}^{-1}$. In view of these theoretical results, our hypothesis that diaurated species could arise from gold hydroxy species, formed by interaction of cationic gold(I) fragments and adventitious water, seems plausible. More precisely, the formation of dinuclear species could in fact involve complexes of type $[(\text{LAu})_2\text{OH}]^+$.

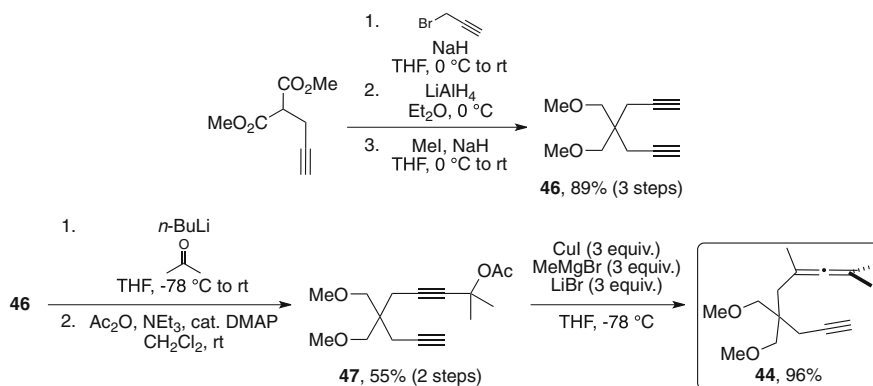
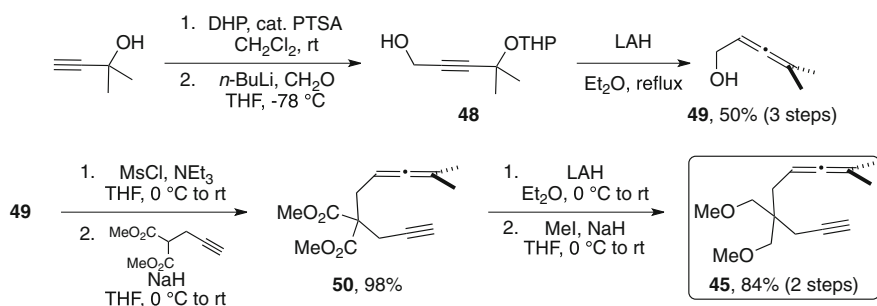


Scheme 4.26 Theoretical study on the formation of diaurated species (free energies in kcal.mol^{-1})

4.5 Preliminary Results with Allenynes

4.5.1 Reactivity of 1,6-Allenynes with Gold Catalyst 38

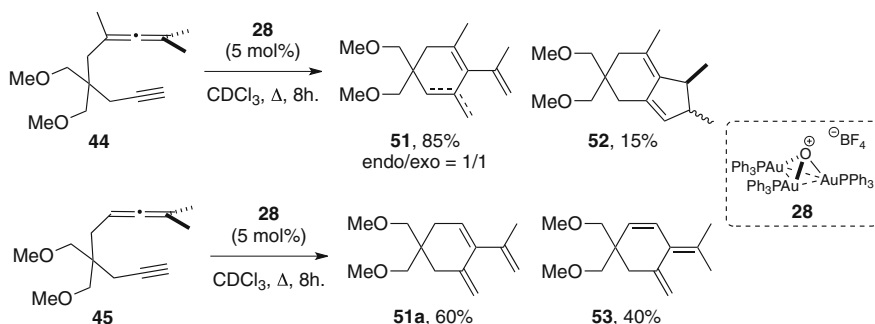
We then turned our attention toward allenynes, to come closer to Toste's and Houk's study. Our study on enynes revealed that gold acetylides are most likely not cyclization intermediates, but their formation could occur, and is favored by traces of water. This is in contrast with Toste's and Houk's observation that 1,5-allenynes acetylides reacted with gold catalyst **28** to give Alder-Ene products, which is not our case. We synthesized 1,6-allenynes **44** and **45** we used in a previous study [45, 46]. 1,6-Allenyne **44** was synthesized through a linear procedure from commercially available dimethyl propargylmalonate. Alkylation with propargyl bromide in the presence of sodium hydride was followed by reduction of the ester groups using lithium aluminium hydride. Final alkylation with methyl iodide furnished diyne **46**. Addition of the mono lithium acetylide of **46** onto acetone and subsequent acetylation of the resulting alcohol produces acetate **49**

Scheme 4.27 Synthesis of 1,6-allenynes **44**Scheme 4.28 Synthesis of 1,6-allenynes **45**

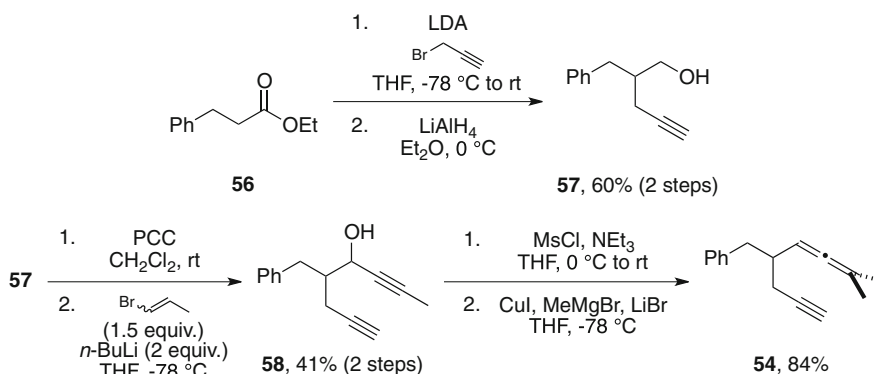
(55 %, 2 steps). $\text{S}_{\text{N}}2'$ using in situ synthesized dimethylcuprate reagent gives the desired allenyne **44** in 96 % yield (Scheme 4.27).

Allenyne **45** was synthesized through a convergent procedure. From propargyl alcohol derivative **50**. Protection of 2,2-methylbutynol with dihydropyran is followed by addition of the lithium acetylide of the resulting THP-protected propargylic alcohol **48** onto formaldehyde. Subsequent treatment with lithium aluminium hydride furnishes allenic alcohol **49**. The mesylate of **49** is then reacted with deprotonated propargyl malonate to give allenyne **50** in 98 % yield. The synthesis ends with a reduction/alkylation sequence to afford dimethoxy derivative **45** (Scheme 4.28).

The reactivity of allenyne **44** and **45** with catalyst **28** are reported in Scheme 4.29. Both substrates gave formal Alder-ene compounds and their double bonds isomers (**51** and **53**) as major (**44**) or exclusive (**45**) products. Intriguingly, allenyne **44** also delivered small amounts of hydrindiene **55**, a compound that is expected to form exclusively with chloride containing catalysts [46].



Scheme 4.29 Reactivity of 1,6-allenyl ether **44–45** with catalyst **28**

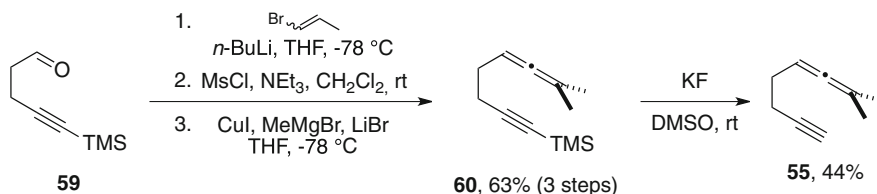


Scheme 4.30 Synthesis of 1,5-allenyl ether **54**

4.5.2 Reactivity of 1,*n*-Allenyl Gold Acetylides

We next decided to check the reactivity of the corresponding gold acetylides. As a starting point of this study, we attempted to reproduce Toste's and Houk's results in the 1,5-allenyl series. 1,5-allenyl ether **54** was prepared from ethyl hydro cinnamate **56**, which was first alkylated in the presence of LDA and propargyl bromide. The resulting α -alkylated ester was then reduced using LAH, affording alcohol **57**. A two-step sequence consisting in oxidation of **57** followed by addition of the in situ generated propyne lithium acetylide furnished propargyl alcohol **58**. Mesylation of the latter and addition of methyl cuprate furnished allenyl ether **54** in 84 % yield (Scheme 4.30).

1,5-Allenyl ether **55** was prepared from aldehyde **64** which synthesis has been described in Chap. 3, according to a comparable procedure than for **54** (Scheme 4.31).

Scheme 4.31 Synthesis of 1,5-allenynes **55**Table 4.2 Cycloisomerizations of 1,5-allenynes **54–55** with gold catalyst **28**

Entry	1,5-allenynes	Product (NMR yield)
1	 54	 61 (99%)
2	 55	 62 (99%)

Their reactivity with gold catalyst **28** was rapidly checked, and the clean formation of Alder-ene product was observed, as Toste and Houk did, in 99 % yield assessed from the NMR of the reaction mixture (Table 4.2).

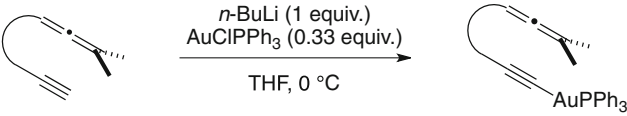
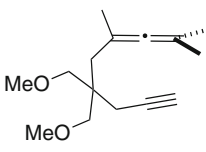
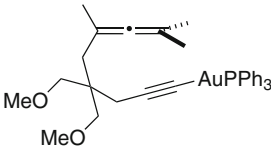
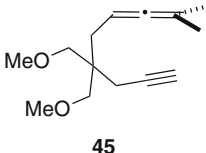
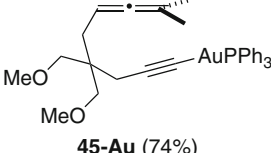
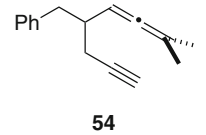
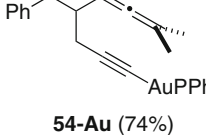
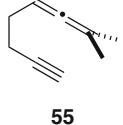
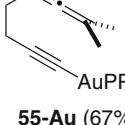
We then prepared the gold acetylides of allenynes **44–45** and **54–55**, in order to check their behaviour in the presence of catalyst **28**. This was done according to the same procedure than for the synthesis of enyne acetylides **24-Au** and **25-Au**, using *n*-butyllithium and triphenylphosphine gold chloride. Acetylides **44/45-Au** and **54/55-Au** were obtained in good yields after precipitation in CHCl_3 /hexane (Table 4.3).

The results of Toste and Houk were totally reproducible in our hands, and 1,5-allenynes gold acetylides **54-Au/55-Au** furnished the Alder-Ene products **61** and **62**, respectively, upon catalysis with complex catalyst **28** (Scheme 4.32).

Contrastingly, the gold acetylides of 1,6-allenynes **44-Au/45-Au** did not give any Alder-Ene products or hydriindiene when submitted to 5 mol% of catalyst **28**. While **45-Au** was totally recovered after 12 h in refluxing CDCl_3 , **44-Au** surprisingly furnished cycloadduct **63** in 55 % isolated yield (Scheme 4.33).

To this date we have no explanation of this reactivity dichotomy between **42** and **42-Au**. The [2 + 2] cycloaddition of allenyne to cyclobutenes has already

Table 4.3 Synthesis of gold acetylides **44-Au**, **45-Au**, **54-Au** and **55-Au**

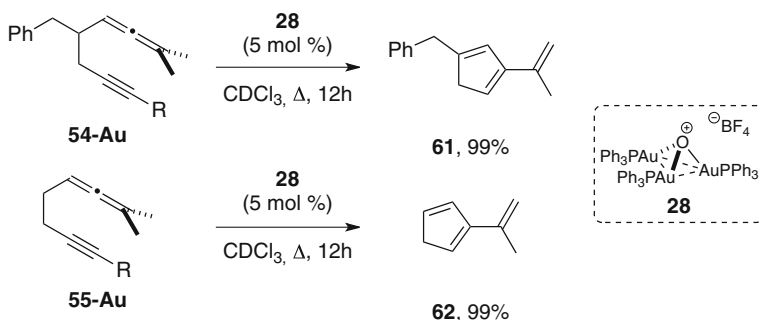
		
Entry	Allenyne	Product (yield)
1	 44	 44-Au (55%)
2	 45	 45-Au (74%)
3	 54	 54-Au (74%)
4	 55	 55-Au (67%)

been reported and is known to occur under thermal conditions. We thus checked the stability of **42-Au** and **42** in refluxing chloroform. The starting material was totally recovered after 12 h in the case of **42-Au**, and **42** led to an inseparable mixture of unidentified compounds, probably arising from allene decumulation but no [2 + 2] adduct was detected (Scheme 4.34).

Gold catalysis, as well as a gold atom as acetylenic substituent is therefore required to perform this reaction.

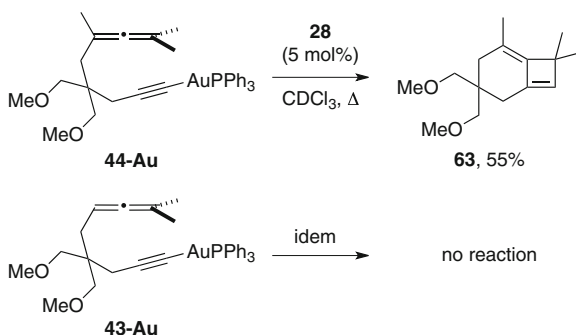
4.5.3 Preliminary Results in Mass Spectrometry

We carried out ESI experiments as above. Allenyne **44** was introduced in infusion in CDCl₃ with catalyst **28**, and similar observations than for 1,6-enynes were made. Among the resulting peaks, two of them caught our attention: a first one at

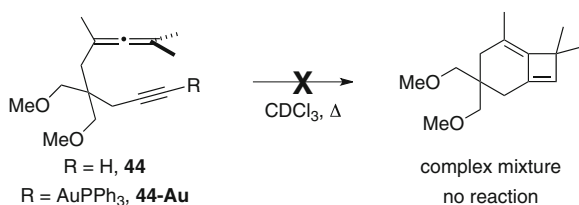


Scheme 4.32 Reactivity of 1,5-allenynes gold acetylides **54-Au** and **55-Au**

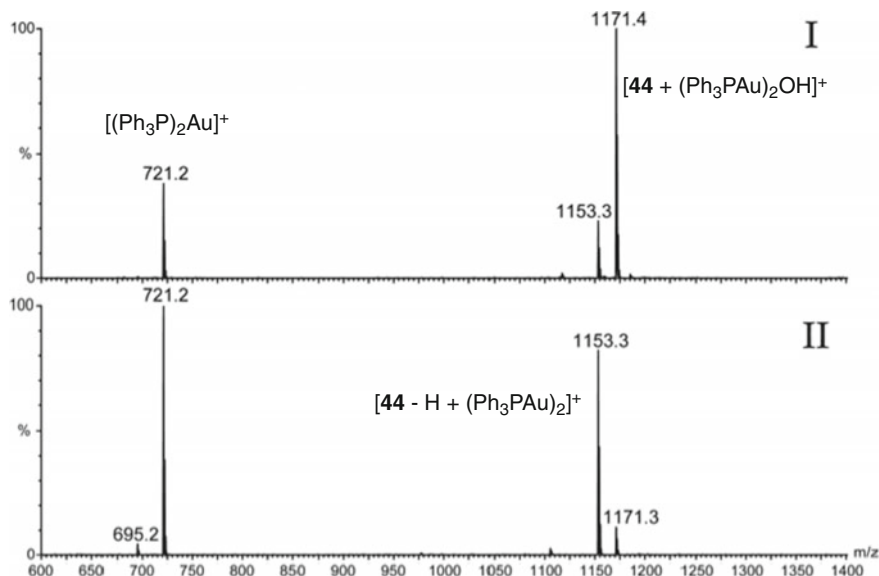
Scheme 4.33 Reactivity of 1,6-allenynes gold acetylides **42-Au** and **43-Au**



Scheme 4.34 Thermal behaviour of allenyne **44** and its related acetylide



$m/z = 1,153$ corresponding to $[\mathbf{44}\text{-H} + (\text{Ph}_3\text{PAu})_2]^+$, and a second one at $m/z = 1,171$ corresponding to $[\mathbf{44} + (\text{Ph}_3\text{PAu})_2\text{OH}]^+$ (Scheme 4.35, I). Again, collision induced dissociation (CID) applied to $m/z = 1,153$ led to $m/z = 721$ ($[(\text{Ph}_3\text{P})_2\text{Au}]^+$), as in the case of enynes. If so, the neutral counterpart could be a cyclic vinylgold as shown before (see Scheme 4.15). On replacing catalyst **28** by **27** ($[(\text{Ph}_3\text{PAu})\text{NTf}_2]$), we found again the peaks at $m/z = 1,153$ and $1,171$, the latter being in this case less abundant (Scheme 4.35, II). Thus, in a similar fashion to enyne **25**, allenyne **44** gives rise to a diaurated species as stable adduct ($m/z = 1,153$) and an adduct with $[(\text{Ph}_3\text{PAu})_2\text{OH}]^+$.



Scheme 4.35 MS spectra recorded by infusion of a CDCl_3 solution of **44** + **28** (I) and **44** + **27** (II)

4.6 Conclusion

This study has shown that gold acetylides are not viable intermediates in the gold catalyzed cycloisomerization of 1,6-enynes, and preliminary results on 1,6-allenynes indicates that they are not likely to occur in their cycloisomerization reactions. These conclusions, however, are in sharp contrast with the ones of Toste and Houk in the 1,5-allenynes series, as substantial experimental and theoretical evidences of their involvement in the formal Alder-Ene of 1,5-allenynes have been collected. The explanation of such mechanistic dichotomy in these closely related reactions has, to this date, no explanation. Aside from these unanswered questions, we have shown that gold acetylides and their corresponding diaurated species could form in the reaction mixture, provided a source of cationic gold(I) is employed as well as substrates bearing a terminal alkyne. Traces of water in the considered solution would greatly favor their formation.

References

1. Scherbaum F, Grohmann A, Huber B, Kruger C, Schmidbaur H (1988) "Aurophilicity" as a Consequence of Relativistic Effects: The Hexakis(triphenylphosphaneaurio)methane Dication $[(\text{Ph}_3\text{PAu})_6\text{C}]^{2+}$. *Angew Chem Int Ed* 27: 1544
2. Schmidbaur H, Schier A (2008) A briefing on aurophilicity. *Chem Soc Rev* 37:1931

3. LaLonde RL, Brenzovich WE, Benitez D, Tkatchouk E, Kelley K, Goddard WA, Toste FD (2010) Alkylgold complexes by the intramolecular aminoauration of unactivated alkenes. *Chem Sci* 1:226
4. Liu L-P, Xu B, Mashuta MS, Hammond GB (2008) Synthesis and Structural Characterization of Stable Organogold(I) Compounds. Evidence for the Mechanism of Gold-Catalyzed Cyclizations. *J Am Chem Soc* 130:17642
5. Hashmi ASK, Schuster AM, Rominger F (2009) Gold Catalysis: Isolation of Vinylgold Complexes Derived from Alkynes. *Angew Chem Int Ed* 48:8247
6. Hashmi ASK, Ramamurthi TD, Rominger F (2009) Synthesis, structure and reactivity of organogold compounds of relevance to homogeneous gold catalysis. *J Organomet Chem* 694:592
7. Weber D, Tarselli MA, Gagne MR (2009) Mechanistic Surprises in the Gold(I)-Catalyzed Intramolecular Hydroarylation of Allenes. *Angew Chem Int Ed* 48:5733
8. Weber D, Gagne MR (2009) Dinuclear Gold–Silver Resting States May Explain Silver Effects in Gold(I)-Catalysis. *Org Lett* 11:4962
9. Seidel G, Lehmann CW, Furstner A (2010) Elementary Steps in Gold Catalysis: The Significance of *gem*-Diauration. *Angew Chem Int Ed* 49:8466
10. Tarselli MA, Gagne MR (2008) Gold(I)-Catalyzed Intramolecular Hydroarylation of Allenes. *J Org Chem* 73:2439
11. Nesmeyanov AN, Perevalova EG, Grandberg KI, Lemenovskii DA, Baukova TV, Afanassova OB (1974) A new type of organogold compound. *J Organomet Chem* 65:131
12. Schmidbaur H, Inoguchi Y (1980) Cyclische μ -(4-Methylcyclohexadien-1-ylidenio)-bis[phosphangold(I)]-Kationen. *Chem Ber* 113:1646
13. Schmidbaur H, Porter KA (2004) In: Olah GA, Prakash GKS (eds) *Carbocation chemistry*, Wiley-Interscience, Hoboken, p 291
14. Cheong PHY, Morganelli P, Luzung MR, Houk KN, Toste FD (2008) Gold-Catalyzed Cycloisomerization of 1,5-Allenynes via Dual Activation of an Ene Reaction. *J Am Chem Soc* 130:4517
15. Hooper TN, Green M, Russell CA (2010) Cationic Au(I) alkyne complexes: synthesis, structure and reactivity. *Chem Commun* 46:2313
16. Blanco MC, Camara J, Gimeno MC, Jones PG, Laguna A, López-de-Luzuriaga JM, Olmos ME, Villacampa MD (2011) Luminescent Homo- and Heteropolynuclear Gold Complexes Stabilized by a Unique Acetylide Fragment. *Organometallics* 31:2597
17. Odabachian Y, Le Goff XF, Gagosz F (2009) An Unusual Access to Medium Sized Cycloalkynes by a New Gold(I)-Catalysed Cycloisomerisation of Diynes. *Chem Eur J* 15:8966
18. Leyva-Perez A, Rubio-Marques P, Al-Deyab SS, Al-Resayes SI, Corma A (2011) Cationic Gold Catalyzes ω -Bromination of Terminal Alkynes and Subsequent Hydroaddition Reactions. *ACS Catalysis* 1:601
19. Gonzalez-Arellano C, Corma A, Iglesias M, Sanchez F (2006) Gold (I) and (III) catalyze Suzuki cross-coupling and homocoupling, respectively. *J Catal* 238:497
20. Gonzalez-Arellano C, Abad A, Corma A, Garcia H, Iglesias M, Sanchez F (2007) Catalysis by Gold(I) and Gold(III): A Parallelism between Homo- and Heterogeneous Catalysts for Copper-Free Sonogashira Cross-Coupling Reactions. *Angew Chem Int Ed* 46:1536
21. Li PH, Wang L, Wang M, You F (2008) Gold(I) Iodide Catalyzed Sonogashira Reactions. *Eur J Org Chem*, 32: 5946
22. Lauterbach T, Livendahl M, Rosellon A, Espinet P, Echavarren AM (2010) Unlikelihood of Pd-Free Gold(I)-Catalyzed Sonogashira Coupling Reactions. *Org Lett* 12:3006
23. Corma A, Juarez R, Boronat M, Sanchez F, Iglesias M, Garcia H (2011) Gold catalyzes the Sonogashira coupling reaction without the requirement of palladium impurities. *Chem Commun* 47:1446
24. Brand JP, Charpentier J, Waser J (2009) Direct Alkynylation of Indole and Pyrrole Heterocycles. *Angew Chem Int Ed* 48:9346

25. Brand JP, Waser J (2010) Direct Alkynylation of Thiophenes: Cooperative Activation of TIPS–EBX with Gold and Brønsted Acids. *Angew Chem Int Ed* 49:7304
26. de Haro T, Nevado C (2010) Gold-Catalyzed Ethynylation of Arenes. *J Am Chem Soc* 132:1512
27. Hopkinson MN, Ross JE, Giuffredi GT, Gee AD, Gouverneur V (2010) Gold-Catalyzed Cascade Cyclization—Oxidative Alkynylation of Allenolates. *Org Lett* 12:4904
28. Mezaillies N, Ricard L, Gagosz F (2005) Phosphine Gold(I) Bis-(trifluoromethanesulfonyl)imide Complexes as New Highly Efficient and Air-Stable Catalysts for the Cycloisomerization of Enynes. *Org Lett* 7:4133
29. Ricard L, Gagosz F (2007) Synthesis and Reactivity of Air-Stable N-Heterocyclic Carbene Gold(I) Bis(trifluoromethanesulfonyl)imide Complexes. *Organometallics* 26:4704
30. Herrero-Gomez E, Nieto-Oberhuber C, Lopez S, Benet-Buchholz J, Echavaren AM (2006) Cationic η^1/η^2 -Gold(I) Complexes of Simple Arenes. *Angew Chem Int Ed* 45:5455
31. Nesmeyanov AN, Perevalova EG, Struchkov YT, Antipin MY, Grandberg KI, Dyadchenko VP (1980) Tris(triphenylphosphine)gold(oxonium) salts. *J Organomet Chem* 201:343
32. Sherry BD, Toste FD (2004) Gold(I)-Catalyzed Propargyl Claisen Rearrangement. *J Am Chem Soc* 126:15978
33. Iribarne JV, Thomson BA (1976) On the evaporation of small ions from charged droplets. *J Chem Phys* 64:2287
34. Thomson BA, Iribarne JV (1979) Field induced ion evaporation from liquid surfaces at atmospheric pressure. *J Chem Phys* 71:4451
35. Plattner DA (2001) Electrospray mass spectrometry beyond analytical chemistry: studies of organometallic catalysis in the gas phase. *Int J Mass Spectrom* 207:125
36. Baumgarten S, Lesage D, Gandon V, Goddard J-P, Malacria M, Tabet J-C, Gimbert Y, Fensterbank L (2009) The Role of Water in Platinum-Catalyzed Cycloisomerization of 1,6-Enynes: A Combined Experimental and Theoretical Gas Phase Study. *ChemCatChem* 1:138
37. Gimbert Y, Lesage D, Milet A, Fournier F, Greene AE, Tabet JC (2003) On Early Events in the Pauson–Khand Reaction. *Org Lett* 5:4073
38. Thota R, Lesage D, Gimbert Y, Giordano L, Humbel S, Milet A, Buono G, Tabet JC (2009) Gas-Phase Study of Phenylacetylene and Norbornadiene on a Palladium(II) Phosphinous Acid Complex: Importance of the Order of Introduction of the Organic Partners. *Organometallics* 28:2735
39. Gaillard S, Slawin AMZ, Nolan SP (2010) A N-heterocyclic carbene gold hydroxide complex: a golden synthon. *Chem Commun* 46:2742
40. Fortman GC, Poater A, Levell JW, Gaillard S, Slawin AMZ, Samuel IDW, Cavallo L, Nolan SP (2010) A versatile gold synthon for acetylene C–H bond activation. *Dalton Trans* 39:10382
41. Marion N, Carlqvist P, Gealageas R, de Fremont P, Maseras F, Nolan SP (2007) [(NHC)Au^I]-Catalyzed Formation of Conjugated Enones and Enals: An Experimental and Computational Study. *Chem Eur J* 13:6437
42. Ramon RS, Marion N, Nolan SP (2009) [(NHC)AuCl]-catalyzed Meyer–Schuster rearrangement: scope and limitations. *Tetrahedron* 65:1767
43. Gaillard S, Bosson J, Ramon RS, Nun P, Slawin AMZ, Nolan SP (2010) Development of Versatile and Silver-Free Protocols for Gold(I) Catalysis. *Chem Eur J* 16:13729
44. Ramon RS, Gaillard S, Poater A, Cavallo L, Slawin AMZ, Nolan SP (2011) [{Au(IPr)}₂(μ -OH)]X Complexes: Synthetic, Structural and Catalytic Studies. *Chem Eur J* 17:1238
45. Cadran N, Cariou K, Hervé G, Aubert C, Fensterbank L, Malacria M, Marco-Contelles J (2004) PtCl₂-Catalyzed Cycloisomerizations of Allenynes. *J Am Chem Soc* 126:3408
46. Lemiere G, Gandon V, Agenet N, Goddard JP, de Kozak A, Aubert C, Fensterbank L, Malacria M (2006) Gold(I)- and Gold(III)-Catalyzed Cycloisomerization of Allenynes: A Remarkable Halide Effect. *Angew Chem Int Ed* 45:7596

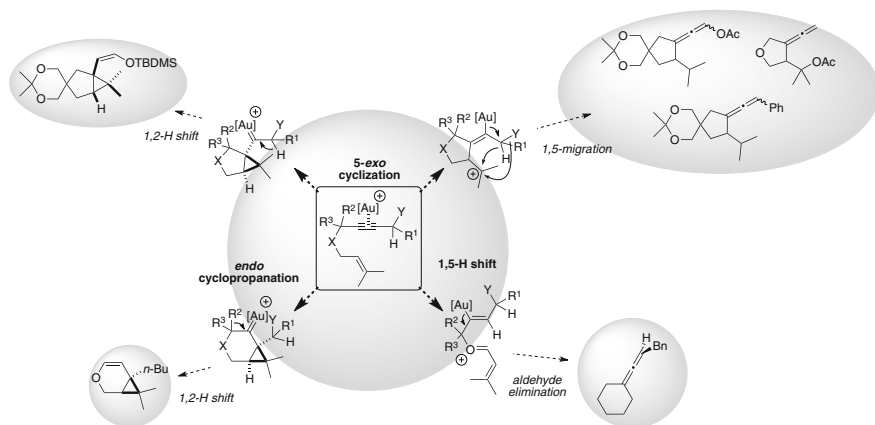
General Conclusion

This Ph.D. work was initially aimed at the discovery of new and original methods to form C–C bonds through activation of triple bonds by gold complexes. Our study started first in the 1,6-enyne series. The behavior of this kind of substrates toward transition metal catalysis has been intensively studied since the pioneering studies led by Trost in the 80s. With the emergence of gold and platinum catalysis in the early 2000s, the rearrangement of enynes has experienced a revival. In our group, we discovered that oxygenated propargylic substituents had a dramatic influence on the cycloisomerization process. This work has brought its contribution in the study of this trend, as we disclosed that unprecedented migration processes from the external propargylic position to a carbocation in 1,5 relationship were possible. The conditions for such a process to occur is the use of prenyl double bonds, which guarantee the stabilization of the carbocation acceptor, and a π -donor substituent (like a hydroxy group) at the external propargylic position. A fine-tuning of these parameters is crucial to avoid the other cyclization pathways to overcome. Thus, we were able to cycloisomerize 1,6-enynes into functionalized allenes, provided the substrate carries the appropriate chemical functionalities [1].

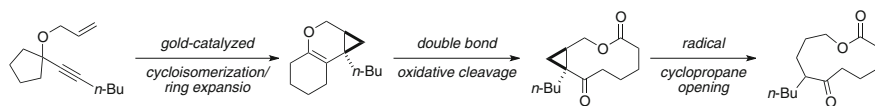
The *endo* cyclopropanation of enyne can give rise to cycle extension if a small ring is placed at the internal propargylic position. This rearrangement served as a starting point to the synthesis of macrocyclic skeletons encountered in nature [2].

In the group, we were also interested in the gold and platinum cyclization of allenynes, a particular case of enyne. The development of a cascade reaction where the allene moiety is generated in situ by the mean of the rearrangement of a propargylic ester was envisioned. In this case, we observed that the acyloxy moiety could fragment after C–C bond formation and give rise to a 1,5-acyl transfer process [3]. This allowed the access to highly conjugated dicarbonyl compounds. The scope was broadened to other type of esters such as acrylate. In this case, the resulting products could be rearranged upon acidic conditions into complex polycyclic skeletons. With an allenolate ester, the resulting allenyl ketone readily cyclized, leading to the isolation of a furan-containing compound.

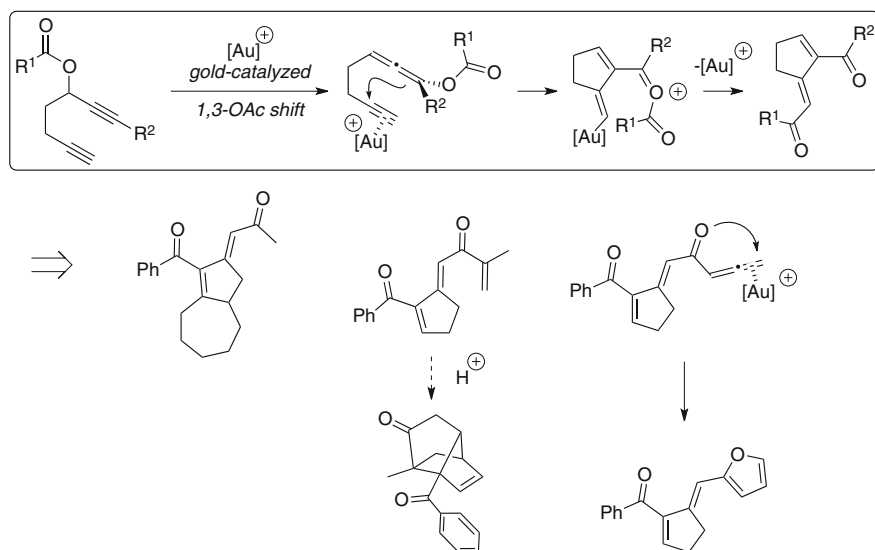
To finish, we conducted an investigation on the role of gold acetylides in C–C bond forming reaction involving terminal alkynes. This study was a joint research program with theoretical chemists and mass spectrometry specialists. It was shown



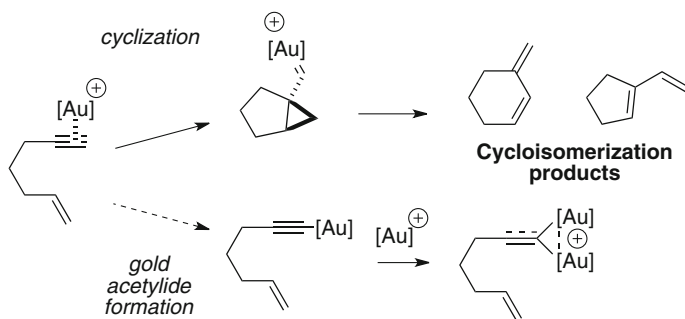
Scheme 1 Brief summary of the enyne reactivities disclosed through this work



Scheme 2 Synthetic approach toward macrocycles



Scheme 3 Au-catalyzed 1,3-OAc shift/Cyclization/1,5-acyl transfer cascade reaction



Scheme 4 Possible evolution of a gold-complexed enyne: cyclization versus gold acetylide

in the case of enynes that such species could form in solution, probably by assistance of adventitious water as revealed by computations and mass spectrometry, and they favorably bind another gold atom to evolve into polynuclear species. However, the data collected from theory and experiment did not support acetylides or resulting polynuclear species as viable intermediates in the gold-catalyzed cycloisomerization of enynes, but rather as catalyst resting states [4].

Experimental Section

General Remarks

Unless special mention, all reactions were carried out under an anhydrous atmosphere of argon. Glassware was flame-dried under an argon gas flow prior to use. Anhydrous solvents were systematically used unless otherwise indicated.

Solvents and Reagents

Following solvents and reagents were systematically distilled under an anhydrous and inert atmosphere prior to use.

- THF and Et₂O were distilled over sodium/benzophenone,
- Et₃N and DCM were distilled from CaH₂,
- toluene was distilled over a Na/K amalgam.

n-Butyllithium was purchased as 2.5 M solutions in hexanes and titrated before use. NaH was purchased as a 60 % suspension in mineral oil. Triphenylphosphinegold chloride 98+ % was purchased from Strem, [bis(trifluoromethanesulfonyl)imide] (triphenyl-phosphine)gold (2:1 toluene adduct) and (Acetonitrile)[(2-biphenyl) di-*tert*-butylphosphine]gold(I) hexafluoroantimonate were purchased from Aldrich and silver hexafluoroantimonate(V) 99 % was obtained from Alfa Aesar.

Thin Layer Chromatography

Thin layer chromatographies were performed on Merck silica gel 60 F 254 and revealed with ultra-violet lamp ($\lambda = 254$ nm) and by dipping in *p*-anisaldehyde, phosphomolybdic acid prepared solution and heating.

Flash Chromatography

Silica gel Merck Geduran SI 60 Å (35–70 µm) was used for column chromatography.

Infra-Red Spectroscopy

IR spectra were recorded on a Tensor 27 (ATR diamond) Bruker spectrometer. IR are reported as characteristic bands (cm^{-1}) in their maximal intensity.

Nuclear Magnetic Resonance

NMR spectra (^1H , ^{13}C , ^{31}P , DEPT, COSY ^1H – ^1H and ^1H – ^{13}C , NOE) were recorded at room temperature on 300 or 400 MHz AVANCE Bruker spectrometers. ^1H NMR spectra are referenced at 7.26 ppm for CDCl_3 and 7.16 ppm for C_6D_6 . ^{13}C NMR spectra are referenced at 77.16 ppm for CDCl_3 and 128.62 ppm for C_6D_6 . Chemical shifts are given in ppm. Coupling constants (J) are given in Hertz (Hz). The letters m, s, d, t, q, quint, sept, bs, bd mean respectively multiplet, singlet, doublet, triplet, quadruplet, quintuplet, septuplet. The letter b mean the signal is broad.

Melting Point

The melting points reported were measured with a SMP3 Stuart Scientific melting point apparatus or on a Wagner and Munz HEIZBANK Kofler bench and were uncorrected.

High Resolution Mass Spectra

High Resolution Mass Spectra (HRMS) were performed by Laboratoire Structure et Fonction de Molécules Bioactives (UPMC).

Optical Rotation

Optical rotations were determined using a Perkin Elmer 343 polarimeter.

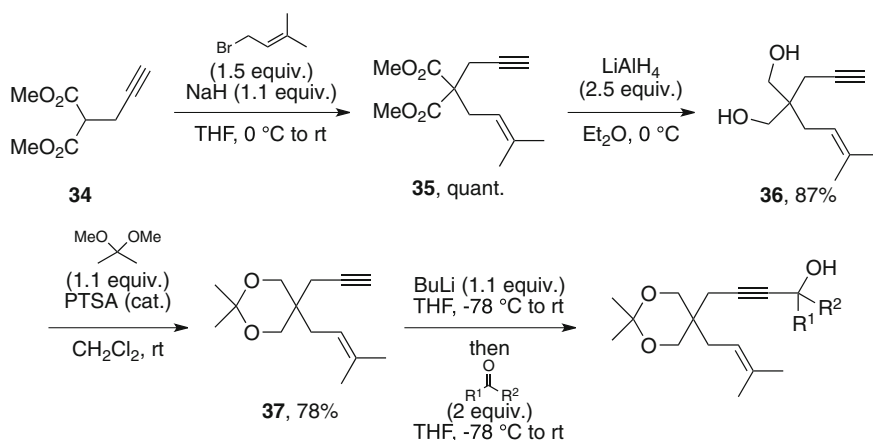
General Procedures

GP1. The catalyst (2 mol%) was added to a solution of the substrate in anhydrous DCM. The mixture was stirred at rt. The reaction progress was monitored by TLC. When the reaction was complete, the mixture was filtered through a short pad of silica. The solvent was removed under vacuum, and purification by flash chromatography afforded the cycloisomerization product.

GP2. The catalyst (2 mol%) was added to a solution of the substrate in anhydrous toluene. The mixture was stirred at 80 °C. The reaction progress was monitored by TLC. When the reaction was complete, the mixture was filtered through a short pad of silica. The solvent was removed under vacuum, and purification by flash chromatography afforded the cycloisomerization product.

GP3. LAuCl (2 mol%) was added to a solution of AgSbF₆ (2 mol%) in anhydrous DCM (0.025 M). The mixture was stirred for 5 min and the substrate was added. The reaction was followed by TLC. When the reaction was complete the mixture was filtered through a short pad of silica. The solvent was then evaporated under vacuum, and purification by flash chromatography afforded the cycloisomerization products.

Experimental Section Related to Chap. 2

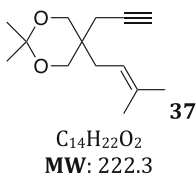


To a suspension of NaH (1.29 g, 31.8 mmol, 1.1 equiv.) in THF (50 mL) is added dropwise at 0 °C propargyl malonate **34** (5 g, 29.4 mmol, 1 equiv.). The reaction mixture is stirred for 5 min at 0 °C and then dimethylallyl bromide (4.1 mL, 35.3 mmol, 1.2 equiv.) is added. The solution is allowed to warm at rt and stirred overnight, and quenched with a saturated aqueous NH₄Cl solution. The aqueous layer is extracted with Et₂O (2 × 40 mL), and the combined organic extracts are

washed with brine and water, dried over MgSO_4 , filtered and the solvent removed under reduced pressure. The crude enyne **35** is engaged in the next step without purification.

To a suspension of LAH (1.2 g, 31.5 mmol, 2.5 equiv.) in Et_2O (13 mL) is added dropwise at $0\text{ }^\circ\text{C}$ enyne **35** (3 g, 12.6 mmol, 1 equiv.). The mixture is allowed to warm to rt and stirred for 4 h, then cooled down to $0\text{ }^\circ\text{C}$ and quenched by a dropwise addition of a saturated aqueous solution of MgSO_4 until the aluminium salts have been hydrolyzed. The mixture is then filtered over a short pad of silica/celite, the remaining solids are washed with Et_2O , and the filtrate evaporated under reduced pressure to afford diol **36** in pure form as a colorless oil in 87 % yield.

To a solution of diol **36** (1.97 g, 11.0 mmol, 1 equiv.) and 2,2-dimethoxypropane (1.7 mL, 13.9 mmol, 1.1 equiv.) in CH_2Cl_2 (20 mL) is added PTSA (0.13 g, 0.7 mmol, 0.05 equiv.), and the resulting mixture is stirred overnight at rt. The solution is quenched with a saturated aqueous NaHCO_3 solution, and the aqueous layer extracted with CH_2Cl_2 . The combined organic extracts are washed with water, dried over MgSO_4 , filtered and the solvent removed under reduced pressure. The crude product is purified by flash column chromatography over silica gel using 14:1 PE/ Et_2O as eluent to afford pure enyne **37** as a colorless oil in 78 % yield.

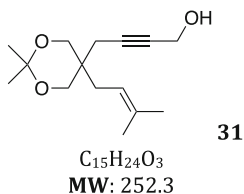


^1H NMR (300 MHz, CDCl_3) δ 5.06 (t, $J = 7.4$ Hz, 1H), 3.63 (s, 3H), 2.32 (s, 1H), 2.09 (d, $J = 7.7$ Hz, 2H), 2.03–1.92 (m, 1H), 1.70 (s, 2H), 1.62 (s, 2H), 1.38 (s, 5H).

^{13}C NMR (75 MHz, CDCl_3) δ 135.5, 117.9, 98.1, 81.2, 70.8, 66.8 (2C), 36.3, 31.0, 26.1, 25.6, 22.4, 22.2, 18.0.

IR (neat) $\nu = 1452, 1371, 1228, 1195, 1103, 1067, 829, 631\text{ cm}^{-1}$.

To a solution of enyne **37** (189 mg, 0.85 mmol, 1 equiv.) in THF (2 mL) is added dropwise at $-78\text{ }^\circ\text{C}$ $n\text{-BuLi}$ (1.7 M in hexanes, 0.55 mL, 0.93 mmol, 1.1 equiv.). The mixture is allowed to warm to rt within 1 h then cooled down again at $-78\text{ }^\circ\text{C}$, and the aldehyde/ketone (1.70 mmol, 2 equiv.) is added dropwise. The mixture is allowed to warm to rt and stirred for 2 h. The solution is then quenched with a saturated aqueous NH_4Cl solution and the aqueous layer is extracted with Et_2O . The combined organic extracts are washed with brine and water, dried over MgSO_4 , filtered and the solvent removed under reduced pressure. The crude product is purified by flash column chromatography over silica gel gradient mixtures of pentane and diethyl ether as eluent to afford the pure alcohol.

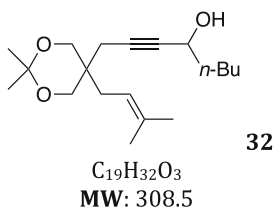


Colorless oil, 71 %. 1H NMR (400 MHz, $CDCl_3$) δ 5.06 (m, 1H), 4.24 (s br, 2H), 3.63 (s, 4H), 2.40 (t, $J = 2.4$, 2H), 2.07 (d, $J = 8.0$, 2H), 1.73 (br, OH), 1.71 (s, 3H), 1.63 (s, 3H), 1.40 (s, 3H), 1.39 (s, 3H).

^{13}C NMR (100 MHz, $CDCl_3$) δ 135.4, 117.7, 98.1, 83.0, 80.9, 66.8 (2C), 51.3, 36.4, 31.0, 25.9 (2C), 22.6, 21.6, 17.9.

IR (neat) $\nu = 3391, 2964, 2860, 1451, 1194, 1062, 827\text{ cm}^{-1}$.

HRMS calculated for $[C_{15}H_{24}O_3Na]^+$: 275.1617, found: 275.1615.

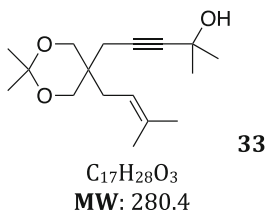


Colorless oil, 85 %. 1H NMR (400 MHz, $CDCl_3$) δ 5.07 (m, 1H), 4.33 (m, 1H), 3.63 (s, 4H), 2.35 (d, $J = 1.6$, 2H), 2.09 (d, $J = 8.0$, 2H), 1.93 (br, OH), 1.71 (s, 3H), 1.68 (m, 2H), 1.63 (s, 3H), 1.40 (s, 3H), 1.39 (s, 3H), 1.36 (m, 4H), 0.89 (t, $J = 7.2$, 3H).

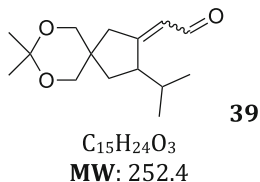
^{13}C NMR (100 MHz, $CDCl_3$) δ 135.4, 117.9, 98.0, 84.0, 81.7, 66.7 (2C), 62.6, 37.9, 36.4, 31.0, 27.4, 25.5, 25.1, 22.6, 22.4, 22.1, 17.9, 14.0.

IR (neat) $\nu = 3402, 2956, 2859, 1452, 1371, 1227, 1101, 828\text{ cm}^{-1}$.

HRMS calculated for $[C_{19}H_{32}O_3Na]^+$: 331.2244, found: 331.2239.



Colorless oil, 88 %. 1H NMR (400 MHz, C_6D_6) δ 5.02–4.95 (m, 1H), 3.59–3.51 (s, 4H), 2.29–2.17 (s, 2H), 2.05–1.95 (d, $J = 7.8$ Hz, 2H), 1.76–1.69 (s, 1H), 1.66–1.60 (d, $J = 1.4$ Hz, 3H), 1.59–1.52 (m, 3H), 1.43–1.37 (s, 6H), 1.32–1.31 (s, 3H), 1.31–1.30 (s, 3H).

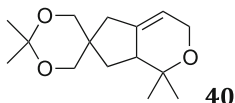


Prepared according to **GPI**, colorless oil, 40 % (*Z/E* ratio 1:1). **¹H NMR (400 MHz, CDCl₃)** δ 9.88 (m, 1H), 6.00 and 5.95 [(d, *J* = 8.0) and (d, *J* = 7.2), 1H], 3.78–3.46 (m, 4H), 3.24 (m, 1H), 2.65 (m, 1H), 2.32 (m, 1H), 1.91 (m, 1H), 1.75 (m, 2H), 1.42 (m, 6H), 0.95–0.77 (m, 6H).

¹³C NMR (100 MHz, CDCl₃) δ 191.5, 190.6, 172.3, 172.2, 125.7, 124.6, 98.2, 98.1, 69.5, 69.3, 67.4, 67.3, 49.9, 45.4, 43.8, 40.7, 39.7, 38.6, 34.2, 33.1, 31.1, 29.8, 25.0, 24.9, 22.6, 22.5, 21.3, 21.1, 17.4, 16.5.

IR (neat) ν = 2990, 2859, 1672, 1383, 1198, 829 cm⁻¹.

HRMS calculated for [C₁₅H₂₄O₃Na]⁺: 275.1617, found: 275.1616.



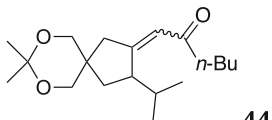
C₁₅H₂₄O₃
MW: 252.3

Prepared according to **GPI**, colorless oil, 20 %. **¹H NMR (400 MHz, CDCl₃)** δ 5.41 (br s, 1H), 4.10 (m, 2H), 3.71–3.53 (m, 4H), 2.50 (m, 1H), 2.29 (d, *J* = 16 Hz, 1H), 2.19 (d, *J* = 16 Hz, 1H), 1.98 (dd, *J* = 12.8, 8, 1H), 1.40 (m, 1H), 1.42 (s, 6H), 1.25 (s, 3H), 1.03 (s, 3H).

¹³C NMR (100 MHz, CDCl₃) δ 138.3, 116.0, 97.9, 72.4, 69.6, 68.5, 61.3, 46.6, 39.7, 38.2, 34.6, 29.2, 24.4, 23.2, 18.2.

IR (neat) ν = 2928, 2854, 1453, 1368, 1092, 830 cm⁻¹.

HRMS calculated for [C₁₅H₂₄O₃Na]⁺: 275.1617, found: 275.1616.



C₁₉H₃₂O₃
MW: 308.5

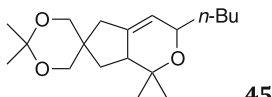
Prepared according to **GPI**. Colorless oil, 39 % (*Z/E* ratio 1:1). **¹H NMR (400 MHz, CDCl₃)** δ 6.13 (dd, *J* = 4.6, 2.4, 1H), 3.84 (d, *J* = 11.2, 1H), 3.58–3.47 (m, 3H), 3.03 (d, *J* = 20.0, 1H), 2.68 (m, 1H), 2.44 (t, *J* = 7.2, 2H), 2.27 (dt, *J* = 19.6, 2.8, 1H), 2.13–2.01 (m, 2H), 1.67–1.48 (m, 3H), 1.43 (s, 3H), 1.41 (s, 3H), 1.40–1.24 (m, 2H), 0.98 (d, *J* = 6.8, 3H), 0.91 (t, *J* = 7.6, 3H), 0.77 (d, *J* = 6.8, 3H).

¹³C NMR (100 MHz, CDCl₃) δ 201.0, 166.4, 120.4, 98.1, 69.8, 67.6, 50.0, 44.1, 41.1, 40.5, 31.8, 29.8, 26.6, 26.4, 22.6, 21.7, 21.4, 16.4, 14.0.

IR (neat) ν = 2958, 2931, 2872, 1709, 1199, 1031, 830 cm⁻¹.

HRMS calculated for [C₁₉H₃₂O₃Na]⁺: 331.2249, found: 331.2255.

The two minor diastereomers of **44** and **45** could not be separated from each other.



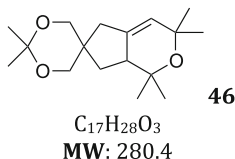
C₁₉H₃₂O₃
MW: 308.5

Prepared according to **GPI**, colorless oil, 46 % (dr > 25:1). **¹H NMR** (400 MHz, CDCl₃) δ 5.37 (quint., *J* = 2.4, 1H), 4.00–3.94 (m, 1H), 3.71–3.53 (m, 4H), 2.48–2.40 (m, 1H), 2.34–2.25 (m, 1H), 2.21–2.15 (m, 1H), 1.94 (dd, *J* = 12.8, 8.4, 1H), 1.53–1.45 (m, 2H), 1.42 (s, 6H), 1.38–1.30 (m, 4H), 1.24 (s, 3H), 1.04–1.01 (m, 1H), 1.02 (s, 3H), 0.89 (t, *J* = 6.8, 3H).

¹³C NMR (100 MHz, CDCl₃) δ 138.6, 120.1, 98.0, 73.2, 70.1, 69.8, 68.8, 47.0, 39.9, 38.3, 35.6, 34.7, 29.6, 27.4, 24.5, 23.5, 23.0, 19.0, 14.2.

IR (neat) ν = 2922, 2853, 1713, 1372, 1197, 829 cm⁻¹.

HRMS calculated for [C₁₉H₃₂O₃Na]⁺: 331.2249, found: 331.2244.

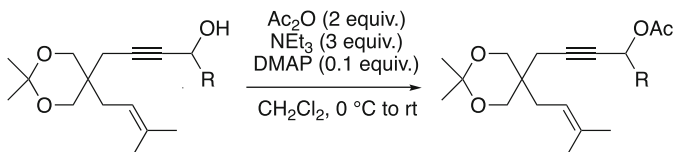


Prepared according to **GPI**, colorless oil, 40 %. **¹H NMR** (400 MHz, CDCl₃) δ 5.47–5.39 (m, 1H), 3.75–3.55 (m, 3H), 2.52–2.32 (m, 1H), 2.29–2.12 (d, *J* = 17.2 Hz, 1H), 2.04–1.90 (dd, *J* = 12.8, 8.6 Hz, 1H), 1.81–1.64 (d, *J* = 18.5 Hz, 1H), 1.50–1.40 (s, 4H), 1.25–1.25 (s, 3H), 1.25–1.24 (s, 2H), 1.22–1.19 (s, 2H), 1.10–1.04 (s, 2H).

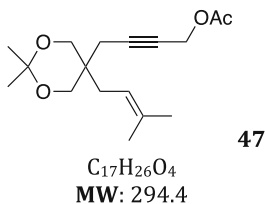
¹³C NMR (100 MHz, CDCl₃) δ 136.5, 125.3, 98.0, 73.9, 72.4, 69.7, 68.4, 46.5, 40.3, 38.5, 35.2, 32.1, 30.4, 29.3, 24.1, 23.8, 22.6.

IR (neat) ν = 2963, 1258, 1010 cm⁻¹.

HRMS calculated for [C₁₇H₂₈O₃Na]⁺: 303.1931, found: 303.1927.



To a stirred solution of the alcohol (1 mmol, 1.0 equiv.), Et₃N (0.4 mL, 3 mmol, 3 equiv.) and 4-DMAP (12 mg, 0.1 mmol, 0.1 equiv.) in CH₂Cl₂ (10 mL) was added acetic anhydride (0.19 mL, 2 mmol, 2 equiv.) at 0 °C. The solution was then allowed to warm to rt and was stirred further until completion (3–4 h at rt). The reaction was quenched with aqueous saturated NH₄Cl solution and the resulting aqueous layer was extracted with CH₂Cl₂. The combined organic layers were washed with brine, dried over anhydrous Na₂SO₄, filtered and evaporated to give crude acetate as oil. Purification was achieved by flash column chromatography on silica gel (PE/Et₂O gradient).

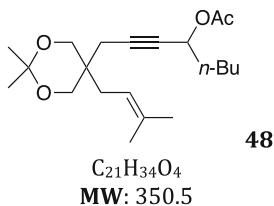


Colorless oil, 88 %. **¹H NMR (400 MHz, CDCl₃)** δ 5.06 (m, 1H), 4.64 (t, J = 2, 2H), 3.63 (s, 4H), 2.38 (t, J = 2.4, 2H), 2.07 (d, J = 7, Hz, 2H), 2.05 (s, 3H), 1.71 (s, 3H), 1.62 (s, 3H), 1.39 (s, 3H), 1.38 (s, 3H).

¹³C NMR (100 MHz, CDCl₃) δ 170.3, 135.5, 117.7, 98.0, 84.2, 76.5, 66.7 (2C), 52.7, 36.4, 31.0, 26.0, 25.8, 22.6, 21.8, 20.7, 17.8.

IR (neat) ν = 2935, 1746, 1438, 1218, 1023 cm⁻¹.

HRMS calculated for [C₁₇H₂₆O₄Na]⁺: 317.1723, found: 317.1719.

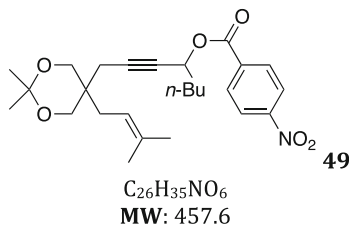


Colorless oil, 86 %. **¹H NMR (400 MHz, CDCl₃)** δ 5.33 (dt, J = 6.8, 1.6, 1H), 5.07 (dt, J = 8.0, 1H), 3.63 (s, 4H), 2.33 (s, 2H), 2.10 (d, J = 7.6, 2H), 2.04 (s, 3H), 1.74 (m, 2H), 1.73 (s, 3H), 1.63 (s, 3H), 1.40 (s, 3H), 1.39 (s, 3H), 1.33 (m, 4H), 0.89 (t, J = 6.4, 3H).

¹³C NMR (100 MHz, CDCl₃) δ 170.0, 135.3, 117.8, 98.0, 84.0, 81.7, 66.7 (2C), 64.5, 36.4, 34.8, 31.0, 27.2, 26.0, 25.1, 22.6, 22.4, 22.2, 21.0, 17.9, 13.9.

IR (neat) ν = 2990, 2861, 1739, 1370, 829 cm⁻¹.

HRMS calculated for [C₂₁H₃₄NaO₄]⁺: 373.2349, found: 373.2342.

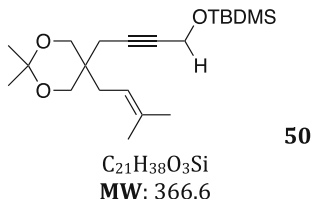


To a stirred solution of alcohol **32** (1 mmol, 1.0 equiv.), Et₃N (0.3 mL, 2.1 mmol, 2.1 equiv.) and 4-DMAP (12 mg, 0.1 mmol, 0.1 equiv.) in CH₂Cl₂ (10 mL) was added *para*-nitrobenzoyl chloride (242 mg, 1.3 mmol, 1.3 equiv.) at 0 °C. The solution was then allowed to warm to rt and was stirred further until completion (3–4 h at rt). The reaction was quenched with aqueous saturated NH₄Cl solution and the resulting aqueous layer was extracted with CH₂Cl₂. The combined organic layers were washed with brine, dried over anhydrous Na₂SO₄, filtered and evaporated to give crude acetate as oil. Purification was achieved by flash column chromatography on silica gel (PE/Et₂O gradient) to afford pure ester **49** as a colorless oil in 86 % yield. **¹H NMR (400 MHz, CDCl₃)** δ 8.28 (m, 2H), 8.21 (m, 2H), 5.60 (m, 1H), 5.05 (m, 1H), 3.64 (s, 2H), 3.63 (s, 2H), 2.38 (d, J = 2.0, 2H), 2.80 (d, J = 7.6, 2H), 1.88 (m, 2H), 1.70 (s, 3H), 1.60 (s, 3H), 1.48 (m, 2H), 1.39 (s, 3H), 1.38 (m, 2H), 1.35 (s, 3H), 0.92 (t, J = 7.2, 3H).

^{13}C NMR (100 MHz, CDCl_3) δ 163.7, 150.6, 135.6, 135.5, 130.8 (2C), 123.5 (2C), 117.7, 98.0, 83.7, 79.7, 66.7 (2C), 66.3, 36.5, 34.8, 31.0, 27.3, 26.0, 25.4, 22.6, 22.2, 22.1, 17.9, 13.9.

IR (neat) ν = 2956, 2862, 1753, 1443, 1212, 867 cm^{-1} .

HRMS calculated for $[\text{C}_{26}\text{H}_{35}\text{NaO}_6]^+$: 480.2356, found: 480.2351.

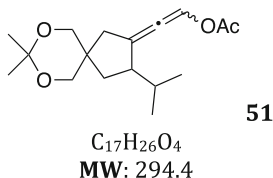


To a solution of alcohol **31** (125 mg, 0.5 mmol, 1 equiv.) in 5 mL of CH_2Cl_2 were added Et_3N (0.35 mL, 2.57 mmol, 5 equiv.), DMAP (6.3 mg, 0.05 mmol, 0.1 equiv.) and *tert*-butyldimethylsilyl chloride (115 mg, 0.75 mmol, 1.5 equiv.). The solution was stirred at rt overnight and was quenched with saturated NH_4Cl solution and extracted with CH_2Cl_2 . The combined organic layers were washed with brine, dried over MgSO_4 and evaporated to give crude **50**. Purification by flash chromatography on silica gel (PE/ Et_2O 99/1) gives 166 mg of pure **50** (91 % yield) as a colorless oil. **^1H NMR (400 MHz, CDCl_3)** δ 5.08 (t, J = 8 Hz, 1H), 4.30 (t, J = 2 Hz, 2H), 3.65 (d, J = 11.6 Hz, 2H), 3.62 (d, J = 11.6 Hz, 2H), 2.34 (t, J = 2 Hz, 2H), 2.11 (d, J = 7.6, 2H), 1.72 (s, 3H), 1.64 (s, 3H), 1.40 (s, 3H), 1.39 (s, 3H), 0.90 (s, 9H), 0.10 (s, 6H).

^{13}C NMR (100 MHz, CDCl_3) δ 135.3, 118.0, 97.9, 81.6, 81.2, 66.8 (2C), 51.9, 36.4, 30.9, 26.0, 25.8 (3C), 25.1, 22.7, 22.4, 22.5, 18.3, 17.9 (2C).

IR (neat) ν = 2954, 2857, 1472, 1452, 1252, 1066, 831 cm^{-1} .

HRMS calculated for $[\text{C}_{21}\text{H}_{38}\text{NaO}_3\text{Si}]^+$: 389.2482, found: 389.2478.

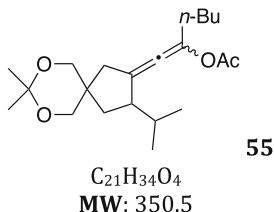


Prepared according to **GPI**, colorless oil, 75 % (dr 1:1). **^1H NMR (400 MHz, CDCl_3)** δ 7.34 (m, 1H), 3.63 (m, 4H), 2.58 (m, 2H), 2.19 (m, 1H), 2.10 (s, 3H), 1.84 (m, 1H), 1.39 (m, 6H), 1.23 (m, 2H), 0.93–0.79 (m, 6H).

^{13}C NMR (100 MHz, CDCl_3) δ 186.9, 186.6, 168.8, 168.7, 121.3, 120.7, 111.8, 111.7, 98.0 (2C), 69.2 (2C), 67.5, 67.4, 48.5, 47.8, 40.8, 40.7, 40.2, 40.1, 34.3, 33.5, 30.6, 30.1, 24.3, 24.2, 23.3, 23.2, 21.1 (2C), 20.9 (2C), 18.3, 17.7.

IR (neat) ν = 2955, 2858, 1750, 1383, 1199 cm^{-1} .

HRMS calculated for $[\text{C}_{17}\text{H}_{26}\text{O}_4\text{Na}]^+$: 317.1723, found: 317.1721.

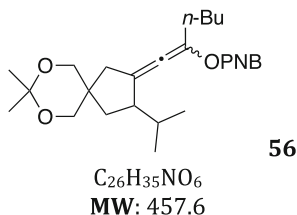


Prepared according to *GPI*, colorless oil, 42 % (dr 1:1, isolated as a 1:1 mixture with **57**). ¹H NMR (400 MHz, CDCl₃) δ 3.66 (m, 4H), 2.62 (m, 1H), 2.47 (d, *J* = 16.0, 1H), 2.21 (m, 3H), 2.10 (s, 3H), 1.91 (m, 2H), 1.42–1.21 (m, 10H), 0.93–0.81 (m, 9H).

¹³C NMR (100 MHz, CDCl₃) δ 188.1, 168.8, 125.3, 117.7, 97.9, 69.3, 67.6, 48.1, 40.7, 39.7, 34.0, 31.3, 30.4, 28.4, 23.9, 23.6, 22.0, 21.0 (2C), 18.0, 13.8.

IR (neat) ν = 2955, 2858, 1751, 1382, 1198, 831 cm⁻¹.

HRMS calculated for [C₂₁H₃₄O₄Na]⁺: 373.2349, found: 373.2343.

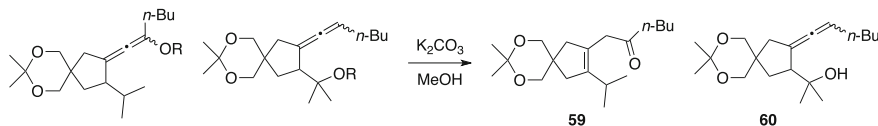


Prepared according to *GPI*, colorless oil, 40 % (dr 1:1, isolated as a 1:1 mixture with **58**). ¹H NMR (400 MHz, CDCl₃) δ 8.27–8.19 (m, 4H), 3.62 (m, 4H), 2.67 (m, 1H), 2.56 (dd, *J* = 15, 4, 1H), 2.31 (m, 3H), 1.86 (m, 2H), 1.43–1.22 (m, 11H), 0.91–0.77 (m, 9H).

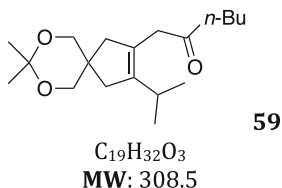
¹³C NMR (100 MHz, CDCl₃) δ 187.8, 187.7, 162.6, 162.3, 150.5 (2C), 135.7 (2C), 130.8 (4C), 125.6, 124.8, 123.4 (4C), 119.0 (2C), 97.9 (2C), 69.2 (2C), 67.5, 67.4, 48.3, 47.8, 40.7 (2C), 40.0, 39.8, 34.0, 33.7, 31.7, 31.3, 30.4, 30.3, 28.7, 28.4, 24.2, 23.9, 23.5, 23.3, 22.0 (2C), 21.2, 21.0, 18.1 (2C), 13.8 (2C).

IR (neat) ν = 2955, 2860, 1733, 1528, 1318, 1089, 716 cm⁻¹.

HRMS calculated for [C₂₆H₃₅NO₆Na]⁺: 480.2356, found: 480.2345.



To a mixture of **55/57** or **56/58** in MeOH (0.5 M) is added K_2CO_3 (3 equiv.). After stirring for 2 h, about 90 % of the solvent is removed under reduced pressure, and the resulting solution is diluted with water and Et_2O . The aqueous layer is extracted twice with Et_2O and the combined organic extracts are washed with brine and water, dried over $MgSO_4$ and evaporated under reduced pressure. Purification by flash chromatography on silica gel using gradient mixtures of pentane/ Et_2O as eluent afforded ketone **59** and alcohol **60**.

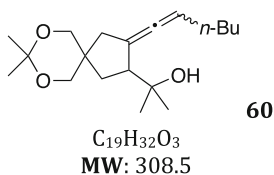


Colorless oil, 80 % from **55**. 1H NMR (400 MHz, $CDCl_3$) δ 3.65 (d, $J = 11.2$, 2H), 3.60 (d, $J = 11.2$, 2H), 3.08 (s, 2H), 2.62 (h, $J = 7.2$, 1H), 2.36 (t, $J = 7.2$, 2H), 2.29 (s, 2H), 2.13 (s, 2H), 1.51 (m, 2H), 1.41 (s, 6H), 1.27 (m, 2H), 0.96 (d, $J = 6.8$, 6H), 0.87 (t, $J = 7.2$, 3H).

^{13}C NMR (100 MHz, $CDCl_3$) δ 208.6, 143.4, 124.1, 97.7, 69.3, 43.6, 42.9, 41.8, 38.7, 38.5, 27.0, 25.8, 24.8, 22.8, 22.3, 21.1 (3C), 13.8.

IR (neat) $\nu = 3150, 2890, 1731, 1176, 1012\text{ cm}^{-1}$.

HRMS calculated for $[C_{19}H_{32}O_3Na]^+$: 331.2249, found: 331.2253.

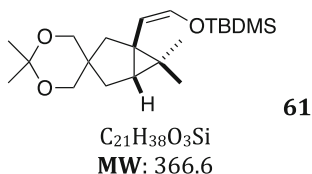


Colorless oil, 82 % from **56**. 1H NMR (400 MHz, $CDCl_3$) δ 5.20 (m, 1H), 3.63 (m, 4H), 2.82 (m, 1H), 2.44 (m, 1H), 2.18 (m, 2H), 1.98–1.89 (m, 2H), 1.42–1.17 (m, 18H), 0.89 (m, 3H).

^{13}C NMR (100 MHz, $CDCl_3$) δ 199.2, 198.6, 102.9, 102.4, 98.0 (2C), 93.6, 93.4, 69.2 (2C), 67.3, 67.2, 51.9, 51.5, 41.0 (2C), 39.9, 39.8, 35.4 (2C), 31.5, 30.9, 29.2, 28.9, 27.9 (2C), 25.2 (2C), 25.1, 24.2, 23.9, 23.6, 23.6, 22.2 (2C), 22.1, 13.9 (2C).

IR (neat) $\nu = 3312, 2866, 1377, 1145, 798\text{ cm}^{-1}$.

HRMS calculated for $[C_{19}H_{32}O_3Na]^+$: 331.2249, found: 331.2243.

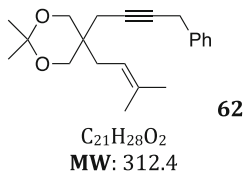


Prepared according to **GPI**, colorless oil, 80%. ^1H NMR (400 MHz, CDCl_3) δ 6.13 (d, $J = 6$ Hz, 1H), 4.44 (d, $J = 6$ Hz, 1H), 3.66 (d, $J = 11.2$, 1H), 3.61 (d, $J = 11.2$, 1H), 3.58 (d, $J = 11.2$, 1H), 3.55 (d, $J = 11.2$, 1H), 1.95–1.85 (m, 2H), 1.54 (d, $J = 14$ Hz, 1H), 1.38 (s, 6H), 1.20 (m, 2H), 0.98 (s, 3H), 0.96 (s, 3H), 0.92 (s, 9H), 0.11 (s, 6H).

^{13}C NMR (100 MHz, CDCl_3) δ 139.4, 112.1, 97.5, 69.6, 67.5, 49.7, 39.0, 35.9, 35.0, 32.7, 27.7, 25.9, 25.6 (3C), 24.4, 24.4, 24.2, 23.5, 18.1, 16.2.

IR (neat) $\nu = 3293, 2857, 1649, 1380, 864\text{ cm}^{-1}$.

HRMS calculated for $[\text{C}_{21}\text{H}_{38}\text{NO}_3\text{SiNa}]^+$: 389.2482, found: 389.2477.

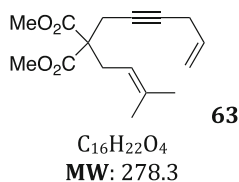


To a solution of enyne **37** (189 mg, 0.85 mmol, 1 equiv.) in THF (2 mL) is added dropwise at -78°C $n\text{-BuLi}$ (1.7 M in hexanes, 0.55 mL, 0.93 mmol, 1.1 equiv.). The mixture is allowed to warm to rt within 1 h then cooled down again at -78°C , and benzyl bromide (0.4 mL, 3.40 mmol, 4 equiv.) is added dropwise. The mixture is allowed to warm to rt and stirred for 2 h. The solution is then quenched with a saturated aqueous NH_4Cl solution and the aqueous layer is extracted with Et_2O . The combined organic extracts are washed with brine and water, dried over MgSO_4 , filtered and the solvent removed under reduced pressure. The crude product is purified by flash column chromatography over silica gel gradient mixtures of pentane and diethyl ether as eluent to afford pure **62** as a colorless oil, 55 % yield. ^1H NMR (400 MHz, CDCl_3) δ 7.30 (m, 5H), 5.12 (t, $J = 7.6$, 1H), 3.70 (d, $J = 11.6$, 2H), 3.65 (d, $J = 11.6$, 2H), 3.59 (t, $J = 2.4$, 2H), 2.36 (t, $J = 2.4$, 2H), 2.14 (d, $J = 7.6$, 2H), 1.73 (s, 3H), 1.63 (s, 3H), 1.42 (s, 3H), 1.40 (s, 3H).

^{13}C NMR (100 MHz, CDCl_3) δ 137.4, 135.2, 128.4 (2C), 127.8 (2C), 126.4, 118.1, 97.9, 80.2, 78.8, 66.9 (2C), 36.5, 31.1, 26.1, 25.2, 25.0, 22.9, 22.7, 17.9.

IR (neat) $\nu = 2989, 2361, 1452, 1195, 827\text{ cm}^{-1}$.

HRMS calculated for $[\text{C}_{21}\text{H}_{28}\text{O}_2\text{Na}]^+$: 335.1981, found: 335.1977.



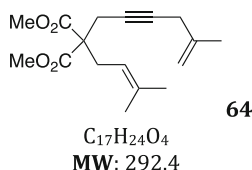
To a stirred solution of propargyl malonate derivative (1 g, 4.2 mmol, 1 equiv.) in dry DMF (5 mL, 0.1 M) under argon were sequentially added K_2CO_3 (1.16 g, 8.4 mmol, 2 equiv.), tetrabutylammonium iodide (465 mg, 1.3 mmol, 0.3 equiv.), and copper(I) iodide (240 mg, 1.3 mmol, 0.3 equiv.) at room temperature. After 15 min, allyl bromide (1.1 mL, 12.6 mmol, 3 equiv.) was added. The reaction

mixture was stirred for 24 h. Then it was poured into water and extracted with Et₂O. The combined organic layers were washed with a saturated aqueous sodium chloride solution, dried over MgSO₄, filtered and the solvents were removed under reduced pressure. The residue was purified by flash column chromatography (Silica gel, PE/Et₂O 95:5) to give the desired product as a colorless oil in 89 % yield. **¹H NMR (400 MHz, CDCl₃)** δ 5.77 (m, 1H), 5.27 (m, 1H), 5.08 (m, 1H), 4.92 (m, 1H), 3.72 (s, 6H), 2.90 (m, 2H), 2.78 (m, 4H), 1.70 (s, 3H), 1.65 (s, 3H).

¹³C NMR (100 MHz, CDCl₃) δ 170.7 (2C), 136.2, 132.7, 117.2, 115.8, 79.3, 70.8, 57.4, 51.9 (2C), 30.6, 25.8, 22.5 (2C), 17.8.

IR (neat) ν = 2953, 1735, 1199, 1056 cm⁻¹.

HRMS calculated for [C₁₆H₂₂O₄Na]⁺: 301.1411, found: 301.1408.

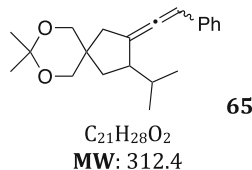


Prepared according to the same procedure than for **63**, using methallyl bromide in place of allyl bromide, colorless oil, 87 %. **¹H NMR (400 MHz, CDCl₃)** δ 4.90 (m, 2H), 4.79 (m, 1H), 3.71 (s, 6H), 2.83 (s br, 2H), 2.78 (m, 4H), 1.74 (s, 3H), 1.68 (d, J = 1, 3H), 1.63 (s, 3H).

¹³C NMR (100 MHz, CDCl₃) δ 170.7 (2C), 140.7, 136.5, 117.2, 111.3, 80.1, 76.8, 57.4, 52.5 (2C), 30.8, 27.4, 25.9, 22.9, 21.9, 17.8.

IR (neat) ν = 2953, 1736, 1377, 1199, 1055 cm⁻¹.

HRMS calculated for [C₁₇H₂₄O₄Na]⁺: 315.1567, found: 315.1563.

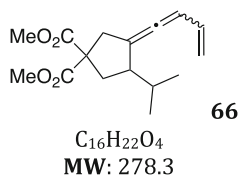


Prepared according to **GPI**, colorless oil, 75 % (dr 1:1). **¹H NMR (400 MHz, CDCl₃)** δ 7.27 (m, 5H), 6.16 (m, 1H), 3.70 (m, 4H), 2.73 (m, 1H), 2.54 (m, 1H), 2.30 (m, 1H), 1.95–1.80 (m, 2H), 1.45 (s, 3H), 1.43 (s, 3H), 1.27 (m, 1H), 0.96–0.89 (m, 6H).

¹³C NMR (100 MHz, CDCl₃) δ 200.0, 199.4, 135.6 (2C), 128.5 (4C), 126.6 (6C), 108.8 (2C), 98.0 (2C), 96.1 (2C), 69.3 (2C), 67.7, 67.5, 48.0, 47.0, 41.1, 41.0, 39.1, 38.9, 34.8, 34.6, 31.2, 31.0, 24.1 (2C), 23.4 (2C), 21.1 (2C), 18.9, 18.4.

IR (neat) ν = 2990, 2855, 1949, 1495, 1382, 1281, 732 cm⁻¹.

HRMS calculated for [C₂₁H₂₈O₂Na]⁺: 335.1981, found: 335.1978.

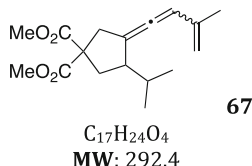


Prepared according to **GPI**, colorless oil, 71 % (dr 1:1). **¹H NMR (400 MHz, CDCl₃)** δ 6.13 (dt, J = 17.2, 10.0, 1H), 5.85 (m, 1H), 5.14 (dd, J = 17.0, 4.0, 1H), 4.94 (dd, J = 10.0, 6.8, 1H), 3.73 (m, 6H), 3.03–2.92 (m, 2H), 2.66 (m, 1H), 2.43 (dd, J = 12.8, 7.6, 1H), 1.89 (q, J = 12.0, 1H), 1.76 (m, 1H), 0.94–0.83 (m, 6H).

¹³C NMR (100 MHz, CDCl₃) δ 201.3 (2C), 171.8 (4C), 133.4 (2C), 115.2 (2C), 104.7 (2C), 97.0 (2C), 59.0 (2C), 52.7 (4C), 47.7 (2C), 38.9 (2C), 35.8 (2C), 29.8 (2C), 20.9, 20.6, 18.1 (2C).

IR (neat) ν = 2954, 1732, 1433, 1243, 898 cm⁻¹.

HRMS calculated for [C₁₆H₂₂O₄Na]⁺: 301.1411, found: 301.1405.

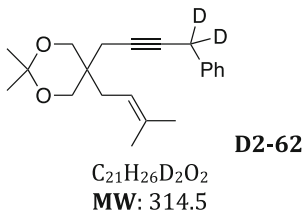


Prepared according to **GPI**, colorless oil, 71 % (dr 1:1). **¹H NMR (400 MHz, CDCl₃)** δ 5.95 (m, 1H), 4.88 (m, 1H), 4.79 (m, 1H), 3.72 (m, 6H), 3.00 (m, 2H), 2.64 (m, 1H), 2.41 (m, 1H), 1.91–1.70 (m, 5H), 0.96–0.86 (m, 6H).

¹³C NMR (100 MHz, CDCl₃) δ 201.1, 199.3, 171.8 (4C), 141.8, 140.2, 113.5, 113.1, 106.9, 106.4, 100.9, 100.0, 59.3, 59.1, 52.7 (4C), 47.9 (2C), 39.5 (2C), 36.1, 35.7, 30.9, 30.7, 22.1, 21.1, 20.7, 19.9, 19.5, 18.6.

IR (neat) ν = 2955, 1731, 1433, 1242, 898 cm⁻¹.

HRMS calculated for [C₁₇H₂₄O₄Na]⁺: 315.1567, found: 315.1563.

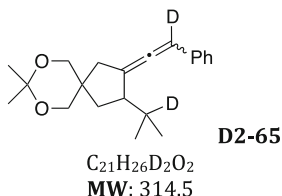


Prepared according to the same procedure than for **62**, using dideuterobenzyl bromide in place of benzyl bromide, colorless oil, 60 %. **¹H NMR (400 MHz, CDCl₃)** δ 7.30 (m, 5H), 5.12 (m, 1H), 3.71 (d, J = 11.2, 2H), 3.65 (d, J = 11.6, 2H), 2.37 (s, 2H), 2.15 (d, J = 8.0, 2H), 1.74 (s, 3H), 1.64 (s, 3H), 1.43 (s, 3H), 1.41 (s, 3H).

¹³C NMR (100 MHz, CDCl₃) δ 137.3, 135.2, 128.4 (2C), 127.8 (2C), 126.4, 118.1, 97.9, 80.1, 78.7, 66.8 (2C), 36.4, 31.0, 26.0, 25.1 (m, CD₂), 25.0, 22.8, 22.6, 17.8.

IR (neat) ν = 2988, 2363, 1448, 1190, 825 cm⁻¹.

HRMS calculated for $[C_{21}H_{26}D_2O_2Na]^+$: 337.2107, found: 337.2098.

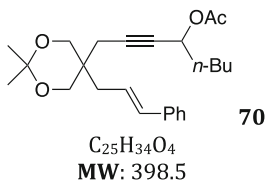


Prepared according to **GPI**, colorless oil, 72 % (dr 1:1). **1H NMR (400 MHz, $CDCl_3$)** δ 7.29 (m, 5H), 3.76–3.68 (m, 4H), 2.74 (m, 1H), 2.52 and 2.57 [(d, $J = 16.4$, 1H-dias(1)), (d, $J = 16.4$, 1H-dias(2)), 1H], 2.37 and 2.29 [(d, $J = 15.6$, CH-dias(1)), (d, $J = 16.4$, CH-dias(2)), 1H], 1.90 (m, 1H), 1.46 (s, 3H), 1.45 (s, 3H), 1.26 (m, 1H), 0.96 (s, 3H), 0.93 and 0.90 [(s, CH_3 -dias(1)) and (s, CH_3 -dias(2)), 3H].

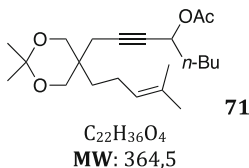
^{13}C NMR (100 MHz, $CDCl_3$) δ 200.1, 199.7, 135.7 (2C), 128.6 (4C), 126.7 (6C), 108.9 (2C), 98.1 (2C), 96.1 (m, C-D, 2C), 69.5 (2C), 67.9, 67.7, 48.1, 47.1, 41.2, 41.1, 39.3, 39.0, 34.9, 34.7, 30.7 (m, C-D, 2C), 24.3 (2C), 23.6 (2C), 21.2, 21.1, 18.9, 18.5.

IR (neat) $\nu = 2991, 2852, 1953, 1496, 1381, 733\text{ cm}^{-1}$.

HRMS calculated for $[C_{21}H_{26}D_2O_2Na]^+$: 337.2107, found: 337.2096.

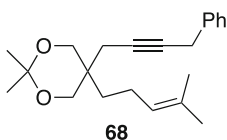


The first step of the synthesis of **70** was realized according to the same procedure than for **35**, using cinnamyl bromide in place of dimethallyl bromide. The following steps are identical to those leading to **48** from **35**. Colorless oil. **1H NMR (400 MHz, $CDCl_3$)** δ 7.32 (dt, $J = 15.2, 7.3\text{ Hz}$, 4H), 7.22 (t, $J = 7.1\text{ Hz}$, 1H), 6.48 (d, $J = 15.6\text{ Hz}$, 1H), 6.15 (dt, $J = 15.6, 7.7\text{ Hz}$, 1H), 5.36 (t, $J = 6.6\text{ Hz}$, 1H), 3.70 (s, 4H), 2.40 (d, $J = 1.8\text{ Hz}$, 2H), 2.34 (d, $J = 7.7\text{ Hz}$, 2H), 2.07 (s, 3H), 1.80–1.71 (m, 2H), 1.44 (s, 3H), 1.42 (s, 3H), 1.48–1.29 (m, 4H), 0.91 (t, $J = 7.1\text{ Hz}$, 3H).



The first step of the synthesis of **71** was realized according to the same procedure than for **35**, using 5-bromo-2-methyl-2-pentene in place of dimethallyl bromide. The following steps are identical to those leading to **48** from **35**. Colorless oil. **1H NMR (400 MHz, $CDCl_3$)** δ 5.35 (t, $J = 6.8\text{ Hz}$, 1H), 5.14–5.02

(m, 1H), 3.64 (s, 4H), 2.49 (s, 2H), 2.05 (s, 3H), 2.01–1.86 (m, 2H), 1.79–1.65 (m, 2H), 1.69 (s, 3H), 1.61 (s, 3H), 1.41 (s, 3H), 1.40 (s, 3H), 1.47–1.29 (m, 4H), 0.91 (t, $J = 7.0$ Hz, 3H).

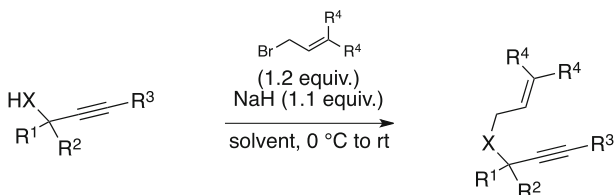


The first step of the synthesis of **72** was realized according to the same procedure than for **35**, using 5-bromo-2-methyl-2-pentene in place of dimethylallyl bromide. The following steps are identical to those leading to **62** from **35**. Colorless oil. ^1H NMR (400 MHz, CDCl_3) δ 7.39–7.28 (m, 4H), 7.27–7.20 (m, 1H), 5.14–5.07 (m, 1H), 3.74–3.64 (m, 4H), 3.61 (s, 2H), 2.52 (s, 2H), 1.98 (q, $J = 7.4$ Hz, 2H), 1.70 (s, 3H), 1.61 (s, 3H), 1.43 (s, 3H), 1.42 (s, 3H), 1.47–1.34 (m, 2H).

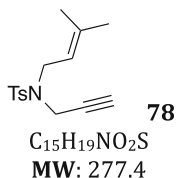
^{13}C NMR (100 MHz, CDCl_3) δ 137.5, 131.8, 128.5 (2C), 127.9 (2C), 126.5, 124.3, 98.1, 80.0, 78.8, 67.4 (2C), 35.5, 33.0, 26.7, 25.8, 25.3, 22.5, 21.5, 21.1, 17.6.

IR (neat) $\nu = 2917, 2863, 1454, 1373, 1262, 1200, 1075, 832, 730, 698\text{ cm}^{-1}$.

HRMS calculated for $[\text{C}_{22}\text{H}_{30}\text{NaO}_2]^+$: 349.2138, found: 349.2138.

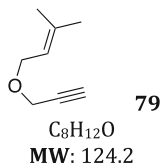


To a suspension of NaH (1.1 equiv.) in the appropriate solvent (THF or DMF, 0.5 M) is added dropwise at 0 °C the propargyl alcohol/amine (1 equiv.). The reaction is stirred at 0 °C for 5 min, and the allyl bromide derivative is added. The mixture is stirred overnight and then quenched with a saturated aqueous NH_4Cl solution. The aqueous layer is extracted with Et_2O , and the combined organic extracts are washed with brine and water, dried over MgSO_4 , filtered and the solvent removed under reduced pressure. The crude product is purified by flash column chromatography over silica gel gradient mixtures of pentane and diethyl ether as eluent to afford the pure enyne.



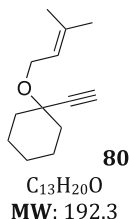
The reaction was performed in DMF, colorless oil, 79 %. ^1H NMR (300 MHz, CDCl_3) δ 7.70 (d, $J = 8.2$ Hz, 2H), 7.25 (d, $J = 8.3$ Hz, 2H), 4.90–5.30 (m, 1H),

4.05 (d, $J = 2.2$ Hz, 2H), 3.80 (d, $J = 7.4$ Hz, 2H), 2.40 (s, 3H), 1.97 (t, $J = 2.3$ Hz, 1H), 1.70 (s, 6H).



The reaction was performed in THF, colorless oil, 83 %. **¹H NMR (300 MHz, CDCl₃)** δ 5.31–5.37 (m, 1H), 4.13 (d, $J = 2.3$ Hz, 2H), 4.06 (d, $J = 7.1$ Hz, 2H), 2.41 (t, $J = 2.3$ Hz, 1H), 1.76 (d, $J = 1.0$ Hz, 3H), 1.71 (d, $J = 1.0$ Hz, 3H).

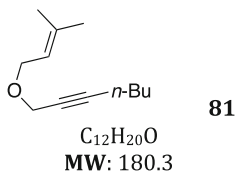
¹³C NMR (75 MHz, CDCl₃) δ 138.0 (C), 120.1 (CH), 79.8 (C), 73.9 (CH), 65.7 (CH₂), 56.5 (CH₂), 25.6 (CH₃), 17.8 (CH₃).



The reaction was performed in THF. Colorless oil, 72 %. **¹H NMR (300 MHz, CDCl₃)** δ 5.06 (t, $J = 7.4$ Hz, 1H), 3.63 (s, 3H), 2.32 (s, 1H), 2.09 (d, $J = 7.7$ Hz, 2H), 2.03–1.92 (m, 1H), 1.70 (s, 2H), 1.62 (s, 2H), 1.38 (s, 5H).

¹³C NMR (75 MHz, CDCl₃) δ 135.5, 117.9, 98.1, 81.2, 70.8, 66.8 (2C), 36.3, 31.0, 26.1, 25.6, 22.4, 22.2, 18.0.

IR (neat) $\nu = 2933, 2858, 1447, 1074, 1020, 947, 649, 624$ cm⁻¹.

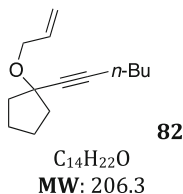


The reaction was performed in THF. Colorless oil, 79 %. **¹H NMR (400 MHz, CDCl₃)** δ 5.30 (dddt, $J = 7.0, 5.6, 2.8, 1.4$ Hz, 1H), 4.05 (t, $J = 2.2$ Hz, 2H), 3.98 (d, $J = 7.1$ Hz, 2H), 2.18 (tt, $J = 7.0, 2.1$ Hz, 2H), 1.70 (s, 3H), 1.65 (s, 3H), 1.50–1.32 (m, 4H), 0.86 (t, $J = 7.2$ Hz, 3H).

¹³C NMR (100 MHz, CDCl₃) δ 137.8, 120.6, 86.7, 76.2, 65.7, 57.4, 30.7, 25.8, 21.9, 18.5, 18.0, 13.6.

IR (neat) $\nu = 2959, 2932, 2872, 2238, 1717, 1673, 1453, 1379, 1250, 1136, 1066$ cm⁻¹.

HRMS calculated for [C₁₂H₂₀NaO]⁺: 203.1406, found: 203.1410.

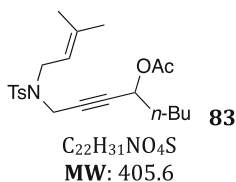


The reaction was performed in THF. Colorless oil, 73%. **¹H NMR (400 MHz, CDCl₃)** δ 5.97 (ddt, J = 17.2, 10.3, 5.6 Hz, 1H), 5.29 (dq, J = 17.3, 1.8 Hz, 1H), 5.13 (dq, J = 10.3, 1.3 Hz, 1H), 4.10 (dt, J = 5.6, 1.5 Hz, 2H), 2.23 (t, J = 6.9 Hz, 2H), 1.92–1.81 (m, 2H), 1.74–1.38 (m, 9H), 1.33–1.23 (m, 1H), 0.92 (t, J = 7.2 Hz, 3H).

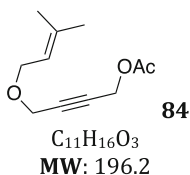
¹³C NMR (75 MHz, CDCl₃) δ 136.1, 115.9, 86.4, 81.4, 74.0, 65.9, 64.4, 37.7, 31.1, 25.7, 23.1, 22.0, 18.4, 13.7.

IR (neat) ν = 2932, 2858, 2238, 1647, 1447, 1126, 1066, 916 cm⁻¹.

HRMS calculated for [C₁₄H₂₂NaO]⁺: 229.1563, found: 229.1558.



Prepared from enyne **78**, through an identical two-step procedure than the one leading to **47** from **37**. Colorless oil. **¹H NMR (400 MHz, CDCl₃)** δ 7.76 (d, J = 8.3 Hz, 2H), 7.32 (d, J = 7.9 Hz, 2H), 5.12 (m, 2H), 4.13 (d, J = 1.7 Hz, 2H), 3.81 (d, J = 7.4 Hz, 2H), 2.45 (s, 3H), 2.04 (s, 3H), 1.75 (s, 3H), 1.68 (s, 3H), 1.51 (qt, J = 13.4, 6.4 Hz, 2H), 1.35–1.14 (m, 4H), 0.90 (t, J = 7.1 Hz, 3H).

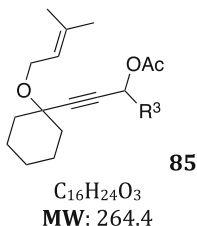


Prepared from enyne **79**, through an identical two-step procedure than the one leading to **47** from **37**. Colorless oil. **¹H NMR (400 MHz, CDCl₃)** δ 5.30 (m, 1H), 4.69 (t, J = 1.6, 2H), 4.13 (t, J = 2.0, 2H), 4.01 (d, J = 7.2, 2H), 2.07 (s, 3H), 1.73 (s, 3H), 1.67 (s, 3H).

¹³C NMR (100 MHz, CDCl₃) δ 170.2, 138.4, 120.1, 83.1, 80.0, 66.1, 56.9, 52.3, 25.8, 20.7, 18.0.

IR (neat) ν = 2935, 2855, 1746, 1376, 1223 cm⁻¹.

HRMS calculated for [C₁₁H₁₆O₃Na]⁺: 219.0992, found: 219.0989.

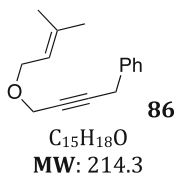


Prepared from enyne **80**, through an identical two-step procedure than the one leading to **47** from **37**. Colorless oil. ^1H NMR (400 MHz, CDCl_3) δ 5.42 (t, $J = 6.6$, 1H), 5.36 (t, $J = 7.2$, 1H), 4.07 (d, $J = 6.6$, 2H), 2.07 (s, 3H), 1.94–1.91 (m, 2H), 1.74 (s, 3H), 1.69 (s, 3H), 1.80–1.23 (m, 14H), 0.91 (t, $J = 7.2$, 3H).

^{13}C NMR (100 MHz, CDCl_3) δ 209.2, 170.1, 136.7, 121.7, 86.8, 73.5, 64.4, 60.1, 37.4 (2C), 34.8, 27.4, 26.0, 25.6, 23.1 (2C), 22.4, 21.2, 18.1, 14.1.

IR (neat) $\nu = 2934, 2861, 1741, 1231\text{ cm}^{-1}$.

HRMS calculated for $[\text{C}_{20}\text{H}_{32}\text{NaO}_3]^+$: 343.2244, found: 343.2239.

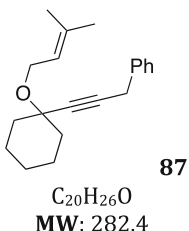


Prepared from enyne **79**, through the same procedure than the one leading to **62** from **37**. Colorless oil. ^1H NMR (400 MHz, CDCl_3) δ 7.32–7.21 (m, 5H), 5.35 (t, $J = 8.0$, 1H), 4.17 (t, $J = 2.4$, 2H), 4.05 (d, $J = 7.2$, 2H), 3.65 (s, 2H), 1.75 (s, 3H), 1.68 (s, 3H).

^{13}C NMR (100 MHz, CDCl_3) δ 138.2, 136.8, 128.6 (2C), 128.1 (2C), 126.9, 120.6, 84.2, 78.6, 66.1, 57.6, 25.9, 25.3, 18.2.

IR (neat) $\nu = 2912, 2851, 1495, 1453, 1064, 728, 695\text{ cm}^{-1}$.

HRMS calculated for $[\text{C}_{15}\text{H}_{18}\text{NaO}]^+$: 237.1250, found: 237.1254.

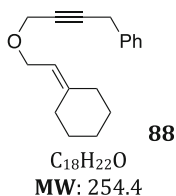


Prepared from enyne **80**, through an identical two-step procedure than the one leading to **62** from **37**. Colorless oil. ^1H NMR (400 MHz, CDCl_3) δ 7.33 (m, 4H), 7.23 (m, 1H), 5.37 (tt, $J = 7.0, 1.5\text{ Hz}$, 1H), 4.12 (d, $J = 6.8\text{ Hz}$, 2H), 3.68 (s, 2H), 1.99–1.90 (m, 2H), 1.73 (s, 3H), 1.66 (s, 3H), 1.70–1.48 (m, 10H).

^{13}C NMR (100 MHz, CDCl_3) δ 137.2, 136.4, 128.6 (2C), 128.0 (2C), 126.6, 122.0, 84.2, 83.6, 74.0, 60.0, 37.7 (2C), 26.0, 25.8, 25.3, 23.2 (2C), 18.2.

IR (neat) $\nu = 2932, 2857, 1706, 1449, 1063, 730, 696\text{ cm}^{-1}$.

HRMS calculated for $[\text{C}_{20}\text{H}_{26}\text{NaO}]^+$: 305.1876, found: 305.1880.



To a solution of NaH (2.45 g, 61.1 mmol, 1.2 equiv.) in THF (40 mL) is added dropwise triethyl phosphonoacetate (15.2 mL, 76.4 mmol, 1.5 equiv.). The reaction is stirred for 20 min at rt and then cooled down to 0 °C. Cyclohexanone is added dropwise, and the mixture is stirred overnight. The solution is quenched with a saturated aqueous NH_4Cl solution, and the aqueous layer is extracted with Et_2O . The combined organic extracts are washed with brine and water, dried over MgSO_4 , filtered and the solvent removed under reduced pressure. Distillation under reduced pressure afforded the desired acrylate derivative (90 °C, 5 mm Hg) in 71 % yield.

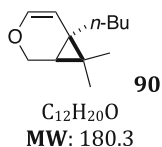
To a suspension of LAH (2.75 g, 72.5 mmol, 2 equiv.) in Et_2O (70 mL) is added dropwise at 0 °C the acrylate derivative (6.1 g, 36.3 mmol, 1 equiv.). The mixture is allowed to warm to rt and stirred for 4 h, then cooled down to 0 °C and quenched by a dropwise addition of a saturated aqueous solution of MgSO_4 until the aluminium salts have been hydrolyzed. The mixture is then filtered over a short pad of silica/celite, the remaining solids are washed with Et_2O , and the filtrate evaporated under reduced pressure to afford the desired alcohol in pure form as a colorless oil in 82 % yield.

O-alkylation of the resulting alcohol was performed through a similar procedure than for the preparation of enynes **78-82**, using propargyl bromide in place of allyl bromide derivatives, and final benzylation of the acetylenic position was realized in an identical manner than for the synthesis of **62** from **37**, affording the desired enyne as a colorless oil in 40 % yield over two steps. **^1H NMR (400 MHz, CDCl_3)** δ 7.32 (m, 5H), 5.30 (dt, $J = 7.2, 0.8$, 1H), 4.19 (t, $J = 2.4$, 2H), 4.10 ($J = 7.2$, 2H), 3.66 (s, 2H), 2.20 (m, 2H), 2.14 (s br, 2H), 1.56 (m, 6H).

^{13}C NMR (100 MHz, CDCl_3) δ 145.9, 136.6, 128.5 (2C), 127.9 (2C), 126.6, 117.1, 84.0, 78.6, 65.0, 57.2, 37.1, 29.0, 28.5, 27.8, 26.7, 25.2.

IR (neat) $\nu = 2924, 2850, 1494, 1068, 803 \text{ cm}^{-1}$.

HRMS calculated for $[\text{C}_{18}\text{H}_{22}\text{NaO}]^+$: 277.1563, found: 277.1560.

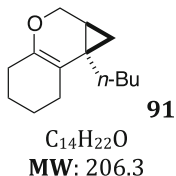


Prepared according to **GPI**, colorless oil, 90 %. **^1H NMR (400 MHz, CDCl_3)** δ 6.23 (d, $J = 6.4$, 1H), 4.75 (dd, $J = 6, 0.8$, 1H), 4.00 (d, $J = 3.2$, 2H), 1.31 (m, 6H), 1.20 (s, 3H), 1.02 (s, 3H), 0.88 (t, $J = 7$, 3H), 0.72 (t, $J = 3.2$, 1H).

^{13}C NMR (100 MHz, CDCl_3) δ 140.7, 104.0, 60.8, 33.0, 29.9, 29.4, 27.6, 22.9 (2C), 22.4, 17.1, 14.1.

IR (neat) ν = 2924, 2860, 1644, 1459, 1240, 736 cm^{-1} .

HRMS calculated for $[\text{C}_{12}\text{H}_{20}\text{ONa}]^+$: 203.1414, found: 203.1418.

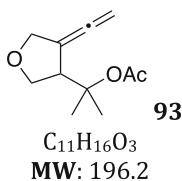


Prepared according to *GPI*, colorless oil, 60 %. **^1H NMR (400 MHz, CDCl_3)** δ 4.08 (dd, J = 10.9, 4.8 Hz, 1H), 3.75 (dd, J = 10.9, 3.3 Hz, 1H), 2.25–2.13 (m, 1H), 2.06–1.89 (m, 4H), 1.69–1.46 (m, 4H), 1.35–1.20 (m, 4H), 1.16–1.08 (m, 1H), 0.94–0.84 (m, 3H), 0.75–0.62 (m, 1H), 0.67 (dd, J = 8.0, 3.8 Hz, 1H), 0.48 (t, J = 3.9 Hz, 1H).

^{13}C NMR (100 MHz, CDCl_3) δ 146.7, 110.7, 65.9, 35.1, 29.7, 27.5, 25.1, 23.4, 23.1, 23.1, 21.3, 20.4, 18.6, 14.3.

IR (neat) ν = 2923, 2857, 1675, 1457, 1382, 1196, 1152, 1031, 1009 cm^{-1} .

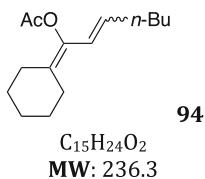
HRMS calculated for $[\text{C}_{14}\text{H}_{22}\text{NaO}]^+$: 229.1563, found: 229.1562.



Prepared according to *GPI*, colorless oil, 75 %. **^1H NMR (400 MHz, CDCl_3)** δ 4.85 (m, 2H), 4.33 (m, 2H), 3.88 (d, J = 5.2, 2H), 3.64 (m, 1H), 1.95 (s, 3H), 1.49 (s, 3H), 1.47 (s, 3H).

^{13}C NMR (100 MHz, CDCl_3) δ 200.6, 170.4, 100.4, 83.7, 78.5, 70.7, 69.9, 50.9, 24.1, 23.3, 22.4.

HRMS calculated for $[\text{C}_{11}\text{H}_{16}\text{O}_3\text{Na}]^+$: 219.0992, found: 219.0993.



Prepared according to *GPI*, colorless oil, quantitative (*Z/E* ratio 0.4:1).

(*Z*)-diastereomer: **^1H NMR (CDCl_3 , 400 MHz)** δ 5.97 (d, J = 11.6, 1H), 5.44 (dt, J = 7.6, 11.6, 1H), 2.18–2.12 (m, 4H), 2.14 (s, 3H), 2.07 (t, J = 5.6, 2H), 1.65–1.49 (m, 6H), 1.41–1.30 (m, 4H), 0.89 (t, J = 6.8, 3H).

^{13}C NMR (100 MHz, CDCl_3) δ 169.2, 136.8, 134.0, 130.2, 120.5, 31.9, 29.6, 29.0, 27.9, 27.4, 27.2, 26.5, 22.6, 20.9, 14.1.

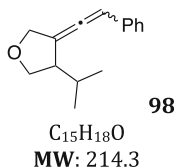
IR (neat) $\nu = 1753\text{ cm}^{-1}$.

(*E*)-diastereomer (colorless oil): **^1H NMR** (CDCl_3 , 400 MHz) δ 6.28 (d, $J = 15.2$, 1H), 5.55 (dt, $J = 6.8$, 15.2, 1H), 2.30 (t, $J = 5.2$, 2H), 2.20 (s, 3H), 2.13–2.04 (m, 4H), 1.59–1.52 (m, 6H), 1.40–1.26 (m, 4H), 0.88 (t, $J = 7.2$, 3H).

^{13}C NMR (100 MHz, CDCl_3) δ 169.1, 137.7, 129.9, 129.1, 120.4, 32.5, 31.6, 29.0, 28.6, 27.5, 27.1, 26.5, 22.4, 20.6, 14.0.

IR (neat) $\nu = 1757\text{ cm}^{-1}$.

HRMS calculated for $[\text{C}_{15}\text{H}_{24}\text{O}_2\text{Na}]^+$: 259.1674, found: 259.1672.

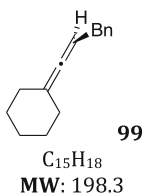


Prepared according to *GPI*, colorless oil, 90 % (dr 1:1). **^1H NMR** (CDCl_3 , 400 MHz) δ 7.34–7.18 (m, 5H), 6.30 (m, 1H), 4.52–4.39 (m, 2H), 4.03 (m, 1H), 3.82–3.75 (m, 1H), 2.92–2.83 (m, 1H), 1.95–1.85 (m, 1H), 1.03–0.95 (m, 6H).

^{13}C NMR (100 MHz, CDCl_3) δ 196.6, 196.1, 135.1 (2C), 128.8 (4C), 127.0 (2C), 126.9 (4C), 108.0 (2C), 98.4, 98.3, 72.3, 72.1, 69.8, 69.7, 51.0, 49.9, 31.1, 30.6, 20.9 (2C), 20.0, 19.7.

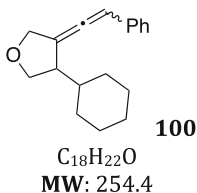
IR (neat) $\nu = 2958$, 2869, 1956, 1496, 1460, 1064 cm^{-1} .

HRMS calculated for $[\text{C}_{15}\text{H}_{19}\text{O}]^+$: 215.1436, found: 215.1430.



Prepared according to *GPI*, colorless oil, 57 %. **^1H NMR** (400 MHz, CDCl_3) δ 7.35–7.18 (m, 5H), 5.17 (ddq, $J = 6.8$, 4.4, 2.1 Hz, 1H), 3.34 (d, $J = 6.6$ Hz, 2H), 1.66–1.39 (m, 10H).

^{13}C NMR (100 MHz, CDCl_3) δ 199.3, 141.1, 128.7 (2C), 128.4 (2C), 126.0, 103.2, 88.5, 36.5, 31.8 (2C), 27.5 (2C), 26.3.

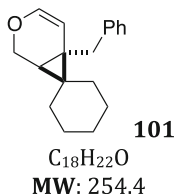


Prepared according to *GPI*, colorless oil, 49% (dr 1:1). **^1H NMR** (400 MHz, CDCl_3) δ 7.30 (m, 5H), 6.30 (m, 1H), 4.41 (m, 2H), 3.99 (m, 1H), 3.82 (m, 1H), 2.87 (m, 1H), 1.73 (m, 1H), 1.56 (m, 5H), 1.17 (m, 5H).

^{13}C NMR (100 MHz, CDCl_3) δ 196.4, 195.8, 135.0 (2C), 128.6 (4C), 126.9 (2C), 126.8 (4C), 107.8, 107.6, 98.1 (2C), 72.2, 72.1, 69.6, 69.4, 50.1, 49.1, 41.3, 40.4, 31.2 (2C), 30.0 (2C), 26.4 (6C).

IR (neat) ν = 3030, 2849, 1954, 1598, 1447, 1063, 691 cm^{-1} .

HRMS calculated for $[\text{C}_{18}\text{H}_{23}\text{O}]^+$: 254.1670, found: 254.1678.

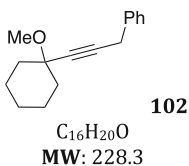


Prepared according to **GPI**, colorless oil, 32 %. **^1H NMR (400 MHz, CDCl_3)** δ 7.27 (m, 5H), 6.21 (dd, J = 6.4, 2.0, 1H), 4.77 (d, J = 6.4, 1H), 4.13 (d, J = 11.6, 1H), 4.04 (m, 1H), 2.99 (d, J = 15.0, 1H), 2.86 (d, J = 15.0, 1H), 1.60 (m, 6H), 1.48 (m, 4H), 1.00 (d, J = 4.4, 1H).

^{13}C NMR (100 MHz, CDCl_3) δ 141.0, 140.6, 128.8 (2C), 128.1 (2C), 125.7, 103.9, 60.8, 38.3, 35.4, 33.9, 29.0, 27.5, 26.6, 26.5, 26.0, 23.2.

IR (neat) ν = 2918, 2848, 1643, 1443, 1234, 1015, 697 cm^{-1} .

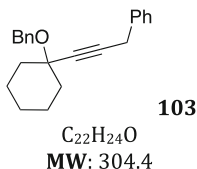
HRMS calculated for $[\text{C}_{18}\text{H}_{22}\text{ONa}]^+$: 277.1565, found: 277.1570.



Prepared from 1-ethynylcyclohexanol **77**. *O*-alkylation was performed through a similar procedure than for the preparation of enynes **78–82**, using methyl iodide in place of allyl bromide derivatives, and final benzylation of the acetylenic position was realized in an identical manner than for the synthesis of **62** from **37**, affording the desired propargylic ether as a colorless oil in 32 % yield over two steps. **^1H NMR (400 MHz, CDCl_3)** δ 7.44–7.33 (m, 4H), 7.31–7.24 (m, 1H), 3.72 (s, 2H), 3.44 (s, 3H), 2.05–1.89 (m, 3H), 1.78–1.50 (m, 7H), 1.42–1.30 (m, 1H).

^{13}C NMR (100 MHz, CDCl_3) δ 132.5, 128.6 (2C), 127.9 (2C), 126.7, 83.6, 77.9, 58.9, 50.8, 37.1 (2C), 25.7, 25.2, 23.0 (2C).

HRMS calculated for $[\text{C}_{16}\text{H}_{20}\text{NaO}]^+$: 251.1406, found: 251.1411.



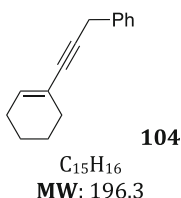
Prepared from 1-ethynylcyclohexanol **77**. *O*-alkylation was performed through a similar procedure than for the preparation of enynes **78–82**, using benzyl bromide in place of allyl bromide derivatives, and final benzylation of the

acetylenic position was realized in an identical manner than for the synthesis of **62** from **37**, affording the desired propargylic ether as a colorless oil in 10 % yield over two steps. **¹H NMR (400 MHz, CDCl₃)** δ 7.41–7.29 (m, 8H), 7.28–7.21 (m, 2H), 4.67 (s, 2H), 3.70 (s, 2H), 1.98 (d, J = 5.3 Hz, 2H), 1.78–1.66 (m, 4H), 1.66–1.47 (m, 4H).

¹³C NMR (75 MHz, CDCl₃) δ 139.63, 137.11, 128.61 (2C), 128.37 (2C), 127.96 (2C), 127.84 (2C), 127.31, 126.66, 93.69, 84.14, 74.43, 65.58, 37.74 (2C), 25.71 (2C), 25.26, 23.09 (2C).

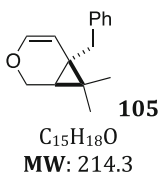
IR (neat) ν = 2933, 2857, 1704, 1495, 1452, 1063, 1027, 937, 730, 694 cm⁻¹.

HRMS calculated for [C₂₂H₂₄ONa]⁺: 327.1719, found: 327.1717.



Prepared according to **GP1**, colorless oil, 41 %. **¹H NMR (400 MHz, CDCl₃)** δ 7.39–7.28 (m, 4H), 7.27–7.19 (m, 1H), 6.09 (dt, J = 4.0, 2.1 Hz, 1H), 3.73 (s, 2H), 2.18–2.14 (m, 2H), 2.13–2.05 (m, 2H), 1.68–1.55 (m, 4H).

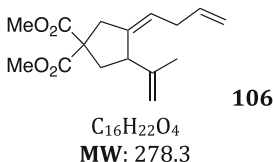
¹³C NMR (101 MHz, CDCl₃) δ 137.3, 134.0, 128.6 (2C), 128.0 (2C), 126.6, 121.0, 84.6, 77.5, 29.7, 25.8, 25.7, 22.5, 21.7.



Prepared according to **GP2**, colorless oil, 94 %. **¹H NMR (400 MHz, CDCl₃)** δ 7.34–7.29 (m, 2H), 7.27–7.19 (m, 3H), 6.20 (d, J = 6.3 Hz, 1H), 4.76 (d, J = 6.3 Hz, 1H), 4.13–3.95 (m, 2H), 2.91 (s, 2H), 1.29 (s, 3H), 1.16 (s, 3H), 0.98 (d, J = 4.2 Hz, 1H).

¹³C NMR (75 MHz, CDCl₃) δ 140.9, 140.4, 128.9 (2C), 128.3 (2C), 125.9, 103.9, 60.5, 39.2, 29.9, 28.4, 23.7, 22.6, 17.2.

HRMS calculated for [C₁₅H₁₈NaO]⁺: 237.1250, found: 237.1248.



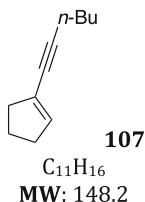
Prepared according to **GP3**, colorless oil, 64 % [α]_D²⁰ = +0.6 (c 1.58, CHCl₃). **¹H NMR (400 MHz, CDCl₃)** δ 5.72 (ddt, J = 16.4, 10.1, 6.3 Hz, 1H), 5.43 (t, J = 7.2 Hz, 1H), 5.00–4.87 (m, 2H), 4.75 (d, J = 24.5 Hz, 2H), 3.71 (s, 3H),

3.70 (s, 3H), 3.36 (t, $J = 8.4$ Hz, 1H), 2.99 (dt, $J = 15.4, 2.3$ Hz, 1H), 2.85 (d, $J = 15.3$ Hz, 1H), 2.69 (ddd, $J = 13.4, 8.7, 1.9$ Hz, 1H), 2.65 (t, $J = 6.7$ Hz, 2H), 1.99 (dd, $J = 13.2, 8.5$ Hz, 1H), 1.67 (s, 3H).

^{13}C NMR (100 MHz, CDCl_3) δ 172.0, 171.9, 145.9, 140.2, 136.7, 122.9, 114.7, 111.4, 59.2, 52.8, 52.8, 47.3, 42.9, 40.0, 32.7, 19.4.

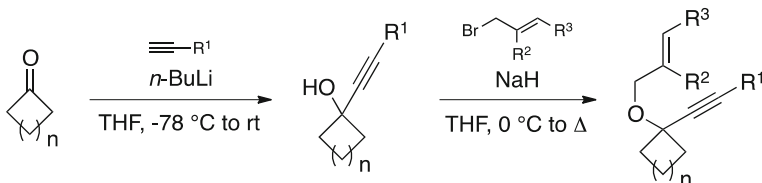
IR (neat) $\nu = 1730, 1435, 1247, 1201, 1166, 895\text{ cm}^{-1}$.

HRMS calculated for $[\text{C}_{16}\text{H}_{22}\text{NaO}_4]^+$: 301.1410, found: 301.1414.

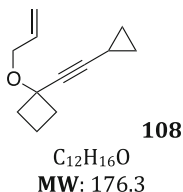


Prepared according to *GPI*, colorless oil, 33 %. ^1H NMR (400 MHz, CDCl_3) δ 5.93 (dt, $J = 3.7, 2.0$ Hz, 1H), 2.46–2.34 (m, 4H), 2.32 (t, $J = 7.0$ Hz, 2H), 1.88 (p, $J = 7.5$ Hz, 2H), 1.57–1.36 (m, 4H), 0.92 (t, $J = 7.3$ Hz, 3H).

^{13}C NMR (100 MHz, CDCl_3) δ 136.1, 125.2, 91.7, 77.9, 36.8, 33.2, 31.1, 23.4, 22.1, 19.3, 13.8.



To a solution of alkyne (1.2 equiv.) in THF (0.5 M) is added dropwise at $-78\text{ }^\circ\text{C}$ *n*-butyllithium (1.1 equiv.). The mixture is allowed to warm to rt within 1 h, then cooled down again to $-78\text{ }^\circ\text{C}$ and the ketone (1 equiv.) is added dropwise. The resulting solution is warmed up to rt and stirred for 2 h. The reaction mixture is then quenched with a saturated aqueous NH_4Cl solution, and the aqueous layer is extracted with Et_2O . The combined organic extracts are washed with brine and water, dried over MgSO_4 , filtered and the solvent removed under reduced pressure to afford the crude alcohol, which is engaged in the next step without purification. *O*-alkylation was performed through a similar procedure than for the preparation of enynes **78–82**.



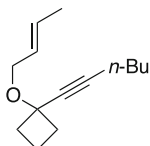
Colorless oil, 63 % over two steps. ^1H NMR (400 MHz, C_6D_6) δ 5.95 (ddt, $J = 17.3, 10.5, 5.7$ Hz, 1H), 5.30 (dq, $J = 17.3, 1.8$ Hz, 1H), 5.19–5.08 (m, 1H),

3.96 (dt, $J = 5.7, 1.4$ Hz, 2H), 2.32–2.12 (m, 4H), 1.91–1.69 (m, 2H), 1.28 (tt, $J = 8.1, 5.0$ Hz, 1H), 0.81–0.75 (m, 2H), 0.71–0.65 (m, 2H).

^{13}C NMR (100 MHz, CDCl_3) δ 135.3, 116.8, 86.3, 77.8, 65.5, 36.3 (2C), 13.4, 8.5 (2C), -0.3 .

IR (neat) $\nu = 2991, 2942, 2858, 2232, 1732, 1648, 1423, 1360, 1275, 1246, 1133, 1028, 919\text{ cm}^{-1}$.

HRMS calculated for $[\text{C}_{12}\text{H}_{16}\text{NaO}]^+$: 199.1093, found: 199.1090.

**109**

$\text{C}_{14}\text{H}_{22}\text{O}$

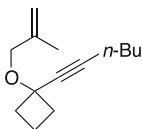
MW: 206.3

Colorless oil, 77 % over two steps. ^1H NMR (200 MHz, CDCl_3) δ 5.85–5.47 (m, 2H), 3.91 (d, $J = 5.3$ Hz, 2H), 2.34–2.13 (m, 6H), 1.92–1.74 (m, 2H), 1.70 (d, $J = 5.0$ Hz, 3H), 1.57–1.16 (m, 4H), 0.91 (t, $J = 7.1$ Hz, 3H).

^{13}C NMR (100 MHz, CDCl_3) δ 129.4, 128.0, 85.5, 81.7, 72.8, 65.2, 59.9, 36.4 (2C), 31.0, 22.1, 18.6, 18.0, 13.8, 13.4.

IR (neat) $\nu = 2935, 2860, 1458, 1272, 1246, 1127, 965\text{ cm}^{-1}$.

HRMS calculated for $[\text{C}_{14}\text{H}_{22}\text{NaO}]^+$: 229.1563, found: 229.1566.

**110**

$\text{C}_{14}\text{H}_{22}\text{O}$

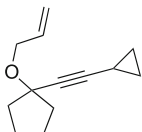
MW: 206.3

Colorless oil, 86 % over two steps. ^1H NMR (200 MHz, CDCl_3) δ 4.93 (d, $J = 28.4$ Hz, 1H), 3.86 (s, 2H), 2.35–2.10 (m, 6H), 1.97–1.67 (m, 2H), 1.77 (s, 3H), 1.57–1.31 (m, 4H), 0.91 (t, $J = 7.1$ Hz, 3H).

^{13}C NMR (100 MHz, CDCl_3) δ 142.8, 111.8, 85.4, 81.7, 73.0, 68.3, 36.2 (2C), 31.0, 22.1, 20.0, 18.6, 13.7, 13.4.

IR (neat) $\nu = 2933, 2860, 1456, 1272, 1246, 1129, 1042, 895\text{ cm}^{-1}$.

HRMS calculated for $[\text{C}_{14}\text{H}_{22}\text{NaO}]^+$: 229.1563, found: 229.1565.

**111**

$\text{C}_{13}\text{H}_{18}\text{O}$

MW: 190.3

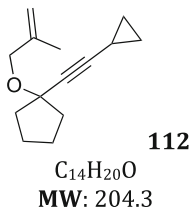
Colorless oil, 78 % over two steps. ^1H NMR (400 MHz, CDCl_3) δ 5.94 (ddd, $J = 17.1, 10.7, 5.2$ Hz, 1H), 5.27 (dd, $J = 17.2, 1.7$ Hz, 1H), 5.12

(d, $J = 10.4$ Hz, 1H), 4.08–3.98 (m, 2H), 2.02–1.92 (m, 2H), 1.88–1.77 (m, 2H), 1.77–1.63 (m, 4H), 1.31–1.20 (m, 1H), 0.80–0.72 (m, 2H), 0.69–0.61 (m, 2H).

^{13}C NMR (100 MHz, CDCl_3) δ 135.9, 116.2, 80.7, 78.1, 67.9, 65.9, 39.9 (2C), 23.5 (2C), 8.5 (2C), -0.4 .

IR (neat) $\nu = 2963, 2872, 2234, 1730, 1424, 1359, 1187, 1060, 1029, 917, 812\text{ cm}^{-1}$.

HRMS calculated for $[\text{C}_{13}\text{H}_{18}\text{NaO}]^+$: 213.1250, found: 213.1250.

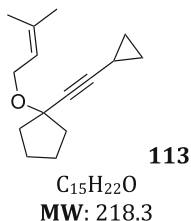


Colorless oil, 61 % over two steps. ^1H NMR (400 MHz, CDCl_3) δ 4.98–4.96 (m, 1H), 4.83 (d, $J = 0.8$ Hz, 1H), 3.91 (s, 2H), 2.03–1.93 (m, 2H), 1.85–1.76 (m, 2H), 1.75 (s, 3H), 1.74–1.63 (m, 2H), 1.30–1.21 (m, 2H), 0.94–0.80 (m, 1H), 0.79–0.72 (m, 2H), 0.68–0.61 (m, 2H).

^{13}C NMR (100 MHz, CDCl_3) δ 143.3, 111.4, 88.3, 80.6, 77.0, 68.7, 39.8 (2C), 23.5 (2C), 20.0, 8.5 (2C), -0.4 .

IR (neat) $\nu = 2956, 2855, 2235, 1657, 1451, 1360, 1187, 1091, 1051, 1028, 978, 938, 895, 812\text{ cm}^{-1}$.

HRMS calculated for $[\text{C}_{14}\text{H}_{20}\text{NaO}]^+$: 227.1406, found: 227.1404.

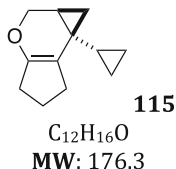


Colorless oil, 67 % over two steps. ^1H NMR (300 MHz, CDCl_3) δ 5.40–5.29 (m, 1H), 4.01 (d, $J = 7.0$ Hz, 2H), 1.97 (dd, $J = 11.9, 5.1$ Hz, 2H), 1.90–1.77 (m, 2H), 1.77–1.59 (m, 4H), 1.74 (s, 3H), 1.70 (s, 3H), 1.33–1.19 (m, 1H), 0.81–0.70 (m, 2H), 0.70–0.61 (m, 2H).

^{13}C NMR (100 MHz, CDCl_3) δ 136.47, 121.87, 88.32, 80.37, 77.22, 61.35, 39.84 (2C), 26.03, 23.43 (2C), 18.13, 8.45 (2C), -0.34 .

IR (neat) $\nu = 2965, 2873, 2235, 1717, 1449, 1381, 1231, 1148, 1071\text{ cm}^{-1}$.

HRMS calculated for $[\text{C}_{15}\text{H}_{22}\text{NaO}]^+$: 241.1563, found: 241.1560.

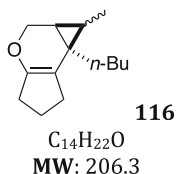


Prepared according to *GPI*, colorless oil, 81 %. ^1H NMR (400 MHz, CDCl_3) δ 4.07 (dd, $J = 10.6, 1.5$ Hz, 1H), 3.95 (dd, $J = 10.5, 2.8$ Hz, 1H), 2.71–2.55 (m, 1H), 2.52–2.38 (m, 1H), 2.36–2.16 (m, 2H), 1.87–1.74 (m, 2H), 1.16 (tt, $J = 8.1, 5.1$ Hz, 1H), 0.99 (ddd, $J = 10.1, 5.0, 2.2$ Hz, 1H), 0.61 (dd, $J = 8.8, 4.2$ Hz, 1H), 0.54–0.47 (m, 1H), 0.44–0.35 (m, 1H), 0.35–0.24 (m, 1H), 0.05 (dq, $J = 9.5, 5.3$ Hz, 1H), -0.06 (dq, $J = 9.9, 5.2$ Hz, 1H).

^{13}C NMR (101 MHz, CDCl_3) δ 147.4, 114.5, 64.8, 31.1, 29.7, 19.7, 19.4, 19.1, 16.8, 13.1, 2.4, 1.7.

IR (neat) $\nu = 3003, 2953, 2872, 1739, 1321, 1129, 1072, 1015, 956, 823\text{ cm}^{-1}$.

HRMS calculated for $[\text{C}_{12}\text{H}_{16}\text{NaO}]^+$: 199.1093, found: 199.1098.

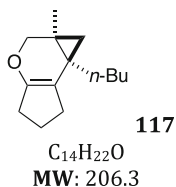


Prepared according to *GPI*, colorless oil, 51 %. ^1H NMR (400 MHz, CDCl_3) δ 4.27 (major dias, dd, $J = 11.4, 5.0$ Hz, 1H), 4.15 (minor dias, d, $J = 10.6$ Hz, 1H), 4.04 (major dias, d, $J = 11.3$ Hz, 1H), 3.96 (minor dias, dd, $J = 10.6, 2.9$ Hz, 1H), 2.51–2.09 (major + minor, m, 4H), 1.89–1.62 (major + minor, m, 2H), 1.38–1.16 (major + minor, m, 6H), 1.07 (minor dias, d, $J = 6.3$ Hz, 3H), 0.99–0.80 (major + minor, m, 3H {major 1H, minor 2H}), 0.89 (major dias, d, $J = 7.3$ Hz, 3H), 0.87 (major + minor, t, $J = 5.4$ Hz, 3H), 0.72–0.68 (major dias, m, 1H).

^{13}C NMR (101 MHz, CDCl_3) major + minor δ 149.6, 148.3, 114.4, 106.7, 64.6, 63.5, 36.7, 31.2, 31.2, 30.5, 30.1, 30.1, 29.9, 29.8, 29.4, 28.9, 26.2, 25.8, 23.3, 23.1, 22.4, 21.9, 21.0, 19.3, 19.3, 14.3, 13.8, 8.5.

IR (neat) $\nu = 2955, 2927, 2858, 1692, 1465, 1095, 1022, 1003, 791\text{ cm}^{-1}$.

HRMS calculated for $[\text{C}_{14}\text{H}_{22}\text{NaO}]^+$: 229.1563, found: 229.1567.

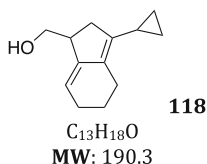


Prepared according to *GPI*, colorless oil, 85 %. ^1H NMR (400 MHz, CDCl_3) δ 3.98 (d, $J = 10.6$ Hz, 1H), 3.71 (d, $J = 10.3$ Hz, 1H), 2.49–2.13 (m, 4H), 1.87–1.75 (m, 2H), 1.41–1.22 (m, 4H), 1.13 (s, 3H), 0.90 (t, $J = 7.0$ Hz, 3H), 0.87 (d, $J = 4.0$ Hz, 1H), 0.45 (d, $J = 3.7$ Hz, 1H).

^{13}C NMR (100 MHz, CDCl_3) δ 148.7, 105.0, 70.0, 43.5, 42.5, 35.2, 31.0, 30.8, 29.7, 25.8, 23.4, 19.9, 16.3, 14.2.

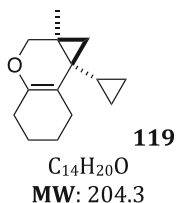
IR (neat) $\nu = 2930, 2858, 1684, 1466, 1378, 1179, 1079, 1048, 1023, 962\text{ cm}^{-1}$.

HRMS calculated for $[C_{14}H_{22}NaO]^+$: 229.1563, found: 229.1562.



Prepared according to **GP2**, colorless oil, 50 %. **1H NMR (400 MHz, $CDCl_3$)** δ 5.72–5.48 (m, 1H), 3.84–3.78 (dd, J = 10.9, 4.2 Hz, 1H), 3.75–3.69 (dd, J = 10.9, 6.1 Hz, 1H), 2.96–2.90 (m, 1H), 2.65–2.57 (m, 2H), 2.40–2.32 (m, 2H), 2.20–2.12 (dd, J = 13.6, 4.7 Hz, 1H), 1.97–1.82 (m, 3H), 1.80–1.71 (ddd, J = 13.2, 8.3, 5.0 Hz, 1H), 0.70–0.65 (m, 2H), 0.57–0.50 (td, J = 5.2, 2.4 Hz, 2H).

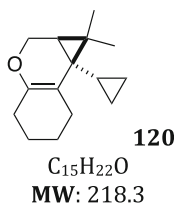
^{13}C NMR (100 MHz, $CDCl_3$) δ 143.9, 139.1, 134.2, 126.0, 64.9, 40.0, 33.8, 32.4, 27.9, 23.6, 11.2, 5.6, 5.5.



Prepared according to **GP2**, colorless oil, 37 %. **1H NMR (400 MHz, $CDCl_3$)** δ 3.78 (d, J = 10.2 Hz, 1H), 3.53 (d, J = 10.2 Hz, 1H), 2.56–2.45 (m, 1H), 2.27–2.13 (m, 1H), 1.99–1.92 (m, 2H), 1.71–1.61 (m, 2H), 1.52–1.43 (m, 2H), 1.17 (s, 3H), 0.94–0.81 (m, 2H), 0.68 (d, J = 4.3 Hz, 1H), 0.67–0.59 (m, 1H), 0.43–0.34 (m, 1H), 0.31 (d, J = 4.3 Hz, 1H), 0.23–0.15 (m, 1H), 0.12–0.02 (m, 1H).

^{13}C NMR (100 MHz, $CDCl_3$) δ 145.1, 113.9, 68.8, 28.0, 27.7, 26.0, 24.9, 24.1, 23.6, 22.9, 18.4, 15.4, 10.3, 5.1, 3.8, 1.2.

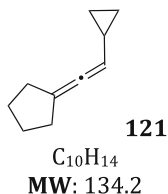
HRMS calculated for $[C_{14}H_{20}NaO]^+$: 227.1406, found: 227.1408.



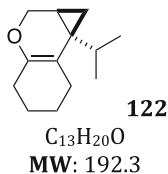
Prepared according to **GP2**, colorless oil, 12 %. **1H NMR (400 MHz, $CDCl_3$)** δ 4.06 (dd, J = 11.7, 7.2 Hz, 1H), 3.79 (dd, J = 11.7, 3.9 Hz, 1H), 2.47–2.36 (m, 1H), 2.00–1.91 (m, 1H), 1.88–1.79 (m, 1H), 1.75–1.63 (m, 3H), 1.61–1.40 (m, 3H), 1.18 (s, 3H), 1.11–1.04 (m, 1H), 1.03 (s, 3H), 0.71 (dd, J = 7.1, 3.9 Hz, 1H), 0.57–0.43 (m, 2H), 0.21 (dq, J = 8.9, 4.8 Hz, 1H), 0.16–0.10 (m, 1H).

^{13}C NMR (100 MHz, $CDCl_3$) δ 145.8, 109.2, 62.8, 28.0, 27.3, 27.2, 26.0, 25.0, 23.5, 23.3, 22.6, 17.4, 11.3, 7.2, 4.3.

HRMS calculated for $[C_{15}H_{22}NaO]^+$: 241.1563, found: 241.1564.



Prepared according to **GP2**, colorless oil, 48 %. **¹H NMR (400 MHz, CDCl₃)** δ 5.92 (s, 1H), 2.43–2.34 (m, 2H), 1.91–1.80 (m, 2H), 1.36 (ddd, J = 13.2, 8.4, 5.1 Hz, 1H), 0.83–0.76 (m, 2H), 0.74–0.68 (m, 2H).

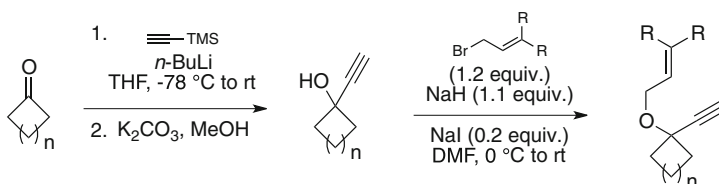


Prepared according to **GP2**, colorless oil, 77 %. **¹H NMR (400 MHz, CDCl₃)** δ 4.13 (dd, J = 11.0, 5.5 Hz, 1H), 3.68 (dd, J = 11.0, 4.0 Hz, 1H), 2.29–2.17 (m, 1H), 2.02–1.93 (m, 3H), 1.86 (p, J = 6.8 Hz, 1H), 1.74–1.61 (m, 2H), 1.60–1.39 (m, 2H), 1.19–1.12 (m, 1H), 0.91 (d, J = 6.8 Hz, 3H), 0.86 (dd, J = 8.2, 4.1 Hz, 1H), 0.69 (d, J = 6.9 Hz, 3H), 0.35–0.27 (m, 1H).

¹³C NMR (100 MHz, CDCl₃) δ 147.7, 111.8, 67.0, 28.9, 27.7, 25.9, 23.6, 23.0, 20.9, 19.2, 17.6, 16.2, 13.2.

IR (neat) ν = 2927, 2870, 1736, 1671, 1462, 1383, 1020, 802 cm⁻¹.

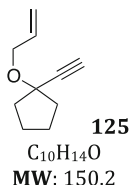
HRMS calculated for $[C_{13}H_{20}NaO]^+$: 215.1406, found: 215.1401.



To a solution of trimethylsilyl acetylene (1.2 equiv.) in THF (0.5 M) is added dropwise at -78 °C *n*-butyllithium (1.1 equiv.). The mixture is allowed to warm to rt within 1 h, then cooled down again to -78 °C and the ketone (1 equiv.) is added dropwise. The resulting solution is warmed up to rt and stirred for 2 h. The reaction mixture is then quenched with a saturated aqueous NH₄Cl solution, and the aqueous layer is extracted with Et₂O. The combined organic extracts are washed with brine and water, dried over MgSO₄, filtered and the solvent removed under reduced pressure to afford the crude alcohol, which is engaged in the next step without purification.

To a solution of the propargyl alcohol in MeOH (0.5 M) is added K₂CO₃ (3 equiv.). After stirring for 2 h, about 90 % of the solvent is removed under reduced pressure, and the resulting solution is diluted with water and Et₂O.

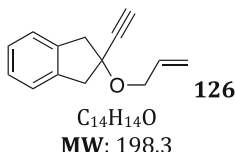
The aqueous layer is extracted twice with Et₂O and the combined organic extracts are washed with brine and water, dried over MgSO₄ and evaporated under reduced pressure to afford the pure alcohol. *O*-alkylation was performed through a similar procedure than for the preparation of enynes **78–82**.



Colorless oil, purified by Kugelrohr distillation (110 °C, 20 mmHg), 43 % over three steps. **¹H NMR (300 MHz, CDCl₃)** δ 6.04–5.85 (ddd, *J* = 17.1, 10.7, 5.2 Hz, 1H), 5.36–5.24 (dd, *J* = 17.2, 1.7 Hz, 1H), 5.16–5.11 (dd, *J* = 10.4, 1.8 Hz, 1H), 4.12–4.01 (dt, *J* = 5.5, 1.4 Hz, 2H), 2.47 (s, 1H), 2.10–1.85 (m, 4H), 1.83–1.67 (m, 4H).

¹³C NMR (75 MHz, CDCl₃) δ 136.1, 115.9, 86.4, 81.4, 74.0, 65.9, 64.4, 37.7, 31.1, 25.7, 23.1, 22.0, 18.4, 13.7.

HRMS calculated for [C₁₀H₁₄NaO]⁺: 173.0937, found: 173.0934.

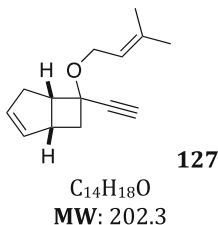


Colorless oil, purified by Kugelrohr distillation (180 °C, 20 mmHg), 22 % over three steps. **¹H NMR (400 MHz, CDCl₃)** δ 7.21–7.15 (m, 4H), 5.93 (ddt, *J* = 17.2, 10.9, 5.5 Hz, 1H), 5.26 (dq, *J* = 17.2, 1.7 Hz, 1H), 5.13 (dq, *J* = 10.4, 1.5 Hz, 1H), 4.20 (dt, *J* = 5.5, 1.5 Hz, 2H), 3.36 (s, 4H), 2.48 (s, 1H).

¹³C NMR (100 MHz, CDCl₃) δ 140.0, 135.0, 127.0, 124.7, 116.8, 85.1, 80.2, 73.1, 66.7, 46.7.

IR (neat) ν = 1089, 1059, 920, 741, 634 cm⁻¹.

HRMS calculated for [C₁₄H₁₄NaO]⁺: 221.0937, found: 221.0940.

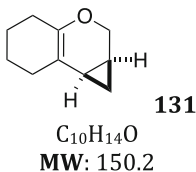


Colorless oil, 67 % over three steps (dr > 25:1). **¹H NMR (300 MHz, CDCl₃)** δ 5.83–5.73 (m, 2H), 5.39–5.30 (m, 1H), 4.04 (dd, *J* = 10.6, 7.0 Hz, 1H), 3.88 (dd, *J* = 10.7, 7.2 Hz, 1H), 3.28–3.17 (m, 1H), 3.16–3.04 (m, 1H), 2.87–2.73 (m, 1H), 2.66 (ddd, *J* = 12.0, 7.9, 2.8 Hz, 1H), 2.58 (s, 1H), 2.44 (dd, *J* = 17.4, 10.1 Hz, 1H), 1.97 (dd, *J* = 12.2, 6.1 Hz, 1H), 1.74 (s, 3H), 1.67 (s, 3H).

^{13}C NMR (75 MHz, CDCl_3) δ 136.8, 133.8, 132.9, 120.9, 87.1, 73.1, 70.2, 61.7, 48.4, 43.3, 37.9, 32.3, 25.9, 18.2.

IR (neat) ν = 3300, 2933, 2857, 1444, 1211, 1118, 1074, 1021, 701, 653, 619 cm^{-1} .

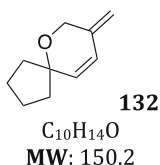
HRMS calculated for $[\text{C}_{14}\text{H}_{18}\text{NaO}]^+$: 225.1250, found: 225.1256.



Prepared according to **GP2**, colorless oil, 65 %. **^1H NMR (400 MHz, CDCl_3)** δ 3.94 (dd, J = 10.5, 2.0 Hz, 1H), 3.83 (dd, J = 10.5, 3.0 Hz, 1H), 2.12 (td, J = 6.1, 5.7, 2.8 Hz, 2H), 1.95–1.85 (m, 2H), 1.70–1.48 (m, 4H), 1.45–1.36 (m, 1H), 0.97 (td, J = 8.4, 4.3 Hz, 1H), 0.82 (td, J = 8.1, 4.0 Hz, 1H), 0.64 (q, J = 4.3 Hz, 1H).

^{13}C NMR (100 MHz, CDCl_3) δ 144.8, 110.4, 63.7, 28.6, 27.1, 23.2, 23.1, 16.1, 11.9, 10.8.

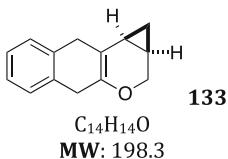
HRMS calculated for $[\text{C}_{10}\text{H}_{14}\text{NaO}]^+$: 173.0937, found: 173.0934.



Prepared according to **GP2**, colorless oil, 18 %. **^1H NMR (400 MHz, CDCl_3)** δ 6.22 (d, J = 10.0 Hz, 1H), 5.83 (d, J = 10.1 Hz, 1H), 4.93 (s, 1H), 4.79 (s, 1H), 4.21 (t, J = 2.3 Hz, 5H), 2.00–1.88 (m, 3H), 1.85–1.67 (m, 10H).

^{13}C NMR (101 MHz, CDCl_3) δ 145.6, 127.2, 127.1, 108.9, 84.8, 61.1, 53.6, 36.4, 36.4, 23.8.

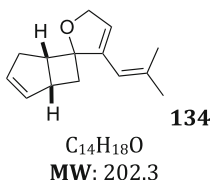
HRMS calculated for $[\text{C}_{10}\text{H}_{14}\text{NaO}]^+$: 173.0937, found: 173.0936.



Prepared according to **GPI**, colorless oil, 62 % (NMR yield using sulfolene as standard). **^1H NMR (400 MHz, CDCl_3)** δ 7.18–7.10 (m, 4H), 4.07 (dd, J = 10.5, 1.9 Hz, 1H), 3.96 (dd, J = 10.5, 3.0 Hz, 1H), 3.59 (td, J = 5.2, 2.5 Hz, 2H), 3.34 (qt, J = 20.4, 5.2 Hz, 2H), 1.57–1.45 (m, 1H), 1.16 (td, J = 8.2, 4.7 Hz, 1H), 0.94 (td, J = 8.0, 4.2 Hz, 1H), 0.76 (q, J = 4.4 Hz, 1H).

^{13}C NMR (100 MHz, CDCl_3) δ 142.1, 134.2, 133.8, 128.5, 128.1, 126.0, 125.9, 107.8, 63.9, 34.2, 31.8, 15.9, 12.3, 10.1.

HRMS calculated for $[C_{14}H_{14}NaO]^+$: 221.0937, found: 221.0938.

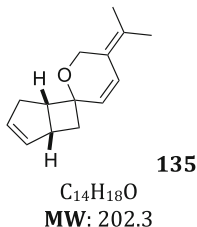


Prepared according to **GPI**, colorless oil, 58 % (dr > 25:1). **1H NMR** (400 MHz, $CDCl_3$) δ 6.47 (d, J = 10.3 Hz, 1H), 5.88–5.72 (m, 3H), 4.07 (s, 2H), 3.52 (t, J = 8.5 Hz, 1H), 3.31 (s, 1H), 2.98–2.85 (m, 1H), 2.51 (dd, J = 12.9, 8.5 Hz, 1H), 2.34 (dd, J = 17.2, 9.5 Hz, 1H), 2.13 (s, 3H), 2.01 (dd, J = 12.9, 4.3 Hz, 1H), 1.84 (s, 3H).

^{13}C NMR (100 MHz, $CDCl_3$) δ 133.5, 132.8, 132.7, 128.17, 124.8, 124.3, 77.8, 60.4, 46.9, 40.3, 39.7, 32.9, 22.9, 22.4.

IR (neat) ν = 2928, 1753, 1215, 1067, 959, 717 cm^{-1} .

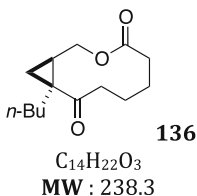
HRMS calculated for $[C_{14}H_{18}NaO]^+$: 225.1250, found: 225.1245.



Prepared according to **GPI**, colorless oil, 11 % (dr > 25:1). **1H NMR** (400 MHz, $CDCl_3$) δ 5.88–5.83 (m, 1H), 5.80 (dq, J = 4.7, 2.3 Hz, 1H), 5.76 (dd, J = 2.7, 1.4 Hz, 1H), 5.55 (s, 1H), 4.69 (d, J = 13.5 Hz, 1H), 4.60 (d, J = 13.5 Hz, 1H), 3.11–3.04 (m, 1H), 2.99–2.91 (m, 1H), 2.74 (ddt, J = 17.0, 5.2, 2.2 Hz, 1H), 2.61 (ddd, J = 13.1, 8.1, 1.5 Hz, 1H), 2.38 (ddq, J = 17.0, 9.3, 1.9 Hz, 1H), 1.95–1.88 (m, 1H), 1.92 (s, 3H), 1.85 (s, 3H).

^{13}C NMR (100 MHz, $CDCl_3$) δ 141.6, 140.1, 134.1, 132.2, 120.3, 116.0, 91.1, 75.3, 46.6, 41.8, 39.1, 33.6, 27.3, 20.4.

HRMS calculated for $[C_{14}H_{18}NaO]^+$: 225.1250, found: 225.1251.



- (i) To a solution of pyridinium chlorochromate (314 mg, 1.45 mmol, 4 equiv.) and celite (270 mg) in dichloromethane (3.5 mL) is added dropwise a solution of bicyclic enol ether **91** (75 mg, 0.36 mmol, 1 equiv.) in 0.5 mL of dichloromethane. The mixture is stirred at rt and the reaction progress is

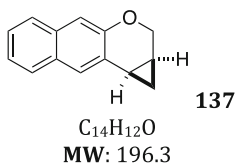
monitored by TLC. Once the starting material is totally consumed, the solution is filtered on a short pad of silica and the dark brown deposit is washed several times with ether. The filtrate is evaporated under reduced pressure and the resulting brown oil is purified by flash column chromatography (pentane/AcOEt 85:15) to afford ketolactone **136** as colorless oil in 58 % yield.

- (ii) To a solution of bicyclic enol ether **91** (81 mg, 0.39 mmol, 1 equiv.) and ruthenium dioxide (2.6 mg, 0.02 mmol, 0.05 equiv.) in a 1:1 mixture of carbon tetrachloride/water (8 mL) is added sodium periodate (334 mg, 1.56 mmol, 4 equiv.). The reaction is stirred at rt overnight, and then extracted 3 times with dichloromethane. The combined organic extracts are dried over magnesium sulfate, filtered and the solvent removed under reduced pressure. The crude product is purified by flash column chromatography (pentane/AcOEt 85:15) to afford ketolactone **136** as colorless oil in 59 % yield. ^1H NMR (400 MHz, CDCl_3) δ 4.48 (dd, $J = 11.7, 6.1$ Hz, 1H), 3.83 (dd, $J = 11.8, 6.4$ Hz, 1H), 2.83 (ddd, $J = 16.7, 10.0, 2.1$ Hz, 1H), 2.46–2.33 (m, 2H), 2.28 (td, $J = 8.4, 3.2$ Hz, 2H), 1.97–1.85 (m, 1H), 1.85–1.76 (m, 1H), 1.74–1.62 (m, 2H), 1.57–1.46 (m, 2H), 1.33–1.12 (m, 4H), 0.89–0.80 (m, 1H), 0.84 (t, $J = 6.9$ Hz, 3H), 0.75 (q, $J = 3.5$ Hz, 1H).

^{13}C NMR (100 MHz, CDCl_3) δ 209.4, 172.7, 63.3, 39.8, 36.6, 36.2, 34.8, 29.8, 28.4, 22.8, 22.8, 22.5, 18.4, 14.0.

IR (neat) $\nu = 2928, 2861, 1730, 1696, 1231, 1032\text{ cm}^{-1}$.

HRMS calculated for $[\text{C}_{14}\text{H}_{22}\text{NaO}_3]^+$: 261.1461, found: 261.1464.

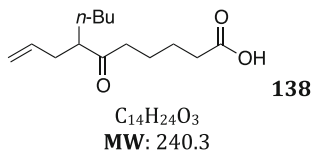


Prepared according to the same procedures than for **136** (i) 54 %, (ii) 82 % or (iii) Ozone is bubbled in a 0.1 M solution of **133** in a 4:1 mixture of dichloromethane/methanol at -78°C . When the solution becomes blue, ozone bubbling is removed and the solution is allowed to warm up to rt under a continuous flow of air. Once the mixture is decolorated, the solvent is removed and the crude oil is purified by flash column chromatography (pentane/AcOEt 85:15) to afford ketolactone **137** as a white solid in 22 % yield. ^1H NMR (400 MHz, CDCl_3) δ 7.74–7.63 (m, 2H), 7.68 (s, 1H), 7.39–7.28 (m, 2H), 7.19 (s, 1H), 4.41 (dd, $J = 10.5, 0.9$ Hz, 1H), 3.97 (dd, $J = 10.5, 1.5$ Hz, 1H), 2.21 (td, $J = 8.5, 4.4$ Hz, 1H), 1.80 (tdt, $J = 8.2, 5.4, 1.4$ Hz, 1H), 1.17 (q, $J = 5.2$ Hz, 1H), 1.14–1.06 (m, 1H).

^{13}C NMR (100 MHz, CDCl_3) δ 151.7, 132.7, 129.8, 128.9, 126.8, 126.6, 125.4, 124.2, 112.7, 63.4, 17.6, 13.6, 9.9, 1.2.

IR (neat) $\nu = 2924, 2855, 1744, 1455, 1268, 991, 917, 875, 747\text{ cm}^{-1}$.

HRMS calculated for $[C_{14}H_{12}NaO]^+$: 219.0780, found: 219.0783.

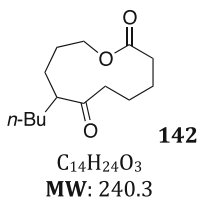


Samarium metal (242 mg) is recovered by THF (15 mL), and subsequently are added 416 mg (1.47 mmol) of diiodoethane. The solution is sonicated until it takes a dark blue color (about 1.5–2 h), then cooled down to 0 °C and anhydrous HMPA (dried over activated molecular sieve, 0.512 mL, 2.95 mmol, 6.68 equiv.) is added, followed by dropwise addition of a solution of cyclopropylketone **154** (105 mg, 0.44 mmol, 1 equiv.) in 10 mL of THF. The mixture is stirred at 0 °C for 45 min and quenched with a saturated aqueous solution of $NaHCO_3$. The aqueous layer is extracted twice with Et_2O , the combined organic extracts dried over $MgSO_4$, filtered and the solvent removed under reduced pressure. The crude product is purified by flash column chromatography (pentane/ $AcOEt$ 3:2) to afford acid **156** as yellow oil in 69 % yield. 1H NMR (300 MHz, $CDCl_3$) δ 9.67 (br s, 1H), 5.67 (ddt, $J = 17.1, 10.1, 7.0$ Hz, 1H), 5.06–4.91 (m, 2H), 2.52 (ddd, $J = 13.7, 7.9, 5.9$ Hz, 1H), 2.45–2.30 (m, 4H), 2.30–2.22 (m, 1H), 2.20–2.07 (m, 1H), 1.66–1.49 (m, 5H), 1.45–1.09 (m, 6H), 0.85 (t, $J = 7.1$ Hz, 3H).

^{13}C NMR (100 MHz, $CDCl_3$) δ 213.8, 179.6, 135.8, 116.8, 52.0, 42.2, 36.0, 34.0, 31.2, 29.6, 24.3, 22.9, 22.8, 14.0.

IR (neat) $\nu = 2932, 1707, 917\text{ cm}^{-1}$.

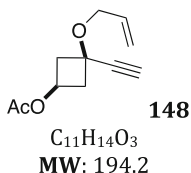
HRMS calculated for $[C_{14}H_{24}NaO_3]^+$: 263.1618, found: 263.1618.



A solution of cyclopropylketone **136** (40 mg, 0.17 mmol, 1 equiv.), Bu_3SnH (0.113 mL, 0.42 mmol, 2.5 equiv.) and AIBN (recrystallized from acetone, 28 mg, 0.17 mmol, 1 equiv.) in benzene (1.7 mL) is heated in a sealed tube for 5 h. The solution is evaporated under reduced pressure and the crude oil is purified by flash column chromatography (pentane/ $AcOEt$ 85:15) to afford ketolactone **142** as colorless oil in 65 % yield (73 % brsm). 1H NMR (300 MHz, $CDCl_3$) δ 4.24–4.13 (m, 1H), 4.02–3.90 (m, 1H), 2.61 (ddd, $J = 17.7, 10.3, 2.4$ Hz, 1H), 2.54–2.32 (m, 3H), 2.30–2.16 (m, 1H), 2.08–1.44 (m, 8H), 1.37–1.12 (m, 4H), 0.86 (t, $J = 6.8$ Hz, 3H).

^{13}C NMR (75 MHz, $CDCl_3$) δ 213.4, 173.6, 65.2, 52.1, 39.9, 34.3, 33.2, 29.7, 29.3, 25.9, 22.9, 22.9, 21.5, 14.0.

IR (neat) ν = 2932, 1730, 1246, 1171, 1041 cm^{-1} .



Over 4 h is added via a dropping funnel a solution of trichloroacetyl chloride (Aldrich, 12.3 mL, 20.0 g, 110 mmol) and phosphorus oxychloride (1.0 mL, 1.69 g, 11 mmol, 0.1 equiv.) in anhydrous methyl acetate (100 mL) to a suspension of zinc dust (14.2 g, 220 mmol, 2 equiv.), copper powder (7.0 g, 110 mmol, 1 equiv.) and vinyl acetate (50 mL, 47.4 g, 550 mmol, 5 equiv.) in anhydrous methyl acetate (100 mL) at rt. The mixture was stirred for 12 h after addition was completed. Zinc dust (14.2 g, 220 mmol, 2 equiv.) was then added and the mixture was cooled to 0–5 °C. Acetic acid (45 mL) was added dropwise at a rate to keep the internal temperature <10 °C. After addition was complete, the mixture was stirred for 3 h at rt, concentrated to remove ca. 90 % of the methyl acetate, and stirred for 12 h at rt. The mixture was then diluted with heptane (40 mL) and methyl acetate (40 mL), and filtered to remove the solids. The solids were washed with methyl acetate (2 × 20 mL) and the yellow/brown filtrate was quenched with a 10 % aqueous solution of NaHCO_3 . The organic layer is washed with brine and water, dried over MgSO_4 , filtered and the solvent removed under reduced pressure. The crude product is purified by flash column chromatography (pentane/ AcOEt 85:15) to afford 3-acetoxycyclobutanone as a yellow oil, 13 % yield.

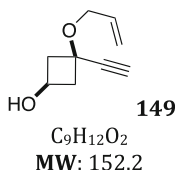
Alkynylation of 3-acetoxycyclobutanone with trimethylsilyl acetylene was realized identically as reported in the synthesis of enynes **125–127** (47 % yield). To a solution of the resulting alcohol (547 mg, 2.42 mmol, 1 equiv.) in DMSO (5 mL) is added KF (561 mg, 9.68 mmol, 4 equiv.) and few drops of water. The reaction mixture is stirred at rt for 1 h, then diluted with 5 mL of water and 10 mL of Et_2O . The aqueous layer is extracted twice with Et_2O (15 mL), and the combined organic extracts are washed with brine and water, dried over MgSO_4 , filtered and the solvent removed under reduced pressure to afford 3-acetoxy-1-ethynylcyclobutanol as a yellow oil (290 mg, 78 %).

To a solution of NaH (68 mg, 2.83 mmol, 1.5 equiv.), NaI (28 mg, 0.19 mmol, 0.1 equiv.) and allyl bromide (0.65 mL, 7.52 mmol, 4 equiv.) in DMF (5 mL) is added at 0 °C *via* a canula a solution of 3-acetoxy-1-ethynylcyclobutanol (290 mg, 1.88 mmol, 1 equiv.) in DMF (5 mL). The resulting solution is stirred at rt for 18 h, then quenched with water (2 mL). The aqueous layer is extracted with Et_2O (3 × 5 mL), and the combined organic extracts are washed with water and brine, dried over MgSO_4 , filtered and the solvent removed under reduced pressure. The crude product is purified by flash column chromatography (pentane/ Et_2O 8:2) to afford enyne **148** in pure form as a colorless oil in 63 % yield (dr > 25:1). ^1H NMR (400 MHz, CDCl_3) δ 5.94 (ddt, J = 17.0, 11.2, 5.7 Hz, 1H), 5.38–5.29

(m, 1H), 5.19 (d, $J = 10.4$ Hz, 1H), 4.93 (p, $J = 7.3$ Hz, 1H), 4.04–4.02 (m, 2H), 2.91 (ddd, $J = 10.0, 7.1, 2.9$ Hz, 2H), 2.54 (s, 1H), 2.35 (ddd, $J = 10.4, 7.7, 2.8$ Hz, 2H), 2.04 (s, 3H).

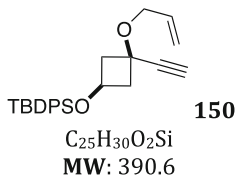
^{13}C NMR (100 MHz, CDCl_3) δ 170.6, 134.5, 117.5, 84.3, 74.0, 66.2, 65.8, 61.6, 44.4, 21.0.

HRMS calculated for $[\text{C}_{11}\text{H}_{14}\text{NaO}_3]^+$: 217.0835, found: 217.0839.



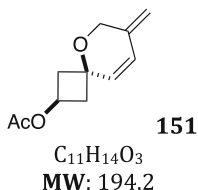
Prepared from enyne **148** through the same procedure than for the synthesis of **59** and **60**. Colorless oil, quantitative yield. ^1H NMR (400 MHz, CDCl_3) δ 5.95 (ddt, $J = 17.1, 10.4, 5.7$ Hz, 1H), 5.32 (dq, $J = 17.2, 1.6$ Hz, 1H), 5.18 (dq, $J = 10.4, 1.3$ Hz, 1H), 4.32–4.19 (m, 1H), 4.02 (dt, $J = 5.7, 1.4$ Hz, 2H), 2.89–2.78 (m, 2H), 2.50 (s, 1H), 2.27–2.16 (m, 2H), 1.84 (d, $J = 5.7$ Hz, 1H).

^{13}C NMR (100 MHz, CDCl_3) δ 134.6, 117.3, 84.9, 73.4, 66.1, 66.0, 60.1, 47.3 (2C).



To a solution of alcohol **149** (157 mg, 1.03 mmol, 1 equiv.) in DMF are added imidazole (84 mg, 1.24 mmol, 1.2 equiv.) and *tert*-butyldiphenylsilyl chloride (340 mg, 1.24 mmol, 1.2 equiv.). The reaction mixture is stirred at rt overnight then quenched with water. The aqueous layer is extracted three times with diethyl ether, and the combined organic extracts are washed with water and brine, dried over MgSO_4 and filtered. The solvent is removed under reduced pressure and the silyl ether is obtained spectroscopically pure in 98 % yield as colorless oil. ^1H NMR (400 MHz, CDCl_3) δ 7.66–7.62 (m, 3H), 7.46–7.35 (m, 7H), 5.95 (ddt, $J = 17.2, 10.4, 5.7$ Hz, 1H), 5.32 (dq, $J = 17.2, 1.6$ Hz, 1H), 5.18 (dq, $J = 10.4, 1.3$ Hz, 1H), 4.26–4.15 (m, 1H), 3.98 (dt, $J = 5.7, 1.4$ Hz, 2H), 2.65 (ddd, $J = 11.7, 6.0, 2.6$ Hz, 2H), 2.37 (s, 1H), 2.36–2.30 (m, 2H), 1.07 (s, 3H), 1.03 (s, 6H).

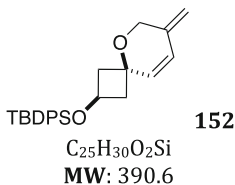
^{13}C NMR (100 MHz, CDCl_3) δ 135.6 (4C), 135.3, 135.0, 134.7, 134.0, 129.8, 127.9, 127.8 (4C), 117.3, 85.2, 73.2, 66.1, 64.9, 60.5, 47.5, 26.8 (2C), 26.7, 19.1 (3C).



Prepared according to **GPI**, colorless oil, 53 % (dr > 25:1). ^1H NMR (400 MHz, CDCl_3) δ 6.21–6.14 (m, 1H), 5.88–5.80 (m, 1H), 5.03 (s, 1H), 4.90–4.81 (m, 2H), 4.23 (td, J = 2.1, 1.1 Hz, 2H), 2.76–2.67 (m, 2H), 2.35–2.26 (m, 2H), 2.05 (s, 3H).

^{13}C NMR (100 MHz, CDCl_3) δ 170.8, 144.2, 127.8, 125.9, 108.9, 71.2, 61.8, 61.4, 41.0 (2C), 21.1.

HRMS calculated for $[\text{C}_{11}\text{H}_{14}\text{NaO}_3]^+$: 217.0835, found: 217.0834.

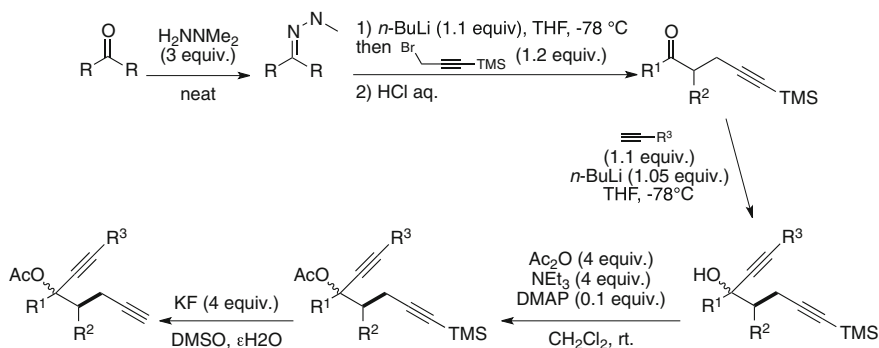


Prepared according to **GPI**, colorless oil, 40 %. ^1H NMR (400 MHz, CDCl_3) δ 7.69–7.62 (m, 4H), 7.47–7.33 (m, 6H), 6.12–6.04 (m, 1H), 5.85–5.77 (m, 1H), 4.66 (d, J = 5.8 Hz, 2H), 4.23–4.21 (m, 2H), 4.10 (p, J = 7.1 Hz, 1H), 2.51–2.43 (m, 2H), 2.36–2.26 (m, 2H), 1.03 (s, 9H).

^{13}C NMR (101 MHz, CDCl_3) δ 144.8 (2C), 135.6 (4C), 134.2, 129.8 (2C), 127.9, 127.8 (4C), 125.9, 108.4, 70.1, 61.4, 60.7, 44.1 (2C), 26.7, 19.1 (3C).

HRMS calculated for $[\text{C}_{25}\text{H}_{30}\text{NaO}_2\text{Si}]^+$: 413.1907, found: 413.1910.

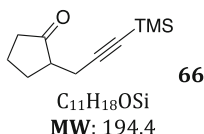
Experimental Section Related to Chap. 3



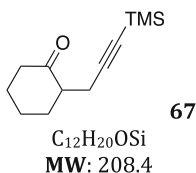
N,N-dimethylhydrazine (1.15 mL, 15 mmol, 3 equiv.) was added to the ketone (5 mmol, 1 eq) at rt. The reaction mixture was stirred overnight, quenched with saturated NH_4Cl , and extracted with diethyl ether. The combined organic extracts were washed with brine, dried over magnesium sulfate and filtered. The solvent was removed by rotary evaporation. The residue was engaged in the next step without further purification.

Hydrazone (5 mmol, 1 equiv.) was diluted in 5 mL of THF under argon. Then, *n*-butyllithium (2.4 mL, 5.5 mmol, 1.1 equiv, 2.3 M in hexane) was added to the

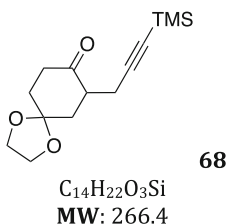
solution at $-78\text{ }^{\circ}\text{C}$. The mixture was stirred at this temperature for 1 h. The bromide (1.25 g, 6 mmol, 1.2 equiv.) was added to the solution, which was allowed to stir at rt overnight. The reaction mixture was quenched with 2 M aqueous HCl and stirred for 2 h, then extracted with diethyl ether. The combined organic extracts were washed with brine, dried over magnesium sulfate and filtered. The solvent was removed by rotary evaporation. The crude ketone was engaged in the next step without further purification.



Yellow oil, 88 %. ^1H NMR (300 MHz, CDCl_3) δ 2.59 (d, $J = 16.3$ Hz, 2H), 2.34 (d, $J = 17.0$ Hz, 4H), 2.06 (s, 2H), 1.79 (s, 1H), 0.13 (s, 9H).



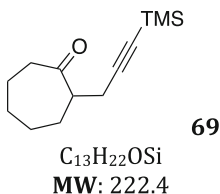
Yellow oil, 88 %. ^1H NMR (300 MHz, CDCl_3) δ 2.68 (dd, $J = 17.2, 4.0$ Hz, 1H), 2.55–2.37 (m, 3H), 2.32 (dd, $J = 13.1, 5.5$ Hz, 1H), 2.20 (dd, $J = 17.2, 9.0$ Hz, 1H), 2.14–2.04 (m, 1H), 1.98–1.81 (m, 1H), 1.80–1.58 (m, 2H), 1.48–1.28 (m, 1H), 0.14 (s, 9H).



Brown solid, 91 %. ^1H NMR (300 MHz, CDCl_3) δ 4.17–3.88 (m, 4H), 2.90–2.49 (m, 3H), 2.48–2.16 (m, 3H), 2.16–1.89 (m, 2H), 1.89–1.61 (m, 1H), 0.11 (s, 9H).

^{13}C NMR (75 MHz, CDCl_3) δ 209.3, 107.4, 104.7, 86.4, 64.9, 64.7, 45.6, 39.5, 38.1, 34.7, 19.9, 0.2 (3C).

IR (neat) $\nu = 2958, 2175, 1715, 1250, 1051, 840, 760, 643\text{ cm}^{-1}$.



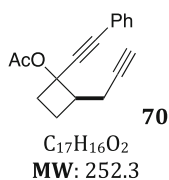
Yellow oil, 95 %. ^1H NMR (300 MHz, CDCl_3) δ 2.78–2.64 (m, 1H), 2.61–2.38 (m, 3H), 2.30 (dd, $J = 17.1, 8.7$ Hz, 1H), 2.08–1.95 (m, 1H), 1.96–1.76 (m, 3H), 1.75–1.58 (m, 1H), 1.52–1.25 (m, 3H), 0.14 (s, 9H).

To a stirred solution of alkyne (2.2 mmol, 1.1 equiv.) in 22 mL of THF under argon at -78°C was added dropwise *n*-butyllithium (1.2 mL, 2.8 mmol, 1.4 eq, 2.4 M in hexane). After 1 h, the ketone (2 mmol, 1 equiv.) was added to the solution. The reaction was allowed to warm up to RT and stirred for 2 h. The reaction mixture was quenched with saturated NH_4Cl and extracted with diethyl ether. The combined organic extracts were washed with brine, dried over magnesium sulfate and filtered. The solvent was removed by rotary evaporation. The crude propargyl alcohol was engaged in the next step without further purification.

To a stirred solution of alcohol (1 mmol, 1.0 equiv.), Et_3N (0.53 mL, 4 mmol, 4 equiv.) and 4-DMAP (12 mg, 0.1 mmol, 0.1 equiv.) in CH_2Cl_2 (10 mL) was added acetic anhydride (0.38 mL, 4 mmol, 4 equiv.) at 0°C . The solution was then allowed to warm to rt and was stirred further until completion (3–4 h at rt). The reaction was quenched with aqueous saturated NH_4Cl solution and the resulting aqueous layer was extracted with CH_2Cl_2 . The combined organic layers were washed with brine, dried over anhydrous MgSO_4 , filtered and evaporated to give crude acetate as oil. Purification was achieved by flash column chromatography on silica gel (PE/ Et_2O gradient).

To a solution of the silylated alkyne in DMSO (0.5 M) are added few drops of water and potassium fluoride (4 equiv.). The reaction is stirred at rt during 2–4 h and then diluted in diethyl ether. The resulting mixture is washed twice with water and dried over MgSO_4 . The solvent is evaporated under reduced pressure and the crude product purified by flash column chromatography over silica gel using gradient mixtures of pentane and diethyl ether.

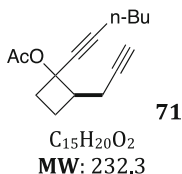
Products **70–84** were obtained as mixture of diastereomers (dr assessed by ^1H NMR) in 36–56 % overall yield.



Colorless oil (75:25 mixture of diastereomers). ^1H NMR (400 MHz, CDCl_3) δ 7.51–7.41 (m, 2H), 7.38–7.27 (m, 3H), 2.84–2.71 (m, 1H), 2.69–2.51 (m, 2H), 2.39–2.26 (m, 1H), 2.23–2.09 (m, 2H), 2.06 (s, 3H), 1.98–1.92 (m, 1H), 1.78–1.62 (m, 1H).

^{13}C NMR (100 MHz, CDCl_3) δ 169.1, 132.0, 128.7 (2C), 128.3 (2C), 122.3, 87.7, 85.8, 82.1, 75.1, 69.0, 45.3, 34.0, 21.4, 21.2, 20.4.

HRMS calculated for $[C_{17}H_{16}NaO_2]^+$: 275.1043, found: 275.1040.

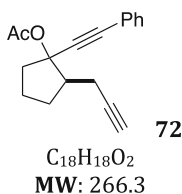


Colorless oil (75:25 mixture of diastereomers). **1H NMR (400 MHz, $CDCl_3$)** δ 2.74–2.55 (m, 1H), 2.54–2.33 (m, 2H), 2.31–2.14 (m, 3H), 2.13–1.98 (m, 1H), 2.02 (s, 3H), 1.95–1.89 (m, 1H), 1.65–1.54 (m, 1H), 1.55–1.45 (m, 2H), 1.46–1.34 (m, 2H), 0.91 (t, J = 7.2 Hz, 3H).

^{13}C NMR (100 MHz, $CDCl_3$) δ 169.4, 88.8, 82.5, 75.2, 73.2, 72.9, 68.7, 45.1, 34.3, 30.8, 22.1, 21.5, 21.1, 18.7, 13.8.

IR (neat) ν = 3293, 2956, 1743, 1368, 1226, 1089, 1030, 630 cm^{-1} .

HRMS calculated for $[C_{15}H_{20}NaO_2]^+$: 255.1356, found: 255.1360.

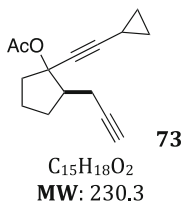


Yellow solid (87:13 mixture of diastereomers), mp = 64 °C. **1H NMR (400 MHz, $CDCl_3$)** δ 7.44–7.42 (m, 2H), 7.31–7.29 (m, 3H), 2.75 (ddd, J = 16.2, 3.8, 2.7 Hz, 1H), 2.53 (ddd, J = 13.6, 8.4, 6.7 Hz, 1H), 2.48–2.41 (m, 1H), 2.36 (ddd, J = 16.2, 10.3, 2.6 Hz, 1H), 2.21–2.07 (m, 2H), 2.06 (s, 3H), 1.96 (t, J = 2.6 Hz, 1H), 1.88–1.70 (m, 2H), 1.60 (m, 1H).

^{13}C NMR (100 MHz, $CDCl_3$) δ 169.4 (C), 131.8 (CH), 128.5 (CH), 128.2 (CH), 122.5 (C), 87.7 (C), 86.4 (C), 83.2 (CH), 82.9 (C), 68.9 (CH), 48.9 (CH), 39.6 (CH₂), 28.4 (CH₂), 21.7 (CH₃), 21.3 (CH₂), 20.8 (CH₂).

IR (neat) ν = 633, 690, 756, 1014, 1232, 1366, 1740, 2230, 2874, 2958, 3295.

HRMS calculated for $[C_{18}H_{18}O_2Na]^+$: 289.1199, found: 289.1198.

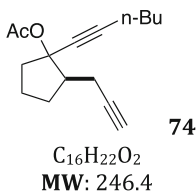


White solid (80:20 mixture of diastereomers), mp = 45 °C. **1H NMR (400 MHz, $CDCl_3$)** δ 2.61 (ddd, J = 16.4, 4.1, 2.7 Hz, 1H), 2.41–2.25 (m, 2H), 2.24–2.14 (m, 1H), 2.11–1.98 (m, 2H), 2.00 (s, 3H), 1.93 (t, J = 2.7 Hz, 1H), 1.80–1.62 (m, 2H), 1.53–1.43 (m, 1H), 1.31–1.21 (m, 1H), 0.76 (ddd, J = 7.2, 6.5, 3.8 Hz, 2H), 0.69–0.64 (m, 2H).

^{13}C NMR (100 MHz, CDCl_3) δ 169.6 (C), 91.9 (C), 83.6 (C), 83.0 (C), 72.4 (C), 68.7 (CH), 48.9 (CH), 39.6 (CH_2), 21.9 (CH_3), 21.3 (CH_2), 20.8 (CH_2), 8.7 (CH_2), 8.6 (CH_2), 0.29 (CH).

IR (neat) ν = 697, 1021, 1244, 1371, 1723, 2232, 2342, 2360, 2874, 2966, 3007, 3243.

HRMS calculated for $[\text{C}_{15}\text{H}_{18}\text{O}_2\text{Na}]^+$: 253.1199, found: 253.1202.

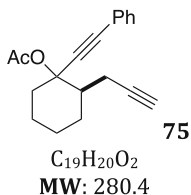


Orange oil (87:13 mixture of diastereomers). **^1H NMR (400 MHz, CDCl_3)** δ 2.64 (ddd, J = 16.0, 3.7, 2.6 Hz, 1H), 2.40 (ddd, J = 13.8, 8.4, 6.6 Hz, 1H), 2.36–2.18 (m, 4H), 2.10–1.98 (m, 2H), 2.01 (s, 3H), 1.94 (t, J = 2.6 Hz, 1H), 1.81–1.64 (m, 2H), 1.57–1.34 (m, 5H), 0.90 (t, J = 7.3 Hz, 3H).

^{13}C NMR (100 MHz, CDCl_3) δ 169.7 (C), 88.7 (C), 83.7 (C), 83.1 (C), 77.3 (C), 68.6 (CH), 48.8 (CH), 39.6 (CH_2), 30.9 (CH_2), 28.3 (CH_2), 22.1 (CH_2), 21.9 (CH_2), 21.2 (CH_2), 20.8 (CH_2), 18.6 (CH_3), 13.7 (CH_3), one carbone missed due to overlapping.

IR (neat) ν = 628, 1012, 1038, 1229, 1366, 1742, 2119, 2873, 2933, 2957, 3292.

HRMS calculated for $[\text{C}_{16}\text{H}_{22}\text{O}_2\text{Na}]^+$: 269.1512, found: 269.1517.

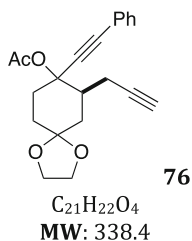


Colorless oil (67:33 mixture of diastereomers). **^1H NMR (400 MHz, CDCl_3)** δ 7.44 (dt, J = 8.0, 3.5 Hz, 2H), 7.33–7.27 (m, 3H), 2.96–2.84 (m, 1H), 2.76 (dt, J = 16.7, 3.1 Hz, 1H), 2.33–2.12 (m, 2 H), 2.07 (s, 1H), 2.05 (s, 2H), 1.98 (t, J = 2.6 Hz, 1H), 1.80–1.55 (m, 4H), 1.52–1.29 (m, 3H).

^{13}C NMR (100 MHz, CDCl_3) δ 169.2 (C), 132.0 (CH), {128.7 (CH), 128.6 (CH)}, {128.4 (CH), 128.3 (CH)}, {122.7 (C), 122.6 (C)}, 89.1 (C), 85.5 (C), 83.6 (CH), 79.9 (C), {69.3 (C), 69.2 (C)}, {46.2 (CH), 46.1 (CH)}, {36.4 (CH_2), 34.9 (CH_2)}, {28.5 (CH_2), 26.2 (CH_2)}, {25.2 (CH_2), 24.7 (CH_2)}, {23.8 (CH_2), 21.3 (CH_2)}, {22.2 (CH_3), 21.9 (CH_3)}, {20.4 (CH_2), 20.3 (CH_2)}.

IR (neat) ν = 690, 756, 1015, 1223, 1366, 1443, 1490, 1740, 2118, 2859, 2933, 3294.

HRMS calculated for $[\text{C}_{19}\text{H}_{20}\text{O}_2\text{Na}]^+$: 303.1356, found: 303.1358.

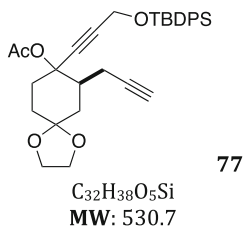


Pale yellow solid (85:15 mixture of diastereomers), mp = 81 °C. **^1H NMR** (400 MHz, CDCl_3) δ 7.46–7.42 (m, 2H), 7.32–7.28 (m, 3H), 4.03–3.93 (m, 4H), 2.90 (td, J = 12.8, 3.7 Hz, 1H), 2.76 (td, J = 16.4, 2.7 Hz, 1H), 2.39–2.23 (m, 2H), 2.17 (td, J = 14.2, 3.2 Hz, 1H), 2.06 (s, 3H), 1.99 (t, J = 2.8 Hz, 1H), 1.97–1.83 (m, 1H), 1.82–1.70 (m, 2H), 1.62–1.51 (m, 1H).

^{13}C NMR (100 MHz, CDCl_3) δ 169.1 (C), 131.9 (CH), 128.7 (CH), 128.2 (CH), 122.1 (C), 107.4 (C), 89.0 (C), 84.2 (C), 82.6 (C), 78.2 (C), 69.6 (CH), 64.6 (CH_2), 64.3 (CH_2), 43.6 (CH), 36.5 (CH_2), 33.0 (CH_2), 32.2 (CH_2), 21.9 (CH_3), 20.0 (CH_2).

IR (neat) ν = 918, 1221, 1364, 1444, 1491, 1741, 2117, 2227, 2892, 2954, 3253 cm^{-1} .

HRMS calculated for $[\text{C}_{21}\text{H}_{22}\text{O}_4\text{Na}]^+$: 361.1410, found: 361.1413.

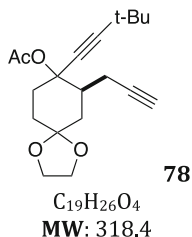


Pale yellow oil (96:4 mixture of diastereomers). **^1H NMR** (400 MHz, CDCl_3) δ 7.73–7.68 (m, 4H), 7.46–7.38 (m, 6H), 4.41 (s, 2H), 4.01–3.91 (m, 4H), 2.80–2.75 (m, 1H), 2.63 (td, J = 17.1, 3.2 Hz, 1H), 2.29–2.21 (m, 1H), 2.17–2.06 (m, 2H), 2.01 (s, 3H), 1.98 (t, J = 2.5 Hz, 1 H), 1.86–1.58 (m, 4 H), 1.06 (s, 9 H).

^{13}C NMR (100 MHz, CDCl_3) δ 169.0 (C), 135.6 (CH), 133.1 (C), 133.0 (C), 129.9 (CH), 127.8 (CH), 107.4 (C), 87.5 (C), 82.7 (C), 80.0 (C), 77.8 (C), 69.5 (CH), 64.5 (CH_2), 64.3 (CH_2), 43.4 (CH), 36.2 (CH_2), 32.8 (CH_2), 32.0 (CH_2), 26.7 (CH_3), 21.9 (CH_3), 19.8 (CH_2), 19.2 (CH_2).

IR (neat) ν = 1111, 1280, 1428, 1472, 1744, 2120, 2859, 2888, 2932, 2958, 3052, 3304 cm^{-1} .

HRMS calculated for $[\text{C}_{32}\text{H}_{38}\text{O}_5\text{SiNa}]^+$: 553.2386, found: 553.2385.

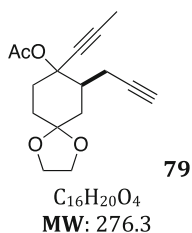


White solid (dr > 25:1), mp = 73 °C. **^1H NMR (400 MHz, CDCl_3)** δ 3.99–3.88 (m, 4H), 2.76–2.69 (m, 1H), 2.63 (dt, J = 17.1, 2.9 Hz, 1H), 2.27–2.16 (m, 1H), 2.15–2.03 (m, 2H), 1.99 (s, 3H), 1.96 (t, J = 2.5 Hz, 1H), 1.88–1.65 (m, 3H), 1.58 (t, J = 22.5 Hz, 1H), 1.20 (s, 9H).

^{13}C NMR (100 MHz, CDCl_3) δ 168.9 (C), 107.5 (C), 98.1 (C), 82.8 (C), 78.0 (C), 73.6 (C), 69.4 (CH), 64.5 (CH_2), 64.2 (CH_2), 43.4 (CH), 36.5 (CH_2), 33.0 (CH_2), 32.2 (CH_2), 30.8 (CH_3), 27.5 (C), 22.0 (CH_3), 19.8 (CH_2).

IR (neat) ν = 931, 1018, 1108, 1228, 1366, 2120, 2230, 2870, 2964, 3262 cm^{-1} .

HRMS calculated for $[\text{C}_{19}\text{H}_{26}\text{O}_4\text{Na}]^+$: 341.1723, found: 341.1724.

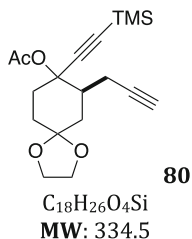


White solid (83:17 mixture of diastereomers), mp = 119 °C. **^1H NMR (400 MHz, CDCl_3)** δ 4.00–3.92 (m, 4H), 2.78–2.74 (m, 1H), 2.69–2.63 (m, 1H), 2.27–2.07 (m, 3H), 2.02 (s, 3H), 1.97 (t, J = 2.5 Hz, 1H), 1.88 (s, 3H), 1.80–1.52 (m, 4H).

^{13}C NMR (100 MHz, CDCl_3) δ 169.3 (C), 107.5 (C), 85.3 (C), 82.7 (C), 78.3 (C), 74.2 (C), 69.4 (CH), 64.5 (CH_2), 64.3 (CH_2), 43.5 (CH), 36.3 (CH_2), 32.9 (CH_2), 32.1 (CH_2), 22.0 (CH_3), 19.8 (CH_2), 3.7 (CH_3).

IR (neat) ν = 985, 1046, 1230, 1370, 1440, 1743, 2117, 2240, 2889, 2937, 2962, 3272 cm^{-1} .

HRMS calculated for $[\text{C}_{16}\text{H}_{20}\text{O}_4\text{Na}]^+$: 299.1254, found: 299.1251.

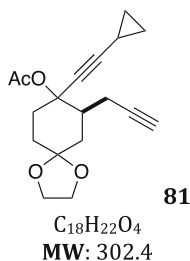


White solid (81:19 mixture of diastereomers), mp = 79 °C. **¹H NMR** (400 MHz, CDCl₃) δ 3.99–3.91 (m, 4H), 2.80–2.75 (m, 1H), 2.70–2.64 (m, 1H), 2.28–2.21 (m, 1H), 2.19–2.09 (m, 2H), 2.02 (s, 3H), 1.97 (t, *J* = 2.6 Hz, 1H), 1.90–1.85 (m, 1H), 1.81–1.55 (m, 3H), 0.17 (s, 9H).

¹³C NMR (100 MHz, CDCl₃) δ 169.3 (C), 107.4 (C), 94.4 (C), 82.5 (C), 77.9 (C), 76.7 (C), 69.4 (CH), 64.5 (CH₂), 64.3 (CH₂), 43.2 (CH), 36.4 (CH₂), 32.7 (CH₂), 32.1 (CH₂), 21.9 (CH₃), 19.8 (CH₂), 0.1 (CH₃).

IR (neat) ν = 843, 1250, 1369, 1740, 2119, 2168, 2874, 2892, 2957, 3256 cm⁻¹.

HRMS calculated for [C₁₈H₂₆O₄SiNa]⁺: 357.1492, found: 357.1489.

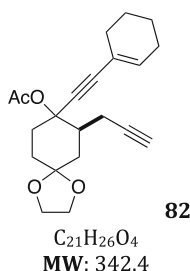


Pale yellow oil (94:6 mixture of diastereomers). **¹H NMR** (400 MHz, CDCl₃) δ 3.99–3.88 (m, 4H), 2.75–2.54 (m, 2H), 2.17–1.99 (m, 3H), 1.97–1.89 (m, 4H), 1.86–1.75 (m, 1H), 1.72–1.49 (m, 3H), 1.25–1.18 (m, 1H), 0.76–0.69 (m, 2H), 0.65–0.59 (m, 2H).

¹³C NMR (100 MHz, CDCl₃) δ 169.1 (C), 107.4 (C), 93.0 (C), 82.7 (C), 78.1 (C), 70.1 (C), 69.5 (CH), 64.5 (CH₂), 64.2 (CH₂), 43.4 (CH), 36.4 (CH₂), 33.0 (CH₂), 32.1 (CH₂), 21.9 (CH₃), 19.8 (CH₂), 8.6 (CH₂), 8.5 (CH₂), 0.5 (CH).

IR (neat) ν = 934, 1230, 1366, 1430, 1742, 2117, 2240, 2881, 2956, 3272 cm⁻¹.

HRMS calculated for [C₁₈H₂₂O₄Na]⁺: 325.1410, found: 325.1406.



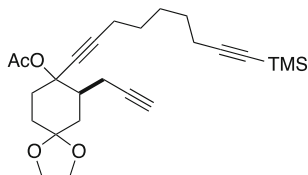
Yellow oil (93:7 mixture of diastereomers). **¹H NMR** (400 MHz, CDCl₃) δ 6.13–6.10 (m, 1H), 4.00–3.85 (m, 4H), 2.81–2.77 (m, 1H), 2.70–2.65 (m, 1H), 2.31–2.05 (m, 7H), 2.01 (s, 3H), 1.97 (t, *J* = 2.3 Hz, 1H), 1.91–1.64 (m, 3H), 1.62–1.51 (m, 5H).

¹³C NMR (100 MHz, CDCl₃) δ 169.1 (C), 136.0 (CH), 130.0 (C), 107.5 (C), 90.9 (C), 82.8 (C), 81.3 (C), 78.4 (C), 69.4 (CH), 64.5 (CH₂), 64.3 (CH₂), 43.5

(CH), 36.4 (CH₂), 33.0 (CH₂), 32.1 (CH₂), 29.1 (CH₂), 25.6 (CH₂), 22.2 (CH₃), 21.9 (CH₂), 21.4 (CH₂), 19.9 (CH₂).

IR (neat) ν = 935, 1111, 1230, 1365, 1645, 1740, 2117, 2885, 2954, 3260 cm⁻¹.

HRMS calculated for [C₂₁H₂₆O₄Na]⁺: 365.1725, found: 365.1728.



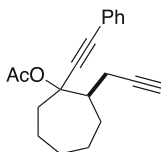
83

C₂₅H₃₆O₄Si

MW: 428.6

Pale yellow oil (97:3 mixture of diastereomers). **¹H NMR** (400 MHz, CDCl₃) δ 3.95–3.89 (m, 4H), 2.78–2.69 (1H), 2.66–2.59 (m, 1H), 2.26–2.04 (m, 7H), 2.01–1.93 (m, 4H), 1.90–1.59 (m, 4H), 1.58–1.43 (m, 6H), 0.10 (s, 9H). **¹³C NMR** (CDCl₃) δ 169.0 (C), 107.4 (C), 89.6 (C), 84.4 (C), 82.7 (C), 78.2 (C), 77.5 (C), 75.2 (C), 69.4 (CH), 64.5 (CH₂), 64.2 (CH₂), 43.4 (CH), 36.4 (CH₂), 33.0 (CH₂), 28.2 (CH₂), 28.1 (CH₂), 28.0 (CH₂), 21.9 (CH₃), 19.8 (CH₂), 19.7 (CH₂), 18.6 (CH₂), 0.1 (CH₃), one carbon missed due to overlapping. **IR** (neat) ν = 840, 1230, 1367, 1745, 2119, 2172, 2238, 2936, 3282 cm⁻¹.

HRMS calculated for [C₂₅H₃₆O₄SiNa]⁺: 451.2275, found: 451.2270.



84

C₂₀H₂₂O₂

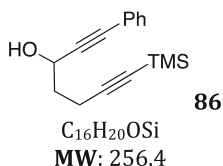
MW: 294.4

Pale yellow oil (8:2 mixture of diastereomers). **¹H NMR** (400 MHz, CDCl₃) δ 7.46–7.41 (m, 2H), 7.31–7.26 (m, 3H), 2.85–2.79 (m, 0.5H), 2.65–2.57 (m, 0.5H), 2.38–2.06 (m, 3H), 2.05 (s, 2H), 2.04 (s, 2H), 2.00–1.96 (m, 1H), 1.90–1.72 (m, 2H), 1.70–1.52 (m, 4H), 1.51–1.39 (m, 2H).

¹³C NMR (100 MHz, CDCl₃) δ 169.0 (C), {131.9 (CH), 131.8 (CH)}, 128.4 (CH), {128.2 (CH), 128.1 (CH)}, 122.6 (C), {90.3 (C), 89.9 (C)}, {85.4 (C), 85.3 (C)}, 84.2 (C), {79.9 (C), 79.3 (C)}, 68.8 (CH), 50.4 (CH), 40.3 (CH₂), 38.1 (CH₂), {28.6 (CH₂), 28.3 (CH₂)}, {27.4 (CH₂), 26.9 (CH₂)}, 22.4 (CH₂), {22.2 (CH₃), 21.8 (CH₃)}, {21.6 (CH₂), 21.4 (CH₂)}.

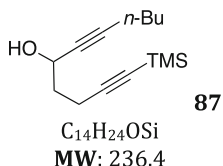
IR (neat) ν = 896, 1264, 1421, 1737, 2227, 2860, 2933, 2987, 3054, 3302 cm⁻¹.

HRMS calculated for $[\text{C}_{20}\text{H}_{22}\text{O}_2\text{Na}]^+$: 317.1512, found: 317.1508.

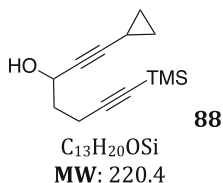


To a solution of 4-pentynol (5.9 g, 70 mmol, 1 equiv.) in THF (100 mL) is added dropwise at -78°C *n*-butyllithium (2.5 M in hexanes, 60 mL, 147 mmol, 2.1 equiv.). The mixture is slowly allowed to warm to rt, then cooled down again to -78°C . Freshly distilled TMSCl (20 mL, 154 mmol, 2.2 equiv.) is added dropwise to the mixture, which is then allowed to warm to rt and stirred for 2 h. The mixture is then quenched with a 3 M HCl aqueous solution, and the resulting biphasic system is vigorously stirred for 3 h. The aqueous layer is extracted twice with Et_2O , and the combined organic extracts are washed with brine, dried over anhydrous MgSO_4 , filtered and evaporated to give 5-trimethylsilyl-4-pentynol in pure form in quantitative yield.

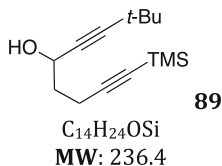
5-Trimethylsilyl-4-pentynol (4 g, 25.6 mmol, 1 equiv.) is added dropwise at rt to a suspension of PCC (8.3 g, 38.4 mmol, 1.5 equiv.) in CH_2Cl_2 (60 mL). The reaction mixture is stirred at rt for 2 h, then diluted with Et_2O and filtered over silica/celite. The solids are washed several times with Et_2O , and the filtrate is concentrated under reduced pressure. Purification by flash column chromatography over silica gel using a 8:2 mixture of pentane/ Et_2O afforded pure 5-trimethylsilyl-4-pentynal in 68 % yield over two steps. Alkynylation of the aldehyde was realized with phenyl acetylene according to the same procedure than for the synthesis of precursors **70–84**. Yellow oil, 88 %. ^1H NMR (400 MHz, CDCl_3) δ 7.37–7.29 (m, 5H), 4.76 (q, $J = 6.2$ Hz, 1H), 2.59–2.41 (m, 2H), 2.13 (d, $J = 5.7$ Hz, 1H), 2.02 (q, $J = 7.0$ Hz, 2H), 0.16 (s, 9H).



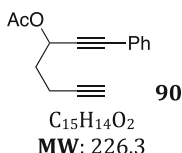
Alkynylation of 5-trimethylsilyl-4-pentynal was realized with 1-hexyne according to the same procedure than for the synthesis of precursors **70–84**. Yellow oil, 85 %. ^1H NMR (400 MHz, CDCl_3) δ 4.53–4.43 (m, 1H), 2.50–2.31 (m, 2H), 2.21 (td, $J = 7.0, 2.0$ Hz, 2H), 1.95–1.82 (m, 3H), 1.54–1.36 (m, 4H), 0.91 (t, $J = 7.2$ Hz, 3H), 0.15 (s, 9H).



Alkynylation of 5-trimethylsilyl-4-pentynal was realized with cyclopropylacetylene according to the same procedure than for the synthesis of precursors **70–84**. Yellow oil, 87 %. ^1H NMR (400 MHz, CDCl_3) δ 4.46 (qd, $J = 6.2, 1.7$ Hz, 1H), 2.49–2.27 (m, 2H), 1.92–1.83 (m, 4H), 1.30–1.18 (m, 1H), 0.81–0.74 (m, 2H), 0.71–0.64 (m, 2H), 0.14 (s, 9H).



Alkynylation of 5-trimethylsilyl-4-pentynal was realized with 3,3-dimethyl-1-butyne according to the same procedure than for the synthesis of precursors **70–84**. Yellow oil, 80 %. ^1H NMR (400 MHz, CDCl_3) δ 4.48 (q, $J = 6.1$ Hz, 1H), 2.51–2.29 (m, 2H), 1.92–1.86 (m, 3H), 1.22 (s, 9H), 0.15 (s, 9H).



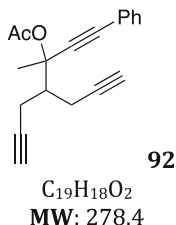
Acetylation of the propargyl alcohol **86** and final desilylation of the alkyne were realized in the same manner than for the synthesis of precursors **70–84**.

Yellow oil. ^1H NMR (400 MHz, CDCl_3) δ 7.46–7.42 (m, 2H), 7.34–7.27 (m, 3H), 5.72 (t, $J = 6.5$ Hz, 1H), 2.49–2.38 (m, 1H), 2.12 (s, 3H), 2.15–2.07 (m, 3H), 2.00 (t, $J = 2.7$ Hz, 1H).

^{13}C NMR (100 MHz, CDCl_3) δ 169.9 (C), 132.0 (CH), 128.8 (CH), 128.4 (CH), 122.2 (C), 85.7 (C), 82.8 (C), 77.4 (CH), 69.3 (C), 63.5 (CH), 33.9 (CH_2), 21.2 (CH_3), 14.7 (CH_2).

IR (neat) $\nu = 639, 690, 756, 1021, 1370, 1443, 1491, 1740, 2120, 2936, 3294\text{ cm}^{-1}$.

HRMS calculated for $[\text{C}_{15}\text{H}_{14}\text{O}_2\text{Na}]^+$: 249.0886, found: 249.0888.



To a stirred solution of NaH (176 mg, 4.4 mmol, 1.1 equiv, 60 % dispersion in mineral oil) in 15 mL of DMF at 0 °C under argon was added dropwise 3-oxobutyric acid methyl ester (960 mg, 2 mmol, 1 equiv.). After 30 min, propargyl bromide (0.64 mL, 6 mmol, 3 equiv., 80 %wt in toluene) was added to the solution. Then, the reaction was stirred at rt overnight. LiCl (336 mg, 8 mmol,

4 equiv.) was added to the solution and the reaction mixture was refluxed for 3 h until completion of the reaction. The mixture was quenched with saturated NH_4Cl and extracted with diethyl ether. The combined organic extracts were washed with brine and dried over magnesium sulfate and filtered. The solvent was removed by rotary evaporation. The crude product was engaged in the next step without further purification.

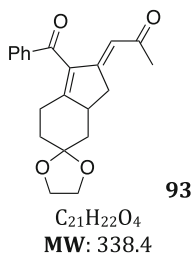
Alkynylation of the resulting ketone **91** and subsequent acetylation of the resulting propargylic alcohol were performed through the same procedures than for compounds **70–84**.

Pale yellow oil, 75 % yield over 4 steps. ^1H NMR (400 MHz, CDCl_3) δ 7.46–7.39 (m, 2H), 7.30–7.25 (m, 3H), 2.78–2.71 (m, 1H), 2.69–2.54 (m, 3H), 2.51–2.45 (m, 1H), 2.06–2.02 (m, 5H), 1.86 (s, 3H).

^{13}C NMR (100 MHz, CDCl_3) δ 168.9 (C), 131.8 (CH), 128.6 (CH), 128.2 (CH), 122.2 (C), 87.4 (C), 87.0 (C), 82.2 (2C), 77.6 (C), 70.2 (CH), 70.1 (CH), 45.7 (CH), 24.3 (CH_3), 22.0 (CH_3), 19.0 (CH_2), 18.5 (CH_2).

IR (neat) ν = 1229, 1366, 1740, 2119, 2236, 2930, 3293 cm^{-1} .

HRMS calculated for $[\text{C}_{19}\text{H}_{18}\text{O}_2\text{Na}]^+$: 301.1204, found: 301.1206.

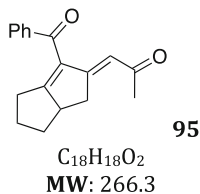


Prepared according to **GP3**, 99 %. Yellow solid, mp = 137 °C. ^1H NMR (400 MHz, CDCl_3) δ 7.89–7.85 (m, 2H), 7.65–7.59 (m, 1H), 7.51–7.46 (m, 2H), 6.05 (s, 1H), 4.03–3.95 (m, 4H), 3.47 (ddd, J = 20.2, 7.0, 2.1 Hz, 1H), 3.19–3.11 (m, 1H), 2.74 (td, J = 19.9, 2.6 Hz, 1H), 2.40–2.34 (m, 2H), 2.25–2.18 (m, 1H), 2.12 (s, 3H), 1.84–1.77 (m, 1H), 1.59–1.48 (m, 2H).

^{13}C NMR (100 MHz, CDCl_3) δ 198.6 (C), 195.1 (C), 166.1 (C), 162.8 (C), 137.2 (C), 136.9 (C), 134.1 (CH), 129.3 (CH), 128.9 (CH), 116.5 (CH), 107.9 (C), 64.6 (CH_2), 64.5 (CH_2), 43.9 (CH), 42.3 (CH_2), 38.1 (CH_2), 34.2 (CH_2), 31.4 (CH_3), 25.6 (CH_2).

IR (neat) ν = 1045, 1214, 1577, 1655, 2948 cm^{-1} .

HRMS calculated for $[\text{C}_{21}\text{H}_{22}\text{O}_4\text{Na}]^+$: 361.1410, found: 361.1410.

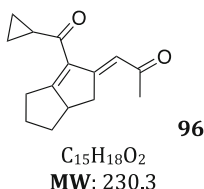


Prepared according to **GPI**, 80 %. Brown oil. ^1H NMR (400 MHz, CDCl_3) δ 7.81–7.76 (m, 2H), 7.58 (t, $J = 7.3$ Hz, 1H), 7.46 (t, $J = 7.7$ Hz, 2H), 6.31 (s, 1H), 3.62 (ddd, $J = 19.1, 6.9, 1.6$ Hz, 1H), 3.20 (d, $J = 7.0$ Hz, 1H), 2.69 (dt, $J = 19.3, 3.3$ Hz, 1H), 2.16 (s, 3H), 2.33–1.93 (m, 4H), 1.28–1.15 (m, 2H).

^{13}C NMR (100 MHz, CDCl_3) δ 198.9 (C), 194.2 (C), 181.6 (C), 166.9 (C), 138.2 (C), 133.6 (C), 133.4 (C), 129.3 (CH), 128.8 (CH), 117.2 (CH), 53.1 (CH), 37.8 (CH_2), 31.8 (CH_2), 30.8 (CH_2), 27.5 (CH_2), 26.3 (CH_3).

IR (neat) $\nu = 693, 727, 912, 1219, 1360, 1448, 1578, 1595, 1654, 1716, 2867, 2954$ cm^{-1} .

HRMS calculated for $[\text{C}_{18}\text{H}_{18}\text{O}_2\text{Na}]^+$: 289.1199, found: 289.1202.

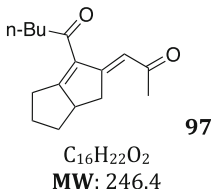


Prepared according to **GPI**, 98 %. Brown oil. ^1H NMR (400 MHz, CDCl_3) δ 6.72 (s, 1H), 3.51 (ddd, $J = 18.8, 6.9, 1.6$ Hz, 1H), 3.10–2.99 (m, 1H), 2.75–2.66 (m, 2H), 2.49 (ddd, $J = 13.2, 7.3, 3.8$ Hz, 1H), 2.14 (s, 3H), 2.22–1.96 (m, 4H), 1.22–1.07 (m, 2H), 1.05–0.96 (m, 1H), 0.96–0.83 (m, 2H).

^{13}C NMR (100 MHz, CDCl_3) δ 199.1 (C), 198.9 (C), 184.3 (C), 165.2 (C), 134.3 (C), 117.8 (CH), 53.4 (CH), 37.6 (CH_2), 31.8 (CH_2), 30.6 (CH_2), 27.8 (CH_2), 27.6 (CH_3), 21.0 (CH), 11.9 (CH_2), 10.9 (CH_2).

IR (neat) $\nu = 732, 1188, 1278, 1358, 1576, 1656, 2866, 2955$ cm^{-1} .

HRMS calculated for $[\text{C}_{15}\text{H}_{18}\text{O}_2\text{Na}]^+$: 253.1199, found: 253.1194.

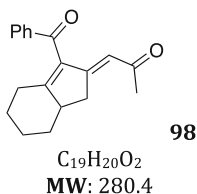


Prepared according to **GPI**, 73 %. Brown oil. ^1H NMR (300 MHz, CDCl_3) δ 6.97 (s, 1H), 3.59 (ddd, $J = 18.6, 7.0, 1.5$ Hz, 1H), 3.07 (m, 1H), 2.79–2.57 (m, 4H), 2.53–2.40 (m, 1H), 2.17 (s, 3H), 2.30–1.92 (m, 3H), 1.68–1.55 (m, 2H), 1.45–1.30 (m, 2H), 1.29–1.17 (m, 1H), 0.93 (t, $J = 7.4$ Hz, 3H).

^{13}C NMR (100 MHz, CDCl_3) δ 199.5 (C), 199.2 (C), 184.2 (C), 165.2 (C), 133.1 (C), 118.1 (CH), 54.0 (CH), 42.7 (CH_2), 37.5 (CH_2), 31.9 (CH_2), 30.6 (CH_2), 28.4 (CH_2), 28.2 (CH_2), 25.9 (CH_3), 22.4 (CH_2), 14.0 (CH_3).

IR (neat) $\nu = 1186, 1357, 1577, 1672, 2869, 2932, 2956$.

HRMS calculated for $[\text{C}_{16}\text{H}_{22}\text{O}_2\text{Na}]^+$: 269.1512, found: 269.1510.

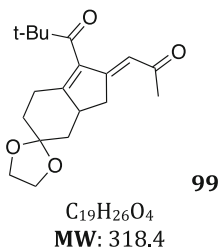


Prepared according to **GPI**, 75 %. Brown oil. **^1H NMR (400 MHz, CDCl_3)** δ 7.87 (d, $J = 7.2$ Hz, 2H), 7.60 (t, $J = 7.4$ Hz, 1H), 7.49 (t, $J = 7.6$ Hz, 2H), 5.80 (s, 1H), 3.55 (ddd, $J = 20.0, 6.8, 1.9$ Hz, 1H), 3.09 (brs, 1H), 2.75 (d, $J = 15.6$ Hz, 1H), 2.57–2.32 (m, 2H), 2.27–2.12 (m, 1H), 2.08 (s, 3H), 2.07–1.94 (m, 1H), 1.88–1.73 (m, 2H), 1.65–1.34 (m, 2H), 1.31–1.10 (m, 1H).

^{13}C NMR (100 MHz, CDCl_3) δ 198.4 (C), 195.5 (C), 169.4 (C), 163.2 (C), 137.4 (C), 135.9 (C), 133.9 (CH), 129.4 (CH), 128.8 (CH), 116.0 (CH), 46.6 (CH), 38.6 (CH_2), 35.4 (CH_2), 31.5 (CH_3), 29.3 (CH_2), 27.0 (CH_2), 25.3 (CH_2).

IR (neat) $\nu = 689, 724, 1176, 1212, 1359, 1370, 1446, 1570, 1656, 2851, 2924 \text{ cm}^{-1}$.

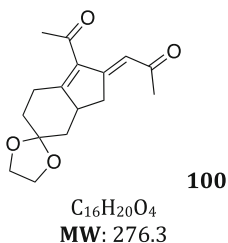
HRMS calculated for $[\text{C}_{19}\text{H}_{20}\text{O}_2\text{Na}]^+$: 303.1356, found: 303.1355.



Prepared according to **GP3**, 97 %. White solid, mp = 115 °C. **^1H NMR (400 MHz, CDCl_3)** δ 5.74 (s, 1H), 4.00–3.93 (m, 4H), 3.36 (ddd, $J = 19.7, 6.8, 2.0$ Hz, 1H), 3.05–2.95 (m, 1H), 2.60 (td, $J = 20.0, 2.4$ Hz, 1H), 2.46–2.37 (m, 2H), 2.14 (s, 3H), 2.14–2.07 (m, 1H), 1.89–1.84 (m, 1H), 1.63–1.54 (m, 1H), 1.38 (t, $J = 12.7$ Hz, 1H), 1.18 (s, 9H).

^{13}C NMR (100 MHz, CDCl_3) δ 213.6 (C), 197.9 (C), 163.6 (C), 160.5 (C), 139.3 (C), 116.2 (CH), 108.0 (C), 64.6 (CH_2), 64.5 (CH_2), 45.0 (C), 43.5 (CH), 42.1 (CH_2), 38.0 (CH_2), 34.2 (CH_2), 31.4 (CH_3), 26.8 (CH_3), 25.9 (CH_2).

HRMS calculated for $[\text{C}_{19}\text{H}_{26}\text{O}_4\text{Na}]^+$: 341.1723, found: 341.1718.

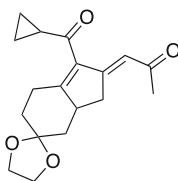


Prepared according to **GP3**, 98 %. Yellow solid, mp = 97 °C. **¹H NMR** (400 MHz, CDCl₃) δ 6.29 (s, 1H), 4.05–3.98 (m, 4H), 3.42 (ddd, *J* = 20.8, 7.3, 2.3 Hz, 1H), 3.10–3.00 (m, 1H), 2.91–2.84 (m, 1H), 2.63 (td, *J* = 20.8, 2.7 Hz, 1H), 2.55 (dt, *J* = 13.5, 4.4 Hz, 1H), 2.43 (s, 3H), 2.23 (s, 3H), 2.21–2.14 (m, 1H), 2.00–1.94 (m, 1H), 1.65 (dt, *J* = 14.4, 5.0 Hz, 1H), 1.46 (t, *J* = 6.8 Hz, 1H).

¹³C NMR (100 MHz, CDCl₃) δ 200.6 (C), 198.4 (C), 166.6 (C), 161.2 (C), 138.7 (C), 116.3 (CH), 107.8 (C), 64.6 (CH₂), 64.5 (CH₂), 43.9 (CH), 42.1 (CH₂), 37.9 (CH₂), 34.3 (CH₂), 31.6 (CH₃), 31.5 (CH₃), 25.5 (CH₂).

IR (neat) ν = 930, 1120, 1195, 1363, 1432, 1576, 1678, 2890, 2926, 2952 cm⁻¹.

HRMS calculated for [C₁₆H₂₀O₄Na]⁺: 299.1259, found: 299.1257.

**101**

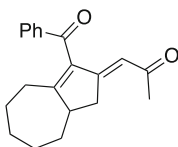
C₁₈H₂₂O₄
MW: 302.4

Prepared according to **GP3**, 90 %. Yellow solid, mp = 109 °C. **¹H NMR** (400 MHz, CDCl₃) δ 6.32 (s, 1H), 4.01–3.95 (m, 4H), 3.40 (ddd, *J* = 19.9, 7.0, 2.1 Hz, 1H), 3.06–2.92 (m, 2H), 2.61 (td, *J* = 20.0, 2.6 Hz, 1H), 2.51 (dt, *J* = 14.2, 5.5 Hz, 1H), 2.19 (s, 3H), 2.17–2.10 (m, 2H), 1.96–1.90 (m, 1H), 1.67–1.58 (m, 1H), 1.42 (t, *J* = 12.8 Hz, 1H), 1.27–1.21 (m, 2H), 1.07–1.01 (m, 2H).

¹³C NMR (100 MHz, CDCl₃) δ 202.7 (C), 198.5 (C), 166.6 (C), 161.5 (C), 139.1 (C), 116.3 (CH), 107.9 (C), 64.6 (CH₂), 64.5 (CH₂), 43.8 (CH), 42.1 (CH₂), 37.9 (CH₂), 34.4 (CH₂), 31.6 (CH₃), 25.5 (CH₂), 22.6 (CH), 12.7 (CH₂), 12.5 (CH₂).

IR (neat) ν = 1045, 1192, 1391, 1575, 1657, 1675, 2891, 2968 cm⁻¹.

HRMS calculated for [C₁₈H₂₂O₄Na]⁺: 325.1410, found: 325.1407.

**102**

C₂₀H₂₂O₂
MW: 294.4

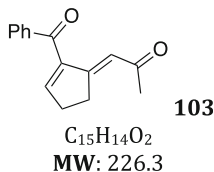
Prepared according to **GPI**, 94 %. Yellow oil. **¹H NMR** (300 MHz, CDCl₃) δ 7.89–7.83 (m, 2H), 7.63–7.56 (m, 1H), 7.50–7.43 (m, 2H), 5.78 (s, 1H), 3.44 (ddd, *J* = 20.3, 6.8, 1.8 Hz, 1H), 3.11–3.01 (m, 1H), 2.73 (d, *J* = 19.5, 1H), 2.53–2.32 (m, 2H), 2.05 (s, 3H), 2.04–1.80 (m, 1H), 1.80–1.70 (m, 2H), 1.67–1.26 (m, 5H).

¹³C NMR (75 MHz, CDCl₃) δ 198.5 (C), 196.5 (C), 171.0 (C), 163.6 (C), 139.1 (C), 136.6 (C), 134.0 (CH), 129.4 (CH), 128.9 (CH), 115.4 (CH), 49.4 (CH),

40.3 (CH₂), 35.2 (CH₂), 31.4 (CH₃), 30.8 (CH₂), 30.5 (CH₂), 28.9 (CH₂), 26.4 (CH₂).

IR (neat) ν = 1172, 1227, 1374, 1448, 1570, 1662, 2247, 2852, 2921, 3261 cm⁻¹.

HRMS calculated for [C₂₀H₂₂O₂Na]⁺: 317.1512, found: 317.1511.

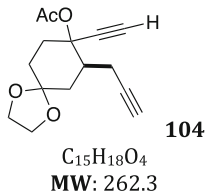


Prepared according to **GP3**, 81 %. Orange oil. **¹H NMR (300 MHz, CDCl₃)** δ 7.85 (dd, J = 8.2, 1.3 Hz, 2H), 7.60 (ddd, J = 8.6, 2.4, 1.2 Hz, 1H), 7.49 (t, J = 7.8 Hz, 2H), 7.09 (s, 1H), 6.76 (s, 1H), 3.29 (dd, J = 5.1, 2.4 Hz, 2H), 2.81 (dd, J = 5.0, 2.7 Hz, 2H), 2.25 (s, 3H).

¹³C NMR (75 MHz, CDCl₃) δ 199.1 (C), 193.3 (C), 161.1 (C), 156.9 (CH), 143.6 (C), 138.0 (C), 133.4 (CH), 129.5 (CH), 128.7 (CH), 118.5 (CH), 32.8 (CH₂), 32.0 (CH₂), 31.9 (CH₃).

IR (neat) ν = 670, 693, 715, 859, 968, 1201, 1270, 1591, 1653, 2341, 2361, 2923, 3058 cm⁻¹.

HRMS calculated for [C₁₅H₁₄O₂Na]⁺: 249.0886, found: 249.0890.

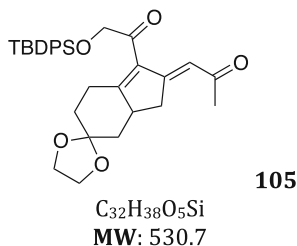


Prepared from **80** under classical desilylation conditions with KF in DMSO (76 % yield). White solid (86:14 mixture of diastereomers), mp = 119 °C. **¹H NMR (400 MHz, CDCl₃)** δ 3.94–3.85 (m, 4H), 2.77–2.70 (m, 1H), 2.65–2.57 (m, 2H), 2.20–1.99 (m, 3H), 1.98 (s, 3H), 1.93 (t, J = 2.5 Hz, 1H), 1.87–1.74 (m, 1H), 1.70–1.54 (m, 3H).

¹³C NMR (100 MHz, CDCl₃) δ 169.1 (C), 107.2 (C), 82.3 (C), 78.7 (C), 77.4 (CH), 74.5 (C), 69.7 (CH), 64.5 (CH₂), 64.3 (CH₂), 43.1 (CH), 36.1 (CH₂), 32.6 (CH₂), 31.9 (CH₂), 21.8 (CH₃), 19.6 (CH₂).

IR (neat) ν = 975, 1146, 1230, 1310, 1369, 1439, 1739, 2108, 2876, 2951, 3241 cm⁻¹.

HRMS calculated for $[\text{C}_{15}\text{H}_{18}\text{O}_4\text{Na}]^+$: 285.1103; found: 285.1107.

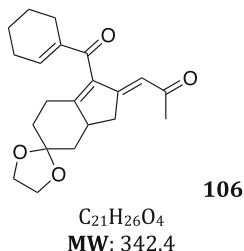


Prepared according to **GP3**, 95 %. Brown solid, mp = 65 °C. **^1H NMR** (400 MHz, CDCl_3) δ 7.74–7.67 (m, 4H), 7.43–7.25 (m, 6H), 5.93 (s, 1H), 4.44 (s, 2H), 3.97–3.93 (m, 4H), 3.30 (dd, J = 20.6, 7.1, 2.5 Hz, 1H), 3.01–2.91 (m, 1H), 2.55 (dt, J = 14.2, 5.5 Hz, 1H), 2.39–2.25 (m, 2H), 2.08 (s, 3H), 2.08–2.03 (m, 1H), 1.79–1.75 (m, 1H), 1.43–1.20 (m, 2H), 1.09 (s, 9H).

^{13}C NMR (100 MHz, CDCl_3) δ 201.9 (C), 198.4 (C), 166.2 (C), 161.9 (C), 136.6 (C), 135.8 (CH), 135.7 (CH), 132.8 (C), 132.7 (C), 130.2 (CH), 128.0 (CH), 115.9 (CH), 107.9 (C), 70.7 (CH_2), 64.7 (CH_2), 64.6 (CH_2), 44.1 (CH), 42.1 (CH_2), 38.1 (CH_2), 34.5 (CH_2), 31.7 (CH_3), 26.8 (CH_3), 25.3 (CH_2), 19.4 (C).

IR (neat) ν = 903, 1113, 1363, 1428, 1472, 1578, 1716, 2252, 2932 cm^{-1} .

HRMS calculated for $[\text{C}_{32}\text{H}_{39}\text{O}_5\text{Si}]^+$: 531.2561, found: 531.2557.

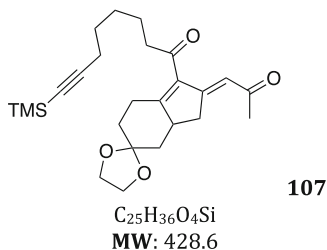


Prepared according to **GP3**, 70 %. Yellow oil. **^1H NMR** (300 MHz, CDCl_3) δ 6.77 (s, 1H), 5.96 (s, 1H), 4.04–3.93 (m, 4H), 3.41 (ddd, J = 20.0, 6.8, 2.0 Hz, 1H), 3.10–3.00 (m, 1H), 2.64 (td, J = 20.0, 2.4 Hz, 1H), 2.54–2.48 (m, 1H), 2.40–2.31 (m, 3H), 2.29–2.23 (m, 2H), 2.16 (s, 3H), 1.90–1.84 (m, 1H), 1.72–1.62 (m, 4H), 1.55 (dt, J = 13.4, 5.0 Hz, 1H), 1.43 (t, J = 12.7 Hz, 2H).

^{13}C NMR (100 MHz, CDCl_3) δ 198.6 (C), 196.6 (C), 163.9 (C), 163.5 (C), 146.2 (CH), 140.5 (C), 137.4 (C), 116.1 (CH), 108.2 (C), 64.8 (CH_2), 64.7 (CH_2), 43.7 (CH), 42.4 (CH_2), 38.2 (CH_2), 34.3 (CH_2), 31.6 (CH_3), 26.6 (CH_2), 25.6 (CH_2), 22.6 (CH_2), 21.9 (CH_2), 21.7 (CH_2).

IR (neat) ν = 1066, 1118, 1202, 1574, 1631, 1671, 2855, 2924 cm^{-1} .

HRMS calculated for $[C_{21}H_{26}O_4Na]^+$: 365.1725, found: 468.1423.

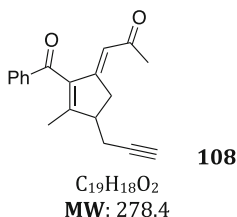


Prepared according to **GP3**, 99 %. Pale yellow oil. **1H NMR (400 MHz, $CDCl_3$)** δ 6.12 (s, 1H), 4.01–3.97 (m, 4H), 3.37 (ddd, J = 20.8, 7.3, 2.1 Hz, 1H), 3.05–2.95 (m, 1H), 2.76–2.69 (m, 1H), 2.67–2.56 (m, 2H), 2.50 (dt, J = 14.8, 5.7 Hz, 1H), 2.25–2.19 (m, 2H), 2.19 (s, 3H), 2.16–2.11 (m, 1H), 1.95–1.89 (m, 1H), 1.36–1.70 (m, 9H), 0.13 (s, 9H).

^{13}C NMR ($CDCl_3$) δ 204.0 (C), 198.2 (C), 165.1 (C), 161.8 (C), 139.0 (C), 115.9 (CH), 107.8 (C), 107.1 (C), 84.6 (C), 64.6 (CH_2), 64.5 (CH_2), 44.0 (CH_2), 43.8 (CH), 42.1 (CH_2), 37.9 (CH_2), 34.4 (CH_2), 31.6 (CH), 28.4 (CH_2), 25.4 (CH_2), 23.5 (CH_2), 19.7 (CH_2), 0.1 (CH_3).

IR (neat) ν = 839, 1046, 1119, 1247, 1357, 1430, 1577, 1675, 2171, 2949 cm^{-1} .

HRMS calculated for $[C_{25}H_{36}O_4SiNa]^+$: 451.2281, found: 365.1728.

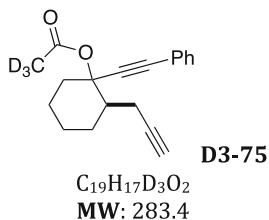


Prepared according to **GP3**, 80 %. Yellow oil. **1H NMR (400 MHz, $CDCl_3$)** δ 8.01–7.94 (m, 2H), 7.66–7.57 (m, 1H), 7.52–7.42 (m, 2H), 5.91 (s, 1H), 3.45 (ddd, J = 20.8, 7.5, 2.2 Hz, 1H), 3.14–3.01 (m, 2H), 2.60–2.50 (m, 2H), 2.10 (s, 3H), 2.01 (t, J = 2.5 Hz, 1H), 1.83 (s, 3H).

^{13}C NMR (100 MHz, $CDCl_3$) δ 205.3 (C), 198.9 (C), 162.6 (C), 162.1 (C), 136.9 (C), 134.6 (CH), 130.1 (CH), 129.9 (CH), 116.5 (CH), 77.6 (C), 70.9 (CH), 47.6 (CH), 37.4 (CH_2), 32.0 (CH_3), 22.3 (CH_2), 15.7 (CH_3), one C unobserved.

IR (neat) ν = 1165, 1223, 1357, 1448, 1575, 1663, 2116, 2914, 3261 cm^{-1} .

HRMS calculated for $[\text{C}_{19}\text{H}_{18}\text{O}_2\text{Na}]^+$: 301.1204, found: 301.1206.

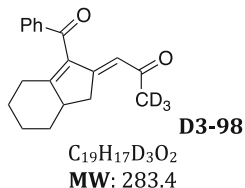


Prepared similarly to compounds **70–84** but deuterated anhydride acetic was used in the acetylation step. Colorless oil (67:33 mixture of diastereomers). **¹H NMR (400 MHz, CDCl₃)** δ 7.44 (dt, J = 8.0, 3.6 Hz, 2H), 7.33–7.28 (m, 3H), 2.95–2.84 (m, 1H), 2.76 (dt, J = 16.7, 3.0 Hz, 1H), 2.34–2.05 (m, 2H), 2.04–1.89 (m, 1H), 1.98 (t, J = 2.6 Hz, 1H), 1.80–1.55 (m, 4H), 1.53–1.28 (m, 2H).

¹³C NMR (100 MHz, CDCl₃) δ 169.2 (C), 132.0 (CH), {128.6 (CH), 128.5 (CH)}, {128.4 (CH), 128.3 (CH)}, {122.6 (C), 122.6 (C)}, {89.1 (C), 88.8 (C)}, {86.1 (C), 85.5 (C)}, {83.6 (CH), 83.5 (CH)}, {79.8 (C), 76.5 (C)}, {69.3 (C), 69.2 (C)}, {46.2 (CH), 46.1 (CH)}, {36.4 (CH₂), 34.9 (CH₂)}, {28.5 (CH₂), 26.2 (CH₂)}, {25.2 (CH₂), 24.7 (CH₂)}, {23.8 (CH₂), 21.3 (CH₂)}, {20.4 (CH₂), 20.3 (CH₂)}, CD₃ was not observed.

IR (neat) ν = 690, 756, 1069, 1227, 1443, 1490, 1737, 2118, 2859, 2933, 3295 cm⁻¹.

HRMS calculated for $[\text{C}_{19}\text{H}_{17}\text{D}_3\text{O}_2\text{Na}]^+$: 306.1544, found: 306.1536.

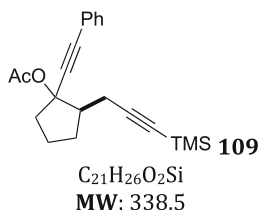


Prepared according to **GPI**, 70 %. Brown oil. **¹H NMR (400 MHz, CDCl₃)** δ 7.87 (d, J = 7.2 Hz, 2H), 7.60 (t, J = 7.4 Hz, 1H), 7.47 (t, J = 7.6 Hz, 2H), 6.02 (s, 1H), 3.45 (ddd, J = 20.0, 6.9, 2.1 Hz, 1H), 2.86–2.67 (m, 2H), 2.40 (dd, J = 13.9, 1.8 Hz, 1H), 2.28–2.17 (m, 1H), 2.02 (ddd, J = 13.8, 9.5, 4.3 Hz, 1H), 1.89–1.77 (m, 2H), 1.53–1.38 (m, 1H), 1.35–1.13 (m, 2H).

¹³C NMR (100 MHz, CDCl₃) δ 198.8 (C), 195.6 (C), 169.5 (C), 163.4 (C), 137.5 (C), 136.0 (C), 134.0 (CH), 129.0 (CH), 128.9 (CH), 116.1 (CH), 46.7 (CH), 38.7 (CH₂), 35.5 (CH₂), 30.7 (q, CD₃), 29.4 (CH₂), 27.1 (CH₂), 25.4 (CH₂).

IR (neat) ν = 2958, 2855, 1660, 1569, 1448, 1372, 1263, 1214, 1179, 1023, 905, 882, 728 cm⁻¹.

HRMS calculated for $[\text{C}_{19}\text{H}_{17}\text{D}_3\text{O}_2\text{Na}]^+$: 306.1544, found: 306.1538.

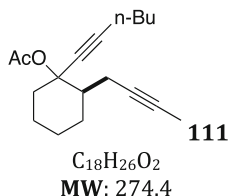


Colorless oil (87:13 mixture of diastereomers). **^1H NMR (200 MHz, CDCl_3)** δ 7.46–7.38 (m, 2H), 7.32–7.26 (m, 3H), 2.85–2.67 (m, 1H), 2.61–2.28 (m, 3H), 2.26–2.02 (m, 2H), 2.04 (s, 3H), 1.93–1.57 (m, 2H), 0.14 (s, 9H).

^{13}C NMR (100 MHz, CDCl_3) δ 188.9, 138.4, 132.0 (2C), 128.6, 128.3 (2C), 87.8, 83.1, 72.3, 69.4, 67.5, 49.2, 39.7, 28.5, 22.3, 21.9, 21.5, 0.3 (3C).

IR (neat) ν = 2925, 2176, 1741, 1682, 1236, 1194, 1147, 1014, 846, 747, 697 cm^{-1} .

HRMS calculated for $[\text{C}_{21}\text{H}_{26}\text{NaO}_2\text{Si}]^+$: 361.1594, found: 361.1591.

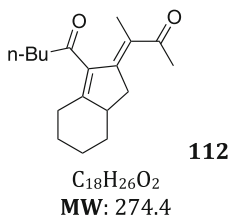


Prepared similarly to compounds **70–84**, but 1-bromo-2-butyne was used in the alkylation step. Colorless oil (81:19 mixture of diastereomers). **^1H NMR (300 MHz, CDCl_3)** δ 2.71 (m, 1H), 2.60 (m, 1H), 2.24 (t, J = 6.9 Hz, 2H), 2.13–2.03 (m, 2H), 2.00 (s, 3H), 1.88–1.83 (m, 1H), 1.80 (t, J = 2.4 Hz, 3H), 1.75–1.15 (m, 10H), 0.91 (t, J = 7.2 Hz, 3H).

^{13}C NMR (75 MHz, CDCl_3) δ 169.3 (C), 89.7 (C), 80.1 (C), 78.2 (C), 76.3 (C), 76.1 (C), 46.4 (CH), 36.5 (CH_2), 30.9 (CH_2), 28.5 (CH_2), 25.2 (CH_2), 23.7 (CH_2), 22.2 (CH_3), 22.1 (CH_2), 20.4 (CH_2), 18.5 (CH_2), 13.6 (CH_3), 3.6 (CH_3).

IR (neat) ν = 2932, 2859, 1744, 1448, 1366, 1225, 1014 cm^{-1} .

HRMS calculated for $[\text{C}_{18}\text{H}_{26}\text{O}_2\text{Na}]^+$: 297.1825, found: 297.1820.



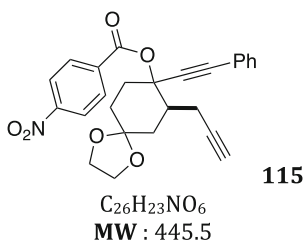
The catalyst (2 mol%) was added to a solution of substrate **114** in anhydrous DCM. The mixture was stirred at 45 °C. After 24 h, the reaction was complete and the mixture was filtered through a short pad of silica. The solvent was removed under vacuum, and purification by flash chromatography afforded the

cycloisomerization product as an orange solid, obtained in 27 % yield, mp = 94 °C. ^1H NMR (400 MHz, CDCl_3) δ 2.57–2.44 (m, 3H), 2.24 (s, 3H), 2.36–1.73 (m, 4H), 1.88 (s, 3H), 1.86–1.69 (m, 2H), 1.63–1.52 (m, 2H), 1.42–1.23 (m, 6H), 0.92 (t, J = 7.3 Hz, 3H).

^{13}C NMR (100 MHz, CDCl_3) δ 210.0 (C), 201.8 (C), 143.2 (C), 137.3 (C), 135.0 (C), 129.9 (C), 45.0 (CH_2), 35.9 (CH), 34.4 (CH_2), 32.7 (CH_2), 30.5 (CH_2), 29.9 (CH_3), 26.0 (CH_2), 25.5 (CH_2), 25.1 (CH_2), 22.4 (CH_2), 17.4 (CH_3), 14.0 (CH_3).

IR (neat) ν = 2927, 2857, 1697, 1668, 1552, 1447, 1353, 1257, 1236, 1176, 1145 cm^{-1} .

HRMS calculated for $[\text{C}_{18}\text{H}_{26}\text{O}_2\text{Na}]^+$: 297.1825, found: 297.1823.

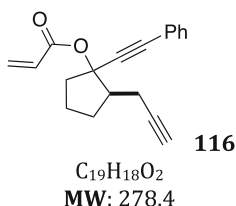


To a stirred solution of alcohol **113** (400 mg, 1.35 mmol, 1.0 equiv.), Et_3N (0.56 mL, 4.05 mmol, 3 equiv.) and 4-DMAP (15.5 mg, 0.1 mmol, 0.1 equiv.) in CH_2Cl_2 (4 mL) was added 4-nitrobenzoyl chloride (630 mg, 3.38 mmol, 1.3 equiv.) at 0 °C. After addition, the solution was allowed to warm to rt and was stirred further until completion (1 h at rt). The reaction was quenched with aqueous saturated NH_4Cl solution and the resulting aqueous layer was extracted with CH_2Cl_2 . The combined organic layers were washed with brine, dried over anhydrous Na_2SO_4 , filtered and evaporated to give the crude ester as an oil. Purification was achieved by flash column chromatography on silica gel (pentane/ AcOEt 85:15) to give pure ester **115** (340 mg, 57 %). Yellow solid, mp = 123 °C. ^1H NMR (400 MHz, CDCl_3) δ 8.21 (d, J = 8.1 Hz, 2H), 7.96–7.89 (m, 4H), 7.67–7.62 (m, 1H), 7.55–7.50 (m, 2H), 6.82 (s, 1H), 4.05–3.98 (m, 4H), 3.72–3.63 (m, 1H), 3.35–3.20 (m, 1H), 2.94 (dd, J = 20.4, 2.4 Hz, 1H), 2.46–2.42 (m, 2H), 2.31–2.25 (m, 1H), 1.88–1.83 (m, 1H), 1.65–1.54 (m, 2H).

^{13}C NMR (75 MHz, CDCl_3) δ 194.7 (C), 188.8 (C), 169.1 (C), 167.6 (C), 149.7 (C), 144.3 (C), 137.3 (C), 137.2 (C), 134.2 (CH), 129.3 (CH), 129.0 (CH), 128.8 (CH), 123.7 (CH), 112.3 (CH), 107.8 (C), 64.7 (CH_2), 64.6 (CH_2), 44.2 (CH), 42.4 (CH_2), 38.9 (CH_2), 34.2 (CH_2), 26.0 (CH_2).

IR (neat) ν = 1100, 1305, 1431, 1520, 1731, 2227, 2938, 3283 cm^{-1} .

HRMS calculated for $[C_{26}H_{23}NO_6Na]^+$: 468.1423, found: 468.1423.



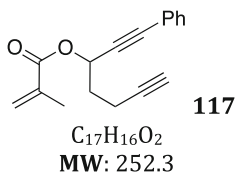
To a stirred solution of alcohol **114** (400 mg, 1.50 mmol, 1.0 equiv.), Et_3N (0.63 mL, 4.51 mmol, 3 equiv.) and 4-DMAP (21 mg, 0.15 mmol, 0.1 equiv.) in CH_2Cl_2 (4 mL) was added acryloyl chloride (0.31 mL, 3.76 mmol, 2.5 equiv.) at $-20\text{ }^\circ\text{C}$. After addition, the solution was stirred below $0\text{ }^\circ\text{C}$ until completion (1–3 h). The reaction was quenched with aqueous saturated NH_4Cl solution and the resulting aqueous layer was extracted with CH_2Cl_2 . The combined organic layers were washed with brine, dried over anhydrous $MgSO_4$, filtered and evaporated to give the crude ester as an oil. Purification was achieved by flash column chromatography on silica gel. Desilylation was carried similarly than in the synthesis of compounds **70–84** using KF in DMSO.

Yellow solid, 72 % over two steps, mp = $74\text{ }^\circ\text{C}$ (90:10 mixture of diastereomers). 1H NMR (400 MHz, $CDCl_3$) δ 7.43 (dt, $J = 5.5, 2.1$ Hz, 2H), 7.32–7.27 (m, 3H), 6.40 (dd, $J = 17.3, 1.4$ Hz, 1H), 6.11 (dd, $J = 17.3, 10.5$ Hz, 1H), 5.82 (dd, $J = 10.5, 1.4$ Hz, 1H), 2.78 (ddd, $J = 16.4, 4.2, 2.7$ Hz, 1H), 2.64–2.45 (m, 2 H), 2.39 (ddd, $J = 16.4, 10.1, 2.6$ Hz, 1H), 2.27–2.07 (m, 2H), 1.97 (t, $J = 2.6$ Hz, 1H), 1.90–1.72 (m, 2H), 1.63 (ddd, $J = 17.3, 12.9, 9.2$ Hz, 1H).

^{13}C NMR (100 MHz, $CDCl_3$) δ 164.7 (C), 132.0 (CH), 130.8 (CH_2), 129.1 (CH), 128.6 (CH), 128.3 (CH), 122.6 (C), 88.0 (C), 86.3 (C), 83.3 (C), 83.2 (C), 69.0 (CH), 49.1 (CH), 39.8 (CH_2), 28.6 (CH_2), 21.5 (CH_2), 20.9 (CH_2).

IR (neat) $\nu = 632, 690, 756, 808, 872, 968, 982, 1036, 1180, 1267, 1402, 1727, 2119, 2231, 2360, 2874, 2957, 3297\text{ cm}^{-1}$.

HRMS calculated for $[C_{19}H_{18}O_2Na]^+$: 301.1199, found: 301.1198.

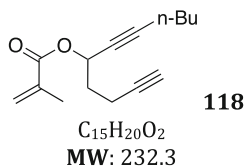


Prepared from alcohol **86** through a similar synthetic sequence than for **114**, using methacryloyl chloride in place of acryloyl chloride. Colorless oil, 46 % over two steps. 1H NMR (400 MHz, $CDCl_3$) δ 7.47–7.40 (m, 2H), 7.35–7.27 (m, 3H), 6.18 (s, 1H), 5.78 (t, $J = 6.4$ Hz, 1H), 5.62 (t, $J = 1.6$ Hz, 1H), 2.46 (m, 2H), 2.22–2.11 (m, 2H), 2.01 (t, $J = 2.7$ Hz, 1H), 1.98 (s, 3H).

^{13}C NMR (100 MHz, $CDCl_3$) δ 166.2 (C), 136.1 (C), 132.0 (CH), 128.8 (CH), 128.4 (CH), 126.4 (CH_2), 122.2 (C), 85.9 (C), 85.8 (C), 82.8 (C), 69.3 (CH), 63.6 (CH), 33.9 (CH_2), 18.4 (CH_3), 14.7 (CH_2).

IR (neat) ν = 3294, 2936, 1740, 1491, 1443, 1370, 1223, 1021, 756, 690, 636 cm^{-1} .

HRMS calculated for $[\text{C}_{17}\text{H}_{16}\text{O}_2\text{Na}]^+$: 275.1043, found: 275.1037.

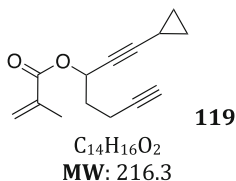


Prepared from alcohol **87** through a similar synthetic sequence than for **114**, using methacryloyl chloride in place of acryloyl chloride. Colorless oil, 53 % over two steps. **^1H NMR (400 MHz, CDCl_3)** δ 6.11 (dd, J = 1.5, 1.0 Hz, 1H), 5.56 (p, J = 1.5 Hz, 1H), 5.49 (tt, J = 6.3, 2.0 Hz, 1H), 2.34 (tt, J = 7.0, 2.7 Hz, 2H), 2.18 (td, J = 7.0, 2.0 Hz, 2H), 2.07–1.96 (m, 2H), 1.95 (t, J = 2.7 Hz, 1H), 1.93 (dd, J = 1.4, 1.0 Hz, 3H), 1.50–1.41 (m, 2H), 1.41–1.31 (m, 2H), 0.88 (t, J = 7.3 Hz, 3H).

^{13}C NMR (100 MHz, CDCl_3) δ 166.3 (C), 136.2 (C), 126.0 (CH_2), 87.0 (C), 82.9 (C), 69.1 (CH), 63.6 (CH), 34.2 (CH_2), 30.6 (CH_2), 22.0 (CH_2), 18.5 (CH_2), 18.4 (CH_3), 14.6 (CH_2), 13.6 (CH_3).

IR (neat) ν = 2958, 2932, 1720, 1451, 1323, 1289, 1150, 1031, 1010, 942, 813, 637 cm^{-1} .

HRMS calculated for $[\text{C}_{15}\text{H}_{20}\text{O}_2\text{Na}]^+$: 255.1356, found: 255.1351.

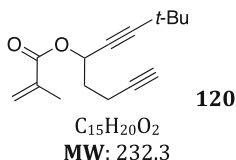


Prepared from alcohol **88** through a similar synthetic sequence than for **114**, using methacryloyl chloride in place of acryloyl chloride. Colorless oil, 54 % over two steps. **^1H NMR (300 MHz, CDCl_3)** δ 6.13 (dq, J = 1.9, 0.9 Hz, 1H), 5.58 (p, J = 1.6 Hz, 1H), 5.49 (td, J = 6.3, 1.8 Hz, 1H), 2.39–2.31 (m, 2H), 2.05–1.93 (m, 6H), 1.30–1.19 (m, 1H), 0.81–0.73 (m, 2H), 0.73–0.65 (m, 2H).

^{13}C NMR (101 MHz, CDCl_3) δ 166.4 (C), 136.3 (C), 126.2 (CH_2), 90.1 (C), 83.0 (C), 72.1 (C), 69.1 (CH), 63.7 (CH), 34.2 (CH_2), 18.4 (CH_3), 14.7 (CH_2), 8.5 (2 CH_2), -0.4 (CH).

IR (neat) ν = 3295, 2245, 1719, 1637, 1433, 1323, 1289, 1151, 1051, 1023, 973, 944, 897, 813, 642 cm^{-1} .

HRMS calculated for $[\text{C}_{14}\text{H}_{16}\text{O}_2\text{Na}]^+$: 239.1043, found: 239.1036.

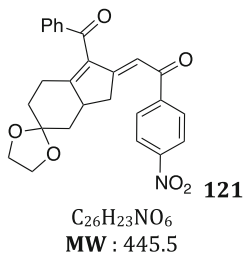


Prepared from alcohol **89** through a similar synthetic sequence than for **114**, using methacryloyl chloride in place of acryloyl chloride. Colorless oil, 47 % over two steps. **¹H NMR (300 MHz, CDCl₃)** δ 6.13 (s, 1H), 5.60–5.57 (m, 1H), 5.53 (t, J = 6.3 Hz, 1H), 2.36 (ddd, J = 8.7, 5.3, 2.4 Hz, 2H), 2.06–1.93 (m, 6H), 1.21 (s, 9H).

¹³C NMR (101 MHz, CDCl₃) δ 166.3 (C), 136.4 (C), 126.0 (CH₂), 95.2 (C), 83.2 (C), 75.3 (C), 69.0 (CH), 63.6 (CH), 34.3 (CH₂), 31.0 (CH₃), 27.5 (C), 18.5 (CH₃), 14.6 (CH₂).

IR (neat) ν = 2970, 1722, 1323, 1290, 1265, 1154, 1025, 943, 634 cm⁻¹.

HRMS calculated for [C₁₅H₂₀O₂Na]⁺: 255.1356, found: 255.1350.

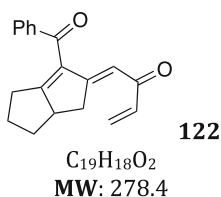


Prepared according to **GP3**, 99 %. Yellow solid, mp = 123 °C. **¹H NMR (400 MHz, CDCl₃)** δ 8.21 (d, J = 8.1 Hz, 2H), 7.96–7.89 (m, 4H), 7.67–7.62 (m, 1H), 7.55–7.50 (m, 2H), 6.82 (s, 1H), 4.05–3.98 (m, 4H), 3.72–3.63 (m, 1H), 3.35–3.20 (m, 1H), 2.94 (dd, J = 20.4, 2.4 Hz, 1H), 2.46–2.42 (m, 2H), 2.31–2.25 (m, 1H), 1.88–1.83 (m, 1H), 1.65–1.54 (m, 2H).

¹³C NMR (75 MHz, CDCl₃) δ 194.7 (C), 188.8 (C), 169.1 (C), 167.6 (C), 149.7 (C), 144.3 (C), 137.3 (C), 137.2 (C), 134.2 (CH), 129.3 (CH), 129.0 (CH), 128.8 (CH), 123.7 (CH), 112.3 (CH), 107.8 (C), 64.7 (CH₂), 64.6 (CH₂), 44.2 (CH), 42.4 (CH₂), 38.9 (CH₂), 34.2 (CH₂), 26.0 (CH₂).

IR (neat) ν = 1100, 1305, 1431, 1520, 1731, 2227, 2938, 3283 cm⁻¹.

HRMS calculated for [C₂₆H₂₃NO₆Na]⁺: 468.1423, found: 468.1423.

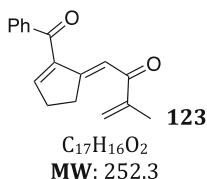


Prepared according to **GPI**, 66%. Yellow solid, mp = 95 °C. **¹H NMR (300 MHz, CDCl₃)** δ 7.78 (d, J = 7.8 Hz, 2H), 7.57 (t, J = 7.4 Hz, 1H), 7.45 (t, J = 7.7 Hz, 2H), 6.54 (s, 1H), 6.39 (dd, J = 17.5, 10.5 Hz, 1H), 6.13 (d, J = 17.4 Hz, 1H), 5.64 (d, J = 10.6 Hz, 1H), 3.67 (ddd, J = 19.1, 6.7, 1.3 Hz, 1H), 3.29–3.14 (m, 1H), 2.75 (dt, J = 19.3, 3.1 Hz, 1H), 2.31–2.19 (m, 1H), 2.18–2.06 (m, 2H), 2.06–1.94 (m, 2H), 1.22 (qd, J = 11.9, 9.8 Hz, 1H).

¹³C NMR (100 MHz, CDCl₃) δ 194.1 (C), 190.3 (C), 182.4 (C), 168.9 (C), 138.5 (CH), 138.2 (C), 133.9 (C), 133.4 (CH), 129.2 (CH), 128.7 (CH), 126.6 (CH₂), 115.2 (CH), 53.1 (CH), 38.1 (CH₂), 30.7 (CH₂), 27.5 (CH₂), 26.4 (CH₂).

IR (neat) ν = 635, 672, 695, 723, 869, 1112, 1213, 1290, 1364, 1399, 1447, 1567, 1650, 2248, 2957 cm^{-1} .

HRMS calculated for $[\text{C}_{19}\text{H}_{18}\text{O}_2\text{Na}]^+$: 301.1199, found: 301.1200.

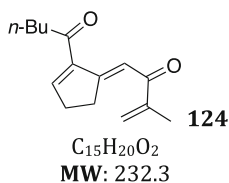


Prepared according to **GPI**, 98 %. Brown solid, mp = 68 °C. **^1H NMR (400 MHz, CDCl_3)** δ 7.82–7.77 (m, 2H), 7.59–7.53 (m, 1H), 7.47–7.41 (m, 2H), 7.24 (t, J = 2.4 Hz, 1H), 7.04 (t, J = 2.8 Hz, 1H), 5.87 (s, 1H), 5.64–5.61 (m, 1H), 3.28 (dt, J = 7.6, 2.5 Hz, 2H), 2.76 (td, J = 5.0, 2.7 Hz, 2H), 1.90 (s, 3H).

^{13}C NMR (100 MHz, CDCl_3) δ 193.3 (C), 193.0 (C), 161.9 (C), 156.7 (CH), 146.4 (C), 143.9 (C), 138.0 (C), 133.2 (CH), 129.4 (CH), 128.6 (CH), 123.1 (CH_2), 114.4 (CH), 32.7 (CH_2), 32.0 (CH_2), 18.0 (CH_3).

IR (neat) ν = 1652, 1590, 1447, 1368, 1351, 1270, 1174, 1094, 932, 868, 714, 694, 668 cm^{-1} .

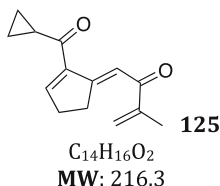
HRMS calculated for $[\text{C}_{17}\text{H}_{16}\text{O}_2\text{Na}]^+$: 275.1043, found: 275.1042.



Prepared according to **GPI**, 64 %. Brown oil. **^1H NMR (400 MHz, CDCl_3)** δ 7.72 (s, 1H), 7.43 (s, 1H), 5.97 (s, 1H), 5.67 (s, 1H), 3.22–3.11 (m, 2H), 2.77–2.69 (m, 2H), 2.69–2.62 (m, 2H), 1.91 (s, 3H), 1.66–1.56 (m, 2H), 1.39–1.27 (m, 2H), 0.90 (t, J = 7.3 Hz, 3H).

^{13}C NMR (CDCl_3) δ 198.9 (C), 193.5 (C), 160.2 (C), 157.4 (CH), 146.5 (C), 143.4 (C), 123.1 (CH_2), 115.4 (CH), 40.7 (CH_2), 32.2 (CH_2), 32.0 (CH_2), 26.4 (CH_2), 22.4 (CH_2), 18.0 (CH_3), 14.0 (CH_3).

HRMS calculated for $[\text{C}_{15}\text{H}_{20}\text{O}_2\text{Na}]^+$: 255.1356, found: 255.1358.

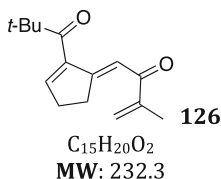


Prepared according to **GPI**, 99 %. Brown oil. **^1H NMR (400 MHz, CDCl_3)** δ 7.65 (t, J = 2.5 Hz, 1H), 7.56 (t, J = 2.9 Hz, 1H), 5.95 (s, 1H), 5.66 (dd, J = 1.4, 0.8 Hz, 1H), 3.23–3.18 (m, 2H), 2.73–2.68 (m, 2H), 2.35 (tt, J = 7.8, 4.6 Hz, 1

H), 1.91 (dd, $J = 1.3, 0.9$ Hz, 3H), 1.13 (dq, $J = 7.0, 3.7$ Hz, 2H), 0.94 (dq, $J = 11.3, 3.6$ Hz, 2H). ^{13}C NMR (100 MHz, CDCl_3) δ 198.5 (C), 193.5 (C), 160.4 (C), 157.3 (CH), 146.5 (C), 144.5 (C), 123.1 (CH_2), 115.2 (CH), 32.4 (CH_2), 32.1 (CH_2), 19.4 (CH), 18.1 (CH), 11.5 (2CH_2).

IR (neat) $\nu = 1663, 1587, 1392, 1368, 1257, 1108, 1092, 952, 923, 875, 810\text{ cm}^{-1}$.

HRMS calculated for $[\text{C}_{14}\text{H}_{16}\text{O}_2\text{Na}]^+$: 239.1043, found: 239.1037.

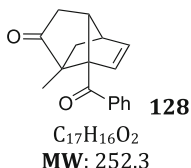


Prepared according to **GPI**, 99 %. Brown oil. ^1H NMR (400 MHz, CDCl_3) δ 6.75 (t, $J = 2.8$ Hz, 1H), 6.62 (t, $J = 2.4$ Hz, 1H), 5.82 (s, 1H), 5.62 (dd, $J = 1.4, 0.7$ Hz, 1H), 3.14–3.09 (m, 2H), 2.67 (td, $J = 4.6, 2.3$ Hz, 2H), 1.89 (dd, $J = 1.3, 0.9$ Hz, 3H), 1.20 (s, 9H).

^{13}C NMR (100 MHz, CDCl_3) δ 209.5 (C), 192.7 (C), 164.3 (C), 147.3 (CH), 146.4 (C), 144.9 (C), 122.8 (CH_2), 113.3 (CH), 45.0 (C), 32.8 (CH_2), 31.0 (CH_2), 26.7 (CH_3), 18.0 (CH_3).

IR (neat) $\nu = 2967, 1685, 1650, 1577, 1477, 1456, 1367, 1303, 1281, 1193, 1096, 997, 933, 902, 858, 658\text{ cm}^{-1}$.

HRMS calculated for $[\text{C}_{15}\text{H}_{20}\text{O}_2\text{Na}]^+$: 255.1356, found: 255.1353.

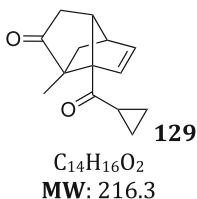


To a solution of the polyconjugated diketone **123** (0.1 mmol) in 2.5 mL of CH_2Cl_2 were added 600 mg (10 mmol) of silica. The mixture was heated at 70 °C in a sealed tube for 2–3 days and then, filtered over a short pad of silica eluted with diethyl ether. The crude material was purified by flash column chromatography (pentane/AcOEt 3:1) to obtain the desired product in pure form, 75 % yield. Orange solid, mp = 92 °C. ^1H NMR (300 MHz, CDCl_3) δ 8.05–8.01 (m, 2H), 7.54 (ddt, $J = 5.4, 4.2, 2.1$ Hz, 1H), 7.47–7.40 (m, 2H), 6.63 (dd, $J = 5.7, 3.0$ Hz, 1H), 6.16 (d, $J = 5.7$ Hz, 1H), 3.02–2.98 (m, 1H), 2.83 (s, 1H), 2.26–2.11 (m, 2H), 1.84 (dd, $J = 12.9, 4.6$ Hz, 1H), 1.12 (s, 3H), 0.96 (dd, $J = 12.9, 1.6$ Hz, 1H).

^{13}C NMR (101 MHz, CDCl_3) δ 213.2 (C), 200.2 (C), 140.2 (CH), 136.9 (C), 133.1 (CH), 130.5 (CH), 129.5 (CH), 128.5 (CH), 73.8 (C), 60.8 (CH), 55.6 (C), 45.8 (CH), 39.4 (CH_2), 35.8 (CH_2), 12.5 (CH_3).

IR (neat) $\nu = 706, 833, 906, 1051, 1063, 1241, 1284, 1447, 1597, 1660, 1748\text{ cm}^{-1}$.

HRMS calculated for $[C_{17}H_{16}O_2Na]^+$: 275.1043, found: 275.1039.

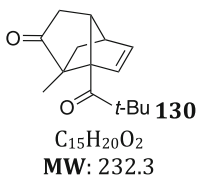


Prepared according to the same procedure than for **128**, quantitative yield. Brown oil. **1H NMR (400 MHz, $CDCl_3$)** δ 6.66 (dd, $J = 5.7, 2.6$ Hz, 1H), 6.22 (d, $J = 6.0$ Hz, 1H), 2.70 (br s, 2H), 2.18 (tt, $J = 7.8, 4.6$ Hz, 1H), 2.12 (d, $J = 3.5$ Hz, 2H), 1.80 (dd, $J = 12.9, 4.2$ Hz, 1H), 1.02 (s, 3 H), 1.09–0.83 (m, 5H).

^{13}C NMR (100 MHz, $CDCl_3$) δ 213.5 (C), 209.6 (C), 142.9 (CH), 128.5 (CH), 75.1 (C), 58.9 (CH), 54.4 (C), 45.5 (CH), 40.0 (CH_2), 35.7 (CH_2), 19.5 (CH), 12.0 (CH_3), 11.7 (CH_2), 11.4 (CH_2).

IR (neat) $\nu = 2959, 1749, 1682, 1446, 1383, 1236, 1215, 1191, 1076, 1056, 944, 750, 731\text{ cm}^{-1}$.

HRMS calculated for $[C_{14}H_{16}O_2Na]^+$: 239.1043, found: 239.1034.

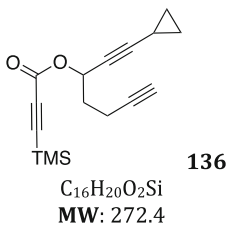


Prepared according to the same procedure than for **128**, 55 %. Brown oil. **1H NMR (300 MHz, $CDCl_3$)** δ 6.53 (dd, $J = 5.8, 3.0$ Hz, 1H), 6.26 (d, $J = 5.8$ Hz, 1H), 2.71–2.61 (m, 2H), 2.09 (m, 2H), 1.70 (dd, $J = 13.0, 4.7$ Hz, 1H), 1.21 (s, 9H), 0.95 (s, 3H), 0.84 (dd, $J = 12.9, 1.6$ Hz, 1H).

^{13}C NMR (101 MHz, $CDCl_3$) δ 213.8 (C), 213.0 (C), 140.5 (CH), 128.6 (CH), 74.2 (C), 59.4 (CH), 56.1 (C), 45.5 (CH), 45.3 (C), 39.3 (CH_2), 35.4 (CH_2), 27.1 (CH_3), 12.2 (CH_3).

IR (neat) $\nu = 2962, 1749, 1677, 1479, 1460, 1367, 1138, 1056, 1025, 914, 733\text{ cm}^{-1}$.

HRMS calculated for $[C_{15}H_{20}O_2Na]^+$: 255.1356, found: 255.1348.



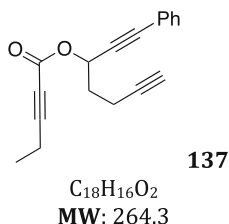
To a solution of alcohol **88** (139 mg, 0.96 mmol, 1 equiv.) in MeOH is added K_2CO_3 (400 mg, 2.88 mmol, 3 equiv.). After stirring for 2 h, about 90 % of the solvent is removed under reduced pressure, and the resulting solution is diluted with water and Et_2O . The aqueous layer is extracted twice with Et_2O and the combined organic extracts are washed with brine and water, dried over $MgSO_4$ and evaporated under reduced pressure to afford the pure alcohol as colorless oil in 98 % yield.

To a solution of the alcohol (92 mg, 0.62 mmol, 1 equiv.), trimethylsilylpropynoic acid (132 mg, 1.93 mmol, 1.5 equiv.) and DMAP (8 mg, 0.06 mmol, 0.1 equiv.) in CH_2Cl_2 (3 mL) is added at 0 °C EDCI (143 mg, 0.75 mmol, 1.2 equiv.). The mixture is stirred at rt overnight, then quenched with brine. The aqueous layer is extracted with CH_2Cl_2 , and the combined organic extracts are washed with a saturated aqueous solution of $NaHCO_3$, dried over $MgSO_4$ and filtered. The solvent is removed under reduced pressure and the residue is purified by flash column chromatography to yield the desired product in 18 % yield. 1H NMR (400 MHz, $CDCl_3$) δ 4.44 (ddd, $J = 7.2, 5.9, 1.7$ Hz, 1H), 2.33–2.25 (m, 2H), 1.92 (t, $J = 2.7$ Hz, 1H), 1.87–1.78 (m, 2H), 1.27–1.18 (m, 1H), 0.77–0.71 (m, 2H), 0.68–0.61 (m, 2H), 0.15 (s, 9H).

^{13}C NMR (101 MHz, $CDCl_3$) δ 207.7, 88.4, 83.9, 76.2, 72.9, 71.6, 68.6, 61.5, 37.6, 14.6, 8.2, 8.1, 0.3 (3C), –0.4.

IR (neat) $\nu = 3307, 2959, 1599, 1490, 1251, 1088, 1068, 978, 838, 753, 689, 630\text{ cm}^{-1}$.

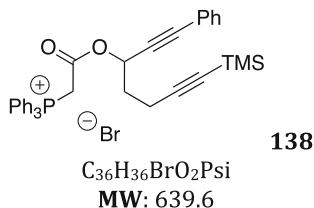
HRMS calculated for $[C_{15}H_{20}O_2Na]^+$: 255.1356, found: 255.1348.



Prepared according to the same procedure than for **136** replacing trimethylsilylpropynoic acid by pent-2-ynoic acid, 53 % (78 % brsm). 1H NMR (400 MHz, $CDCl_3$) δ 7.44 (dd, $J = 7.6, 1.9$ Hz, 2H), 7.36–7.28 (m, 3H), 5.76 (t, $J = 6.5$ Hz, 1H), 2.45 (td, $J = 6.9, 2.6$ Hz, 2H), 2.37 (q, $J = 7.5$ Hz, 2H), 2.15 (p, $J = 6.9$ Hz, 2H), 2.00 (t, $J = 2.6$ Hz, 1H), 1.22 (t, $J = 7.5$ Hz, 3H).

^{13}C NMR (101 MHz, $CDCl_3$) δ 152.6, 131.9 (2C), 128.8, 128.3 (2C), 121.9, 91.8, 86.5, 84.8, 82.4, 72.1, 69.4, 64.7, 33.6, 14.6, 12.5, 12.5.

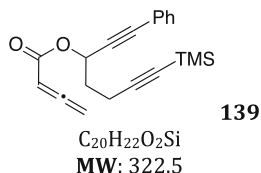
IR (neat) $\nu = 3297, 2234, 1711, 1232, 1047, 751, 636\text{ cm}^{-1}$.



To a solution of alcohol **86** (750 mg, 2.93 mmol, 1 equiv.) in CH_2Cl_2 (30 mL), is added dropwise at 0 °C bromoacetyl bromide (0.512 mL, 5.86 mmol, 2 equiv.). The mixture is stirred at rt for 4 d, then quenched with a 10 % aqueous solution of K_2CO_3 . The aqueous layer is extracted with CH_2Cl_2 , and the combined organic extracts are washed with brine, dried over MgSO_4 and filtered. After removal of the solvents under reduced pressure, the crude residue is purified by flash column chromatography (PE/AcOEt 95:5 to 9:1) to yield the desired bromoacetate derivative in 55 % yield as a brown oil. ^1H NMR (300 MHz, CD_3CN) δ 7.44 (dd, $J = 7.3, 2.1$ Hz, 2H), 7.36–7.28 (m, 3H), 5.74 (t, $J = 6.4$ Hz, 1H), 3.88 (s, 2H), 2.49 (t, $J = 7.5$ Hz, 2H), 2.15 (q, $J = 6.8$ Hz, 2H), 0.87 (q, $J = 6.7, 5.8$ Hz, 1H), 0.16 (s, 9H).

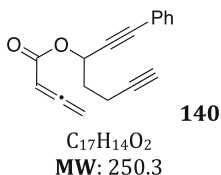
To a solution of the bromoacetate (465 mg, 1.2 mmol, 1 equiv.) in MeCN (91 mL) is added PPh_3 (388 mg, 1.5 mmol, 1.2 equiv.). The reaction mixture is stirred at rt for 24 h, and then the solvent is removed under reduced pressure to give a brown foaming solid. The latter is washed twice with Et_2O to give phosphonium salt **138** as a brown solid in quantitative yield. ^1H NMR (400 MHz, CD_3CN) δ 7.92–7.76 (m, 10H), 7.71–7.61 (m, 7H), 7.43–7.30 (m, 6H), 5.56 (t, $J = 6.4$ Hz, 1H), 5.47–5.24 (m, 2H), 2.37–2.15 (m, 2H), 1.84 (q, $J = 7.4$ Hz, 2H), 0.10 (s, 9H). ^{31}P NMR (162 MHz, CD_3CN) δ 21.8 (t, $J = 26.4$ Hz).

^{13}C NMR (101 MHz, CD_3CN) δ 164.3, 136.1 (d, $J = 2.8$ Hz, 3C), 134.9 (d, $J = 10.8$ Hz, 6C), 134.27 (d, $J = 19.6$ Hz, 3C), 132.6 (2C), 130.9 (d, $J = 13.2$ Hz, 6C), 130.1, 129.5 (2C), 122.1, 119.1, 106.1, 87.2, 86.2, 85.2, 66.4, 34.0, 32.5, 32.0, 16.1, 0.0 (3C).



Phosphonium salt **138** (495 mg, 0.77 mmol, 1 equiv.) is diluted in CH_2Cl_2 and the solution is introduced in a small separatory funnel. 1.3 mL of a 1.2 M aqueous solution of NaOH (1.55 mmol, 2 equiv.) is then added, and the biphasic system is shaken vigorously. The aqueous layer is extracted with CH_2Cl_2 , and the combined organic extracts are dried over MgSO_4 and filtered. Removal of the solvent under reduced pressure affords a brown oil, which is diluted in CH_2Cl_2 (8 mL). NEt_3 is added to the solution, followed by dropwise addition of acyl chloride at rt. The resulting mixture is stirred at rt overnight, and then filtered on short plug of silica using a 2:1 mixture of pentane/ Et_2O as eluent. Allenic derivative **155** is obtained pure as a brown oil in 80 % yield. ^1H NMR (400 MHz, CDCl_3) δ 7.46–7.42 (m, 2H), 7.34–7.28 (m, 3H), 5.73 (t, $J = 6.4$ Hz, 1H), 5.68 (t, $J = 6.5$ Hz, 1H), 5.26 (d, $J = 6.6$ Hz, 2H), 2.51–2.44 (m, 2H), 2.17–2.09 (m, 2H), 0.15 (s, 9H).

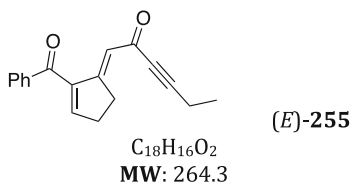
^{13}C NMR (101 MHz, CDCl_3) δ 216.3, 164.6, 132.1 (2C), 128.8, 128.4 (2C), 122.2, 105.4, 87.8, 86.1, 85.7, 85.6, 79.7, 64.0, 34.1, 16.0, 0.2 (3C).



Desilylation was performed under classical conditions using KF in DMSO. Brown oil, 63 %. **^1H NMR (400 MHz, CDCl_3)** δ 7.46–7.42 (m, 2H), 7.34–7.28 (m, 3H), 5.77 (t, J = 6.4 Hz, 1H), 5.68 (t, J = 6.5 Hz, 1H), 5.26 (d, J = 6.5 Hz, 2H), 2.47–2.41 (m, 2H), 2.18–2.10 (m, 2H), 2.00 (t, J = 2.7 Hz, 1H).

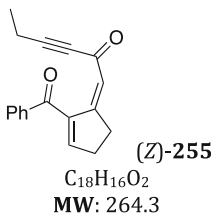
^{13}C NMR (101 MHz, CDCl_3) δ 216.4, 164.7, 132.1 (2C), 128.9, 128.4 (2C), 122.2, 87.8, 86.1, 85.6, 82.8, 79.7, 69.4, 63.9, 33.9, 14.7.

IR (neat) ν = 3296, 2232, 1969, 1715, 1244, 1149, 854, 757, 690, 636 cm^{-1} .



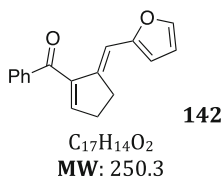
Prepared according to *GPI*, 39 %. **^1H NMR (400 MHz, CDCl_3)** δ 7.81–7.76 (m, 2H), 7.65–7.55 (m, 1H), 7.51–7.42 (m, 2H), 6.95 (t, J = 2.9 Hz, 1H), 6.18 (t, J = 2.3 Hz, 1H), 3.08–2.98 (m, 2H), 2.83–2.74 (m, 2H), 2.62 (q, J = 7.4 Hz, 2H), 1.19 (t, J = 7.4 Hz, 3H).

^{13}C NMR (101 MHz, CDCl_3) δ 192.8, 188.8, 163.2, 155.6, 142.5, 138.1, 133.2, 129.4 (2C), 128.7 (2C), 99.2, 94.3, 90.7, 38.9, 31.7, 31.1, 8.5.



Prepared according to *GPI*, 59 %. **^1H NMR (400 MHz, CDCl_3)** δ 7.85–7.79 (m, 2H), 7.63–7.57 (m, 1H), 7.53–7.43 (m, 2H), 7.10 (t, J = 2.8 Hz, 1H), 6.80 (t, J = 2.4 Hz, 1H), 3.35–3.27 (m, 2H), 2.81 (dq, J = 4.7, 2.5 Hz, 2H), 2.36 (q, J = 7.5 Hz, 2H), 1.19 (t, J = 7.5 Hz, 3H).

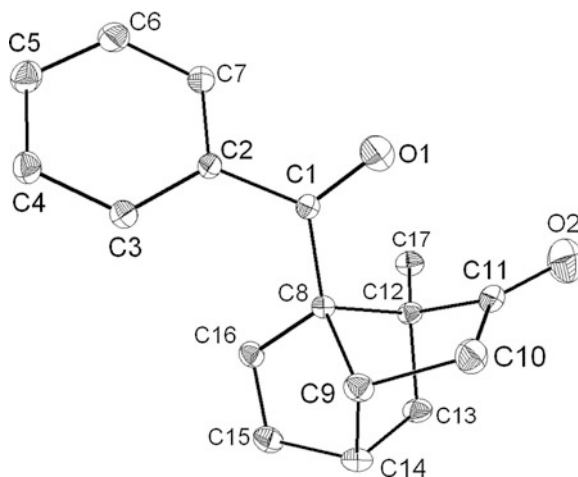
^{13}C NMR (101 MHz, CDCl_3) δ 193.02, 177.42, 162.78, 157.44, 143.74, 137.88, 133.46, 129.58 (2C), 128.71 (2C), 120.75, 93.96, 83.11, 33.02, 32.34, 12.95, 12.91.



Prepared according to *GPI*, 74 %. **^1H NMR (400 MHz, CDCl_3)** δ 7.88–7.83 (m, 2H), 7.62–7.54 (m, 1H), 7.50–7.42 (m, 2H), 7.41 (d, $J = 1.6$ Hz, 1H), 6.82 (t, $J = 2.4$ Hz, 1H), 6.62 (t, $J = 2.8$ Hz, 1H), 6.42 (dd, $J = 3.3, 1.8$ Hz, 1H), 6.26 (d, $J = 3.3$ Hz, 1H), 3.12–3.02 (m, 2H), 2.83–2.73 (m, 2H).

^{13}C NMR (101 MHz, CDCl_3) δ 194.2, 154.3, 148.4, 144.2, 142.6, 141.7, 138.5, 133.0, 129.6 (2C), 128.5 (2C), 111.7, 110.6, 108.9, 32.1, 30.5.

X-ray structure of compound 128



Scheme 5 Structure of compound **128** in the solid-state. Anisotropic displacement parameters are drawn at the 50 % probability level and hydrogen atoms are omitted for clarity

Table 1 Crystal structure information:

Formula C17H16O2			
Crystal class	Monoclinic	Space group P 21/c	
a	20.7922(8)	Alpha	90
b	8.9315(3)	Beta	110.436(1)
c	14.7308(5)	Gamma	9
Volume	2563.42(16)	Z	8
Radiation type	Mo K α	Wavelength	0.71073
ρ	1.31	Mr	504.63
μ	0.084	Temperature (K)	200(2)
Size	0.08 \times 0.12 \times 0.20		
Colour	Colourless	Shape	Plate
Cell from	593 reflections	Theta range	4–28
Diffractometer type APEX2	Scan type	2 Theta/OMEG	
Absorption type	Multi-scan	Transmission range	0.97–0.99
Reflections measured	24983	Independent reflections	6784
Rint	0.02	Theta max	29.14
Hmin, Hmax	–28	28	
Kmin, Kmax	–11	12	
Lmin, Lmax	–20	19	
Refinement on Fsqd			
R[I > 2 σ (I)]	0.043	WR2(all)	0.126
Max shift/su	0.0007		
Delta Rho min	–0.20	Delta Rho max	0.40
Reflections used	6766		
Number of parameters	344	Goodness of fit	0.947

Table 2 Fractional atomic coordinates for C17H16O2

Atom	x/a	y/b	z/c	U(eq v)
C(1)	0.98207(5)	0.78181(11)	0.36047(8)	0.0227
C(2)	1.05734(5)	0.76066(11)	0.41192(8)	0.0224
C(3)	1.09520(6)	0.65413(12)	0.38298(8)	0.0248
C(4)	1.16591(6)	0.64570(13)	0.42981(9)	0.0294
C(5)	1.19843(6)	0.74094(14)	0.50687(10)	0.0339
C(6)	1.16093(6)	0.84593(14)	0.53696(9)	0.0337
C(7)	1.09045(6)	0.85693(13)	0.48891(9)	0.0282
C(8)	0.93460(5)	0.64881(11)	0.32637(7)	0.0205
C(9)	0.90499(6)	0.61984(12)	0.21391(8)	0.0250
C(10)	0.85905(6)	0.75333(14)	0.17045(8)	0.0304
C(11)	0.83472(5)	0.80261(13)	.25268(8)	0.0269
C(12)	0.86114(5)	0.68455(12)	0.33132(8)	0.0232
C(13)	0.81875(6)	0.54563(13)	0.27869(9)	0.0309
C(14)	0.86505(6)	0.47867(13)	0.22530(8)	0.0293
C(15)	0.91939(7)	0.39392(13)	0.30357(9)	0.0317

(continued)

Table 2 (continued)

Atom	x/a	y/b	z/c	U(eqv)
C(16)	0.95924(6)	0.49399(12)	0.36426(8)	0.0269
C(17)	0.85688(7)	0.72245(14)	0.42902(9)	0.0329
C(21)	0.51156(5)	0.78664(11)	0.37950(7)	0.0228
C(22)	0.43621(5)	0.76225(11)	0.35398(8)	0.0227
C(23)	0.40123(6)	0.85038(13)	0.39999(8)	0.0286
C(24)	0.33084(6)	0.83177(14)	0.37729(10)	0.0337
C(25)	0.29531(6)	0.72825(14)	0.30778(10)	0.0337
C(26)	0.32960(6)	0.64158(12)	0.26075(9)	0.0297
C(27)	0.40015(5)	0.65725(11)	0.28467(8)	0.0245
C(28)	0.55938(5)	0.65461(11)	0.39016(7)	0.0199
C(29)	0.58985(6)	0.63150(12)	0.30724(7)	0.0239
C(30)	0.63603(6)	0.76643(13)	0.31341(8)	0.0288
C(31)	0.66029(5)	0.80813(12)	0.42085(8)	0.0262
C(32)	0.63230(5)	0.68668(12)	0.46945(7)	0.0222
C(33)	0.67460(6)	0.54909(13)	0.45600(9)	0.0282
C(34)	0.62916(6)	0.48804(12)	0.35488(8)	0.0274
C(35)	0.57409(6)	0.40043(12)	0.37640(9)	0.0289
C(36)	0.53440(5)	0.49854(12)	0.39995(8)	0.0244
C(37)	0.63621(6)	0.71711(15)	0.57203(8)	0.0318
O(1)	0.95826(4)	0.90865(9)	0.34766(7)	0.0339
O(2)	0.79740(5)	0.90725(11)	0.25123(7)	0.0387
O(11)	0.53503(4)	0.91346(9)	0.39428(7)	0.0346
O(12)	0.69878(5)	0.90907(11)	0.46004(7)	0.0382

Table 3 Interatomic distances (Å) for C17H16O2

C(1)–C(2)	1.4936(14)	C(1)–C(8)	1.5137(14)
C(1)–O(1)	1.2243(13)	C(2)–C(3)	1.3932(14)
C(2)–C(7)	1.3980(15)	C(3)–C(4)	1.3910(15)
C(4)–C(5)	1.3904(18)	C(5)–C(6)	1.3874(18)
C(6)–C(7)	1.3906(16)	C(8)–C(9)	1.5743(14)
C(8)–C(12)	1.5867(14)	C(8)–C(16)	1.5121(14)
C(9)–C(10)	1.5221(16)	C(9)–C(14)	1.5508(16)
C(10)–C(11)	1.5314(16)	C(11)–C(12)	1.5203(15)
C(11)–O(2)	1.2100(14)	C(12)–C(13)	1.5621(15)
C(12)–C(17)	1.5108(15)	C(13)–C(14)	1.5594(16)
C(14)–C(15)	1.5065(17)	C(15)–C(16)	1.3294(16)
C(21)–C(22)	1.4940(14)	C(21)–C(28)	1.5149(14)
C(21)–O(11)	1.2224(13)	C(22)–C(23)	1.3972(15)
C(22)–C(27)	1.3964(15)	C(23)–C(24)	1.3928(17)
C(24)–C(25)	1.3859(19)	C(25)–C(26)	1.3903(18)
C(26)–C(27)	1.3908(15)	C(28)–C(29)	1.5736(14)
C(28)–C(32)	1.5839(14)	C(28)–C(36)	1.5119(14)
C(29)–C(30)	1.5237(15)	C(29)–C(34)	1.5498(15)

(continued)

Table 3 (continued)

C(1)–C(2)	1.4936(14)	C(1)–C(8)	1.5137(14)
C(30)–C(31)	1.5298(16)	C(31)–C(32)	1.5229(15)
C(31)–O(12)	1.2100(14)	C(32)–C(33)	1.5636(15)
C(32)–C(37)	1.5094(15)	C(33)–C(34)	1.5575(16)
C(34)–C(35)	1.5092(16)	C(35)–C(36)	1.3300(15)

Table 4 Bond angles (°) for C17H16O2

C(2)–C(1)–C(8)	121.03(9)	C(2)–C(1)–O(1)	119.40(9)
C(8)–C(1)–O(1)	119.56(9)	C(1)–C(2)–C(3)	122.34(9)
C(1)–C(2)–C(7)	117.76(9)	C(3)–C(2)–C(7)	119.83(10)
C(2)–C(3)–C(4)	119.83(10)	C(3)–C(4)–C(5)	120.02(10)
C(4)–C(5)–C(6)	120.46(10)	C(5)–C(6)–C(7)	119.67(11)
C(2)–C(7)–C(6)	120.16(10)	C(1)–C(8)–C(9)	116.64(8)
C(1)–C(8)–C(12)	110.70(8)	C(9)–C(8)–C(12)	93.00(8)
C(1)–C(8)–C(16)	119.84(9)	C(9)–C(8)–C(16)	101.29(8)
C(12)–C(8)–C(16)	111.99(8)	C(8)–C(9)–C(10)	105.74(8)
C(8)–C(9)–C(14)	92.71(8)	C(10)–C(9)–C(14)	113.65(9)
C(9)–C(10)–C(11)	102.98(9)	C(10)–C(11)–C(12)	105.78(9)
C(10)–C(11)–O(2)	126.51(11)	C(12)–C(11)–O(2)	127.45(11)
C(8)–C(12)–C(11)	101.66(8)	C(8)–C(12)–C(13)	101.70(8)
C(11)–C(12)–C(13)	100.46(9)	C(8)–C(12)–C(17)	117.80(9)
C(11)–C(12)–C(17)	116.39(9)	C(13)–C(12)–C(17)	116.11(9)
C(12)–C(13)–C(14)	102.37(8)	C(9)–C(14)–C(13)	101.01(8)
C(9)–C(14)–C(15)	101.80(9)	C(13)–C(14)–C(15)	103.70(10)
C(14)–C(15)–C(16)	107.56(10)	C(8)–C(16)–C(15)	108.38(10)
C(22)–C(21)–C(28)	120.34(9)	C(22)–C(21)–O(11)	119.89(9)
C(28)–C(21)–O(11)	119.74(9)	C(21)–C(22)–C(23)	118.26(9)
C(21)–C(22)–C(27)	122.01(9)	C(23)–C(22)–C(27)	119.71(10)
C(22)–C(23)–C(24)	119.84(11)	C(23)–C(24)–C(25)	120.10(11)
C(24)–C(25)–C(26)	120.38(10)	C(25)–C(26)–C(27)	119.79(11)
C(22)–C(27)–C(26)	120.16(10)	C(21)–C(28)–C(29)	116.69(8)
C(21)–C(28)–C(32)	111.12(8)	C(29)–C(28)–C(32)	93.15(7)
C(21)–C(28)–C(36)	119.52(9)	C(29)–C(28)–C(36)	101.41(8)
C(32)–C(28)–C(36)	111.63(8)	C(28)–C(29)–C(30)	105.43(8)
C(28)–C(29)–C(34)	92.79(8)	C(30)–C(29)–C(34)	113.90(9)
C(29)–C(30)–C(31)	103.15(9)	C(30)–C(31)–C(32)	105.72(9)
C(30)–C(31)–O(12)	126.82(11)	C(32)–C(31)–O(12)	127.16(11)
C(28)–C(32)–C(31)	101.93(8)	C(28)–C(32)–C(33)	101.56(8)
C(31)–C(32)–C(33)	100.13(8)	C(28)–C(32)–C(37)	118.29(9)
C(31)–C(32)–C(37)	116.53(9)	C(33)–C(32)–C(37)	115.62(9)
C(32)–C(33)–C(34)	102.49(8)	C(29)–C(34)–C(33)	101.04(8)
C(29)–C(34)–C(35)	101.82(9)	C(33)–C(34)–C(35)	103.41(9)
C(34)–C(35)–C(36)	107.37(9)	C(28)–C(36)–C(35)	108.52(9)

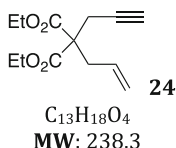
Table 5 Anisotropic thermal parameters for C17H16O2

Atom	u(11)	u(22)	u(33)	u(23)	u(13)	u(12)
C(1)	0.0198(5)	0.0216(4)	0.0266(5)	−0.0018(4)	0.0080(4)	−0.0003(4)
C(2)	0.0186(4)	0.0214(4)	0.0261(5)	0.0008(4)	0.0064(4)	−0.0003(4)
C(3)	0.0233(5)	0.0220(5)	0.0282(5)	0.0003(4)	0.0078(4)	0.0012(4)
C(4)	0.0227(5)	0.0263(5)	0.0384(6)	0.0039(4)	0.0096(4)	0.0045(4)
C(5)	0.0217(5)	0.0339(6)	0.0390(6)	0.0045(5)	0.0015(5)	0.0012(4)
C(6)	0.0281(6)	0.0337(6)	0.0319(6)	−0.0047(5)	0.0011(5)	−0.0034(5)
C(7)	0.0260(5)	0.0270(5)	0.0297(5)	−0.0045(4)	0.0074(4)	−0.0002(4)
C(8)	0.0203(4)	0.0196(4)	0.0211(4)	−0.0010(3)	0.0066(4)	−0.0006(3)
C(9)	0.0289(5)	0.0259(5)	0.0212(5)	−0.0023(4)	0.0099(4)	0.0004(4)
C(10)	0.0341(6)	0.0322(5)	0.0227(5)	0.0033(4)	0.0072(4)	0.0036(5)
C(11)	0.0197(5)	0.0288(5)	0.0291(5)	−0.0015(4)	0.0045(4)	0.0006(4)
C(12)	0.0215(5)	0.0255(5)	0.0238(5)	−0.0035(4)	0.0092(4)	−0.0031(4)
C(13)	0.0266(5)	0.0306(5)	0.0357(6)	−0.0069(5)	0.0112(5)	−0.0089(4)
C(14)	0.0337(6)	0.0260(5)	0.0270(5)	−0.0081(4)	0.0089(4)	−0.0051(4)
C(15)	0.0401(6)	0.0221(5)	0.0340(6)	−0.0007(4)	0.0143(5)	−0.0013(4)
C(16)	0.0302(5)	0.0225(5)	0.0274(5)	0.0026(4)	0.0095(4)	0.0024(4)
C(17)	0.0364(6)	0.0373(6)	0.0307(6)	−0.0058(5)	0.0190(5)	−0.0035(5)
C(21)	0.0203(5)	0.0221(5)	0.0236(5)	−0.0021(4)	0.0047(4)	0.0014(4)
C(22)	0.0201(5)	0.0209(4)	0.0258(5)	0.0011(4)	0.0062(4)	0.0028(4)
C(23)	0.0289(5)	0.0275(5)	0.0292(5)	−0.0012(4)	0.0097(4)	0.0064(4)
C(24)	0.0303(6)	0.0350(6)	0.0400(6)	0.0041(5)	0.0176(5)	0.0098(5)
C(25)	0.0214(5)	0.0325(6)	0.0480(7)	0.0094(5)	0.0131(5)	0.0042(4)
C(26)	0.0222(5)	0.0237(5)	0.0388(6)	0.0026(4)	0.0050(4)	−0.0006(4)
C(27)	0.0220(5)	0.0211(5)	0.0285(5)	0.0002(4)	0.0064(4)	0.0015(4)
C(28)	0.0186(4)	0.0197(4)	0.0205(4)	−0.0003(3)	0.0056(4)	0.0012(3)
C(29)	0.0275(5)	0.0245(5)	0.0202(4)	−0.0010(4)	0.0087(4)	0.0006(4)
C(30)	0.0319(6)	0.0295(5)	0.0279(5)	0.0022(4)	0.0142(4)	−0.0027(4)
C(31)	0.0210(5)	0.0275(5)	0.0303(5)	−0.0006(4)	0.0093(4)	−0.0006(4)
C(32)	0.0187(4)	0.0260(5)	0.0200(4)	−0.0006(4)	0.0044(4)	0.0007(4)
C(33)	0.0220(5)	0.0294(5)	0.0318(5)	0.0031(4)	0.0077(4)	0.0063(4)
C(34)	0.0296(5)	0.0251(5)	0.0304(5)	−0.0012(4)	0.0139(4)	0.0052(4)
C(35)	0.0339(6)	0.0210(5)	0.0321(5)	0.0002(4)	0.0116(5)	0.0008(4)
C(36)	0.0244(5)	0.0227(5)	0.0252(5)	0.0010(4)	0.0076(4)	−0.0018(4)
C(37)	0.0306(6)	0.0412(6)	0.0209(5)	−0.0028(4)	0.0057(4)	−0.0022(5)
O(1)	0.0241(4)	0.0214(4)	0.0530(5)	−0.0013(3)	0.0094(4)	0.0015(3)
O(2)	0.0287(4)	0.0382(5)	0.0455(5)	−0.0012(4)	0.0083(4)	0.0118(4)
O(11)	0.0268(4)	0.0219(4)	0.0499(5)	−0.0058(3)	0.0068(4)	−0.0010(3)
O(12)	0.0319(5)	0.0379(5)	0.0447(5)	−0.0086(4)	0.0132(4)	−0.0126(4)

Table 6 Hydrogen atoms fractional atomic coordinates for C17H16O2

Atom	x/a	y/b	z/c	U(iso)
H(31)	1.0727	0.5863	0.3319	0.0418(8)
H(41)	1.1919	0.5741	0.4089	0.0418(8)
H(51)	1.2468	0.7346	0.5383	0.0418(8)
H(61)	1.1837	0.9099	0.5912	0.0418(8)
H(71)	1.0643	0.9305	0.5082	0.0418(8)
H(91)	0.9390	0.6010	0.1861	0.0418(8)
H(101)	0.8838	0.8306	0.1527	0.0418(8)
H(102)	0.8211	0.7244	0.1143	0.0418(8)
H(131)	0.8119	0.4760	0.3235	0.0418(8)
H(132)	0.7748	0.5746	0.2337	0.0418(8)
H(141)	0.8421	0.4244	0.1672	0.0418(8)
H(151)	0.9240	0.2875	0.3081	0.0418(8)
H(161)	0.9971	0.4714	0.4223	0.0418(8)
H(171)	0.8113	0.7417	0.4233	0.0418(8)
H(172)	0.8845	0.8094	0.4547	0.0418(8)
H(173)	0.8747	0.6411	0.4726	0.0418(8)
H(231)	0.4259	0.9245	0.4469	0.0418(8)
H(241)	0.3066	0.8918	0.4089	0.0418(8)
H(251)	0.2472	0.7148	0.2918	0.0418(8)
H(261)	0.3048	0.5722	0.2124	0.0418(8)
H(271)	0.4238	0.5955	0.2538	0.0418(8)
H(291)	0.5558	0.6165	0.2448	0.0418(8)
H(301)	0.6736	0.7392	0.2943	0.0418(8)
H(302)	0.6113	0.8459	0.2739	0.0418(8)
H(331)	0.7183	0.5770	0.4573	0.0418(8)
H(332)	0.6787	0.4759	0.5055	0.0418(8)
H(341)	0.6531	0.4366	0.3198	0.0418(8)
H(351)	0.5690	0.2937	0.3739	0.0418(8)
H(361)	0.4963	0.4751	0.4196	0.0418(8)
H(371)	0.6828	0.7347	0.6116	0.0418(8)
H(372)	0.6099	0.8040	0.5729	0.0418(8)
H(373)	0.6190	0.6342	0.5960	0.0418(8)

Experimental Section Related to Chap. 4

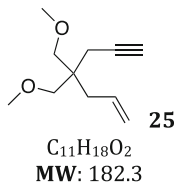


Diethylmalonate **26** (0.45 mL, 2.9 mmol) was added to a suspension of NaH (0.14 g, 2.9 mmol) in THF (40 mL) at 0 °C, under an argon atmosphere and the solution was stirred for 15 min at rt. Propargyl bromide (0.6 g, 2.9 mmol) was added and stirring was kept on for an additional 3 h. After dilution with ether (30 mL), the solution was washed with a saturated NH_4Cl solution ($3 \times 50\text{ mL}$) and the aqueous phase was further extracted with ether ($3 \times 40\text{ mL}$). The combined organic layers were dried over anhydrous MgSO_4 , then concentrated *in vacuo*. The reaction residue was purified by silica gel chromatography (AcOEt/pentane, 5:95) affording the desired product in 54 % yield.

Diethyl 2-(prop-2-ynyl)malonate was added to a suspension of NaH (1.1 equiv.) in THF (0.5 M) at 0 °C, under an argon atmosphere and the solution was stirred for 15 min at room temperature. Allyl bromide (1.2 equiv.) was added and stirring was kept on for an additional 3 h. After dilution with ether, the solution was washed with a saturated NH_4Cl solution ($3 \times 50\text{ mL}$) and the aqueous phase was further extracted with ether. The combined organic layers were dried over anhydrous MgSO_4 , then concentrated *in vacuo*. The reaction residue was purified by silica gel chromatography (AcOEt: pentane, 5:95) affording the desired enyne **24** in 97 % yield. ^1H NMR (300 MHz, CDCl_3) δ 5.66–5.57 (m, 1H), 5.33–4.98 (m, 2H), 4.19 (q, $J = 7.1\text{ Hz}$, 4H), 2.89–2.79 (m, 4H), 2.01 (t, $J = 2.5\text{ Hz}$, 1H), 1.24 (t, $J = 7.1\text{ Hz}$, 6H).

^{13}C NMR (75 MHz, CDCl_3) δ 169.8 (2C), 131.9 (CH), 119.9 (CH_2), 79.0 (C), 71.5 (CH), 61.7 (2CH_2), 56.7 (C), 36.5 (CH_2), 22.7 (CH_2), 14.2 (2CH_3).

IR (neat) $\nu = 2982, 2936, 2587, 1734, 1214, 1192, 926\text{ cm}^{-1}$.



To a suspension of LAH (1.2 g, 31.5 mmol, 2.5 equiv.) in Et_2O (13 mL) is added dropwise at 0 °C enyne **24** (3 g, 12.6 mmol, 1 equiv.). The mixture is allowed to warm to rt and stirred for 4 h, then cooled down to 0 °C and quenched by a dropwise addition of a saturated aqueous solution of MgSO_4 until the aluminium salts have been hydrolyzed. The mixture is then filtered over a short pad of silica/celite, the remaining solids are washed with Et_2O , and the filtrate evaporated under reduced pressure to afford the diol in pure form as a colorless oil in 87 % yield. ^1H NMR (300 MHz, CDCl_3) δ 5.95–5.67 (m, 1H), 5.26–5.02

(m, 2H), 3.61 (br, 4H), 2.93 (br s, 2H), 2.25 (dd, $J = 8.3, 2.7$ Hz, 2H), 2.22–2.09 (m, 2H), 2.02 (dd, $J = 3.5, 1.9$ Hz, 1H).

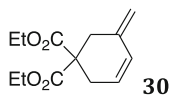
^{13}C NMR (75 MHz, CDCl_3) δ 133.3 (CH), 118.8 (CH_2), 81.0 (C), 71.0 (CH), 67.2 (2CH_2), 42.1 (C), 36.1 (CH_2), 21.5 (CH_2).

IR (neat) $\nu = 3412, 3065, 3001, 2971, 1458, 1023, 973\text{ cm}^{-1}$.

The diol (2.4 g, 15.8 mmol, 1 equiv.) was added to a suspension of NaH (1.325 g, 33.1 mmol, 2.1 equiv.) in THF (30 mL) at 0 °C, under an argon atmosphere and the solution was stirred for 15 min at rt. Methyl iodide (2.16 mL, 34.7 mmol, 2.2 equiv.) was added and stirring was kept on for an additional 3 h. After dilution with ether (30 mL), the solution was washed with a saturated NH_4Cl solution and the aqueous phase was further extracted with ether. The combined organic layers were dried over anhydrous MgSO_4 , then concentrated in vacuo. The reaction residue was purified by silica gel chromatography (Et_2O /pentane, 1:99) affording the desired enyne **25** in 90 % yield. ^1H NMR (400 MHz, CDCl_3) δ 1.97 (t, $J = 1.8$ Hz, 1H), 2.17 (dt, $J = 7.5, 1.2$ Hz, 2H), 2.21 (d, $J = 1.8$ Hz, 2H), 3.25 (d, $J = 2.1$ Hz, 4H), 3.33 (s, 6H), 5.05–5.15 (m, 2H), 5.80 (ddt, $J = 10.2, 17.1, 7.5$ Hz, 1H).

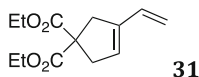
^{13}C NMR (100 MHz, CDCl_3) δ 22.0, 36.2, 41.7, 59.3, 70.1, 74.2, 81.2, 118.1, 133.7.

IR (neat) $\nu = 3292, 2934, 2876, 2100, 1641, 1452, 1200, 1109, 914\text{ cm}^{-1}$.



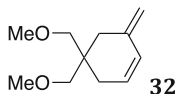
$\text{C}_{13}\text{H}_{18}\text{O}_4$
MW: 238.3

Prepared according to *GPI*. ^1H NMR (400 MHz, CDCl_3) δ 6.14 (dt, $J = 2.0, 10.0$ Hz, 1H), 5.77 (dt, $J = 0.8, 8.8$ Hz, 1H), 4.90 (dt, $J = 0.8, 6.0$ Hz, 2H), 4.21–4.10 (m, 4H), 2.85 (t, $J = 1.4$ Hz, 2H), 2.68–2.66 (m, 2H), 1.22 (t, $J = 7.2$ Hz, 6H). Other spectral data identical to those reported [5].



$\text{C}_{13}\text{H}_{18}\text{O}_4$
MW: 238.3

Prepared according to *GPI*. ^1H NMR (400 MHz, CDCl_3) δ 6.47 (dd, $J = 10.8, 17.6$ Hz, 1H), 5.57 (brs, 1H), 5.11 (d, $J = 6.4$ Hz, 1H), 5.08 (s, 1H), 4.20 (q, $J = 7.2$ Hz, 4H), 3.12 (brs, 2H), 3.09 (brs, 2H), 1.25 (t, $J = 7.2$ Hz, 6H). Other spectral data identical to those reported [6].

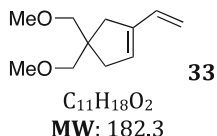


$\text{C}_{11}\text{H}_{18}\text{O}_2$
MW: 182.3

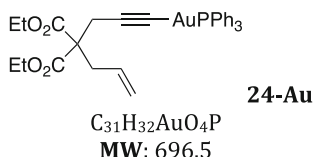
Prepared according to **GPI**. ^1H NMR (400 MHz, CDCl_3) δ = 6.12 (dt, J = 2.0, 9.6 Hz, 1H), 5.69 (dt, J = 3.6, 9.6 Hz, 1H), 4.84 (s, 1H), 4.79 (s, 1H), 3.31 (s, 6H), 3.21 (s, 2H), 3.20 (s, 2H), 2.26 (t, J = 1.6 Hz, 2H), 2.04 (d, J = 1.6 Hz, 2H).

^{13}C NMR (100 MHz, CDCl_3) δ 141.3, 128.9, 127.7, 112.4, 75.9 (2C), 59.5 (2C), 38.8, 35.4, 29.8.

HRMS calculated for $[\text{C}_{13}\text{H}_{18}\text{NaO}_4]^+$: 261.1097, found: 261.1101.



This product could not be separated from **32**. ^1H NMR (400 MHz, CDCl_3) δ 6.50 (dd, J = 10.8, 17.2 Hz, 1H), 5.57 (s, 1H), 5.04 (d, J = 6.8 Hz, 1H), 5.00 (s, 1H), 3.35 (s, 6H), 2.31 (s, 2H), 2.29 (s, 2H).



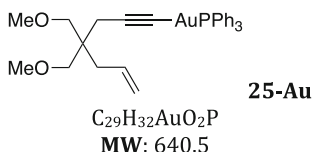
In a dry Schlenk apparatus under argon was dissolved 0.9 mmol of enyne **24** in 12 mL of THF. The solution was cooled down to 0 °C then 0.9 mmol of *n*-BuLi (2.25 M in hexanes, 380 μL) was added. A brown color could appear. The mixture was stirred at 0 °C for 10 min, then 0.3 mmol of AuClPPh_3 was added. The reaction was warmed up to room temperature and allowed to stir for 3 h, after what the reaction was quenched with 6 mL of a saturated aqueous solution of NH_4Cl . The organic layer was removed under vacuum, then 12 mL of CH_2Cl_2 were added. The aqueous layer was extracted with CH_2Cl_2 , and the combined organic extracts were dried over MgSO_4 . After removal of the solvent, a gum was obtained that can be purified in several manners: direct precipitation in CHCl_3 /hexane followed by filtration on a fritted glass and washing with hexane, slow precipitation in a 5:95 CHCl_3 /hexane mixture at -25 °C when the direct precipitation was not effective, flash chromatography on neutral alumina in a 1:1 pentane/ CH_2Cl_2 mixture if the afore mentioned precipitation techniques were not able to furnish the acetylide with the desired purity. Any attempt to purify the acetylide on silica gel led to decomposition (PPh_3 observed). Pale yellow solid, 37 % upon precipitation in CHCl_3 /hexane at -25 °C. ^1H NMR (400 MHz, CDCl_3) δ 7.56–7.40 (m, 15H), 5.75 (dq, J = 10.0, 7.4 Hz, 1H), 5.20 (d, J = 17.0 Hz, 1H), 5.09 (d, J = 10.1 Hz, 1H), 4.26–4.15 (m, 4H), 2.99 (d, J = 1.8 Hz, 2H), 2.93 (d, J = 7.4 Hz, 2H), 1.25 (t, J = 7.1 Hz, 6H).

^{13}C NMR (100 MHz, CDCl_3) δ 170.6 (2C), 134.5 (d, J = 13.8 Hz, 6C), 132.9, 131.6 (3C), 129.2 (d, J = 11.2 Hz, 6C), 119.2, 61.5 (2C), 57.6, 36.7, 24.3, 14.3 (2C).

^{31}P NMR (162 MHz, CDCl_3) δ 42.8.

IR (neat) $\nu = 692, 710, 742, 754, 921, 998, 1018, 1101, 1187, 1210, 1435, 1731, 2360 \text{ cm}^{-1}$.

HRMS calculated for $[\text{C}_{31}\text{H}_{32}\text{O}_4\text{AuNaP}]^+$: 719.1596, found: 719.1604.



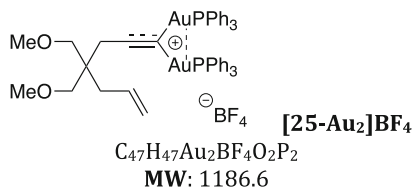
Prepared according to the same procedure than for **24-Au**, using enyne **25** in place of **24**. White solid, 83 % upon precipitation in CHCl_3 /hexane. **^1H NMR (400 MHz, CDCl_3)** δ 7.55–7.42 (m, 15H), 5.93–5.82 (m, 1H), 5.11 (d, $J = 17.1 \text{ Hz}$, 1H), 5.05 (d, $J = 10.0 \text{ Hz}$, 1H), 3.36 (s, 4H), 3.34 (s, 6H), 2.40 (s, 2H), 2.27 (d, $J = 7.5 \text{ Hz}$, 2H).

^{13}C NMR (100 MHz, CDCl_3) δ 134.9 (3C), 134.5 (d, $J = 13.7 \text{ Hz}$, 6C), 131.6, 131.2 (d, $J = 21.9 \text{ Hz}$, 3C), 129.2 (d, $J = 11.2 \text{ Hz}$, 6C), 117.6, 75.0 (2C), 59.4 (2C), 41.9, 36.6, 23.8.

^{31}P NMR (162 MHz, CDCl_3) δ 42.9.

IR (neat) $\nu = 649, 710, 750, 917, 997, 1101, 1435, 1479, 2341, 2360$.

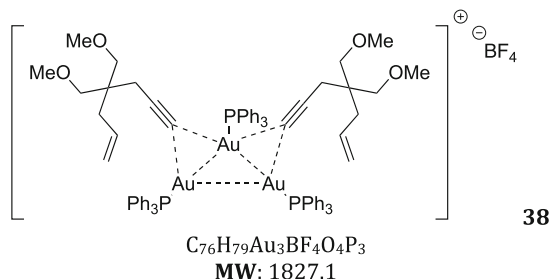
HRMS calculated for $[\text{C}_{29}\text{H}_{32}\text{O}_2\text{AuNaP}]^+$: 663.1698, found: 663.1703.



An oven-dried round-bottom flask was introduced in a glove box and was loaded with Ph_3PAuCl (7.3 mg, 14.7 μmol) and AgBF_4 (2.9 mg, 14.7 μmol). The solids were dissolved in 0.2 mL of distilled and degassed CDCl_3 and the solution was stirred for 5–10 min. The supernatant was then added via a syringe through a UptidiscTM PTFE (13 mm/0.45 μm) syringe filter to a solution of **25-Au** (10 mg, 14 μmol) dissolved in 0.2 mL of CDCl_3 . The mixture was stirred for 5 min. The formation of the digold complex was checked by ^{31}P NMR. A minor residual peak was always observed in ^{31}P NMR which was attributed to $(\text{Ph}_3\text{P})_2\text{AuBF}_4$ in analogy with the previous observations made by Fürstner and co-workers in their study of *gem*-diaurated species. **^1H NMR (400 MHz, CDCl_3)** δ 7.67–7.41 (m, 30H), 5.84–5.74 (m, 1H), 5.15–5.04 (m, 2H), 3.34–3.28 (m, 4H), 3.25 (s, 6H), 2.80 (s, 2H), 2.25 (d, $J = 7.6 \text{ Hz}$, 2H).

^{13}C NMR (100 MHz, CDCl_3) δ 134.2 (d, $J = 13.7 \text{ Hz}$, 12C), 133.6, 132.6 (6C), 129.8 (d, $J = 11.7 \text{ Hz}$, 12C), 118.7, 74.3 (2C), 59.5 (2C), 42.4, 36.7, 25.5.

^{31}P NMR (162 MHz, CDCl_3) δ 37.1 (2P).

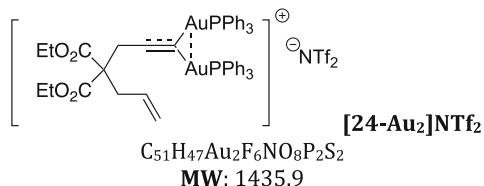


In round-bottom flask was introduced $[(\text{Ph}_3\text{PAu})_3\text{O}]\text{BF}_4$ (54 mg, 0.037 mmol, 0.5 equiv.)¹ and CDCl_3 (3 mL). Enyne **1** (13 mg, 0.074 mmol, 1 equiv.) was then dissolved in the solution, and the mixture took instantaneously a pale yellow color. Formation of the trigold complex was checked by ^1H and ^{31}P NMR and complete disappearance of the free enyne and gold complex was observed after 30 min. **^1H NMR (400 MHz, CDCl_3) δ 7.57–7.37 (m, 45H), 5.82 (dq, J = 10.1, 7.5 Hz, 2H), 5.15–5.02 (m, 4H), 3.33 (q, J = 9.2 Hz, 8H), 3.28 (s, 12H), 2.70 (br s, 4H), 2.27 (d, J = 7.5 Hz, 4H).**

^{13}C NMR (100 MHz, CDCl_3) δ 134.2 (d, J = 13.7 Hz, 18C), 133.9 (9C), 132.44 (9C), 129.7 (d, J = 11.7 Hz, 18C), 128.8 (2C), 118.5 (2C), 74.5 (4C), 59.5 (4C), 42.3 (2C), 36.64 (2C), 24.7 (2C).

^{31}P NMR (162 MHz, CDCl_3) δ 38.3 (3P).

HRMS calculated for $[\text{C}_{76}\text{H}_{79}\text{Au}_3\text{O}_4\text{P}_3]^+$: 1739.4188, found: 1739.4181.



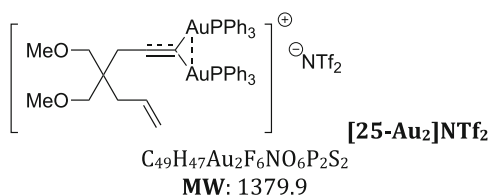
The gold acetylide (14 μmol) was dissolved in 0.2 mL of CDCl_3 . A solution of $\text{Ph}_3\text{PAuNTf}_2$ (2:1 toluene adduct, 14 μmol in 0.2 mL of CDCl_3) was added to the former solution. The mixture was stirred for 5 min. The formation of the digold complex was checked by ^{31}P NMR. A minor residual peak was always observed in ^{31}P NMR which was attributed to $(\text{Ph}_3\text{P})_2\text{AuNTf}_2$ in analogy with our previous observations in the generation of **[25-Au₂] BF_4** . Any attempt to precipitate or crystallize the digold complex failed. **^1H NMR (400 MHz, CDCl_3) δ = 7.44–7.37 (m, 30H), 5.68–5.63 (m, 1H), 5.19 (dd, J = 16.9, 1.7 Hz, 1H), 5.10 (dd, J = 10.1, 1.7 Hz, 1H), 4.18–4.07 (m, 4H), 3.47 (s, 2H), 2.90 (d, J = 7.4 Hz, 2H), 2.35 (toluene), 1.21 (t, J = 7.1 Hz, 6H).**

^{13}C NMR (100 MHz, CDCl_3) δ = 169.2 (2C), 134.0 (d, J = 13.7 Hz, 12C), 133.1 (6C), 132.8 (d, J = 5.6 Hz, 6C), 131.2, 129.8 (d, J = 11.9 Hz, 12C), 129.2

¹ Addition of only 0.33 equiv. led to a mixture of free enyne and trigold complex

(toluene), 128.4 (toluene), 127.9 (not attributed), 125.4 (toluene), 120.8, 62.4 (2C), 57.0, 36.9, 31.7, 25.4, 21.6 (toluene), 14.2 (2C).

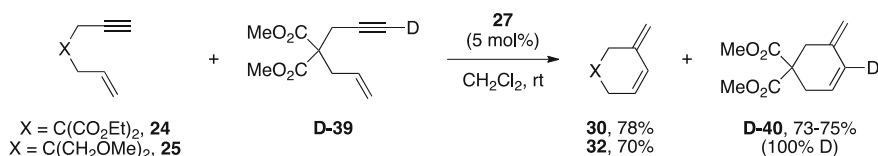
^{31}P NMR (162 MHz, CDCl_3) δ = 36.1 (2P).



Prepared according to the same procedure than **[24-Au₂]NTf₂**, using acetylide **25-Au** in place of **24-Au**. ^1H NMR (400 MHz, CDCl_3) δ = 7.57–7.39 (m, 30H), 7.28–7.15 (m, toluene), 5.82–5.72 (m, 1H), 5.14–5.03 (m, 2H), 3.32 (q, J = 9.2 Hz, 4H), 3.24 (s, 6H), 2.96 (s, 2H), 2.35 (toluene), 2.27 (d, J = 7.6 Hz, 2H).

^{13}C NMR (100 MHz, CDCl_3) δ = 134.0 (d, J = 13.7 Hz, 12C), 133.1 (6C), 132.8 (d, J = 5.6 Hz, 6C), 129.9 (d, J = 11.8 Hz, 12C), 129.2 (toluene), 128.4 (toluene), 128.1, 119.1, 74.0 (2C), 59.5 (2C), 42.6, 36.7, 25.4.

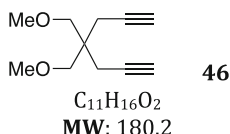
^{31}P NMR (162 MHz, CDCl_3) δ = 36.4 (2P).



A solution of enynes **24** or **25** (0.19 mmol) and **D-39** (40 mg, 0.19 mmol) in DCM (6 ml) was prepared. Then $[\text{PPh}_3\text{AuNTf}_2 \times 0.5 \text{ toluene}]$ (3 mg, 0.004 mmol) was added at room temperature and the reaction was stirred for 1 h. After filtration through a silicon pad and evaporation of the solvent, the obtained products were separated by column chromatography using pentane:diethylether = 8:2 as eluent. **30** or **32** was obtained as colourless oil in 70-78 % yield and **D-40** as a colorless oil in 73 % yield (29 mg, 0.14 mmol). ^1H NMR (400 MHz, CDCl_3) δ 6.17–6.13 (m, 1H), 4.93–4.92 (m, 2H), 3.72 (s, 6H), 2.88 (t, J = 1.4 Hz, 2H), 2.69 (d, J = 1.2 Hz, 2H).

^{13}C NMR (75 MHz, CDCl_3) 171.4, 138.8, 128.6, 126.3 (t, J = 22.5 Hz), 113.6, 53.9, 52.7, 35.8.

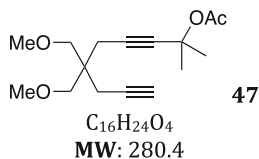
HRMS calculated for $[\text{C}_{11}\text{H}_{13}\text{O}_4\text{D}]^+$: 211.0954, found: 211.0944.



To a suspended solution of sodium hydride (60 %, 6.67 g, 166.3 mmol) in THF (100 mL) at 0 °C was dropped a mixture of dimethyl malonate (10 g, 75.7 mmol) and propargyl bromide (80 % in toluene, 16.9 mL, 151.4 mmol) in THF (60 mL). The mixture was stirred 2 h at 0 °C and overnight at room temperature. Then the reaction mixture was quenched by brine (20 mL). The mixture was diluted with diethyl ether (50 mL) and the layers were separated. The aqueous layer was extracted with ethyl ether (2 × 40 mL). The combined organic layers were dried over magnesium sulfate, and the solvents were removed on rotary evaporator. Final purification was achieved by precipitation in *n*-hexanes to yield a yellowish powder (15.26 g, 97 %).

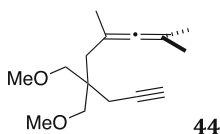
The diester was reduced and the resulting diol alkylated through a similar two-step sequence than the one leading to **25** from **24** (92 % over two steps).

¹H NMR (CDCl₃, 400 MHz) δ 3.31 (s, 4H), 3.29 (s, 6H), 2.30 (d, 4H, *J* = 2.1 Hz), 1.74 (t, 2H, *J* = 2.1 Hz).



To a solution of **46** (2 g, 11.1 mmol, 1 equiv.) in THF (100 mL) at −78 °C was dropped *via* syringe *n*-butyllithium (2.5 M in hexanes, 4.4 mL, 11.1 mmol, 1 equiv.). The resulting solution was stirred at −78 °C for 2 h, and then acetone (0.81 mL, 11.1 mmol, 1 equiv.) was added dropwise. The reaction mixture was allowed to warm up to rt and stirred for 2 h, then quenched with water. The mixture was diluted with diethyl ether (20 mL) and the layers were separated. The aqueous layer was extracted with Et₂O. The combined organic layers were dried over magnesium sulfate, and the solvents were removed on rotary evaporator. Final purification was achieved by flash column chromatography on silica gel (Pentane/Et₂O 3:2) to give the propargylic alcohol as a colorless oil in 58 % yield.

To a stirred solution of the propargylic alcohol (410 mg, 1.72 mmol, 1.0 equiv.), Et₃N (0.96 mL, 6.88 mmol, 4 equiv.) and 4-DMAP (20 mg, 0.17 mmol, 0.1 equiv.) in CH₂Cl₂ (5 mL) was added acetic anhydride (0.65 mL, 6.88 mmol, 4 equiv.) at 0 °C. The solution was then allowed to warm to rt and was stirred further until completion (3–4 h at rt). The reaction was quenched with aqueous saturated NH₄Cl solution and the resulting aqueous layer was extracted with CH₂Cl₂. The combined organic layers were washed with brine, dried over anhydrous Na₂SO₄, filtered and evaporated to give crude acetate as oil. Purification was achieved by flash column chromatography on silica gel (PE/Et₂O gradient) to afford the acetate as a colorless oil, 94 % yield. ¹H NMR (400 MHz, CDCl₃) δ 3.34 (s, 4H), 3.34 (s, 6H), 2.35–2.29 (m, 4H), 2.01 (s, 3H), 1.96 (t, *J* = 2.4 Hz, 1H), 1.64 (s, 6H).

C₁₅H₂₄O₂

MW: 236.4

In an oven-dried round-bottom flask are introduced CuI (790 mg, 4.14 mmol, 3 equiv.) and LiBr (360 mg, 4.14 mmol, 3 equiv.). The solids are dried under vacuum at 70 °C for 2 h, then recovered with 20 mL of anhydrous THF. The solution is cooled down to −78 °C, and MeMgBr is added dropwise. The resulting black mixture is stirred at −78 °C for 2 h. Acetate **49** (386 mg, 1.38 mmol, 1 equiv.) in solution in 5 mL of THF is then added dropwise at −78 °C. The reaction mixture is allowed to warm up to rt and stirred for 20 h, then quenched with a 1:1 mixture of a saturated aqueous solution of NH₄Cl and a 30 % aqueous solution of NH₃ (20 mL). The resulting mixture is extracted with Et₂O, and the combined organic extracts are washed with brine, dried over MgSO₄ and the solvent removed by rotary evaporator. Rapid purification on a short pad of silica using pentane/Et₂O 95:5 as eluent afforded the desired allenyne **44** as a colorless oil in 96 % yield. ¹H NMR (400 MHz, CDCl₃) δ 3.34 (s, 6H, CH₃O), 3.33 (s, 4H, CH₂O), 2.31 (d, *J* = 2.6 Hz, 2H), 2.05 (s, 2H, CH₂), 1.97 (t, *J* = 2.6 Hz, 1H, CH), 1.69 (s, 3H, CH₃), 1.67 (s, 6H, CH₃).

¹³C NMR (100 MHz, CDCl₃) δ 201.1 (C_{allene}), 92.8 (CH₂–C–CH₃), 92.5 (C(CH₃)₂), 81.7 (C_{alkyne}), 74.2 (2C, CH₂O), 69.9 (CH), 59.2 (2C, CH₃O), 42.3 (C), 35.5 (CH₂), 30.4 (CH₂), 22.2 (CH₃), 22.0 (CH₃), 20.9 (CH₃).

IR (neat) ν = 3308, 2940, 1540 cm^{−1}.

C₆H₁₀O

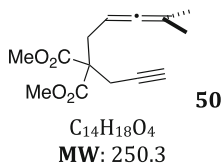
MW: 98.1

2-methyl-3-butyn-2-ol **50** (10 g, 0.118 mol) was solubilized in dry CH₂Cl₂ (100 mL) and cooled to 0 °C. DHP (11 mL, 0.118 mol) was added and then a catalytic amount of APTS (1 g). The reaction mixture was stirred 2 h and quenched by brine (10 mL). The organic layer was washed several times with brine (3 × 15 mL) and then with water (15 mL). The organic layer was dried over magnesium sulfate, and the solvents were removed on rotary evaporator to yield the protected alcohol (16.85 g, 85 %).

Protected alcohol (5 g, 29.6 mmol) was dissolved in THF (20 mL) and cooled to −78 °C. *n*-BuLi (2.3 M, 19.3 mL, 44.3 mmol) was then added with a syringe. The reaction mixture was stirred for 15 min, and formaldehyde (3.6 g, 11.8 mmol) was added. The mixture was stirred and allowed to reach room temperature. The reaction was quenched with a saturated solution of NH₄Cl. The organic layer was washed several times with brine (3 × 15 mL) and then with water (15 mL). The organic layer was dried over magnesium sulfate, and the solvents were removed on

rotary evaporator to yield the desired propargyl alcohol (5.2 g, 88 %). This compound was used in the following step without any further purification.

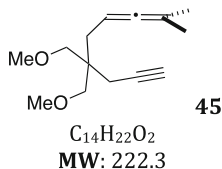
The alcohol (5.2 g, 26.1 mmol) in solution in ether (50 mL) was carefully dropped, at 0 °C over a solution of LiAlH_4 (2 g, 52.2 mmol) in ether (60 mL). The reaction was stirred 30 min at this temperature and then refluxed for 5 h. The reaction mixture was cooled to roomtemperature diluted in dry ether, quenched (at 0 °C) by a saturated solution of sodium sulfate until the formation of a white precipitate and filtered over celite. The solid was washed with ether (2 \times 20 mL) and solvents were evaporated under reduce pressure to yield the corresponding alcohol **52** (1.911 g, 75 %). ^1H NMR (200 MHz, CDCl_3) δ 5.17 (m, 1H), 4.09 (d, 2H, J = 5.6 Hz), 3.64 (t, 1H, J = 6.5 Hz), 1.75 (d, 3H, J = 2.9 Hz).



To a solution of alcohol **52** (1.28 g, 13 mmol, 1 equiv.) and NEt_3 (2 mL, 14.3 mmol, 1.1 equiv.) is added at 0 °C mesyl chloride. After 1 h, the reaction mixture is filtered on a short plug of silica, and the filtrate is evaporated under reduced pressure. The crude mesylate is engaged in the following step without purification.

Malonate **44** (1.98 g, 10 mmol) in solution in THF (15 mL) is dropped, at room temperature, over a solution of NaH (60 %, 0.420 g, 10.5 mmol) in THF (15 mL). The reaction mixture was stirred for 1 h and the mesylate of **52** (10 mmol) was added *via* a syringe. The reaction is stirred for 24 h. and quenched with brine (5 mL). The mixture was diluted with diethyl ether (20 mL) and the layers were separated. The aqueous layer was extracted with ethyl ether (2 \times 20 mL). The combined organic layers were dried over magnesium sulfate, and the solvents were removed. Purification was achieved by flash column chromatography on silica gel using 8:2 PE/diethyl ether as the eluent to give **53** (1.65 g, 59 %) as a colorless oil. ^1H NMR (400 MHz, CDCl_3) δ 4.80–4.74 (m, 1H), 4.24–4.16 (m, 4H), 2.86 (d, 2H, J = 2.8 Hz), 2.71 (d, 2H, J = 7.6 Hz), 1.98 (t, 1H, J = 2.8 Hz), 1.65 (d, 6H, J = 7.1 Hz).

^{13}C NMR (100 MHz, CDCl_3) δ 204.1 (C_{allene}), 169.9 (2CO), 95.5 (C), 82.4 ($\text{CH}_{\text{allene}}$), 79.1 (C), 71.2 (C), 61.7 (2 CH_2), 57.1 (C), 32.5 (CH), 22.5 (CH_2), 20.6 (2 CH_3), 14.2 (2 CH_3). IR (neat) 2982, 2935, 2123, 1969, 1734 cm^{-1} .

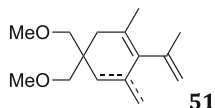


Reduction of the *gem*-diester group in **50** and subsequent alkylation of the diol were performed through identical procedures than those leading to **25** from **24**

(84 % over two steps). **¹H NMR (400 MHz, CDCl₃)** δ 4.87 (m, 1H, H₂), 3.33 (s, 6H, H₅), 3.28 (s, 4H, H₄), 2.23 (d, 2H, J = 2.6 Hz, H₆), 2.04 (d, 2H, J = 8.0 Hz, H₃), 1.94 (t, 1H, J = 2.6 Hz, H₇), 1.67 (d, 6H, J = 2.8 Hz, H₁).

¹³C NMR (100 MHz, CDCl₃) δ 204.2 (C_{allene}), 94.0 (C), 83.8 (CH), 81.5 (C_{alkyne}), 74.5 (2CH₂), 70.3 (CH), 59.6 (2CH₃), 42.3 (C), 32.5 (CH₂), 22.2 (CH₂), 20.9 (2CH₃).

IR (neat) ν = 2117, 1968 cm⁻¹.

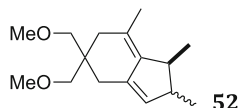


C₁₅H₂₄O₂
MW: 236.4

Prepared according to **GPI** in refluxing CDCl₃, 85 %, colorless oil. **¹H NMR (400 MHz, CDCl₃)** δ 5.22 (s, 1H, =CH, endo), 5.10–5.09 (m, 1H, CH₃C=CHH, exo), 5.06–5.05 (m, 1H, CH₃C=CHH, endo), 4.83 (s, 1H, =CHH, exo), 4.73 (s, 1H, =CHH, exo), 4.63–4.62 (m, 1H, CH₃C=CHH, exo), 4.60–4.59 (m, 1H, CH₃C=CHH, endo), 3.32 (s, 6H, MeO, exo), 3.31 (s, 6H, MeO, endo), 3.24 (AB, J = 8.6 Hz, 2H, CH₂O, endo), 3.20 (s, 4H, CH₂O, exo), 3.19 (AB, J = 8.6 Hz, 2H, CH₂O, endo), 2.25 (s, 2H, CH₂, exo), 2.08 (s, 2H, CH₂, endo), 2.02 (s, 2H, CH₂, exo), 1.78 (s, 3H, CH₃, exo), 1.76 (s, 3H, CH₃, endo), 1.72 (s, 3H, CH₃, endo), 1.70 (d, J = 1.2 Hz), 3H, CH₃, endo), 1.69 (s, 3H, CH₃, exo).

¹³C NMR (100 MHz, CDCl₃) δ 144.1 (C), 143.8 (C), 140.8 (C), 136.0 (C), 134.5 (C), 134.0 (C), 129.7 (C), 127.4 (C), 122.8 (=CH, endo), 114.9 (CH₃C=CH₂, exo), 114.6 (CH₃C=CH₂, endo), 110.4 (s, 1H, =CH₂, exo), 76.0 (2C, CH₂O, exo), 75.2 (2C, CH₂O, 3a''), 59.5 (2C+2C, MeO, exo+ endo), 40.3 (C, one isomer), 38.7 (C, other isomer), 36.6 (CH₂, exo), 36.4 (CH₂, exo), 34.3 (CH₂, 3a''), 24.1 (CH₃, endo), 23.2 (CH₃, exo), 21.0 (CH₃), 20.5 (CH₃), 20.4 (CH₃).

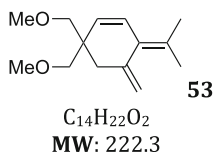
IR (neat) ν = 3077, 2978, 2919, 2886, 2824, 1644, 1625, 1606, 1447, 1376 cm⁻¹.



C₁₅H₂₄O₂
MW: 236.4

Prepared according to **GPI** in refluxing CDCl₃, 15 %, colorless oil. **¹H NMR (400 MHz, CDCl₃)** δ 5.41 (bs), 3.30 (s, 3H), 3.28 (s, 3H), 3.19 (d, 2H, J = 1.5 Hz), 3.13 (s, 2H), 2.83 (qd, 1H, J = 7.1, 6.6 Hz), 2.64 (dd, 1H, J = 16.8, 6.6 Hz), 2.18 (s, 2H), 2.00 (1H, J = 16.9 Hz), 1.90 (d, 1H, J = 16.8 Hz, H₇), 1.88 (1H, J = 16.9 Hz), 1.70 (s, 3H), 1.00 (d, 3H, J = 7.1 Hz). **¹³C NMR (100 MHz, CDCl₃)** δ 143.3 (C), 138.5 (C), 125.2 (CH), 120.3 (C), 76.5 (CH₂), 75.9 (CH₂), 59.6 (CH₃), 59.5 (CH₃), 40.1 (CH₂), 39.5 (C), 36.0 (CH₂), 33.2 (CH), 29.5 (CH₂), 21.7 (CH₃), 19.4 (CH₃).

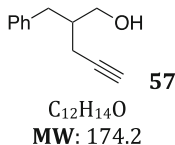
IR (neat) ν = 2953, 2918, 2888, 2846, 1476, 1446, 1116, 1105 cm^{-1} .



Prepared according to **GPI** in refluxing CDCl_3 , 15 %. Colorless oil, isolated in mixture with low amounts of other unidentified products, after column chromatography (Pentane/ Et_2O 98:2). **^1H NMR (400 MHz, CDCl_3)** δ = 6.51 (d, J = 10 Hz, 1H), 5.49 (d, J = 10 Hz, 1H), 5.08 (d, J = 1.2 Hz, 1H), 4.91 (d, J = 2.4 Hz, 1H), 3.33 (s, 6H), 3.32 (s, 2H), 3.31 (s, 2H), 2.26 (s, 2H), 1.95 (s, 3H), 1.84 (s, 3H).

^{13}C NMR (100 MHz, CDCl_3) δ = 141.9, 130.6, 128.8, 127.3, 114.3, 75.8 (2C), 59.5 (2C), 44.0, 38.6, 23.1, 20.6.

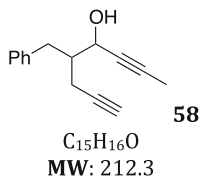
HRMS calculated for $[\text{C}_{14}\text{H}_{22}\text{O}_2\text{Na}]^+$: 245.1517, found: 245.1524.



To diisopropylamine (15.4 mL, 110 mmol) was added *n*-butyllithium (2.5 M in Hexanes, 42.0 mL, 105 mmol) at -78°C with stirring, then THF (100 mL) was added to dissolve all the solids generated. To this LDA solution was added ethyl hydrocinnamate (17.8 mL, 100 mmol) in 30 min. After 1 h, propargyl bromide (80 % in toluene, 11.7 mL, 105 mmol) was added dropwise. The resulting mixture was kept at -78°C for 2 h and warmed to 25°C over 1 h. The reaction was quenched with saturated aqueous NH_4Cl , and extracted three times with EtOAc. The combined organic layers were separated, washed with 2 M aqueous HCl, saturated aqueous NaHCO_3 and brine, dried over MgSO_4 , filtered, and concentrated in vacuo to afford the desired ester (21.2 g, 98 %) as a clear orange yellow liquid. A solution of the ethyl ester (2.16 g, 10.0 mmol) in Et_2O (10 mL) was added to a stirred suspension of LAH (0.40 g, 10.0 mmol) in Et_2O (10 mL) at 0°C . After stirring for 30 min, the reaction mixture was quenched with saturated aqueous NH_4Cl , treated with 2 M aqueous HCl to dissolve the aluminum precipitate, and extracted with EtOAc. The combined organic layers were separated, washed with saturated aqueous NaHCO_3 and brine, dried over MgSO_4 , filtered, and concentrated in vacuo. Flash chromatography (20 % EtOAc/Hexanes) afforded the desired alcohol **57** (1.05 g, 60 % for 2 steps) as a light yellow oil. **^1H NMR (400 MHz, CDCl_3)** δ 7.10–7.36 (m, 5H), 3.70 (dd, J = 11.0 and 5.0 Hz, 1H), 3.65 (dd, J = 11.0 and 6.5 Hz, 1H), 2.74 (dd, J = 13.5 and 7.0 Hz, 1H), 2.69 (dd, J = 13.5 and 8.0 Hz, 1H), 2.31 (ddd, J = 17.0, 6.0 and 3.0 Hz, 1H), 2.23 (ddd, J = 17.0, 6.0 and 3.0 Hz, 1H), 2.04 (t, J = 3.0 Hz, 1H), 2.04 (m, 1H), 1.71 (s, br, 1H).

^{13}C NMR (100 MHz, CDCl_3) δ 140.0, 129.4, 128.7, 126.4, 82.6, 70.5, 64.7, 41.9, 36.7, 20.0.

IR (neat) $\nu = 3364, 3296, 2115, 1030, 743, 701 \text{ cm}^{-1}$.

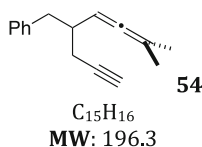


To a solution of PCC (2 equiv.) in CH₂Cl₂ (0.5 M) is added alcohol **57** at rt. The reaction mixture is stirred at rt for 2 h and then filtered over a short pas of silica. The solids are washed several time with Et₂O, then the filtrate evaporated under reduced pressure and the crude mixture is purified by flash column chromatography using gradient mixtures of pentane/Et₂O to afford the desired aldehyde in 71 % yield.

n-BuLi (1.25 M in hexane, 2.2 ml, 2.73 mmol) was slowly added to a solution of bromopropene (0.17 ml, 1.92 mmol) in THF (2.5 mL) at -78°C . After stirring for 2 h a solution of the aldehyde (211 mg, 1.24 mmol) in THF (2 ml) was added and the solution was warmed to room temperature over 1 h. The reaction was quenched with sat. NH₄Cl and extracted with diethyl ether. Drying with MgSO₄ and evaporating the solvent resulted in crude alcohol **58**, which was purified by column chromatography using hexane/AcOEt 7:3 as eluent. The pure product was obtained in 58 % yield (150 mg, 0.71 mmol) as a yellow oil.

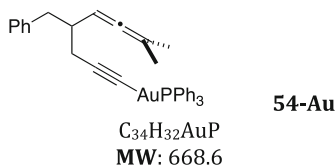
¹H NMR (300 MHz, CDCl₃) δ 7.32–7.22 (m, 5H), 4.48 (m, 1H), 3.0–2.7 (m, 2H), 2.5–2.2 (m, 2H), 2.06 (m, 2H), 1.92 (s, 3H).

IR (neat) $\nu = 3250, 2900, 2115, 1952, 1602, 1485, 1450, 1025 \text{ cm}^{-1}$.



To a solution of alcohol **58** (1 equiv.) and NEt₃ (1.1 equiv.) is added at 0°C mesyl chloride. After 1 h, the reaction mixture is filtered on a short plug of silica, and the filtrate is evaporated under reduced pressure. The crude mesylate is engaged in the following step without purification.

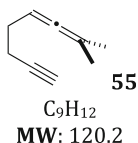
Allenyne **54** was synthesized from the mesylate of **58** through the same procedure than for **44**. **¹H NMR (400 MHz, CDCl₃)** δ 7.31–7.25 (m, 2H), 7.22–7.15 (m, 3H), 5.02–4.94 (m, 1H), 2.82 (dd, $J = 13.6, 7.0 \text{ Hz}$, 1H), 2.70 (dd, $J = 13.6, 7.4 \text{ Hz}$, 1H), 2.52 (q, $J = 7.0 \text{ Hz}$, 1H), 2.23 (d, $J = 2.6 \text{ Hz}$, 1H), 2.21 (dd, $J = 2.6, 0.8 \text{ Hz}$, 1H), 2.02 (t, $J = 2.6 \text{ Hz}$, 1H), 1.62 (d, $J = 2.9 \text{ Hz}$, 3H), 1.60 (d, $J = 2.9 \text{ Hz}$, 3H). Other spectral data identical to those reported.



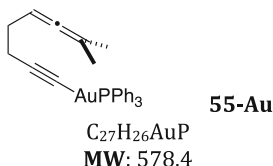
Prepared according to the same procedure than for **24-Au**, using allenyne **54** in place of **24**. White solid, 74 % upon precipitation in CHCl_3 /hexane. ^1H NMR (400 MHz, CDCl_3) δ 7.57–7.40 (m, 15H), 7.31–7.20 (m, 4H), 7.20–7.11 (m, 1H), 5.10–5.00 (m, 1H), 3.03–2.97 (dd, 1H, $J = 6, 16$ Hz), 2.73–2.65 (dd, 1H, $J = 8, 13.6$ Hz), 2.42–2.30 (m, 2H), 1.68–1.60 (d, 3H, $J = 2.8$ Hz), 1.60–1.54 (d, 4H, $J = 3.2$ Hz).

^{13}C NMR (100 MHz, CDCl_3) δ 201.8, 141.5, 134.9, 134.7, 132.0, 130.9, 130.4, 129.9, 129.7, 129.6, 128.5, 126.1, 96.5, 92.5, 54.6, 54.3, 54.0, 53.7, 53.5, 41.6, 40.6, 26.1, 21.0, 20.9.

^{31}P NMR (162 MHz, CDCl_3) δ 42.1. Other spectral data identical to those reported



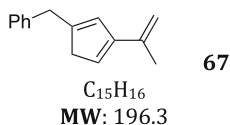
Allenyne **58** was synthesized from aldehyde **64** through an identical procedure than for **54** followed by desilylation of TMS-protected allenyne **68** using KF in DMSO (28 % over 3 steps). ^1H NMR (400 MHz, CDCl_3) δ 5.05–4.98 (m, 1H), 2.30–2.23 (m, 2H), 2.23–2.15 (m, 2H), 1.96 (t, $J = 2.6$ Hz, 1H), 1.69 (s, 3H), 1.69 (s, 3H). Other spectral data identical to those reported.



Prepared according to the same procedure than for **24-Au**, using allenyne **55** in place of **24**. White solid, 67 % upon precipitation in CHCl_3 /hexane. ^1H NMR (400 MHz, CDCl_3) δ 7.56–7.37 (m, 15H), 5.11–5.03 (m, 1H), 2.44 (t, $J = 7.5$ Hz, 2H), 2.28–2.20 (m, 2H), 1.68 (s, 3H), 1.67 (s, 3H).

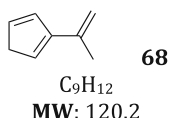
^{13}C NMR (100 MHz, CDCl_3) δ 201.9, 143.9, 134.5 (d, $J = 13.9$ Hz, 6C), 131.6, 130.1 (d, $J = 55.6$ Hz, 3C), 129.2 (d, $J = 11.3$ Hz, 6C), 125.2, 88.2, 30.1, 20.9, 20.2.

HRMS calculated for $[\text{C}_{27}\text{H}_{26}\text{AuNaP}]^+$: 601.1330, found: 601.1333.



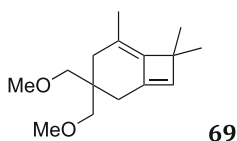
Prepared according to **GPI** in refluxing CDCl_3 , 99 %, colorless oil. ^1H NMR (400 MHz, CDCl_3) δ 7.31–7.25 (m, 2H), 7.22–7.24 (m, 3H), 5.97 (s, 1H), 5.14 (s, 1H), 5.07 (s, 1H), 5.02 (s, 1H), 4.87 (s, 1H), 3.06–2.98 (m, 1H), 2.79–2.58 (m, 3H), 2.33 (ddt, 1H, $J = 16, 3.5$, and 2.2 Hz), 1.91 (s, 3H).

^{13}C NMR (100 MHz, CDCl_3) δ 151.8, 145.8, 140.9, 139.6, 138.8, 129.1, 128.5, 126.2, 114.7, 103.7, 44.4, 42.2, 38.8, 23.2. Other spectral data identical to those reported.



Prepared according to **GPI** in refluxing CDCl_3 , 99 %, colorless oil. **^1H NMR (400 MHz, CDCl_3)** δ 6.06 (s, 1H), 5.11 (s, 1H), 5.06 (s, 1H), 5.02 (s, 1H), 4.89 (s, 1H), 2.66–2.60 (m, 2H), 2.44–2.39 (m, 2H), 1.92 (s, 3H).

^{13}C NMR (100 MHz, CDCl_3) δ 152.9, 146.2, 139.0, 136.5, 114.2, 102.9, 32.0, 30.2, 23.3. Other spectral data identical to those reported.

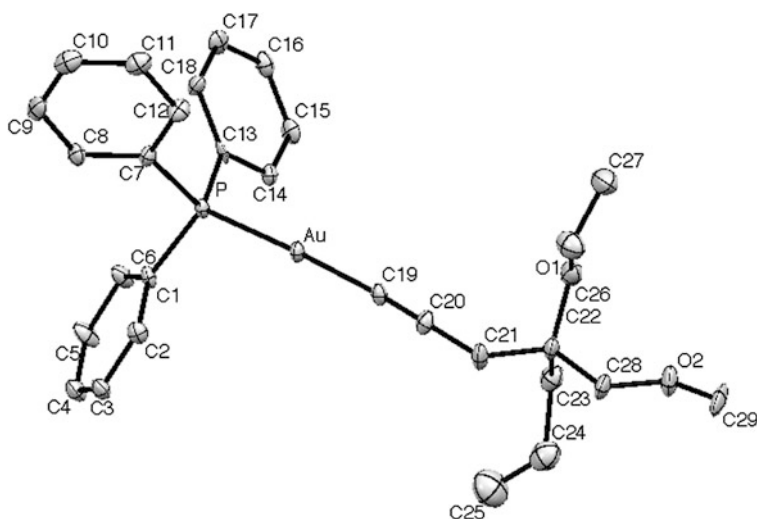


Prepared according to the same procedure than for **[24-Au₂]NTf₂**, using acetylide **42-Au** in place of **24-Au**, then heating of the CDCl_3 solution at 70 °C for 12 h. **^1H NMR (400 MHz, CDCl_3)** δ 6.00 (s, 1H, C=CH), 3.31 (s, 6H, OCH_3), 3.20 (s, 4H, CH_2OMe), 2.05 (d, $J = 1.2$ Hz, 2H, $\text{CH}_2\text{C}=\text{CH}$), 1.92 (s, 2H, $\text{CH}_2\text{MeC}=\text{C}$), 1.59 (s, 3H, $\text{CH}_3\text{C}=\text{C}$), 1.27 (s, 6H, CH_3).

^{13}C NMR (100 MHz, CDCl_3) δ 143.74 (C), 142.97 (C), 136.72 (CH), 111.16 (C), 76.48 (2CH_2), 59.59 (2CH_3), 50.90 (C), 41.66 (C), 34.64 (CH_2), 26.86 (CH_2), 25.24 (2CH_3), 17.53 (CH_3).

HRMS calculated for $[\text{C}_{15}\text{H}_{24}\text{NaO}_2]^+$ 259,1669, found: 259,1667.

X-ray structure of compound 25-Au



Scheme 6 Structure of compound **25-Au** in the solid-state. Anisotropic displacement parameters are drawn at the 50 % probability level and hydrogen atoms are omitted for clarity

Crystal data

$\text{C}_{23}\text{H}_{32}\text{AuO}_2\text{P}$
 $M_r = 640.48$
 Monoclinic, $P2_1/c$
 $a = 16.9075$ (12) Å
 $b = 9.8602$ (7) Å
 $c = 17.2281$ (12) Å
 $\beta = 113.997$ (2)°
 $V = 2623.9$ (3) Å³
 $Z = 4$

$F(000) = 1264$
 $D_x = 1.621$ Mg m⁻³
 Mo $K\alpha$ radiation, $\lambda = 0.71073$ Å
 Cell parameters from 9737 reflections
 $0 = 2.4\text{--}38.9^\circ$
 $\mu = 5.69$ mm⁻¹
 $T = 100$ K
 $0.31 \times 0.27 \times 0.08$ mm

Data collection

CCD area detector
 diffractometer
 Radiation source: fine-focus sealed tube, kappa X8
 APEX II Bruker ICMMO
 graphite
 phi and omega scans
 Absorption correction: ψ scan
 SADABS
 $T_{\text{min}} = 0.324$, $T_{\text{max}} = 0.651$
 42406 measured reflections

13296 independent reflections
 10968 reflections with $I > 2\sigma(I)$
 $R_{\text{int}} = 0.037$
 $0_{\text{max}} = 39.2^\circ$, $0_{\text{min}} = 2.4^\circ$
 $h = -29 \rightarrow 26$
 $k = -13 \rightarrow 17$
 $l = -24 \rightarrow 30$

Refinement

Refinement on F^2
 Least-squares matrix: Full
 $R[F^2 > 2\sigma(F^2)] = 0.063$
 $wR(F^2) = 0.206$
 $S = 1.09$
 13296 reflections
 301 parameters
 0 restraints

Primary atom site location: Structure-invariant direct methods
 Secondary atom site location: Difference Fourier map
 Hydrogen site location: Inferred from neighbouring sites
 H-atom parameters constrained
 $w = 1/[\sigma^2(F_o^2) + (0.0955P)^2 + 49.7274P]$
 where $P = (F_o^2 + 2F_c^2)/3$
 $(\Delta/\sigma)_{\text{max}} = 0.008$
 $\Delta\rho_{\text{max}} = 2.06$ e Å⁻³
 $\Delta\rho_{\text{min}} = -1.97$ e Å⁻³

Fractional atomic coordinates and isotropic or equivalent isotropic displacement parameters (\AA^2)

	x	y	z	U_{eq}
C1	0.1387 (4)	0.8249 (6)	0.3322 (4)	0.0126 (8)
C2	0.1457 (4)	0.9543 (6)	0.3663 (4)	0.0155 (9)
H2	0.1385	1.0302	0.3320	0.019*
C3	0.1637 (4)	0.9693 (6)	0.4522 (4)	0.0174 (10)
H3	0.1681	1.0558	0.4751	0.021*
C4	0.1753 (5)	0.8564 (7)	0.5039 (4)	0.0207 (11)
H4	0.1885	0.8673	0.5614	0.025*
C5	0.1670 (6)	0.7275 (7)	0.4694 (4)	0.0244 (13)
H5	0.1745	0.6517	0.5038	0.029*
C6	0.1474 (5)	0.7112 (6)	0.3825 (4)	0.0199 (11)
H6	0.1404	0.6249	0.3588	0.024*
C7	0.0092 (4)	0.8426 (6)	0.1590 (4)	0.0135 (9)
C8	-0.0527 (4)	0.8177 (7)	0.1916 (4)	0.0174 (10)
H8	-0.0353	0.7950	0.2486	0.021*
C9	-0.1399 (4)	0.8266 (7)	0.1392 (5)	0.0227 (12)
H9	-0.1810	0.8137	0.1616	0.027*
C10	-0.1663 (5)	0.8547 (7)	0.0533 (5)	0.0231 (12)
H10	-0.2250	0.8568	0.0177	0.028*
C11	-0.1053 (5)	0.8796 (7)	0.0209 (5)	0.0227 (12)
H11	-0.1231	0.9000	-0.0364	0.027*
C12	-0.0176 (4)	0.8744 (7)	0.0730 (4)	0.0185 (10)
H12	0.0231	0.8920	0.0508	0.022*
C13	0.1379 (4)	0.6368 (5)	0.2004 (4)	0.0124 (8)
C14	0.2216 (4)	0.5861 (6)	0.2328 (4)	0.0151 (9)
H14	0.2673	0.6397	0.2682	0.018*
C15	0.2370 (5)	0.4553 (7)	0.2125 (5)	0.0189 (10)
H15	0.2929	0.4203	0.2350	0.023*
C16	0.1678 (4)	0.3764 (6)	0.1580 (4)	0.0187 (10)
H16	0.1780	0.2893	0.1435	0.022*
C17	0.0853 (5)	0.4271 (6)	0.1258 (5)	0.0193 (11)
H17	0.0397	0.3737	0.0902	0.023*
C18	0.0692 (4)	0.5580 (6)	0.1461 (4)	0.0157 (9)
H18	0.0131	0.5925	0.1236	0.019*
C19	0.2977 (4)	1.0844 (6)	0.1782 (4)	0.0143 (9)
C20	0.3439 (4)	1.1704 (6)	0.1690 (4)	0.0168 (10)
C21	0.3994 (4)	1.2748 (6)	0.1582 (5)	0.0202 (11)
H21A	0.4219	1.3303	0.2091	0.024*
H21B	0.3646	1.3328	0.1112	0.024*
C22	0.4760 (4)	1.2189 (6)	0.1411 (4)	0.0172 (10)
C23	0.5345 (5)	1.1272 (8)	0.2151 (5)	0.0241 (12)
H23A	0.4989	1.0588	0.2257	0.029*

H23B	0.5756	1.0810	0.1983	0.029*
C24	0.5840 (6)	1.2049 (10)	0.2973 (7)	0.0364 (18)
H24	0.6308	1.2575	0.3002	0.044*
C25	0.5658 (9)	1.2030 (14)	0.3628 (8)	0.051 (3)
H25A	0.5195	1.1516	0.3623	0.062*
H25B	0.5990	1.2531	0.4108	0.062*
C26	0.4431 (5)	1.1367 (8)	0.0596 (5)	0.0243 (12)
H26A	0.4917	1.1041	0.0485	0.029*
H26B	0.4109	1.0588	0.0653	0.029*
C27	0.3735 (6)	1.1629 (12)	-0.0885 (6)	0.038 (2)
H27A	0.3461	1.0761	-0.0935	0.057*
H27B	0.4275	1.1520	-0.0938	0.057*
H27C	0.3364	1.2219	-0.1325	0.057*
C28	0.5273 (4)	1.3406 (7)	0.1317 (5)	0.0202 (11)
H28A	0.4901	1.3975	0.0854	0.024*
H28B	0.5479	1.3940	0.1835	0.024*
C29	0.6327 (5)	1.4032 (11)	0.0844 (5)	0.0316 (18)
H29A	0.5895	1.4350	0.0315	0.047*
H29B	0.6822	1.3717	0.0756	0.047*
H29C	0.6498	1.4760	0.1249	0.047*
O1	0.3888 (4)	1.2195 (7)	-0.0090 (4)	0.0321 (12)
O2	0.5986 (4)	1.2957 (6)	0.1154 (4)	0.0276 (11)
P	0.12306 (10)	0.81362 (14)	0.22173 (9)	0.0110 (2)
Au	0.215238 (14)	0.95522 (2)	0.195819 (13)	0.01300 (7)

Atomic displacement parameters (\AA^2)

	U^{01}	U^{02}	U^{03}	U^{12}	U^{13}	U^{23}
C1	0.016 (2)	0.0119 (19)	0.015 (2)	0.0031 (17)	0.0112 (18)	0.0030 (17)
C2	0.019 (2)	0.0116 (19)	0.018 (2)	0.0023 (18)	0.0092 (19)	0.0016 (18)
C3	0.021 (3)	0.017 (2)	0.017 (2)	0.001 (2)	0.011 (2)	-0.003 (2)
C4	0.027 (3)	0.022 (3)	0.018 (2)	0.000 (2)	0.014 (2)	-0.002 (2)
C5	0.045 (4)	0.018 (2)	0.018 (2)	-0.002 (3)	0.020 (3)	0.002 (2)
C6	0.034 (3)	0.013 (2)	0.018 (2)	-0.003 (2)	0.016 (2)	-0.001 (2)
C7	0.012 (2)	0.0119 (19)	0.018 (2)	-0.0005 (16)	0.0071 (17)	0.0010 (18)
C8	0.015 (2)	0.019 (2)	0.021 (2)	0.0023 (19)	0.010 (2)	-0.002 (2)
C9	0.016 (3)	0.020 (3)	0.035 (3)	0.001 (2)	0.014 (2)	-0.008 (3)
C10	0.017 (3)	0.016 (2)	0.030 (3)	0.004 (2)	0.003 (2)	-0.002 (2)
C11	0.022 (3)	0.017 (2)	0.026 (3)	0.000 (2)	0.007 (2)	0.001 (2)
C12	0.016 (2)	0.018 (2)	0.018 (2)	0.002 (2)	0.0043 (19)	0.005 (2)
C13	0.019 (2)	0.0103 (18)	0.016 (2)	0.0047 (17)	0.0147 (18)	0.0006 (17)
C14	0.013 (2)	0.018 (2)	0.017 (2)	0.0012 (18)	0.0087 (18)	-0.001 (2)
C15	0.017 (2)	0.018 (2)	0.024 (3)	0.008 (2)	0.011 (2)	0.000 (2)
C16	0.023 (3)	0.015 (2)	0.023 (3)	0.005 (2)	0.015 (2)	0.003 (2)
C17	0.025 (3)	0.012 (2)	0.026 (3)	-0.004 (2)	0.016 (2)	0.001 (2)
C18	0.012 (2)	0.012 (2)	0.025 (3)	-0.0013 (16)	0.0085 (19)	-0.0034 (19)
C19	0.015 (2)	0.0125 (19)	0.019 (2)	0.0031 (17)	0.0108 (19)	0.0007 (19)
C20	0.013 (2)	0.015 (2)	0.025 (3)	0.0028 (18)	0.009 (2)	0.001 (2)
C21	0.022 (3)	0.014 (2)	0.034 (3)	-0.002 (2)	0.021 (3)	-0.001 (2)
C22	0.014 (2)	0.016 (2)	0.026 (3)	-0.0025 (19)	0.013 (2)	-0.002 (2)
C23	0.019 (3)	0.022 (3)	0.031 (3)	0.002 (2)	0.010 (2)	0.001 (3)
C24	0.029 (4)	0.036 (4)	0.041 (5)	0.002 (3)	0.011 (3)	0.000 (4)
C25	0.063 (8)	0.051 (7)	0.044 (6)	0.001 (6)	0.026 (5)	0.008 (5)
C26	0.022 (3)	0.023 (3)	0.031 (3)	-0.001 (2)	0.014 (3)	-0.006 (3)
C27	0.029 (4)	0.055 (6)	0.031 (4)	-0.001 (4)	0.012 (3)	-0.013 (4)
C28	0.014 (2)	0.021 (3)	0.030 (3)	-0.004 (2)	0.013 (2)	0.001 (2)
C29	0.016 (3)	0.053 (5)	0.030 (3)	-0.008 (3)	0.013 (3)	0.013 (4)
O1	0.030 (3)	0.036 (3)	0.028 (3)	0.009 (2)	0.010 (2)	-0.002 (2)
O2	0.023 (2)	0.030 (3)	0.041 (3)	-0.001 (2)	0.024 (2)	0.002 (2)
P	0.0124 (6)	0.0098 (5)	0.0138 (5)	0.0005 (4)	0.0087 (5)	0.0012 (4)
Au	0.01350 (10)	0.01226 (9)	0.01647 (10)	-0.00053 (6)	0.00943 (7)	0.00163 (7)

Geometric parameters (Å, °)

C1—C6	1.387 (8)	C17—H17	0.9300
C1—C2	1.389 (8)	C18—H18	0.9300
C1—P	1.815 (6)	C19—C20	1.207 (9)
C2—C3	1.392 (9)	C19—Au	2.000 (6)
C2—H2	0.9300	C20—C21	1.453 (9)
C3—C4	1.389 (9)	C21—C22	1.543 (8)
C3—H3	0.9300	C21—H21A	0.9700
C4—C5	1.386 (10)	C21—H21B	0.9700
C4—H4	0.9300	C22—C26	1.518 (10)
C5—C6	1.404 (9)	C22—C28	1.527 (9)
C5—H5	0.9300	C22—C23	1.547 (10)
C6—H6	0.9300	C23—C24	1.526 (13)
C7—C8	1.396 (8)	C23—H23A	0.9700
C7—C12	1.397 (9)	C23—H23B	0.9700
C7—P	1.807 (6)	C24—C25	1.285 (16)
C8—C9	1.383 (9)	C24—H24	0.9300
C8—H8	0.9300	C25—H25A	0.9300
C9—C10	1.390 (11)	C25—H25B	0.9300
C9—H9	0.9300	C26—O1	1.422 (10)
C10—C11	1.379 (11)	C26—H26A	0.9700
C10—H10	0.9300	C26—H26B	0.9700
C11—C12	1.387 (10)	C27—O1	1.402 (11)
C11—H11	0.9300	C27—H27A	0.9600
C12—H12	0.9300	C27—H27B	0.9600
C13—C14	1.386 (8)	C27—H27C	0.9600
C13—C18	1.395 (8)	C28—O2	1.416 (8)
C13—P	1.820 (5)	C28—H28A	0.9700
C14—C15	1.389 (9)	C28—H28B	0.9700
C14—H14	0.9300	C29—O2	1.412 (9)
C15—C16	1.401 (10)	C29—H29A	0.9600
C15—H15	0.9300	C29—H29B	0.9600
C16—C17	1.369 (10)	C29—H29C	0.9600
C16—H16	0.9300	P—Au	2.2679 (14)
C17—C18	1.392 (9)		
C6—C1—C2	120.6 (5)	C20—C21—H21A	108.8
C6—C1—P	122.6 (4)	C22—C21—H21A	108.8
C2—C1—P	116.8 (4)	C20—C21—H21B	108.8

C1—C2—C3	119.4 (5)	C22—C21—H21B	108.8
C1—C2—H2	120.3	H21A—C21—H21B	107.6
C3—C2—H2	120.3	C26—C22—C28	109.3 (6)
C4—C3—C2	120.6 (6)	C26—C22—C21	110.3 (6)
C4—C3—H3	119.7	C28—C22—C21	107.3 (5)
C2—C3—H3	119.7	C26—C22—C23	108.8 (6)
C5—C4—C3	119.8 (6)	C28—C22—C23	110.3 (6)
C5—C4—H4	120.1	C21—C22—C23	110.9 (5)
C3—C4—H4	120.1	C24—C23—C22	113.4 (6)
C4—C5—C6	120.1 (6)	C24—C23—H23A	108.9
C4—C5—H5	120.0	C22—C23—H23A	108.9
C6—C5—H5	120.0	C24—C23—H23B	108.9
C1—C6—C5	119.5 (6)	C22—C23—H23B	108.9
C1—C6—H6	120.2	H23A—C23—H23B	107.7
C5—C6—H6	120.2	C25—C24—C23	124.8 (11)
C8—C7—C12	119.6 (6)	C25—C24—H24	117.6
C8—C7—P	121.5 (5)	C23—C24—H24	117.6
C12—C7—P	118.5 (4)	C24—C25—H25A	120.0
C9—C8—C7	120.0 (6)	C24—C25—H25B	120.0
C9—C8—H8	120.0	H25A—C25—H25B	120.0
C7—C8—H8	120.0	O1—C26—C22	109.4 (6)
C8—C9—C10	120.2 (6)	O1—C26—H26A	109.8
C8—C9—H9	119.9	C22—C26—H26A	109.8
C10—C9—H9	119.9	O1—C26—H26B	109.8
C11—C10—C9	119.8 (7)	C22—C26—H26B	109.8
C11—C10—H10	120.1	H26A—C26—H26B	108.2
C9—C10—H10	120.1	O1—C27—H27A	109.5
C10—C11—C12	120.7 (7)	O1—C27—H27B	109.5
C10—C11—H11	119.7	H27A—C27—H27B	109.5
C12—C11—H11	119.7	O1—C27—H27C	109.5
C11—C12—C7	119.6 (6)	H27A—C27—H27C	109.5
C11—C12—H12	120.2	H27B—C27—H27C	109.5
C7—C12—H12	120.2	O2—C28—C22	110.0 (6)
C14—C13—C18	120.3 (5)	O2—C28—H28A	109.7
C14—C13—P	117.7 (5)	C22—C28—H28A	109.7
C18—C13—P	121.6 (4)	O2—C28—H28B	109.7
C13—C14—C15	119.9 (6)	C22—C28—H28B	109.7
C13—C14—H14	120.0	H28A—C28—H28B	108.2
C15—C14—H14	120.0	O2—C29—H29A	109.5
C14—C15—C16	119.6 (6)	O2—C29—H29B	109.5
C14—C15—H15	120.2	H29A—C29—H29B	109.5
C16—C15—H15	120.2	O2—C29—H29C	109.5
C17—C16—C15	120.3 (6)	H29A—C29—H29C	109.5
C17—C16—H16	119.9	H29B—C29—H29C	109.5
C15—C16—H16	119.9	C27—O1—C26	112.5 (7)
C16—C17—C18	120.6 (6)	C29—O2—C28	110.7 (6)
C16—C17—H17	119.7	C7—P—C1	106.4 (3)
C18—C17—H17	119.7	C7—P—C13	103.4 (3)
C17—C18—C13	119.3 (6)	C1—P—C13	107.3 (2)
C17—C18—H18	120.3	C7—P—Au	115.81 (19)
C13—C18—H18	120.3	C1—P—Au	110.5 (2)
C20—C19—Au	174.9 (5)	C13—P—Au	112.84 (17)

C19—C20—C21	179.5 (7)	C19—Au—P	177.29 (17)
C20—C21—C22	114.0 (5)		
C6—C1—C2—C3	1.5 (9)	C21—C22—C23—C24	−68.7 (8)
P—C1—C2—C3	−175.6 (5)	C22—C23—C24—C25	105.8 (12)
C1—C2—C3—C4	0.5 (10)	C28—C22—C26—O1	−59.9 (7)
C2—C3—C4—C5	−1.4 (11)	C21—C22—C26—O1	57.8 (7)
C3—C4—C5—C6	0.3 (12)	C23—C22—C26—O1	179.6 (6)
C2—C1—C6—C5	−2.6 (10)	C26—C22—C28—O2	−60.0 (8)
P—C1—C6—C5	174.4 (6)	C21—C22—C28—O2	−179.7 (6)
C4—C5—C6—C1	1.7 (12)	C23—C22—C28—O2	59.5 (8)
C12—C7—C8—C9	−1.0 (9)	C22—C26—O1—C27	165.1 (7)
P—C7—C8—C9	−172.9 (5)	C22—C28—O2—C29	164.3 (6)
C7—C8—C9—C10	2.7 (10)	C8—C7—P—C1	−24.3 (6)
C8—C9—C10—C11	−2.8 (10)	C12—C7—P—C1	163.7 (5)
C9—C10—C11—C12	1.2 (10)	C8—C7—P—C13	88.5 (5)
C10—C11—C12—C7	0.5 (10)	C12—C7—P—C13	−83.4 (5)
C8—C7—C12—C11	−0.6 (9)	C8—C7—P—Au	−147.6 (4)
P—C7—C12—C11	171.5 (5)	C12—C7—P—Au	40.5 (5)
C18—C13—C14—C15	−1.3 (9)	C6—C1—P—C7	101.9 (6)
P—C13—C14—C15	−174.7 (5)	C2—C1—P—C7	−81.1 (5)
C13—C14—C15—C16	1.2 (9)	C6—C1—P—C13	−8.3 (6)
C14—C15—C16—C17	−1.0 (10)	C2—C1—P—C13	168.8 (5)
C15—C16—C17—C18	0.8 (10)	C6—C1—P—Au	−131.7 (5)
C16—C17—C18—C13	−0.8 (10)	C2—C1—P—Au	45.4 (5)
C14—C13—C18—C17	1.0 (9)	C14—C13—P—C7	173.5 (4)
P—C13—C18—C17	174.2 (5)	C18—C13—P—C7	0.1 (5)
C20—C21—C22—C26	61.1 (8)	C14—C13—P—C1	−74.3 (5)
C20—C21—C22—C28	−179.9 (6)	C18—C13—P—C1	112.3 (5)
C20—C21—C22—C23	−59.4 (8)	C14—C13—P—Au	47.6 (5)
C26—C22—C23—C24	169.8 (7)	C18—C13—P—Au	−125.8 (4)
C28—C22—C23—C24	49.9 (8)		

References

1. Harrak Y, Simonneau A, Malacria M, Gandon V, Fensterbank L (2010) *Chem Commun* 46:865
2. Simonneau A, Harrak Y, Jeanne-Julien L, Lemièrre G, Mouriès-Mansuy V, Goddard J-P, Malacria M, Fensterbank L (2013) *ChemCatChem* 5:1096
3. Leboeuf D, Simonneau A, Aubert C, Malacria M, Gandon V, Fensterbank L (2011) *Angew Chem Int Ed* 50:6868
4. Simonneau A, Jaroschik F, Lesage D, Karanik M, Guillot R, Malacria M, Tabet J-C, Goddard J-P, Fensterbank L, Gandon V, Gimbert Y (2011) *Chem Sci*. doi:[10.1039/c1sc00478f](https://doi.org/10.1039/c1sc00478f)
5. Grigg R, Stevenson P, Worakun T (1988) *Tetrahedron* 44:4967
6. Chatani N, Morimoto T, Muto T, Murai S (1994) *J Am Chem Soc* 116:6049